

**CHARACTERISATION OF THE HSV-1 DNA PACKAGING
PROTEIN ENCODED BY THE UL25 GENE.**

By

PAUL TARGETT-ADAMS

A Thesis Presented for the Degree of
Doctor of Philosophy

in

The Faculty of Science
at the University of Glasgow

**MRC Virology Unit
Church Street
Glasgow
G11 5JR**

November 2001

ProQuest Number: 13833989

All rights reserved

INFORMATION TO ALL USERS

The quality of this reproduction is dependent upon the quality of the copy submitted.

In the unlikely event that the author did not send a complete manuscript and there are missing pages, these will be noted. Also, if material had to be removed, a note will indicate the deletion.



ProQuest 13833989

Published by ProQuest LLC (2019). Copyright of the Dissertation is held by the Author.

All rights reserved.

This work is protected against unauthorized copying under Title 17, United States Code
Microform Edition © ProQuest LLC.

ProQuest LLC.
789 East Eisenhower Parkway
P.O. Box 1346
Ann Arbor, MI 48106 – 1346

GLASGOW
UNIVERSITY
LIBRARY

12381

Copy 1

Abstract.

Herpes simplex virus type 1 (HSV-1) DNA replication results in the formation of head-to-tail concatemers which are cleaved into genome size units and packaged into the procapsid in the nuclei of virus-infected cells. The procapsid is a spherical structure with icosahedral symmetry and contains an internal protein scaffold which is removed at the same time viral DNA is encapsidated. During the DNA packaging process the procapsid angularises and the DNA-containing capsid can subsequently mature into an infectious virion. The product of the HSV-1 UL25 gene is a minor component of the viral capsid and has been implicated in the HSV-1 DNA packaging process (Addison *et al.*, 1984, Ali *et al.*, 1996, McNab *et al.*, 1998, Ogasawara *et al.*, 2001).

The overall goal of this thesis was to investigate the role of the UL25 protein in the HSV-1 lytic cycle. Before a detailed study of this protein could be undertaken, a number of reagents had to be prepared, including potent UL25-specific antibodies. Therefore, an initial aim of the project was to express the UL25 protein in a variety of *in vivo* recombinant protein expression systems and to purify the soluble recombinant UL25 protein for use as an antigen in the production of UL25-specific monoclonal antibodies. Maltose binding protein (MBP)-tagged UL25 and polyhistidine (His)-tagged UL25 were expressed in *Escherichia coli* and recombinant baculovirus-infected *Sf21* cells respectively. BALB/c mice were immunised with purified soluble MBP-UL25 fusion protein and given a final boost with purified soluble His-tagged UL25 protein. Twelve hybridoma cell lines secreting UL25-specific monoclonal antibodies were isolated. The monoclonal antibodies were characterised using Western blot, immunoprecipitation and immunofluorescence assays. From this analysis a monoclonal antibody that reacted strongly with the UL25 protein in each of the immunoassays was purified for use in subsequent experiments.

In the absence of other HSV-1 proteins, UL25 localised predominantly to the cytoplasm of cells transiently expressing the protein. In cells infected with HSV-1, however, UL25 protein was concentrated in the nuclei at late times. To investigate whether the HSV-1 capsid shell proteins, VP5, VP23 and VP19C, were required for the nuclear localisation of UL25 in HSV-1-infected cells, the distribution of UL25 protein was examined in cells infected with HSV-1 mutants which fail to express these proteins. In non-complementing cells infected with VP23 or VP5 null mutants, the distribution of UL25 protein was similar to the pattern in wild-type (wt) virus-infected cells indicating that neither VP23 nor VP5 were necessary for the nuclear localisation of the UL25 protein

during HSV-1 infection. Since capsid assembly did not occur under these conditions (Desai *et al.*, 1993), nuclear localisation of UL25 was independent of capsid assembly. The intracellular distribution of UL25 was also examined in non-complementing cells infected with a VP19C null mutant of HSV-1. However, this virus appeared to have an additional mutation, one which affected late viral protein production, and no conclusive results were obtained through the use of this virus. The localisation of the UL25 protein was therefore investigated in cells infected with *ts2*, a mutant of HSV-1 that contains a temperature sensitive (*ts*) lesion in the VP19C protein. In cells infected with *ts2* at the non-permissive temperature (NPT), UL25 co-localised with the capsid shell proteins at the perinuclear region of cells with little, if any, UL25 protein observed in the nuclei. These findings suggested that the VP19C protein was necessary for the nuclear distribution of UL25 during wt HSV-1 infection. However, in cells infected with a *ts2* marker rescuant at the NPT, UL25 remained localised to the perinuclear region while the capsid shell proteins were found in the nuclei. This result indicated that the altered intracellular distribution of UL25 in cells infected with *ts2* at the NPT was not a consequence of the *ts* lesion in the VP19C protein. Furthermore, UL25 also localised to the perinuclear region of cells infected with HSV-1 A44, the parental syncytial strain of *ts2*, at the NPT. This virus formed syncytia to a greater extent in cells infected at the NPT compared to the permissive temperature and it is possible that the altered intracellular distribution of UL25 protein in cells infected with HSV-1 A44 at the NPT may have resulted from the formation of syncytia or from an aberrant interaction with a component of the HSV-1 tegument.

The association of UL25 protein with the capsid was initially examined using the recombinant baculovirus expression system to obtain information about the copy number and the location of the UL25 protein in the capsid as well as its interaction with capsid shell proteins. The UL25 protein was incorporated into capsids generated in insect cells multiply infected with recombinant baculoviruses expressing the HSV-1 capsid shell, scaffolding and the UL25 proteins, suggesting that the UL25 protein can interact with capsids in the absence of other viral proteins. This finding is in agreement with earlier results of McNab *et al.* (1998). The level of the UL25 protein associated with recombinant capsids was consistently found to be about eight-fold higher than the amount of UL25 protein bound to HSV-1 B capsids, and was similar to the levels detected in DNA-containing C capsids by Sheaffer *et al.* (2001). Treatment of the recombinant capsids with 2M guanidine hydrochloride (GuHCl) did not remove significant amounts of the UL25 protein, indicating that the protein was tightly associated with these capsids. The high level

of UL25 protein in recombinant capsids allowed an estimate of the copy number of the UL25 protein in the HSV-1 B capsid to be made, which was found to be approximately 40 copies per capsid. This result suggested that the UL25 protein was not located at a unique site within the B capsid. In contrast to the UL25 bound to recombinant capsids, the UL25 protein appeared to be more loosely associated with HSV-1 B capsids and treatment with 2M GuHCl removed a significant amount of the protein. It is therefore possible that the UL25 protein may be associated with the pentons and/or peripentonal triplexes in B capsids. Interestingly, the UL25 protein co-purified with VP5/19C particles generated in insect cells multiply infected with recombinant baculoviruses expressing the VP5, VP19C and UL25 proteins. Immunoprecipitation analysis of HSV-1 infected cells identified a protein of approximately 55,000 molecular weight that appeared to interact specifically with the UL25 protein. This protein was probably of viral origin although the exact identity of the protein remains unknown. In contrast to data presented by Ogasawara *et al.* (2001) no direct evidence was found for an interaction between UL25 and VP5 or VP19C. In an immunofluorescence assay polyclonal rabbit antiserum, specific for the UL25 protein, reacted with cytoplasmic capsids in HSV-1-infected cells during the initial stages of the virus life cycle, suggesting that at least part of the UL25 protein was located on the exterior of capsids derived from input virions.

Early work by Addison *et al.* (1984) on the *ts* mutant *ts1204*, which has a lesion in the UL25 gene, implicated UL25 at a very early stage in virus infection as well as at a late stage. To obtain more insight into the function of the UL25 protein, *ts1204* and another UL25 mutant, *ts1208*, were further characterised, using electron microscopic, DNA and immunofluorescent analysis. Initial experiments revealed that *ts1204* had an additional *ts* mutation and therefore subsequent work was carried out on *ts1249* which contained only the *ts* lesion from the UL25 gene of *ts1204*. *Ts1249*, like *ts1204*, exhibited two defects in cells infected at the NPT. The first appeared to be in the uncoating of the virus and the second defect was found to be in the DNA packaging process. *Ts1208* had a major defect in the latter stage only. Contrary to a report on the properties of a UL25 null mutant virus grown in non-complementing cells (McNab *et al.*, 1998), both *ts1249* and *ts1208* packaged low-levels of HSV-1 DNA in cells infected at the NPT, encapsidating 1.2% and 0.45% of replicated HSV-1 DNA respectively. Additionally, these mutants packaged amplicon DNA with greater efficiency than the full-length HSV-1 genome. These findings indicated that the UL25 protein has a direct role in the HSV-1 DNA cleavage and packaging process and does not function solely to retain the newly packaged DNA within the viral capsid.

Acknowledgements.

I would like to extend my gratitude to Dr Valerie Preston for her support and advice during the course of this investigation and particularly for her extensive proof-reading of this thesis. Thanks are also due to Dr Nigel Stow and to Dr Frazer Rixon for the provision of some of the reagents used in this study. Additional thanks go to Dr Frazer Rixon for many of the capsid images contained within this thesis. I thank the remaining members of Group 3 for friendship and sound technical assistance.

I would also like to thank Dr Susan Graham for the construction of hybridoma cell lines and Dr Howard Marsden for his helpful discussions. I thank Dr Gary Cohen and Dr Stanley Person for kindly supplying some of reagents used in this investigation. I also thank Professor Duncan McGeoch for providing excellent research facilities in the Institute of Virology.

I would like to thank my parents and some great friends whose support contributed to the completion of this thesis. A special thanks goes to Kat, her continual support, advice and friendship during the last couple of years have been greatly appreciated.

The author of this thesis was a recipient of a Medical Research Council studentship. Except where specified, all of the results described in this study were obtained solely through the author's own efforts.

Contents.

LIST OF FIGURES AND TABLES	I
ABBREVIATIONS	V
CHAPTER 1 - INTRODUCTION	
Section 1.1 – The Herpesviruses	2
1.1.1 The <i>Herpesviridae</i> Family	2
1.1.2 Classification of the Herpesviruses	3
1.1.3 Biological Properties of the <i>Alpha-</i> , <i>Beta-</i> and <i>Gammaherpesvirinae</i>	3
1.1.3.1 The <i>Alphaherpesvirinae</i>	3
1.1.3.2 The <i>Betaherpesvirinae</i>	3
1.1.3.3 The <i>Gammaherpesvirinae</i>	4
1.1.4 Herpesvirus Virions	5
1.1.4.1 Herpesvirus Genome Structures	5
1.1.4.2 Herpesvirus Capsids	6
1.1.4.3 Herpesvirus Tegument	8
1.1.4.4 Herpesvirus Envelope	9
Section 1.2 - The Molecular Biology of HSV-1	10
1.2.1 The HSV-1 Genome	10
1.2.1.1 Structure of the HSV-1 Genome	10
1.2.1.2 The <i>a</i> Sequence	10
1.2.1.3 Functions of the <i>a</i> Sequence	12
a). Genome Isomerisation and Recombination	12
b). Genome Circularisation	12
c). Cleavage and Packaging of Viral DNA	13
1.2.1.4 HSV-1 Genes	13
a). The IE Genes	13
b). The Early Genes	14
c). The Late Genes	14
1.2.1.5 The Structure of Encapsidated HSV-1 DNA	15
1.2.2 The Structure of the HSV-1 Capsid	15
1.2.2.1 Protein Composition of the HSV-1 Capsid	15
1.2.2.2 The Pentons and Hexons	16
1.2.2.3 The VP26 Protein	17
1.2.2.4 The Triplexes	17
1.2.2.5 The Protein Scaffold	18

1.2.2.6 <i>The Capsid Floor</i>	20
1.2.2.7 <i>HSV-1 Capsid-Tegument Attachment Sites</i>	20
1.2.3 <i>The HSV-1 Procapsid</i>	21
1.2.4 <i>The HSV-1 Lytic Cycle</i>	22
1.2.4.1 <i>Attachment to and Penetration into the Host Cell</i>	22
1.2.4.2 <i>Disruption of Host Cell Protein Synthesis</i>	23
1.2.4.3 <i>Transport of the Nucleocapsid to the Nucleus</i>	23
1.2.4.4 <i>HSV-1 Gene Expression</i>	24
1.2.4.5 <i>HSV-1 DNA Replication</i>	24
1.2.4.6 <i>Assembly of Procapsids Within the Nucleus of the Infected Cell</i>	25
1.2.4.7 <i>Tegument Acquisition, Envelopment and Virion Egress</i>	26
1.2.5 <i>HSV-1 Latency: An Overview</i>	27
1.2.6 <i>HSV-1 DNA Cleavage and Packaging</i>	29
1.2.6.1 <i>Introduction</i>	29
1.2.6.2 <i>HSV-1 DNA Cleavage and Packaging Signals</i>	30
1.2.6.3 <i>The Production of Genomic-Length DNA Molecules from Concatemeric DNA</i>	31
a). <i>Staggered Nick-Repair Model (Varmuza, 1985)</i>	32
b). <i>The Theft Model (Varmuza, 1985)</i>	32
c). <i>The Directional Cleavage Model (Modified Theft Model) (Deiss, 1986)</i>	33
1.2.6.4 <i>Translocation of DNA Into the Capsid</i>	33
1.2.6.5 <i>HSV-1 DNA Cleavage and Packaging Proteins</i>	35
a). <i>UL6</i>	35
b). <i>UL12</i>	36
c). <i>UL12.5</i>	37
d). <i>UL15</i>	38
e). <i>UL17</i>	40
f). <i>UL25</i>	40
g). <i>UL28</i>	43
h). <i>UL31</i>	44
i). <i>UL32</i>	45
j). <i>UL33</i>	45

CHAPTER 2 – MATERIALS AND METHODS

Section 2.1 – Materials	47
2.1.1 <i>Chemicals and Reagents</i>	47
2.1.2 <i>Additional Materials</i>	48
2.1.3 <i>Solutions</i>	48
2.1.4 <i>Enzymes</i>	50
2.1.5 <i>Radiochemicals</i>	51

2.1.6 Immunological Reagents	51
2.1.7 Plasmids	52
2.1.8 Bacterial Strains and Culture Media	52
2.1.9 Cell Lines	53
2.1.10 Cell Culture Media	53
2.1.11 Viruses	54
Section 2.2 – Methods	55
2.2.1 Tissue Culture	55
2.2.1.1 <i>Serial Passage of Cells</i>	55
2.2.1.2 <i>Storage of Cells</i>	55
2.2.2 Virus Culture and Purification	56
2.2.2.1 <i>Production of HSV-1 Stocks</i>	56
2.2.2.2 <i>Preparation of High Titre Recombinant Baculovirus Stock</i>	56
2.2.2.3 <i>Sterility of Viral Stocks</i>	57
2.2.2.4 <i>Titration of HSV-1</i>	57
2.2.2.5 <i>Titration of Recombinant Baculovirus (Brown & Faulkner, 1977)</i>	57
2.2.2.6 <i>Purification of HSV-1 Virions (wt and ts mutants)</i>	58
2.2.2.7 <i>Purification of HSV-1 Capsids</i>	58
a). <i>Purification of HSV-1 Capsids from Wt Virus-Infected Cells</i>	58
b). <i>Purification of Recombinant B Capsids from Sf21 Cells Infected with Recombinant Baculoviruses</i>	59
c). <i>Purification of VP5-19C Particles from Sf21 Cells Infected with Recombinant Baculoviruses</i>	59
2.2.3 The Generation of a Polyhistidine-Tagged UL25-Expressing Recombinant Baculovirus	60
2.2.3.1 <i>Overview of the Baculovirus Expression System</i>	60
2.2.3.2 <i>Preparation of PAK6 Baculovirus Vector DNA</i>	60
2.2.3.3 <i>Cotransfection of Sf21 Cells with PAK6 Baculovirus Vector DNA and pPTA10/9</i>	61
2.2.3.4 <i>Selection of Recombinant Baculoviruses</i>	61
2.2.3.5 <i>The Identification of Recombinant Baculoviruses Expressing the His-UL25 Protein</i>	62
2.2.3.6 <i>Plaque Purification of His-UL25 Expressing Baculovirus</i>	62
2.2.4 Isolation of HSV-1 Virion DNA	62
2.2.4.1 <i>Infection of Cells with Virus and Isolation of Cell-Released Virus and Cell-Associated Capsids</i>	62
2.2.4.2 <i>Extraction of Viral DNA</i>	63
2.2.5 Preparation of Soluble/Insoluble Fractions from HSV-1 Infected Cells	63
2.2.6 Preparation of Plasmid DNA	64
2.2.6.1 <i>Large Scale Plasmid Preparation (CsCl banding)</i>	64
2.2.6.2 <i>QIAGEN MIDI Plasmid Purification</i>	65
2.2.6.3 <i>Small Scale Plasmid Preparation (miniprep) (Chowdhury, 1991)</i>	65

2.2.7 Manipulation of DNA	66
2.2.7.1 <i>Synthesis and Purification of Oligonucleotides</i>	66
2.2.7.2 <i>Gel Electrophoresis of DNA</i>	66
2.2.7.3 <i>Southern Blotting and Hybridisation</i>	67
a). <i>Southern Blot Transfer (Southern, 1975)</i>	67
b). <i>Preparation of Radio-Labelled Probe for Southern Blot Hybridisation</i>	67
c). <i>Southern Blot Hybridisation</i>	67
d). <i>Quantitative Analysis</i>	68
2.2.7.4 <i>Restriction Endonuclease Enzyme Digestion of DNA</i>	68
2.2.7.5 <i>Purification of DNA Fragments</i>	68
2.2.7.6 <i>Ligation of DNA Fragments</i>	68
2.2.8 Preparation and Transformation of Competent <i>E. coli</i>	69
2.2.8.1 <i>Preparation and Transformation of Competent BL21 <i>E. coli</i> (CaCl₂ Method)</i>	69
2.2.8.2 <i>Preparation of Electrocompetent DH5α <i>E. coli</i></i>	69
2.2.8.3 <i>Transformation of Electrocompetent DH5α <i>E. coli</i></i>	70
2.2.9 Generation of Monoclonal Antibodies Specific for the HSV-1 UL25 Protein	70
2.2.9.1 <i>Immunisation of Mice with MBP-UL25</i>	70
2.2.9.2 <i>Fusion of Splenic Lymphocytes with Myeloma Cells</i>	70
2.2.9.3 <i>Screening Hybridoma Cell Colonies for Production of Monoclonal Antibodies Specific for UL25</i>	71
2.3.0 Protein Purification	71
2.3.0.1 <i>MBP-UL25 Purification</i>	71
a). <i>Expression of MBP-UL25 Fusion Protein and Generation of Soluble Cell Extracts</i>	71
b). <i>Purification of MBP-UL25 Fusion Protein by Affinity Chromatography</i>	72
2.3.0.2 <i>Purification of His-UL25 from PTA10bac#14 Infected Sf21 Cells</i>	72
a). <i>Preparation of Virus-Infected Cell Extracts</i>	72
b). <i>Purification of His-UL25 by Affinity Chromatography</i>	73
2.3.0.3 <i>Purification of Monoclonal Antibodies by Affinity Chromatography</i>	73
2.3.1 Protein Analysis	74
2.3.1.1 <i>SDS-PAGE</i>	74
2.3.1.2 <i>Coomassie Blue Staining of Polyacrylamide Gels</i>	74
2.3.1.3 <i>Fluorography</i>	75
2.3.1.4 <i>Western Blotting</i>	75
2.3.1.5 <i>Immunofluorescence</i>	75
2.3.1.6 <i>Immunofluorescent Detection of Incoming Capsids</i>	76
2.3.1.7 <i>Immunoprecipitation of HSV-1 Infected Cells</i>	76
2.3.2 Transient Transfection of Cells Using LipofectAMINE	77
2.3.3 Detergent Extraction of Transiently Transfected Cells	78
2.3.4 Analysis of Virus-Infected Cells by Electron Microscopy	78
2.3.4.1 <i>Virus Infection of Cells</i>	78

2.3.4.2 <i>Embedding Virus-Infected Cells in Epon Resin</i>	79
2.3.4.3 <i>Thin Sectioning</i>	79
2.3.4.4 <i>Negative Staining</i>	79
2.3.5 HSV-1 DNA Packaging Assay	80
2.3.5.1 <i>Virus Infection of Cells</i>	80
2.3.5.2 <i>Harvesting the Virus-Infected Cells</i>	80
2.3.5.3 <i>Preparation of HSV-1 Packaged DNA</i>	80
2.3.5.4 <i>Preparation of Total DNA</i>	81
2.3.5.5 <i>Analysis of Total and HSV-1 Packaged DNA</i>	81
2.3.6 HSV-1 Transient DNA Packaging Assay	81
2.3.6.1 <i>Transfection of Vero Cells with pSA1</i>	81
2.3.6.2 <i>Superinfection of Vero Cells with HSV-1</i>	81
2.3.6.3 <i>Detection of Replicated and Packaged Amplicon DNA</i>	82
2.3.7 Marker Rescue of HSV-1 Ts2 with Cloned wt HSV-1 HindIII k DNA Fragment	82
2.3.7.1 <i>Cotransfection of Cells with Ts2 DNA and HindIII k DNA</i>	82
2.3.7.2 <i>Selection and Isolation of Marker Rescue Virus</i>	82

CHAPTER 3 – RESULTS

Section 3.1 - Sequence Analysis of The HSV-1 UL25 Protein	85
3.1.1 <i>Introduction</i>	85
3.1.2 <i>Sequence Alignment of the HSV-1 UL25 Protein and its Homologues</i>	85
3.1.3 <i>Predicted Secondary Structure of the HSV-1 UL25 Protein</i>	85
3.1.3.1 <i>PSIPRED and PHDsec Secondary Structure Predictions</i>	85
3.1.3.2 <i>ISREC COILS Secondary Structure Prediction</i>	86
3.1.4 <i>Discussion</i>	86
Section 3.2 - Generation and Characterisation of Reagents Used In This Study	88
3.2.1 <i>The Generation of a Polyhistidine-Tagged UL25 Expressing Recombinant Baculovirus</i>	88
3.2.1.1 <i>Introduction</i>	88
3.2.1.2 <i>The Generation of Oligonucleotide OG3</i>	88
3.2.1.3 <i>Purification of UL25 Gene Fragments and Linearised pUC19 Plasmid</i>	89
3.2.1.4 <i>Ligation of the OG3 Oligonucleotide and UL25 Gene Fragments to the Linearised pUC19 Plasmid</i>	89
3.2.1.5 <i>An EcoRI/HindIII Screen was Used to Identify Plasmids Containing the Full-Length UL25 ORF Modified at the 5' End</i>	90
3.2.1.6 <i>An EcoRV/HindIII Screen was Used to Identify Constructs containing the UL25 AatII–AatII DNA Fragment in the Correct Orientation Within the pPTA8 Plasmid</i>	90
3.2.1.7 <i>The Cloning of the Modified UL25 Gene Into Baculovirus Transfer Vector pAcCL29.1 to Generate the pPTA10 Plasmid</i>	91

3.2.1.8 <i>A BamHI Screen was Used to Identify Plasmids in Which the Modified UL25 Gene had Ligated Successfully into pAcCL29.1</i>	91
3.2.1.9 <i>A KpnI Screen was Used Identify Plasmids Containing the Modified UL25 Gene in the Correct Orientation Within the pPTA10 Plasmid</i>	91
3.2.1.10 <i>The Isolation of PTA10bac#14: A His-UL25 Expressing Recombinant Baculovirus</i>	92
3.2.2 <i>The Generation of a MBP-UL25 Fusion Protein Expressing Bacterial Clone</i>	92
3.2.3 <i>The Generation and Characterisation of Monoclonal Antibodies Specific for the HSV-1 UL25 Protein</i>	93
3.2.3.1 <i>Introduction</i>	93
3.2.3.2 <i>Purification of MBP-UL25 and His-UL25 Proteins</i>	93
3.2.3.3 <i>Purification of MBP-UL25 Protein for Immunisation of BALB/c Mice</i>	93
3.2.3.4 <i>Purification of His-UL25 Protein for Boosting Immunised BALB/c Mice</i>	94
3.2.3.5 <i>The Reactivity of Monoclonal Antibodies Specific for the UL25 Protein in a Western Blot Assay</i>	94
3.2.3.6 <i>The Reactivity of Monoclonal Antibodies Specific for the UL25 Protein in an Immunoprecipitation Assay</i>	95
3.2.3.7 <i>The Reactivity of Monoclonal Antibodies Specific for the UL25 Protein in Indirect Immunofluorescence Assays</i>	95
3.2.4 <i>Discussion</i>	95
Section 3.3 - A Study of The Factor(s) Required For The Nuclear Localisation of The UL25 Protein In Cells Infected With HSV-1	98
3.3.1 <i>Introduction</i>	98
3.3.2 <i>The Intracellular Localisation of the UL25 Protein in Non-Complementing Cells Infected with K23Z, K5ΔZ and KΔ19C</i>	98
3.3.3 <i>The Intracellular Localisation of the UL25 and Capsid Proteins in Cells Infected with Ts2</i>	99
3.3.4 <i>The Construction of Ts2Hindk MR#6, a Ts2 Marker Rescue Virus</i>	100
3.3.5 <i>The Intracellular Localisation of the UL25 and Capsid Proteins in Cells Infected with Ts2Hindk MR#6</i>	101
3.3.6 <i>The Intracellular Localisation of the UL25 Protein in Cells Infected with Ts⁺ A44</i>	101
3.3.7 <i>Discussion</i>	102
Section 3.4 - Protein-Protein Interactions Involving The UL25 Protein	105
3.4.1 <i>Introduction</i>	105
3.4.2 <i>The Association of the His-UL25 Protein with Recombinant HSV-1 Capsids</i>	106
3.4.3 <i>The Association of the His-UL25 Protein with VP5/19C Particles</i>	106
3.4.4 <i>Is the UL25 Protein Located on the External Surface of the HSV-1 Capsid?</i>	107
3.4.5 <i>An Estimation of the Copy Number of the UL25 Protein in the HSV-1 Capsid</i>	108

3.4.5.1 Elevated Levels of the UL25 Protein are Found in Recombinant Capsids Compared to <i>Wt</i> HSV-1 Capsids	108
3.4.5.2 The UL25 Protein Found in Recombinant Capsids is Resistant to 2 M GuHCl Treatment	108
3.4.5.3 The Additional Levels of the UL25 Protein Found in Recombinant Capsids Allow an Estimation of the Copy Number of the UL25 Protein in HSV-1 Capsids	109
3.4.6 The Analysis of Protein-Protein Interactions Involving the UL25 Protein in HSV-1 <i>ts</i> ⁺ 17 <i>syn</i> ⁺ Infected Cells Using an Immunoprecipitation Assay with Monoclonal Antibody 166	110
3.4.7 The UL25 Protein Associates with the Cellular Cytoskeleton	110
3.4.8 Discussion	111
Section 3.5 - The Characterisation of <i>Ts</i>1204 and <i>Ts</i>1208 Mutants	115
3.5.1 Introduction	115
3.5.2 Sequence Analysis of the <i>Ts</i> 1204 and <i>Ts</i> 1208 Mutations	115
3.5.3 The Construction of <i>Ts</i> 1249	115
3.5.4 The Protein Profile of <i>Ts</i> 1249 and <i>Ts</i> 1208 in Cells Infected at the NPT	116
3.5.5 The Entry of <i>Ts</i> 1249 Into Cells Infected at the NPT	116
3.5.6 Electron Microscopic Analysis of Mutant Virus-Infected Cells	117
3.5.7 The Ability of <i>Ts</i> 1249 and <i>Ts</i> 1208 to Package HSV-1 DNA in Cells Infected at the NPT	118
3.5.8 The Ability of <i>Ts</i> 1249 and <i>Ts</i> 1208 to Package Amplicon DNA in Cells Infected at the NPT	119
3.5.9 Discussion	119
CHAPTER 4 – GENERAL DISCUSSION	
4.1 The UL25 Protein	123
4.2 Interactions Between UL25 and the HSV-1 Capsid Proteins	124
4.3 The Copy Number and Location of the UL25 Protein in HSV-1 Capsids	128
4.4 The Factors Required to Localise the UL25 Protein to the Nucleus During <i>Wt</i> Virus-Infection.	131
4.5 Other Interactions Involving the UL25 Protein	133
4.6 The Further Characterisation of <i>Ts</i> 1249 and <i>Ts</i> 1208	135
CHAPTER 5 – BIBLIOGRAPHY	

List of Figures and Tables.

Figures.

- Figure 1.1** The HSV-1 Virion
- Figure 1.2** Herpesvirus Genome Structures
- Figure 1.3** Structure of the HSV-1 Genome
- Figure 1.4** Structure of the HSV-1 *a* Sequence
- Figure 1.5** The HSV-1 B Capsid
- Figure 1.6** The Arrangement of Hexons in the HSV-1 Capsid
- Figure 1.7** The Asymmetric Unit of the HSV-1 Capsid
- Figure 1.8** The Relationship between the HSV-1 UL26 and UL26.5 Gene Products
- Figure 1.9** Comparison of Procapsids Formed by *Ts1201* at the NPT with Angularised Capsids of wt HSV-1.
- Figure 1.10** Schematic Representation of the HSV-1 Lytic Life Cycle
- Figure 1.11** Protein-Protein Interactions Involving the HSV-1 Capsid Proteins
- Figure 1.12** Sequence Arrangement in Adjacent HSV-1 *a* Sequences
- Figure 1.13** Structure of the Bacteriophage $\phi 29$ Portal Complex (Simpson, 2000)
- Figure 2.1** The Structure of Baculovirus Transfer Vector pAcCL29.1
- Figure 3.1** Sequence Alignment of the HSV-1 UL25 Protein and its Homologues
- Figure 3.2** PSIPRED Predicted Secondary Structure of the HSV-1 UL25 Protein
- Figure 3.3** ISREC COILS Analysis of the HSV-1 17⁺ UL25 Amino Acid Sequence and its Homologues
- Figure 3.4** The Structure of Oligonucleotide OG3
- Figure 3.5** An Outline of the Cloning Strategy used to Generate the pPTA10 Plasmid (pAcCL29.1 Baculovirus Transfer Vector Encoding the Polyhistidine Tagged UL25 Protein)
- Figure 3.6** An *EcoRI/HindIII* Screen was Used to Identify Constructs in which the Modified UL25 Gene had been Introduced Into the pUC19 Plasmid Backbone to Form the pPTA8 Plasmid
- Figure 3.7** An *EcoRV/HindIII* Screen was Used to Identify Plasmids Containing the UL25 *AatII–AatII* DNA Fragment in the Correct Orientation Within the pPTA8 Plasmid
- Figure 3.8** A *BamHI* Screen was Used to Identify Constructs in which the pAcCL29.1 Plasmid and the Modified UL25 Gene had Ligated Successfully to Form the pPTA10 Plasmid
- Figure 3.9** A *KpnI* Screen was Used to Identify Constructs Containing the Modified UL25 Gene in the Correct Orientation Within the pPTA10 Plasmid
- Figure 3.10** His-UL25 Recombinant Protein Screen of Plaque Isolated Small Scale Virus Stocks
- Figure 3.11** Purification of MBP-UL25 from IPTG Induced PTA3 Bacteria Carrying pPTA3
- Figure 3.12** Western blot Analysis of the Specific Immunoreactivity in Serum from Blood Taken in a Test Bleed from MBP-UL25 Immunised Mice
- Figure 3.13** Purification of His-UL25 from *Sf21* Cells Infected with PTA10bac#14

- Figure 3.14** Monoclonal Antibody 166 Functions in a Western blot Assay
- Figure 3.15** Monoclonal Antibody 220 Functions in an Immunoprecipitation Assay
- Figure 3.16** In the Absence of Other Viral Proteins the UL25 Protein Localises to the Cellular Cytoplasm
- Figure 3.17** The UL25 Protein Localises Primarily to the Nucleus During Wt HSV-1 Infection
- Figure 3.18** The UL25 Protein Co-Localises with the VP19C Protein in the Nuclei of Non-Complementing Cells Infected with K23Z
- Figure 3.19** The UL25 Protein Co-Localises with the VP23 Protein in the Nuclei of Non-Complementing Cells Infected with K5ΔZ
- Figure 3.20** The Intracellular Localisation of the UL25 and Capsid Proteins in Cells Infected with *Ts2* at the PT
- Figure 3.21** The UL25 Protein Co-Localises with the VP23 Protein at the Perinuclear Region of Cells Infected with *Ts2* at the NPT
- Figure 3.22** The UL25 Protein Co-Localises with the VP19C Protein at the Perinuclear Region of Cells Infected with *Ts2* at the NPT
- Figure 3.23** The Intracellular Localisation of the VP5 Protein in Cells Infected with *Ts2* at the NPT
- Figure 3.24** Confirmation of the Perinuclear Localisation of the UL25 Protein in Cells Infected with *Ts2* at the NPT
- Figure 3.25** An Analysis of the Solubility of the UL25 and VP23 Proteins in Cells Infected with *Ts2* at the NPT
- Figure 3.26** The UL25 Protein Does Not Co-Localise with the VP23 Protein in the Nuclei of Cells Infected with *Ts2*Hindk MR#6 at the NPT
- Figure 3.27** The UL25 Protein Does Not Co-Localise with the VP19C Protein in the Nuclei of Cells Infected with *Ts2*Hindk MR#6 at the NPT
- Figure 3.28** The Intracellular Localisation of the VP5 Protein in Cells Infected with *Ts2*Hindk MR#6 at the NPT
- Figure 3.29** The Intracellular Localisation of the UL25 and Capsid Proteins in Cells Infected with *Ts2*Hindk MR#6 at the PT
- Figure 3.30** The Altered Intracellular Localisation of the UL25 Protein in Cells Infected with HSV-1 *Ts*⁺ A44 at the NPT
- Figure 3.31** The Intracellular Localisation of the UL25 Protein in Cells Infected with HSV-1 *Ts*⁺ 17 syn and *ts*⁺ 17 syn⁺ at the NPT
- Figure 3.32** His-UL25 Co-Migrates with B Capsids Generated from Co-Infection of *Sf21* Cells with Recombinant Baculoviruses Expressing the HSV-1 Capsid Proteins
- Figure 3.33** His-UL25 Co-Migrates with VP5/19C Particles Generated in *Sf21* Cells Multiply-Infected with Recombinant Baculoviruses Expressing the HSV-1 VP5 and VP19C Capsid Proteins and the His-UL25 Protein
- Figure 3.34** Negatively Stained VP5/19C Particles and Recombinant HSV-1 Capsids
- Figure 3.35** At Least Part of the UL25 Protein is Located on the External Surface of the HSV-1 Capsid
- Figure 3.36** Approximately Eight-Fold More UL25 Protein is Found in Recombinant Capsids Compared to Wt HSV-1 Capsids

- Figure 3.37** The Elevated Levels of the UL25 Protein Associated with Recombinant Capsids are Resistant to 2 M GuHCl Treatment
- Figure 3.38** An Estimation of the Copy Number of the UL25 Protein in the HSV-1 Capsid
- Figure 3.39** Monoclonal Antibody 166 Co-Immunoprecipitates the UL25 Protein and an Unknown Protein of Approximately 55 kDa from Wt Virus-Infected Cells
- Figure 3.40** The UL25 Protein Associates with the Cellular Cytoskeletal Structure
- Figure 3.41** The Protein Profile of *Ts1249* and *Ts1208* in Cells Infected at the NPT
- Figure 3.42** Entry of *Ts1249* Into Cells Infected at the PT
- Figure 3.43** Entry of *Ts1249* Into Cells Infected at the NPT
- Figure 3.44** Electron Microscopic Analysis of Mutant Virus-Infected Cells
- Figure 3.45** Both *Ts1249* and *Ts1208* Package a Low level of HSV-1 DNA in Cells Infected at the NPT
- Figure 3.46** Both *Ts1249* and *Ts1208* Package Amplicon DNA in Cells Infected at the NPT

Tables.

Table 1.1	Taxonomic Structure of the <i>Herpesviridae</i> Family
Table 1.2	The Major Protein Components of HSV-1 B Capsids
Table 1.3	The Essential HSV-1 DNA Replication Proteins
Table 1.4	The HSV-1 DNA Cleavage and Packaging Proteins
Table 2.1	Chemicals and Reagents
Table 2.2	Additional Materials
Table 2.3	Solutions
Table 2.4	Enzymes
Table 2.5	Immunological Reagents
Table 2.6	Plasmids
Table 3.1	Summary of the Characterisation of Monoclonal Antibodies Specific for the HSV-1 UL25 Protein
Table 3.2	The Plating Efficiency of <i>Ts2Hindk</i> MR#6 and Wt Virus at the PT and the NPT
Table 3.3	The Effect of GuHCl Concentration on the Levels of UL25 and VP22a Protein in HSV-1 Capsids and Capsids Generated Using Recombinant Baculoviruses
Table 3.4	Potential HSV-1 Protein Candidates for Interaction with the UL25 Protein
Table 3.5	The Level of DNA Packaged by <i>Ts1249</i> , <i>Ts1208</i> and Marker Rescued Viruses in Cells Infected at the NPT

Abbreviations.

A

A	- adenine
AIDS	- acquired immune deficiency syndrome
ATP	- adenosine triphosphate

B

bp	- base pairs
BHV-1	- bovine herpesvirus 1

C

C	- cytosine
Ci	- curie
CIP	- calf intestinal phosphatase
cpe	- cytopathic effect

D

DMSO	- dimethyl sulphoxide
DNA	- deoxyribonucleic acid
DNase	- deoxyribonuclease
ds	- double-stranded (DNA)

E

EBV	- Epstein-Barr virus
<i>E. coli</i>	- <i>Escherichia coli</i>

F

FITC	- fluorescein isothiocyanate
------	------------------------------

G

G	- guanine
GFP	- green fluorescent protein
GPCMV	- guinea pig cytomegalovirus

H

HCMV	- human cytomegalovirus
------	-------------------------

HGPRT	- hypoxanthine-guanine phosphoribosyltransferase
HHV-6	- human herpesvirus 6
HSV-1	- herpes simplex virus type 1
HSV-2	- herpes simplex virus type 2

I

IE	- immediate-early
kbp	- kilobase pairs
kDa	- kilodaltons

M

M	- molar
MBP	- maltose binding protein
MCMV	- murine cytomegalovirus
mg	- milligram
μCi	- microcurie
μg	- microgram
μl	- microlitre
ml	- millilitre
mM	- millimolar
moi	- multiplicity of infection
MOPS	- 3-[N-morpholino] propane sulphonic acid
mRNA	- messenger ribonucleic acid

N

nm	- nanometre
NPT	- non permissive temperature

O

ORF	- open reading frame
-----	----------------------

P

PBS	- phosphate-buffered saline
pfu	- plaque-forming units
pi	- post-infection
PRV	- pseudorabies virus
PT	- permissive temperature
PVDF	- polyvinylidene difluoride

R

RNA	- ribonucleic acid
RNase	- ribonuclease
rpm	- revolutions per minute

S

SCMV	- simian cytomegalovirus
SDS	- sodium dodecyl sulphate
SDS-PAGE	- sodium dodecyl sulphate polyacrylamide gel electrophoresis
ss	- single-stranded (DNA)

T

T	- thymine
<i>ts</i>	- temperature sensitive
TEMED	- N,N,N',N'-tetra-methyl-ethlene diamine
TRIS	- 2-amino-2-(hydroxymethyl)-1,3-propandiol

U

UV	- ultra violet
----	----------------

V

VHS	- virion associated host shut off protein
v/v	- volume / volume

W

wt	- wild type virus (HSV-1 <i>ts</i> ⁺ 17 <i>syn</i> ⁺)
w/v	- weight / volume

X

X-Gal	- 5-bromo-4-chloro-3-indolyl- β -D-galactosidase
-------	--

CHAPTER 1

INTRODUCTION

1.1 The Herpesviruses.

1.1.1 The *Herpesviridae* Family.

Members of the *Herpesviridae* family are large, structurally similar viruses containing double stranded (ds) DNA genomes. Herpesvirus virions are roughly spherical in shape with an average diameter of approximately 200 nm and are composed of four very distinct morphological elements (Figure 1.1). The dsDNA genome is packaged within a icosahedral protein shell termed the capsid. An amorphous protein layer known as the tegument surrounds the capsid and the whole structure is enclosed within a lipid envelope derived from the host cell. To date, more than 100 herpesviruses have been isolated from a wide variety of eukaryotic organisms. Although the majority of known herpesviruses were isolated from vertebrate organisms (fish, amphibians, reptiles, birds and mammals), a herpesvirus which infects an invertebrate organism has also been identified (Comps & Cochenec, 1993). As a general rule, the natural host range of individual viruses is highly restricted and most herpesviruses are thought to have evolved in association with a single host species, though occasional transfer to other species can occur in nature. *Herpesviridae* family members share four common characteristics:

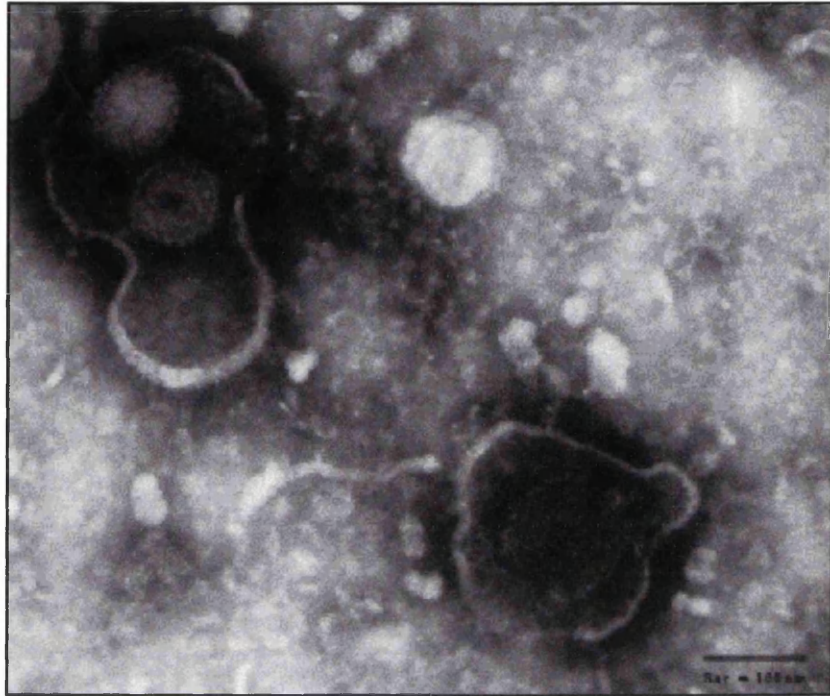
- i. All encode enzymes involved in nucleic acid synthesis and metabolism e.g. DNA polymerase and deoxyuridine triphosphatase. Herpesviruses also encode at least one protease and several protein kinases.
- ii. The synthesis of viral DNA, capsid assembly and the initial envelopment stage all occur in the nucleus of the infected host cell.
- iii. Virion production leads to host cell death.
- iv. Most herpesviruses are known to establish a latent infection in their natural host.

Latency is a central feature of herpesvirus infection and is defined as the persistence of virus in the absence of a clinically apparent infection. After primary infection of their natural host, herpesviruses frequently establish a latent infection. Recurring lytic infections are produced by the reactivation of the quiescent genome in response to certain stimuli.

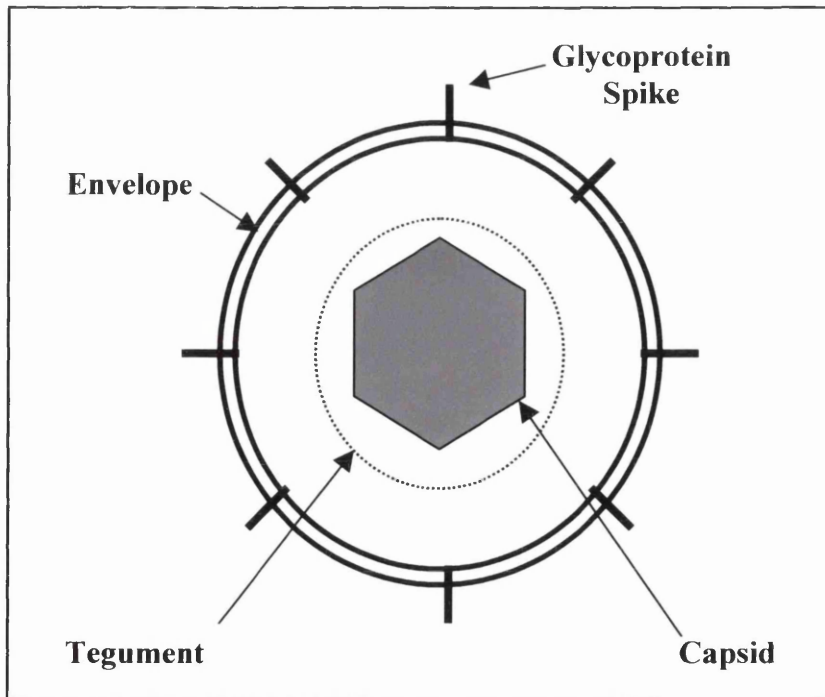
Figure 1.1 The HSV-1 Virion.

Negatively stained HSV-1 virions **(a)** and schematic representation of an HSV-1 virion **(b)**.

a).



b).



1.1.2 Classification of the Herpesviruses.

Table 1.1 illustrates the classification of the *Herpesviridae* family according to the seventh report from the Herpesvirus Study Group of the International Committee on Taxonomy of Viruses.

1.1.3 Biological Properties of the *Alpha-, Beta- and Gammaherpesvirinae*.

1.1.3.1 The *Alphaherpesvirinae*.

The members of this subfamily are classified on the basis of their variable host range *in vitro*, relatively short reproductive cycle, rapid spread in culture, efficient destruction of infected cells and capacity to establish latent infections primarily, but not exclusively, in sensory ganglia. The prototype alphaherpesvirus is HSV-1. Its natural host is man and primary infection usually occurs in the mucosa of the mouth or throat although HSV-1 is also capable of infecting the mucosa of the genital tract. Primary infection is usually asymptomatic but can lead to illness characterised by lesions in the mouth and throat, fever and a general malaise. Latency is usually established in the trigeminal ganglia, from where reactivation may occur. Reactivation is often associated with stress, fever, exposure to UV light, tissue damage or immuno-suppression. Reactivated virus-infection usually results in lesions of the skin in the area served by the trigeminal ganglia e.g. herpes labialis (cold sores). Complications can result from infection with HSV-1 and include encephalitis, although this is usually restricted to neonatal and immuno-compromised individuals, keratitis and disseminated infection involving organs such as the liver and adrenal glands.

Other notable human pathogens which belong to the *Alphaherpesvirinae* subfamily include varicella-zoster virus, the causative agent of chicken pox and shingles, and HSV-2 which is responsible for recurrent genital lesions.

1.1.3.2 The *Betaherpesvirinae*.

Members of this subfamily often exhibit a restricted host range both *in vivo* and *in vitro*, they have long reproductive cycles and virus-infection progresses slowly in culture. The infected cells frequently become enlarged (cytomegalia) and latent infections are established in a variety of tissues including secretory glands, lymphoreticular cells and the kidneys.

SUBFAMILY	<i>Alphaherpesvirinae</i>
Genus	<i>Simplexvirus</i>
Genus	<i>Varicellovirus</i>
Genus	“Marek’s disease-like viruses”
Genus	“Infectious laryngotracheitis-like viruses”
SUBFAMILY	<i>Betaherpesvirinae</i>
Genus	<i>Cytomegalovirus</i>
Genus	<i>Muromegalvirus</i>
Genus	<i>Roseolovirus</i>
SUBFAMILY	<i>Gammaherpesvirinae</i>
Genus	<i>Lymphocryptovirus</i>
Genus	<i>Rhadinovirus</i>
Unassigned Genus	“Ictalurid herpes-like viruses”

Table 1.1 Taxonomic Structure of the *Herpesviridae* Family.

Human cytomegalovirus (HCMV) is a betaherpesvirus which frequently infects man. Primary infection typically occurs in monocytes or endothelial cells (Turtinen *et al.*, 1987, Saltzman *et al.*, 1988) and is usually asymptomatic even in immuno-compromised individuals. Where clinical disease does occur, infection with HCMV results in a persistent fever and myalgia and infrequent complications include pneumonia, hepatitis and encephalitis. The sites of HCMV viral latency remain unclear but HCMV DNA has been identified in monocyte populations of peripheral blood (Taylor-Wiedeman *et al.*, 1991).

AIDS patients are particularly susceptible to HCMV infection and the virus frequently infects the liver, the lungs and the central nervous system of these people. HCMV often infects the gastrointestinal tract of AIDS patients where disease can vary from superficial ulceration to more severe necrosis which often leads to a fatal perforation of the gut (Cotte *et al.*, 1993).

1.1.3.3 The Gammaherpesvirinae.

The experimental host range of the members of this subfamily is limited to the family or order to which the natural host belongs. *In vitro* all members replicate in lymphoblastoid cells, and some cause lytic infections in some types of epithelioid and fibroblastic cells. Viruses in this group are specific for either T- or B-lymphocytes and latent virus is frequently demonstrated in lymphoid tissue. Epstein-Barr virus (EBV) is a gammaherpesvirus that infects man. Primary infection probably occurs in the mucosa of the nose and mouth and rapidly progresses to B-lymphocytes which are transformed into an immortal lymphoblastoid state. Primary infection is usually asymptomatic although EBV has been identified as the causative agent of infectious mononucleosis in a proportion of adolescent primary infections. In immuno-compromised individuals the outcome of infection can be more severe, resulting in tumours such as oral hairy leukoplakia and Burkitt's lymphoma.

A relatively new addition to the *Gammaherpesviridae* subfamily was discovered in 1994 (Chang *et al.*, 1994). Known as human herpesvirus 8 (HHV-8) or Kaposi's sarcoma-associated herpesvirus (KSHV), this herpesvirus is the infectious cause of Kaposi's sarcoma (reviewed by Schulz, 1998).

1.1.4 Herpesvirus Virions.

1.1.4.1 Herpesvirus Genome Structures.

The genomes of all herpesviruses characterised to date are linear dsDNA which range in size from 120-240 kbp and contain a G+C content of 31% to 75%. Herpesvirus genomes often have multiple internal and terminal repeat sequences and exhibit a diverse range of genome structures which differ in the arrangement of unique and repeated regions (Roizman *et al.*, 1992, Davison & McGeoch, 1995) (Figure 1.2). For simplicity, herpesviruses genome structures will be referred to using the classification system designated by Davison and McGeoch (1995).

Genomes which contain a single unique region flanked by direct repeat sequences are designated as group 1 genomes and include the genome of channel catfish virus (Davison, 1992).

Group 2 and group 3 genomes both have multiple copies of a repeat sequence at their termini. However, while group 2 genomes have a single unique region, group 3 genomes have additional copies of the repeat sequence positioned internally. This gives rise to two unique regions which are flanked by inverted copies of the same repeat sequence. In addition, the two unique regions of group 3 genomes invert, giving rise to four genome isomers which are present in an equimolar amount in DNA isolated from virions. Group 2 genomes include the genome of herpesvirus saimiri (Albrecht *et al.*, 1992), while group 3 genomes include the genome of cottontail rabbit herpesvirus (Cebrian *et al.*, 1989).

The genome structure of Epstein-Barr virus is characteristic of group 4 and has a set of internal repeat sequences that are unrelated to the terminal repeat sequences (Baer *et al.*, 1984).

Group 5 genomes have two unique regions which are flanked by inverted repeat sequences. The repeats are not related and the repeat flanking the long unique region (U_L) is significantly shorter than that flanking the short unique region (U_S). The two genomic orientations of U_S are present in an equimolar amount in DNA isolated from virions but U_L is found in predominantly one orientation. The genome structure of varicella-zoster virus is characteristic of group 5 (Davison & Scott, 1986).

Classification as:

Roizman *et al.* (1992) **Davison & McGeoch (1995)**

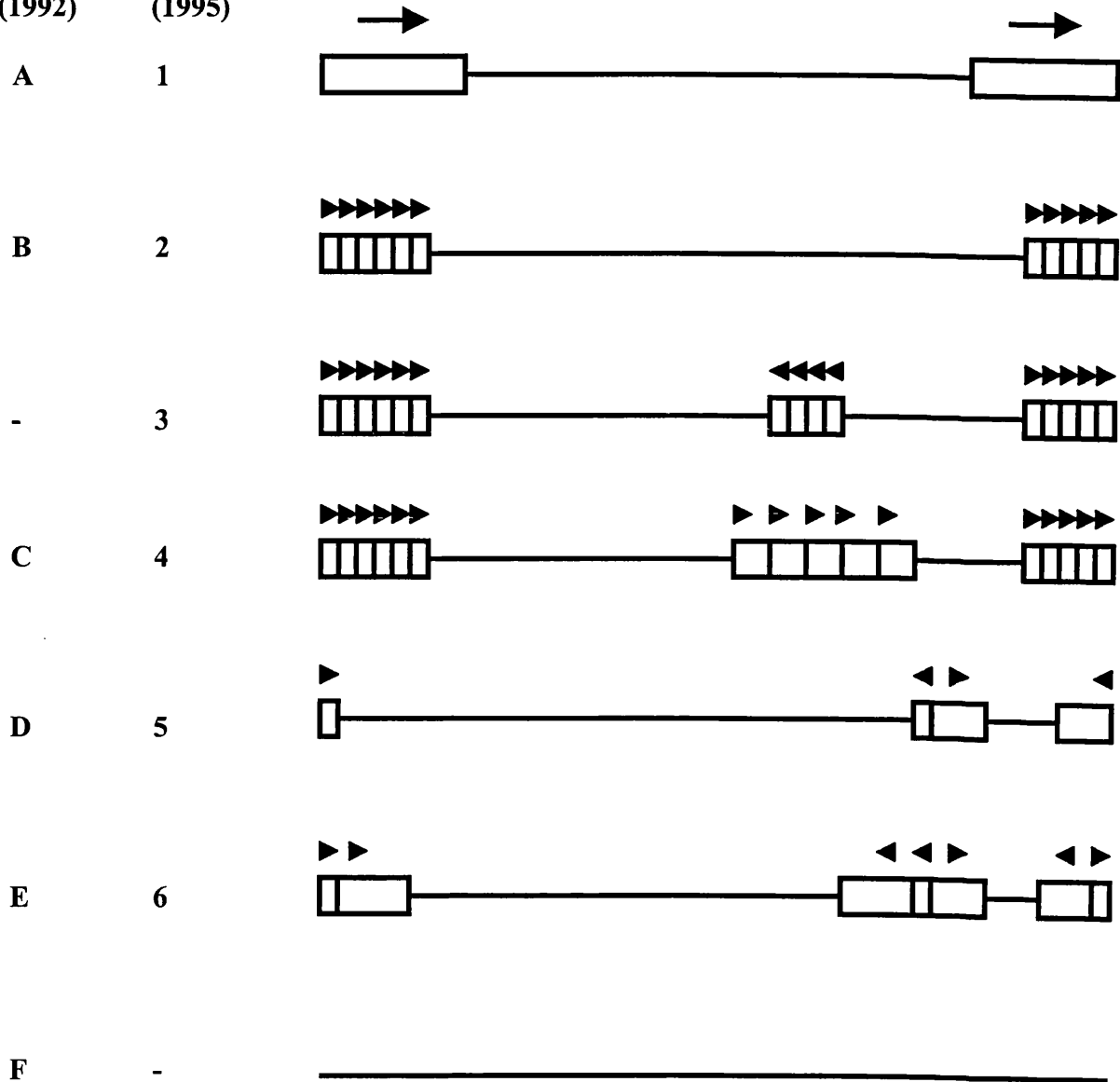


Figure 1.2 Herpesvirus Genome Structures.

The above figure is a schematic representation of the genome structures found within the *Herpesviridae* family. Unique and repeat regions are shown as horizontal lines and rectangles, respectively. The orientations of the repeats are shown by arrowheads and alternative genome structure nomenclature is indicated on the left of the diagram.

Group 6 is similar to group 5 except the inverted repeat sequences flanking the U_L region are larger and an additional repeat sequence known as the *a* sequence is found at the termini and at the junction between the long (L) and short (S) segments. The UL and US regions are both capable of inversion and the resulting four genomic isomers are found in an equimolar amount in DNA isolated from virions. The genome structures of HSV-1 and HSV-2 are characteristic of group 6 genomes (Roizman, 1979).

The genome structure designated as group F by Roizman *et al.* (1992) consists of a single unique sequence which lacks both internal and terminal repeat sequences. The genome structure of tree shrew herpesvirus is characteristic of this group (Koch *et al.*, 1985).

1.1.4.2 Herpesvirus Capsids.

Although within the herpesvirus family there is limited sequence homology between the primary amino acid sequences of any of the herpesvirus major capsid proteins, cryoelectron microscopy and image reconstruction have demonstrated that even evolutionary distinct herpesviruses assemble morphologically similar capsids (Booy *et al.*, 1996). All herpesvirus capsids are approximately 120 nm in diameter and exhibit icosahedral symmetry. The icosahedral capsid is composed of 20 identical equilateral triangles and displays three different forms of rotational symmetry. A fivefold symmetry axis is present through each of the 12 vertices of the icosahedron, each of the 20 faces has a threefold axis of symmetry and each of the 30 edges shows a twofold axis of symmetry.

The minimum number of protein subunits required to form an icosahedral capsid is equal to the number of asymmetric units that comprise the icosahedron. The icosahedron is composed of 60 asymmetric units derived from dividing each of the 20 triangular faces into three equal units. One of the simplest and smallest icosahedral capsids seen in nature belongs to that of satellite tobacco mosaic virus. The capsid of this virus is composed of only 60 protein subunits, each subunit constitutes one asymmetric unit of the icosahedron (Larson *et al.*, 1993). However, complex viruses such as the herpesviruses, require larger icosahedral capsids to contain their genetic material. Increasing the size of the icosahedral capsid within the constraints of symmetry can only be achieved through increasing the number of protein subunits that form the asymmetric units of the icosahedron. Casper and Klug (1962) demonstrated that only certain multiples of the minimum 60 protein subunits are likely to

occur and these multiples are termed triangulation numbers. When the triangulation number is greater than one it is no longer possible to pack the protein subunits in a strictly equivalent way such as in satellite tobacco mosaic virus (which has a triangulation number of $T=1$) where all the subunits have an identical environment and packing interactions. However, Casper and Klug demonstrated that for certain multiples of T it is possible to pack the protein subunits in a 'quasi-equivalent' manner. This meant that in order to construct an icosahedral capsid with a triangulation number above $T=1$, the asymmetric units must be formed by packing together the various protein subunits using slightly different bonding patterns between them.

Herpesvirus capsids consist of a $T=16$ icosahedral lattice and thus, each of the 60 asymmetric units of the icosahedral capsid are composed of 16 quasi-equivalent protein subunits. The 960 protein subunits are arranged into 162 capsomers, of which 150 are hexons and 12 are pentons. The pentons are positioned at the vertices of the icosahedron and the hexons form the faces and edges of the icosahedron. A small decorating protein is located on the rim of the hexons and both the hexons and pentons have a central transcapsomeric channel approximately 3-5 nm in width. The capsomers are connected together by heterotrimeric protein complexes known as triplexes. Each icosahedral capsid contains 320 triplex complexes which are located at points of local threefold symmetry.

The nuclei of cells infected with herpesvirus contain three types of capsid structure known as A, B and C capsids that can be distinguished from one another in electron micrographs (Gibson & Roizman, 1972, Gibson & Roizman, 1974, Perdue *et al.*, 1975) (see Figure 3.44a). Further studies have identified a fourth type of capsid structure termed the procapsid (Trus *et al.*, 1996). The procapsid is not normally seen during wt HSV-1 infection but is observed following infection of cells with a virus lacking a functional maturational protease gene (Preston *et al.*, 1983, Newcomb *et al.*, 2000), and is also generated in *in vitro* capsid assembly systems (Newcomb *et al.*, 1994, Newcomb *et al.*, 1999). Procapsids are spherical structures which exhibit icosahedral symmetry and contain an uncleaved internal protein scaffold. Newly replicated concatameric HSV-1 DNA is cleaved and packaged into procapsids in the nucleus of virus-infected cells. The packaging of viral DNA into the procapsid results in concomitant angularisation of the capsid and loss of the protein scaffold leading to the formation of a DNA-containing (C) capsid which is an intermediate in the pathway to infectious virions. Abortive DNA packaging is thought to result in the formation of A capsids which are

angularised icosahedral structures that lack both an internal protein scaffold and a packaged viral genome. The other form of angularised capsids are B capsids, which contain a small, dense core formed by cleavage of the protein scaffold, and arise in the absence of DNA packaging. The latter capsid type is the predominant form of capsid present in the nuclei of HSV-1 infected cells.

1.1.4.3 Herpesvirus Tegument.

The tegument is a proteinaceous layer of variable thickness surrounding the capsid and is unique to herpesviruses. Approximately 20 proteins comprise the herpesvirus tegument and they are typically defined as being those structural proteins that are not components of purified capsids or of the envelope. Several of them have been shown to be involved in very early events during infection, such as the virion associated host shutoff protein (VHS) (Smibert *et al.*, 1992), and VP16 (Batterson & Roizman, 1983), and their presence in the virion ensures their availability at this time. However, the precise roles of many tegument proteins have not yet been determined and there are several areas of the herpesvirus lytic cycle in which they are likely to be involved. Among these are packaging and release of the viral genome (Batterson *et al.*, 1983, Salmon *et al.*, 1998), intracellular transport of the capsid (Bearer *et al.*, 2000) and formation of the virion envelope. An insight into the nature of the tegument came from the identification of a virus-related particle produced in infected cells, namely the L particle (Szilágyi & Cunningham, 1991, McLauchlan & Rixon, 1992). L particles are composed of tegument and envelope but lack capsids and cores and are consequently non-infectious. Their existence demonstrated that the tegument has an inherent structural integrity and that its assembly can take place independently of capsids. Further insight into the structure of the tegument has come from cryoelectron microscopy and image reconstruction of herpesvirus virions such as HSV-1 (Zhou *et al.*, 1999), HCMV (Chen *et al.*, 1999) and SCMV (Trus *et al.*, 1999). Generally, at least a portion of the tegument is icosahedrally ordered and the attachment areas of the tegument to the capsid vary in herpesviruses from a few sites only, such as the pentons and peripentonal triplexes (HSV-1), to that of a more extensive association involving the penton, hexon and triplex components of the capsid (HCMV and SCMV).

1.1.4.4 Herpesvirus Envelope.

The lipid membrane surrounding herpesviruses is termed the envelope and is derived from patches of altered host cell membranes (Morgan *et al.*, 1959). Envelopment occurs at the inner nuclear membrane, but there is some controversy regarding whether or not this process also takes place in the cytoplasm. Non-enveloped capsids are seen in the cytoplasm of HSV-1 infected cells and whereas some evidence suggests that these are non-infectious particles resulting from terminal de-envelopment (Campadelli-Fiume *et al.*, 1991), other evidence suggests that these de-enveloped capsids are re-enveloped in the cytoplasm to generate infectious virions (Rixon, 1993, Browne *et al.*, 1996).

No host proteins have been unambiguously detected in the envelope of purified herpesviruses but a number of virus-encoded glycoproteins have been identified. Viewed under the electron microscope these glycoproteins appear as spikes, approximately 8 nm in length protruding from the envelope (Wildy & Watson, 1963). The number of glycoproteins encoded by different herpesviruses varies but HSV-1 encodes at least eleven. HSV-1 glycoproteins such as gB (Sarmiento *et al.*, 1979), gC (Trybala *et al.*, 1993), gD (Ligas & Johnson, 1988) and gH (Forrester *et al.*, 1992) are believed to be involved in attachment and/or penetration of virus into the host cell. The glycoproteins also appear to have a role in modulation of the host immune response e.g. the HSV-1 gE/gI complex (Johnson *et al.*, 1988), and in cell-to-cell spread of virus e.g. HSV-1 gK (Hutchinson *et al.*, 1992).

1.2 The Molecular Biology of HSV-1.

1.1.1 The HSV-1 Genome.

1.2.1.1 Structure of the HSV-1 Genome.

The HSV-1 genome is approximately 152 kbp in size with a G+C content of 68%. The genome is classified as a group 6 structure as described in section 1.1.4.1 and consists of two covalently linked regions designated L (long) and S (short). L and S components each contain unique sequences U_L (108 kbp) and U_S (13 kbp) respectively, and both these regions are bracketed by inverted repeat sequences. U_L is flanked by a (250-500 bp) and b (8.8 kbp) sequences and U_S is surrounded by a and c (6.6 kbp) sequences. The terminal L repeat (TR_L) is composed of a variable number of a sequences and one b sequence while the terminal S repeat (TR_S) is composed of one a sequence and one c sequence. The internal repeats are inverted with respect to the terminal repeats and the number of a sequences found at the L-S junction and the L terminus is variable. The HSV-1 genome structure can thus be represented as $a_m b - U_L - b' a' n c' - U_S - c a$ where the numbers designated by m and n are variable (Wadsworth *et al.*, 1975). Figure 1.3 shows a diagrammatic representation of the HSV-1 genome structure (McGeoch *et al.*, 1988). The L and S components of HSV can invert relative to one another, yielding four linear isomers which are present in an equimolar amount in DNA isolated from virions. The four isomers have been designated as P (prototype), I_L (inversion of the L component), I_S (inversion of the S component) and I_{SL} (inversion of both S and L components) (Hayward *et al.*, 1975).

1.2.1.2 The a Sequence.

The a sequence of HSV-1 strain 17 is 380 bp in size and is composed of both quasi unique sequences and repeat elements. The ends of the a sequence are flanked by a repeat element known as the DR1 repeat which is 20 bp in length. Single a sequences are bounded by separate DR1 repeats but two tandemly repeated a sequences share the intervening DR1 repeat. The DR1 repeat contains the site for cleavage of the concatemeric viral DNA during the DNA packaging process although the actual sequence of the DR1 repeat has been shown to be unimportant (Varmuza & Smiley, 1985) (section 1.2.6).

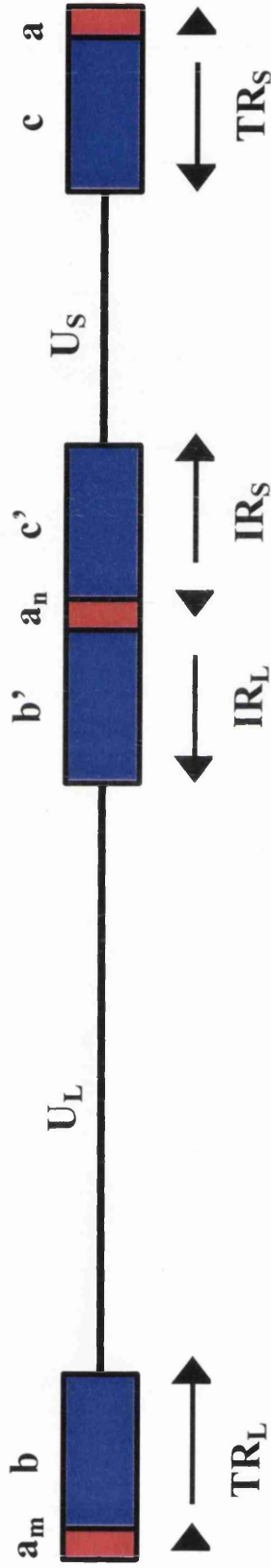


Figure 1.3 Structure of the HSV-1 Genome.

The above figure is a diagrammatic representation of the HSV-1 genome (not to scale). The genome is composed of two freely invertible unique sequences, U_L and U_S , which are flanked by inverted repeat sequences. The 108 kbp U_L region is flanked by a 8.8 kbp repeat known as the b sequence while the 13 kbp U_S region is flanked by a 6.6 kbp repeat known as the c sequence. Multiple copies of the 250-500 bp a sequence are found at the L terminus as well as the L-S junction and a single copy is found at the S terminus. The genome can be represented as $a_m b-U_L-b' a'_n c'-U_S-ca$, where the numbers designated by m and n are variable.

The *a* sequence contains two quasi unique regions, u_b and u_c , separated by a number of repeat elements known as DR2 repeats. The variability in size of *a* sequences from different strains of HSV-1 is due to diversity in the number and length of these internal repeats. Approximately 19 copies of the 12 bp DR2 repeat separates the 80 bp u_b element from the 72 bp u_c element. The DR2 repeats are neither required for DNA encapsidation nor genome isomerisation (Varmuza & Smiley, 1985), and their exact role remains to be elucidated.

Two specific regions of the u_b and u_c elements are necessary for HSV-1 DNA cleavage and packaging. These sequences are termed the *pac1* and *pac2* homologies and correspond to regions of conserved sequence found at the termini of many herpesvirus genomes (Deiss *et al.*, 1986). Using DNA sequence comparisons Deiss *et al.* (1986) identified four distinct regions within the *pac1* and *pac2* homology elements (below and Figure 1.4):

Pac1, in 5' to 3' order,

1. A G+C rich region.
2. A region of uninterrupted runs of C and G residues.
3. A T rich element.
4. A G rich region.

Pac2, in 5' to 3' order,

1. A short DNA consensus sequence of CGCCGCG.
2. An unconserved region of variable length.
3. A T rich element.
4. A G+C rich region.

Using a larger number of herpesvirus sequences, subsequent investigators have preferred to define the *pac2* homology element as two GC rich regions separated by a T rich element (Broll *et al.*, 1999). The regions within the *pac1* and *pac2* homologies have not been investigated further and the functional significance of these elements is not known.

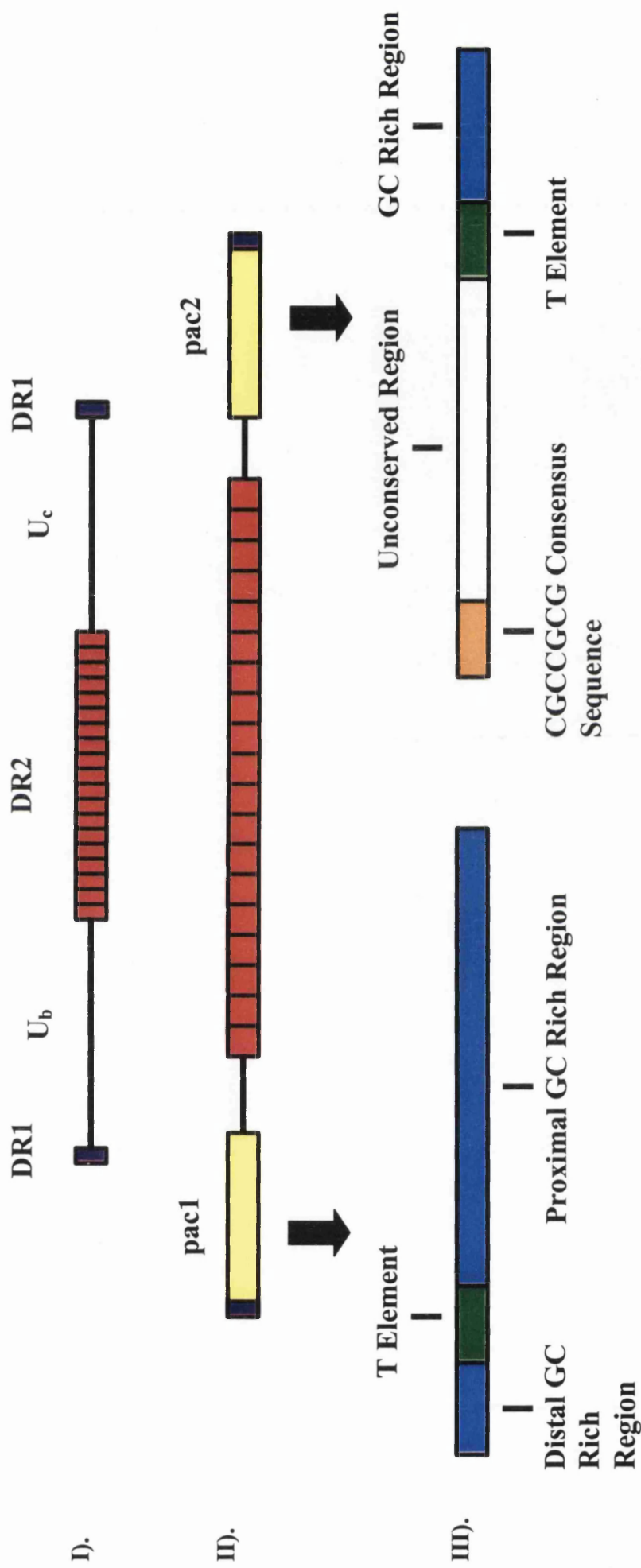


Figure 1.4 Structure of the HSV-1 α Sequence.

The above figure is a diagrammatic representation of the HSV-1 α sequence and shows, I). The a sequence is composed of two quasi unique regions, u_b and u_c , interrupted by an array of DR2 repeats. II). The location of the pac1 and pac2 homology elements. III). An expansion of the two homology elements illustrating the regions identified by Deiss *et al.* (1986).

1.2.1.3 Functions of the *a* Sequence.

a). Genome Isomerisation and Recombination.

Genome isomerisation is tightly linked to viral DNA replication and is believed to occur via sequence-independent homologous recombination mediated by dsDNA breaks generated by cleavage of the viral DNA (Sarisky & Weber, 1994). Initially, it was thought that the viral DNA was cleaved at the *a* sequence to generate the dsDNA breaks necessary for recombination, possibly by a host cell endonuclease (Wohlrab *et al.*, 1991). However, in 1996 it was shown that the *a* sequence was dispensable for isomerisation of the HSV-1 genome using a recombinant virus which was engineered without *a* sequences at the L-S junction or at the L and S termini (Martin & Weber, 1996). In infected cells, this virus, which contained a single *a* sequence within the thymidine kinase gene, was able to invert its L and S segments at wt levels and all four isomers were readily detected at a stage of infection co-incident with the onset of DNA replication. This work suggested that genome isomerisation is mediated by an *a* sequence-independent homologous recombination mechanism which is enhanced by the process of viral DNA replication.

b). Genome Circularisation.

The exact mechanism by which the HSV-1 genome circularises prior to DNA replication remains unknown but it almost certainly involves the terminal repeats and more specifically, the *a* sequence. The L and S termini of the HSV-1 genome end with an 18.5 bp and a 1.5 bp DR1 repeat respectively (Davison & Wilkie, 1981, Mocarski & Roizman, 1982). The 0.5 bp represents a single nucleotide 3' overhang present at each termini and suggests a potential genome circularisation mechanism whereby the two ends are directly ligated via their single base overhang to generate a complete 20 bp DR1 repeat. Although this remains a hypothesis for HSV-1, the genome circularisation mechanism of GPCMV is proposed to occur through the direct ligation of the genome termini and appears to involve the pac2 homology element (McVoy *et al.*, 1997). The direct ligation of the genome termini could also function as a genome circularisation mechanism for those herpesviruses that lack a terminally redundant element. Another possible mechanism for genome circularisation of HSV-1 involves homologous recombination and the *a* sequence of this virus is able to direct circularisation

both by imprecise end joining and non-conservative homologous recombination (Yao *et al.*, 1997). Since the structure of the genomic termini varies amongst the herpesviruses, it is possible that individual herpesviruses utilise different mechanisms for genome circularisation. In the case of HSV-1, there is evidence that this process may also involve cellular proteins. HSV-1 DNA remains linear in infected BHK cells that lack the *RCC1* gene (regulator of chromosome condensation) implicating a possible involvement of this host cell gene product in the circularisation mechanism of the HSV-1 genome (Umene & Nishimoto, 1996).

c). Cleavage and Packaging of Viral DNA.

The role of the *a* sequence in the viral DNA cleavage and packaging process was first identified by Stow *et al.* (1983) who demonstrated that a plasmid containing the HSV-1 origin of replication and sequences from the termini of the virus genome could be packaged into viral particles. Subsequent investigations have determined that the entire viral DNA cleavage and packaging signal lies within a 179 bp sequence containing the *pac1* and *pac2* homology elements from the junction between two tandemly repeated *a* sequences (Nasseri & Mocarski, 1988). The role of the *a* sequence in the viral DNA cleavage and packaging process is discussed in detail in section 1.2.6.

1.2.1.4 HSV-1 Genes.

HSV-1 encodes a total of 74 genes of which 58 are located in the U_L region, 13 are found in U_S , 2 are found in R_L and a single ORF is found in R_S (McGeoch *et al.*, 1985 and 1988, Dolan *et al.*, 1998). HSV-1 genes are divided into three classes according to the timing of their expression during the HSV-1 replication cycle. These classes are designated immediate early or IE (α), early (β) and late (γ) genes and are sequentially expressed in a cascade fashion during HSV-1 infection (Honess & Roizman, 1974, Honess & Roizman, 1975).

a). The IE Genes.

The IE genes are the first to be expressed during the HSV-1 replication cycle and the synthesis of IE polypeptides reaches peak rates at approximately 2 to 4 hours pi. The IE genes are expressed in the absence of prior viral protein synthesis and are characterised by the presence of a TAATGARAT DNA sequence (where r is a purine) within their promoters

(Gaffney *et al.*, 1985). This sequence is a binding site for the cellular factor Oct-1 (octamer DNA-binding protein) which is necessary for IE-gene transcription. Four of the five IE genes are involved in regulation of gene expression (ICP4/Vmw175, ICP0/Vmw110, ICP22/Vmw68 and ICP27/Vmw63). The fifth, (ICP47/Vmw12), functions in the inhibition of antigen presentation by HSV-1-infected cells.

b). The Early Genes.

The early genes are expressed in very low levels in the absence of competent IE proteins. In the presence of IE proteins the early genes reach peak rates of synthesis at about 5 to 7 hours pi. The early gene class is further subdivided into the β_1 and β_2 genes. The β_1 proteins appear very early after infection but are distinguished from IE proteins by their lack of the TAATGARAT DNA sequence within their promoters and their dependence on IE proteins for their synthesis. Most viral proteins involved in nucleic acid metabolism appear to be in the early class of genes, such as the β_1 UL29 gene which encodes the major DNA binding protein (Conley *et al.*, 1981) and the β_2 UL30 gene which encodes the viral DNA polymerase (Chartrand *et al.*, 1980).

c). The Late Genes.

This class of gene generally reach peak rates of expression after the onset of viral DNA synthesis and is further subdivided into the leaky-late (γ_1) and the true-late (γ_2) genes according to their dependence on viral DNA synthesis. The UL27 gene, encoding glycoprotein gB, is a characteristic leaky-late gene which is expressed relatively early in infection and is only minimally affected by inhibitors of DNA synthesis. In contrast, typical true-late genes such as UL44, which encodes glycoprotein gC, are expressed late in infection and at very low levels when viral DNA synthesis is inhibited. Most virion proteins appear to be in the late class of genes. Late gene expression peaks at 8-10 hours pi and persists for the remainder of the lytic cycle (Harris-Hamilton & Bachenheimer, 1985).

1.2.1.5 The Structure of Encapsidated HSV-1 DNA.

Encapsidated HSV-1 DNA exists in a semi liquid-crystalline state closely resembling that of the icosahedral dsDNA bacteriophages. The packaged DNA forms a uniformly dense ball, extending radially as far as the inner surface of the icosahedral capsid shell (Booy *et al.*, 1991, Cerritelli *et al.*, 1997). Electron cryomicroscopy and image reconstruction of HSV-1 virions, computed to a resolution of 20 Å, have allowed the visualisation of encapsidated HSV-1 DNA (Zhou *et al.*, 1999). Inside the HSV-1 virion the DNA appears as concentric spherical shells spaced 26 Å apart and this pattern is similar to the structure of packaged phage DNA.

Early studies using electron microscopy and low-angle X-ray scattering indicated that in icosahedral dsDNA bacteriophages such as T7, the DNA is wound into a spool-like structure surrounding a central protein plug (Earnshaw & Harrison, 1977, Cerritelli *et al.*, 1997). According to the spool model, DNA passes into the capsid through a unique entry port and then wraps around the inner surface of the capsid shell. It accumulates one layer at a time, with the layers becoming less well ordered as their distance from the shell increases (Harrison, 1983). Although HSV-1 does not appear to possess a central protein plug, or spindle, inside the capsid around which the genome is arranged, the close parallels between the structure of the encapsidated HSV-1 genome and that of the icosahedral dsDNA bacteriophages strongly suggests that the spool model may also describe the organisation of the HSV-1 genome.

1.2.2 The Structure of the HSV-1 Capsid.

The experimental work described in this study concerns the characterisation of the HSV-1 UL25 DNA packaging protein, which is also a minor component of the capsid. The following section therefore reviews in greater depth, the molecular structure of the HSV-1 capsid and is an expansion of section 1.1.4.2.

1.2.2.1 Protein Composition of the HSV-1 Capsid.

The HSV-1 capsid shell has a diameter of 1250 Å and is 160 Å thick. The capsid shell of A, B and C capsids is composed of four predominant protein components, a major capsid protein (VP5); and three less abundant proteins, VP19C, VP23 and VP26 (Gibson & Roizman, 1972, Newcomb *et al.*, 1993, Rixon, 1993). The interior of B capsids contain large amounts of the VP22a major scaffolding protein and smaller amounts of the VP24 protease and VP21

minor scaffolding protein (Gibson & Roizman, 1974, Cohen *et al.*, 1980, Newcomb *et al.*, 1993) (Table 1.2). The HSV-1 B capsid also contains several minor proteins, including the products of the UL6, UL12.5, UL15, UL17, UL25, UL28 genes (Table 1.4). These minor capsid proteins are not required for the assembly of icosahedral capsids and the majority are involved in the DNA cleavage and packaging process. These proteins are described in section 1.2.6.

1.2.2.2 The Pentons and Hexons.

The VP5 protein is essential for the capsid assembly process and no capsid structures are assembled in its absence (Desai *et al.*, 1993). VP5 is the major structural subunit of the 162 capsomers, of which 150 are hexons and 12 are pentons (Newcomb *et al.*, 1993). Electron microscopic analysis of HSV-1 capsids revealed that both the pentons and the hexons appeared as cylindrical protrusions from the capsid shell (Newcomb *et al.*, 1993, Zhou *et al.*, 1994) (Figure 1.5). However, biochemical analysis and image reconstruction of capsids to a resolution of 26 Å have shown that structurally, they differ in several respects (Newcomb & Brown, 1991, Trus *et al.*, 1992, Newcomb *et al.*, 1993, Zhou *et al.*, 1994, Wingfield *et al.*, 1997). Pentons each contain five copies of VP5 and exhibit fivefold rotational symmetry while hexons have six copies of VP5 and exhibit sixfold rotational symmetry. All capsomers have an axial channel that traverses their entire length. The axial channel of hexons is approximately 20-30 nm in diameter and is smaller than the axial channel of the pentons. Additionally, the status of the penton axial channel varies according to the type of capsid particle. In A capsids, the axial channel of the pentons is approximately 50 Å in diameter (Zhou *et al.*, 1998), whereas in DNA containing capsids the penton channel appears to be either closed or blocked (Zhou *et al.*, 1999). Newcomb and Brown (1994) demonstrated that viral DNA was extruded from the pentons, but not the hexons, of HSV-1 C capsids treated with 0.5 M GuHCl. These findings led the workers to suggest that during the DNA packaging process the viral DNA genome enters the capsid through the penton channel. The closure of the penton channel, as seen in DNA containing capsids, would then function to retain the packaged genome within the capsid.

Whereas the 12 pentons of the icosahedral capsid appear to be identical, the 150 hexons are composed of three distinct quasi-equivalent populations (Figure 1.6): P (peripentonal),

Gene	Protein	Molecular Weight	* Predicted Copy Number	Structural Function and Location in Capsid
UL19	VP5	149,075	960	Forms hexons and pentons of outer capsid shell.
UL38	VP19C	50,260	375 ± 22	Component of the triplex heterotrimer of outer capsid shell.
UL18	VP23	34,268	572 ± 67	Component of the triplex heterotrimer of outer capsid shell.
UL35	VP26	12,095	952 ± 315	Located on the outer surface of hexons.
UL26	VP21	39,875	87 ± 42	Minor component of the scaffold structure, present inside the capsid shell .
UL26	VP24	26,618	147 ± 67	Protease, present inside the capsid shell.
UL26.5	VP22a	33,765	1153 ± 69	Major component of the scaffold structure, present inside the capsid shell.

* predicted protein copy numbers from cryoelectron microscopic studies on HSV-1 B capsids (Newcomb et al., 1993).

Table 1.2 The Major Protein Components of HSV-1 B Capsids.

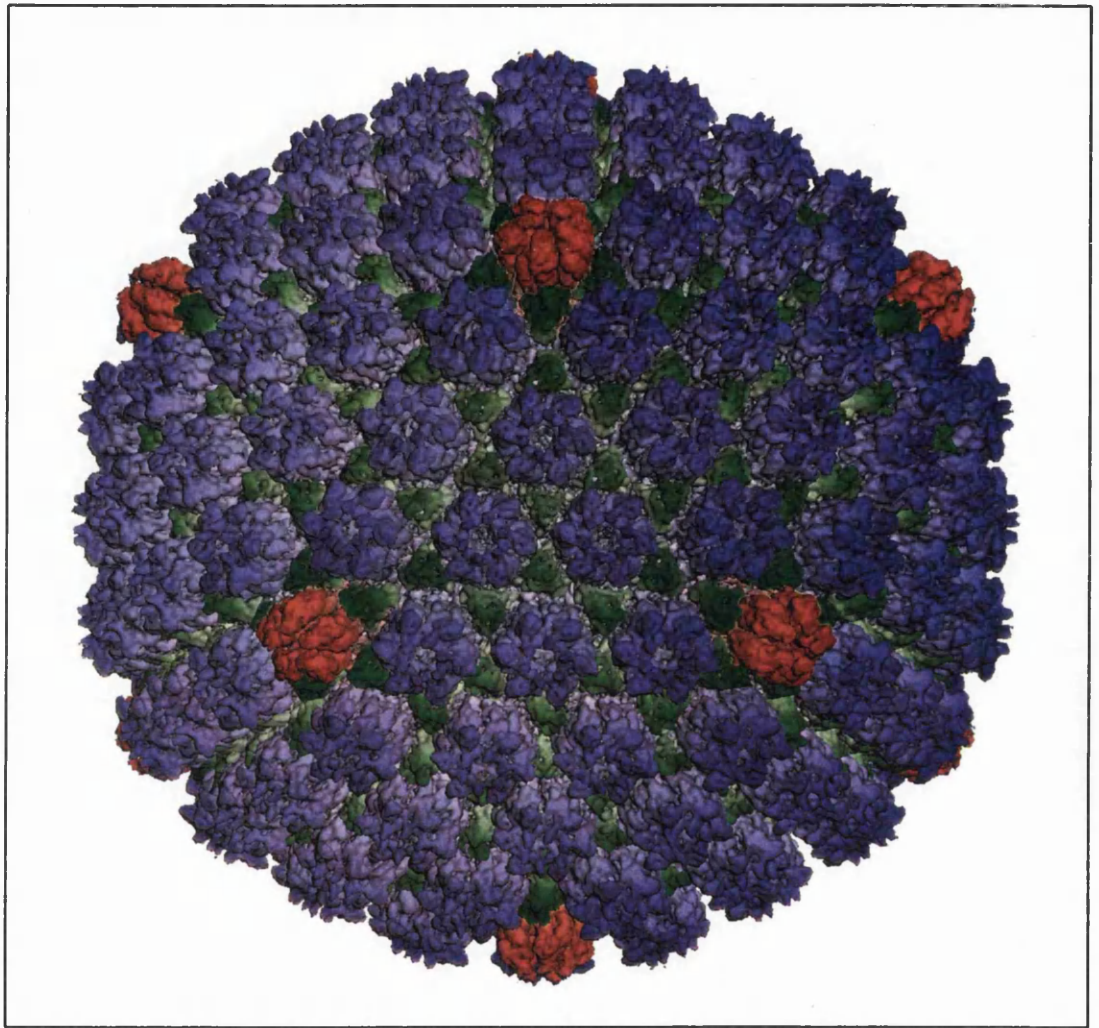


Figure 1.5 The HSV-1 B Capsid.

The above figure is a computer generated reconstruction of a HSV-1 B capsid at a resolution of 8.5 Å viewed through a threefold axis of symmetry. The capsid is composed of 162 capsomers. Pentons, of which there are 12 (coloured red), are located at the icosahedral vertices while the 150 hexons (coloured blue) are found at the faces and edges of the capsid. The 320 triplexes (coloured green) connect the capsomers and are located at points of local threefold symmetry. Image kindly supplied by F. Rixon taken from Zhou *et al.* (1998).

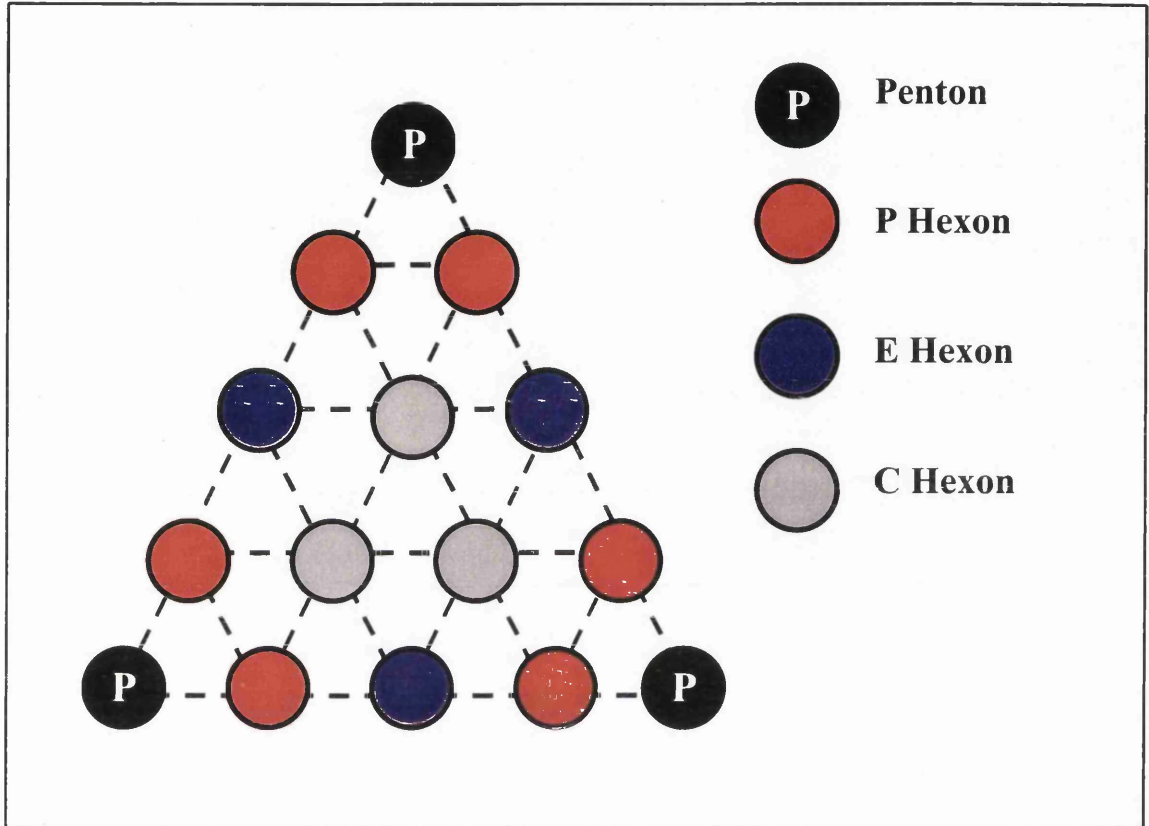


Figure 1.6 The Arrangement of Hexons in the HSV-1 Capsid.

The above figure is a schematic diagram of a single face from the icosahedral HSV-1 capsid viewed along the threefold axis of symmetry. The three quasi-equivalent hexon populations, which differ in terms of their local bonding environments, are indicated, together with the relative locations of the pentons.

those immediately adjacent to the pentons (surrounding the icosahedral fivefold axis of symmetry); E (edge), those located on an edge of a triangular face (on the icosahedral twofold axis of symmetry); and C (central), those lying in the centre of a triangular face (surrounding the icosahedral threefold axis of symmetry) (Steven *et al.*, 1986, Schrag *et al.*, 1989). The quasi-equivalent hexons differ in terms of their local bonding environments through their respective configurations of adjacent capsomers and their relative proximities to the vertices and edges of the icosahedral capsid. The quasi-equivalent hexons also differ in the nature of their interactions with the quasi-equivalent triplex complexes as discussed in section 1.2.2.4. At a resolution of 26 Å, subtle structural differences concerning the size and shape of the quasi-equivalent hexons are also evident (Zhou *et al.*, 1998). The arrangement of the quasi-equivalent hexons and pentons in one of the sixty asymmetric units of the icosahedral capsid is illustrated in Figure 1.7.

1.2.2.3 The VP26 Protein.

The VP26 protein is associated with the hexameric but not the pentameric capsomers of the HSV-1 capsid (Wingfield *et al.*, 1997). Six VP26 subunits are distributed symmetrically around the outer tip of each hexon protrusion and the VP26 protein is readily dissociated from and reattached to the capsid (Booy *et al.*, 1994). Therefore, the protein does not appear to contribute significantly to the structural stability of the capsid and recombinant capsids can be assembled in its absence (Tatman *et al.*, 1994, Thomsen *et al.*, 1994, Trus *et al.*, 1995). The exact function of VP26 is unknown and the protein is not required for the growth of virus in cell culture although it does appear to be important for virion production in the nervous system of HSV-1 infected mice (Desai *et al.*, 1998).

1.2.2.4 The Triplexes.

The triplexes mediate intercapsomeric interactions at sites of local threefold symmetry within the capsid (Figure 1.5). The triplex is a heterotrimeric protein complex composed of two copies of the VP23 protein and one copy of the VP19C protein (Newcomb *et al.*, 1993), and both proteins are essential for the assembly of capsids in HSV-1 infected cells (Desai *et al.*, 1993, Person & Desai, 1998). Although the primary function of the triplexes is the formation of intercapsomeric interactions, it has been reported that the VP19C protein binds

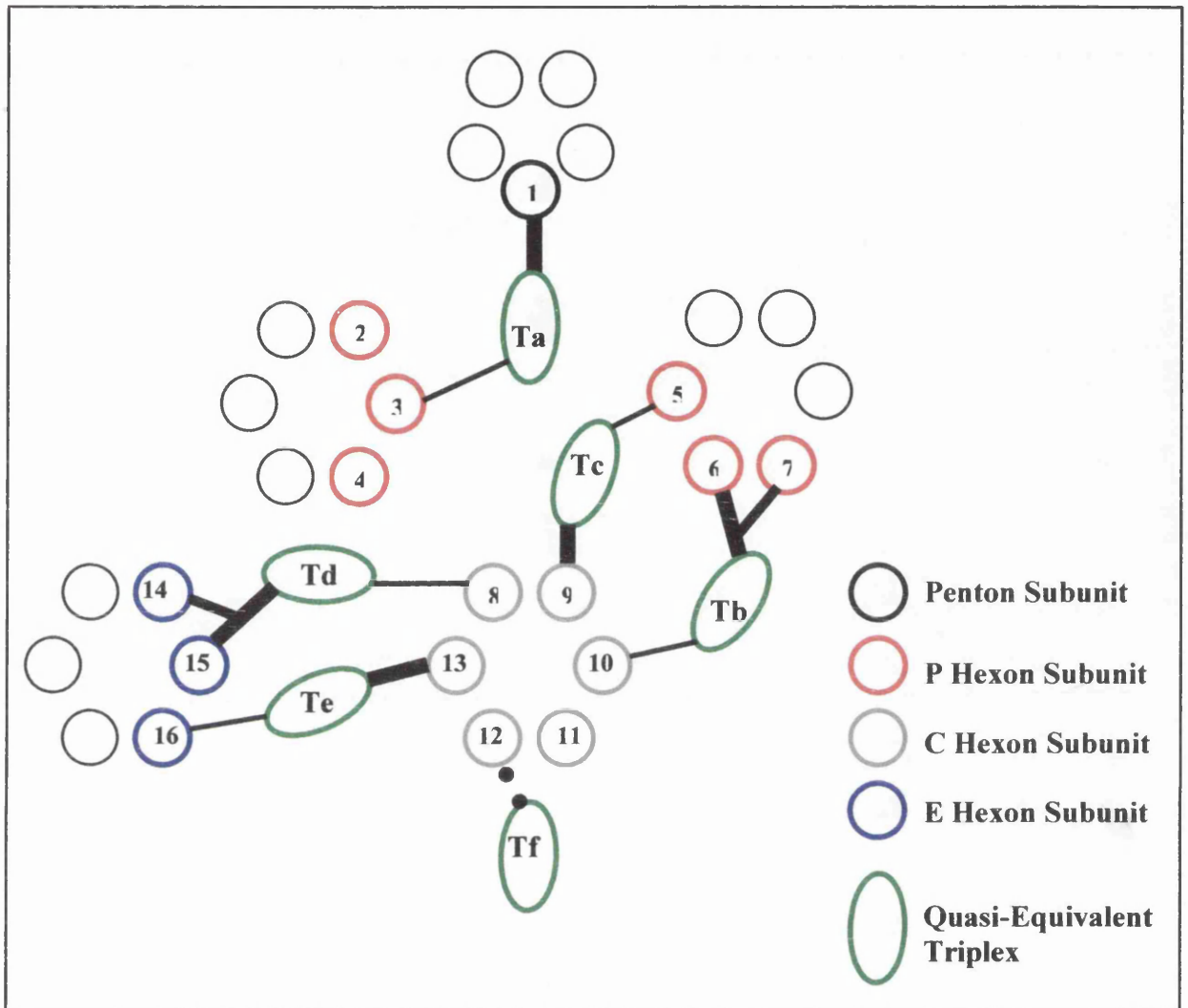


Figure 1.7 The Asymmetric Unit of the HSV-1 Capsid.

The above figure is a diagrammatic representation of one asymmetric unit of the HSV-1 capsid viewed along the threefold axis of symmetry. Each of the 60 asymmetric units of the HSV-1 capsid is composed of one P, one C, and 1/2 E hexons, 1/5 penton, one each of Ta – Te triplexes, and 1/3 Tf triplex. Due to the T=16 icosahedral symmetry of the capsid there are 16 quasi-equivalent positions in each asymmetric unit for the VP5 protein subunits of the pentons and hexons (labelled 1 – 16). The more extensive molecular interactions between the quasi-equivalent triplexes and neighbouring capsomeric subunits are shown with thick lines, the less extensive ones with thin lines and the dotted line represents a low degree of interaction.

DNA (Braun *et al.*, 1984). This suggests that VP19C may also function in anchoring the DNA to the capsid, however, since this finding is unrepeatable, the exact significance of the proposed DNA binding properties of the VP19C protein are unknown.

The VP19C and VP23 proteins directly interact with one other to form triplex complexes in the absence of other proteins (Desai & Person, 1996). *In vitro* assembled triplexes are functional in terms of capsid assembly (Spencer *et al.*, 1998) and therefore, all the information required to form a functional triplex is encoded by the VP19C and VP23 proteins. There are six types of quasi-equivalent triplexes based on their locations within the icosahedral lattice (Zhou *et al.*, 1994). They are labelled Ta – Tf and their arrangement in one of the sixty asymmetric units of the icosahedral capsid is illustrated in Figure 1.7. The quasi-equivalent triplexes vary considerably in the nature of their interactions with neighbouring capsomers and it is believed that the VP23 protein, which exists as a molten globule in solution (Kirkittadze *et al.*, 1998), is involved in imparting this flexibility on the protein complex.

The VP19C protein also interacts with the VP5 protein (Rixon *et al.*, 1996). The significance of this interaction was revealed through the characterisation of recombinant capsid-like particles formed in the presence of only these two proteins (Saad *et al.*, 1999). This study demonstrated that the VP5-VP19C interaction alone was the key to forming an icosahedral particle. However, the VP5-VP19C particles are structurally very different to wt HSV-1 capsids; they are smaller, spherical in size and exhibit T=7 icosahedral symmetry (see Figure 3.34, section 3.4). This study suggested that, together with the scaffolding proteins, the VP23 protein was responsible for modulating the VP5-VP19C interaction to form a T=16 icosahedral lattice. Additionally, this study indicated a potential interaction between the VP5 and VP23 proteins and although no such interaction has been detected in either fluorescence (Nicholson *et al.*, 1994), or yeast two-hybrid (Desai & Person, 1996) assays, Rixon *et al.* (1996) suggested that this interaction might form in the context of the capsid.

1.2.2.5 The Protein Scaffold.

In addition to the shell proteins discussed above, HSV-1 B capsids contain a large amount of the VP22a major scaffolding protein encoded by the UL26.5 gene, and smaller amounts of the VP24 serine protease and VP21 minor scaffolding protein, both encoded by the UL26 gene

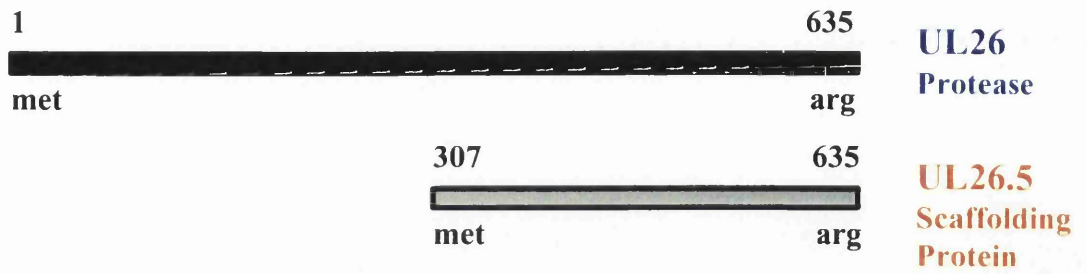
(Gibson & Roizman, 1972, Preston *et al.*, 1983, Rixon *et al.*, 1988, Davison *et al.*, 1992, Person *et al.*, 1993).

The UL26.5 gene overlaps and is in frame with the C-terminal half of the UL26 gene so the 329 amino acid scaffolding protein is identical in sequence to the C-terminal 329 amino acids encoded by the UL26 gene (Figure 1.8 i) (Liu & Roizman, 1991a, Liu & Roizman, 1993). The full-length protease cleaves itself at two places, the R site, which separates the VP24 protease from the VP21 protein, and the M site, which removes the C-terminal 25 amino acids from the VP21 protein as shown in Figure 1.8ii and iii (Dilanni *et al.*, 1993, Liu & Roizman, 1993, Weinheimer *et al.*, 1993).

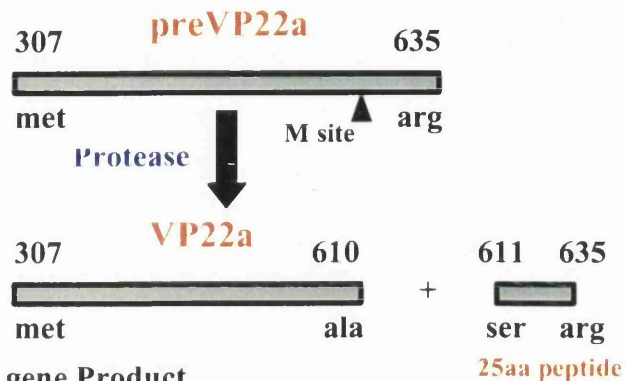
A direct interaction between the preVP22a protein and the VP5 protein is essential for the assembly of 125 nm T=16 icosahedral capsids in virus-infected cells and the site recognised by VP5 has been localised to a hydrophobic domain within the C-terminal region of the preVP22a protein (Thomsen *et al.*, 1994, Newcomb *et al.*, 1994, Nicholson *et al.*, 1994, Tatman *et al.*, 1994, Thomsen *et al.*, 1995, Hong *et al.*, 1996, Desai & Person, 1996, Oien *et al.*, 1997). Since the preVP22a protein is identical in sequence to the C-terminal 329 amino acids of preVP21, the M site is also found in preVP22a where it is cleaved by the VP24 protease releasing the mature VP22a protein and the C-terminal 25 amino acid peptide as shown in Figure 1.8ii and iii (Preston *et al.*, 1992). Cleavage of the preVP22a protein at the M site disrupts the interaction between preVP22a and VP5 as it is the C-terminal region of the preVP22a protein that binds to the VP5 protein. This causes a structural alteration to the scaffold leading to a more condensed form. The initiation of the DNA packaging process results in the selective loss of the VP22a and VP21 scaffolding proteins from the capsid and the subsequent removal of the scaffold structure.

The UL26 gene products are essential for productive infection. The HSV-1 *ts1201* mutant has a *ts* lesion which maps to the UL26 gene and results in the production of an inactive protease in cells infected at the NPT (Preston *et al.*, 1983). Large cored B capsids (procapsids) containing the uncleaved form of the scaffolding protein (preVP22a) accumulate in the nuclei of cells infected with *ts1201* at the NPT and viral DNA is not encapsidated. However, when virus-infected cells are shifted to the PT, preVP22a is cleaved and capsids containing DNA are observed. Mutations within the UL26.5 gene are not lethal (Matusick-Kumar *et al.*, 1994) but result in a marked reduction in the efficiency of capsid production compared to that of wt virus

i). The UL26 and UL26.5 Gene Products.



ii). Proteolysis of the UL26.5 Gene Product.



iii). Proteolysis of the UL26 gene Product.

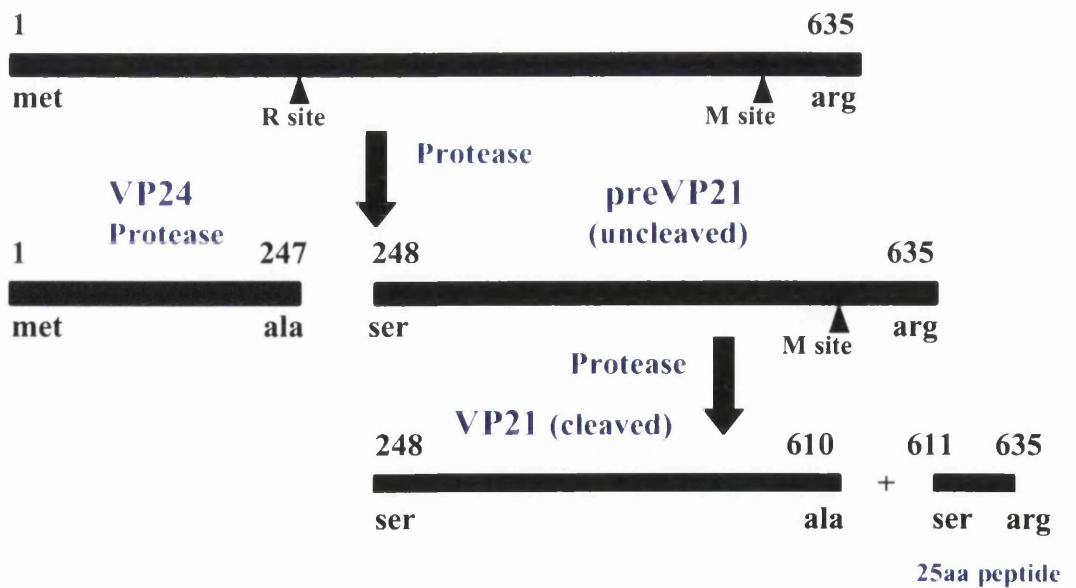


Figure 1.8 The Relationship between the HSV-1 UL26 and UL26.5 Gene Products.

The scaffolding protein (preVP22a) has the same sequence as the C-terminal 329 aa of the protease (i). The protease cleaves preVP22a to create VP22a and a 25aa peptide (ii). It also cleaves itself in two places (iii), to generate VP24, the cleaved form of preVP21 and the same 25aa peptide generated in step ii). This C-terminal 25 aa peptide contains the VP5 binding site.

and it is thought that the VP21 minor scaffolding protein can partially substitute for the VP22a major scaffold protein (Gao *et al.*, 1994, Tatman *et al.*, 1994, Robertson *et al.*, 1997, Sheaffer *et al.*, 2000).

1.2.2.6 The Capsid Floor.

At a computed resolution of 26 Å, the floor of the capsid is seen as a continuous mass density punctuated by the transcapsomeric channels (Zhou *et al.*, 1994). The prominent portion of this continuous density is formed by the close association of the lower domains of the penton and hexon subunits. The VP23 triplex protein also contributes to this continuous density and appears to have a role in connecting the body of the triplex to the capsid floor (Saad *et al.*, 1999). The close interaction between the lower domains of these various subunits is important in maintaining the stability of the capsid. In addition, the inner surface of the capsid floor contains the regions of contact with the scaffolding protein in the B-capsid (Zhou *et al.*, 1998), and would also be expected to contain the regions of contact with the packaged viral genome in the C capsid.

1.2.2.7 HSV-1 Capsid-Tegument Attachment Sites.

The locations of interaction between the capsid and the tegument are confined to the icosahedral vertices and involve contacts between the tegument and the penton and some P hexon subunits and their adjacent triplexes (particularly the Ta and Tc triplexes) (Zhou *et al.*, 1999). The binding of tegument proteins to these positions does not influence the assembly of capsids, or more specifically, the formation of the pentons, since stable capsids are formed in their absence (Tatman *et al.*, 1994, Thomsen *et al.*, 1994). Thus, the locations of these tegument proteins are presumably related to other properties of the capsid such as the release of viral DNA from the capsid. Consistent with this hypothesis, Zhou *et al.* (1999) have suggested that the VP1-3 tegument protein, encoded by the UL36 gene (McGeoch *et al.*, 1988), represents a good candidate for the penton bound tegument material since the estimated copy number of VP1-3 can be accounted for by the mass observed by electron cryomicroscopy at these sites. This protein forms a tight association with the capsid (Gibson & Roizman, 1972), and is essential for the envelopment of capsids within the cytoplasm of HSV-1-infected cells (Desai, 2000). Additionally, the HSV-1 mutant *tsB7* contains a *ts* lesion in the UL36

gene and at the NPT the virus is defective for the release of DNA from infecting capsids (Knipe *et al.*, 1981, Batterson *et al.*, 1983). Since the penton has been suggested to be the route by which the virus DNA leaves the capsid (Newcomb & Brown, 1994), an interaction between the VP1-3 protein and the pentons would place it in an appropriate position to influence the passage of the viral genome.

1.2.3 The HSV-1 Procapsid.

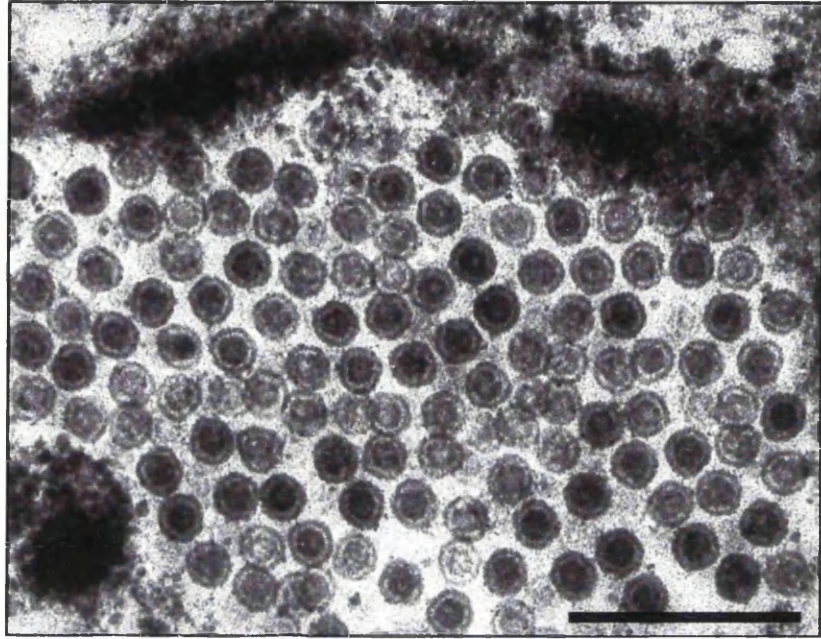
Procapsids are not observed in wt HSV-1 infected cells. They are seen in cells infected with HSV-1 mutants lacking a functional VP24 protease gene (Preston *et al.*, 1983, Gao *et al.*, 1994, Rixon & McNab, 1999, Newcomb *et al.*, 2000) (Figure 1.9), and are also observed as capsid assembly intermediates in HSV-1 cell-free assembly systems (Newcomb *et al.*, 1996, Newcomb *et al.*, 1999). Procapsids are closed structures composed of 162 capsomers lying on a T=16 lattice as in the mature capsid form. Unlike mature capsids, however, procapsids are spherical rather than icosahedral in overall morphology and contain a large, uncleaved, scaffolding core. The procapsid is cryosensitive, indicating that it is structurally less stable than the mature icosahedral capsid, and purified procapsids are able to undergo a structural transformation upon extended incubation *in vitro* to form polyhedral capsids (Newcomb *et al.*, 1996). Although this finding indicated that no additional protein subunits were required for the structural transformation to take place *in vitro*, procapsids formed in cells infected with *ts1201* at the NPT undergo a prompt structural transformation when the temperature is shifted down to the PT (Preston *et al.*, 1983). This suggests that other proteins may be involved in the structural transformation of the procapsid *in vivo*. In wt HSV-1 infected cells, procapsids are believed to have an extremely short half life, rapidly undergoing a structural transformation concomitant with DNA packaging to form an icosahedral DNA-containing (C) capsid. In this respect the procapsid is thought of as an intermediate product in the capsid assembly/DNA packaging process.

The structure of the procapsid has been determined to a resolution of 27 Å by cryoelectron microscopy and three-dimensional image reconstruction (Newcomb *et al.*, 1996, Trus *et al.*, 1996). Compared to the icosahedral B capsid, the procapsid is a more open, porous structure. The transcapsomeric channels are enlarged compared with those of the B capsid and there are small holes between the capsomers that are not found in B capsids. The triplexes appear to

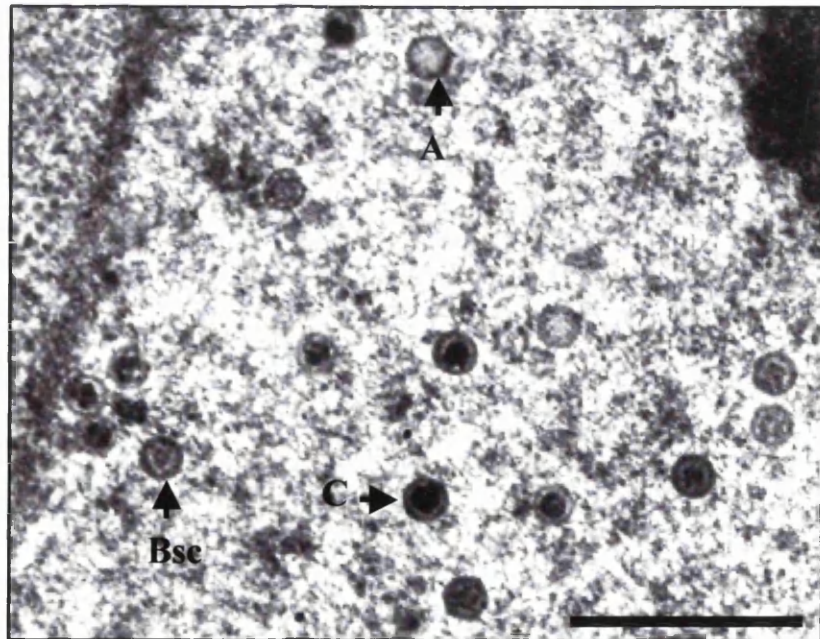
Figure 1.9 Comparison of Procapsids Formed by *Ts1201* at the NPT with Angularised Capsids of wt HSV-1.

(a.) BHK cells were infected with *ts1201* at a moi of 5 pfu.cell⁻¹ for 10 hours at 39°C. The cells were harvested and prepared for analysis by electron microscopy as described in section 2.3.4. The electron micrograph shows the accumulation of large-cored spherical capsids (procapsids) in the nucleus of a cell infected with *ts1201* at the NPT. For comparison, angularised small-cored B capsids (Bsc) formed in wt HSV-1-infected cells are shown in (b.) (A and C capsids are also labelled). Images kindly supplied by F. Rixon, taken from Rixon and McNab (1999). Scale bars represent 500 nm.

a).



b).



constitute the primary links by which the capsomers are held together since the floor layer found in B capsids is largely absent in the procapsid. The hexons of the procapsid also have an altered morphology and are elongated or triangular as opposed to the hexagonal-shaped structures characteristic of the B capsid. The structural transformation of the procapsid to the polyhedral capsid involves extensive morphological changes (Trus *et al.*, 1996). Although cleavage of the scaffolding protein by the maturational protease is known to be involved, the exact step at which cleavage takes place is not known and the overall process is similar to the prohead expansion step involved in dsDNA phage head morphogenesis (Steven *et al.*, 1992).

1.2.4 The HSV-1 Lytic Cycle.

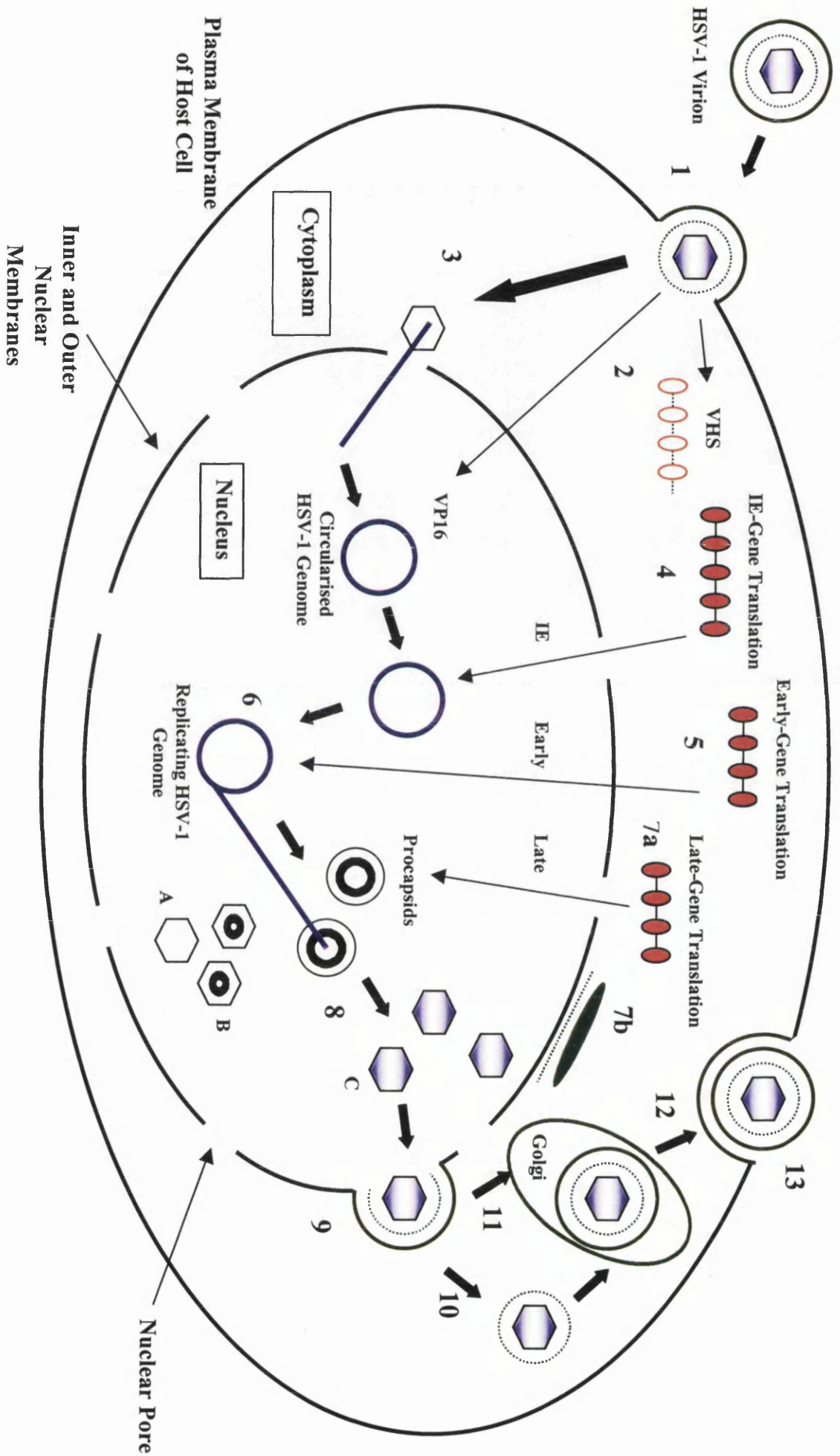
The events starting with the attachment of an HSV-1 virion to the surface of a permissive cell through to the production of infectious progeny virus within that cell are known as the lytic cycle. These events are discussed briefly below and are outlined schematically in Figure 1.10.

1.2.4.1 Attachment to and Penetration into the Host Cell.

The receptor mediated attachment of an HSV-1 virion to the host cell surface involves several of the 11 glycoproteins found within the viral envelope, reviewed by Spear, (1993) and Steven & Spear, (1997) (step 1, Figure 1.10). The initial attachment of the virion to the host cell is thought to involve an interaction of gC and/or gB with heparan sulphate (Shieh & Spear, 1994), a cell surface glycosaminoglycan. However, the binding of viral glycoproteins to heparan sulphate is not sufficient for virus penetration (Lee & Fuller, 1993) and an interaction with a second group of receptors, termed the herpesvirus entry mediators (HveA-D), is required. The specificity of these receptors varies and can depend on the cell type. For example, HveA is a member of the tumour necrosis factor receptor family and while it is the principle receptor for HSV-1 entry into human lymphoid cells, it will not support the entry of other alphaherpesviruses, such as PRV, into this cell type (Montgomery *et al.*, 1996). HveB-D are related to the poliovirus receptor proteins and although HveB and HveD can mediate the entry of a number of alphaherpesviruses, these two receptors do not support the entry of HSV-1 which has been shown to involve HveC. This receptor binds strongly to HSV-1 gD and not

Figure 1.10 Schematic Representation of the HSV-1 Lytic Life Cycle.

Stage 1, The virus initiates infection of the host cell through the fusion of the viral envelope with the cellular plasma membrane following receptor mediated attachment to the cell surface. 2, Fusion of the membranes releases virus tegument proteins into the host cell, including VHS (viral host-shutoff protein) which disrupts host cell protein synthesis (broken RNA in open polyribosomes) and VP16 (IE *trans*-inducing factor) which is transported to the nucleus. 3, Utilising the microtubule network, the capsid is transported to the nuclear pore where the viral genome is released into the nucleus and immediately circularises to form an episome. 4, The transcription of IE genes by cellular enzymes is stimulated by VP16. Viral DNA is transcribed throughout the replication cycle by host RNA polymerase II, but with the participation of viral factors at all stages of infection. The 5 IE mRNAs are translated in the cytoplasm (filled polyribosomes) and the IE proteins are transported into the nucleus. 5, IE proteins enable the expression of the early genes which encode proteins necessary for viral DNA synthesis, acting at the transcriptional or post-transcriptional level. 6, Viral DNA is replicated in the nucleus of infected cells probably by a rolling circle mechanism which yields head-to-tail- concatemers of unit-length viral DNA. 7a, A new round of transcription and translation produces the late proteins, consisting of proteins involved in DNA cleavage and packaging together with the viral structural proteins. Membrane associated structural proteins, predominantly glycoproteins, become incorporated into the rough endoplasmic reticulum. 7b, Membrane proteins may then become glycosylated and some localise to the inner and outer nuclear membranes and the endoplasmic reticulum. Further modification occurs within the Golgi apparatus and mature glycoproteins are transported to the plasma membrane. The capsid proteins are transported to the nucleus and procapsids are assembled. 8, Concatemeric viral DNA is cleaved into unit-length (152 kbp) molecules and packaged into the preformed procapsids. The inner protein scaffold of the procapsid is lost and the procapsid angularises to form a DNA-containing C capsid. A and B capsids are also seen in the nucleus at this stage and are thought to result from defective DNA cleavage and packaging. 9, The DNA-containing capsids, probably in association with some tegument proteins, acquire an envelope by budding through the inner nuclear membrane. Two theories exist concerning virion egress. 10, In the de-envelopment pathway, the enveloped capsids are then de-enveloped at the outer nuclear membrane and the capsid-tegument structure is released into the cytoplasm. The capsids acquire additional tegument proteins within the cytoplasm and the capsid-tegument structure is re-enveloped at Golgi compartments containing mature viral membrane associated proteins. 11, In the luminal pathway, enveloped virus is engulfed by a transport vesicle and delivered to the Golgi apparatus. The precursor viral envelope proteins are processed *in situ* as part of the virion. 12, In both cases the mature virion is transported to the plasma membrane and released by exocytosis. 13, Progeny virus in the extracellular space can either establish lytic infections in surrounding epithelial cells or, following infection of neuronal cells, may be transported to sensory ganglia where latent infection can take place. In fully permissive tissue culture cells, the entire lytic replication cycle takes approximately 18 to 20 hours.



only facilitates the entry of HSV-1 but also HSV-2, PRV and BHV-1 (Geraghty *et al.*, 1998, Krummenacher *et al.*, 1998).

Following receptor mediated attachment of an HSV-1 virion to the host cell surface, the capsid and tegument are internalised through the fusion of the viral envelope with the host cell plasma membrane. This is a rapid process which proceeds in a pH-independent manner and involves a number of viral glycoproteins including gD, gB and the gH-gL complex (Wittels & Spear, 1991, Spear, 1993).

1.2.4.2 Disruption of Host Cell Protein Synthesis.

The fusion of the viral envelope with the plasma membrane of the host cell not only serves to internalise the nucleocapsid but also releases tegument proteins into the cytoplasm. The 55 kDa VHS tegument protein is encoded by the UL41 gene of HSV-1 and is involved in the disruption of host cell protein synthesis during the initial stages of infection (step 2, Figure 1.10). Although this protein degrades both cellular and viral mRNAs in a non-specific manner, the rate of viral mRNA synthesis has been shown to be greater than VHS-induced degradation (Schek & Bachenheimer, 1985, Kwong & Frenkel, 1987, Kwong *et al.*, 1988, Elgadi *et al.*, 1999). VHS is not the only HSV-1 encoded protein that can modulate host cell protein synthesis, the IE protein ICP27 and the virion associated UL13 protein kinase are also believed to function in the regulation host cell protein synthesis (Overton *et al.*, 1994, Sandri-Goldin, 1998, Laurent *et al.*, 1998).

1.2.4.3 Transport of the Nucleocapsid to the Nucleus.

Once inside the cell, the nucleocapsid is actively transported to the nuclear pore (step 3, Figure 1.10). Within neurons, nucleocapsids travel from the presynaptic membrane to the nucleus by retrograde transport along the axon (Lycke *et al.*, 1988, Penfold *et al.*, 1994, Smith *et al.*, 2000). In other cell types, such as epithelial cells, transport of the HSV-1 nucleocapsid to the nuclear pore is thought to be mediated by the cytoskeleton and, in particular, the microtubule network (Sodeik *et al.*, 1997). The UL34 protein may be component of the HSV-1 capsid-tegument structure and has been shown to interact with a cytoplasmic dynein intermediate polypeptide chain (Ye *et al.*, 2000). The cytoplasmic dynein protein is a microtubule associated motor protein involved in intracellular transport. The UL34 protein is

believed to anchor the capsid-tegument structure to the microtubule network through an interaction with dynein to facilitate retrograde transport of the nucleocapsid to the nuclear pore in an ATP dependent manner. The nucleocapsid attaches to the nuclear pore and the viral genome is released into the nucleus where it circularises to form an episome (Batterson *et al.*, 1983, Ojala *et al.*, 2000).

1.2.4.4 HSV-1 Gene Expression.

Transcription of the viral DNA within the nucleus is carried out by host cell DNA-dependent RNA polymerase II with the participation of viral factors. Following HSV-1 penetration into the host cell, the VP16 tegument protein translocates to the nucleus and, in association with cellular factors Oct-1 and HCF (host cell factor), induces the expression of the IE-genes. HSV-1 gene expression then proceeds in a regulated cascade as described in section 1.2.1.4 (steps 4,5 and 7, Figure 1.10).

1.2.4.5 HSV-1 DNA Replication.

HSV-1 DNA synthesis commences shortly after the onset of early-gene expression and at 37°C continues up to 15 hours pi, with a peak between 7-10 hours pi (step 6, Figure 1.10). The HSV-1 genome contains three origins of replication (*ori*) and DNA replication can be initiated from any one of these *cis*-acting elements. In addition, HSV-1 contains seven genes that specify proteins with *trans*-acting functions essential for *ori*-dependent DNA replication. These genes are UL5, UL8, UL9, UL29, UL30, UL42 and UL52 (Table 1.3) and their involvement in the process of HSV-1 DNA replication has been comprehensively reviewed (Challberg, 1991, Boehmer & Lehman, 1997, Lehman & Boehmer, 1999).

Viral DNA synthesis is believed to be preceded by the sequence-specific binding of the UL9/UL29 complex to *ori* regions (He & Lehman, 2001). The other DNA replication proteins are then recruited by virtue of a series of specific protein-protein interactions (described in Table 1.3) to form a replication complex. The *ori* region is unwound, RNA primers are synthesised and replication forks are established. All the HSV-1 replication proteins, with the exception of UL9, are believed to function in the co-ordination of leading and lagging strand synthesis and the RNA primers are probably degraded by the RNase activity of the viral DNA polymerase. Host cell enzymes such as DNA ligase I and topoisomerase II and HSV-1

Gene	Size (kDa)	Function
UL5	98	Complexes with UL8 and UL52 proteins to form the trimeric primosome holoenzyme, enzyme complex has DNA helicase-primase activity.
UL8	79	Component of the primosome holoenzyme, acts as a primase and expresses helicase activity in the presence of UL9 protein. Stabilises interaction between primers and DNA template.
UL9	94	Homodimeric ori binding protein, has helicase and ATPase activity. Complexes with UL29 protein.
UL29	128	Binds ss DNA, increases helicase and DNA-dependent ATPase activity of UL9 protein.
UL30	139	DNA polymerase with 3' to 5' exonuclease and RNaseH activity, forms a heterodimer with UL42.
UL42	51	Ds DNA-binding phosphoprotein, binds to and increases the processivity of UL30 DNA polymerase.
UL52	114	Component of the primosome holoenzyme, required for DNA helicase-primase activity.

Table 1.3 The Essential HSV-1 DNA Replication Proteins.

encoded enzymes involved in nucleic acid metabolism, for example, thymidine kinase (UL23), dUTPase (UL50) and uracil DNA glycosylase (UL2), are also likely to function in viral DNA synthesis.

Although the evidence is not conclusive, it is proposed that, like bacteriophage lambda, the newly circularised HSV-1 genome is initially amplified by theta form of replication followed by a phase of rolling circle DNA synthesis which generates head-tail concatemers of unit-length viral DNA molecules. Prior to cleavage and packaging of the newly replicated viral DNA, it is thought that branched DNA structures arising from recombination are removed by the UL12 alkaline nuclease (Weller *et al.*, 1990, Shao *et al.*, 1993, Martinez *et al.*, 1996a, Goldstein & Weller, 1998a). Viral DNA is then cleaved into unit-length monomers and packaged into preformed viral procapsids (discussed in section 1.2.6).

1.2.4.6 Assembly of Procapsids Within the Nucleus of the Infected Cell.

The HSV-1 capsid proteins, VP26, VP5, VP23 VP19C, preVP22a and the UL26 gene products, are synthesised in the cytoplasm of the host cell following late-gene transcription. These proteins are transported to the nucleus through a network of specific protein-protein interactions which are summarised in Figure 1.11 (Nicholson *et al.*, 1994, , Tatman *et al.*, 1994, Thomsen *et al.*, 1994, Kennard *et al.*, 1995, Rixon *et al.*, 1996, Desai & Person, 1996,).

Newcomb *et al.* (1996) have proposed a model for capsid assembly based upon their observations during cell-free *in vitro* assembly of HSV-1 capsids. Extracts from Sf9 cells infected with recombinant baculoviruses expressing the HSV-1 capsid proteins were prepared and mixed together. Distinct capsid-related structures, presumably capsids in various stages of assembly, were then isolated at different times from the reaction mixture and characterised. Partial capsids were the first type of structure isolated and had the appearance of angular segments of procapsids consisting of a partial region of core surrounded by a partial region of shell. It is believed that in the nuclei of infected cells, preVP22a-VP5-triplex complexes assemble to form partial procapsids through the ability of the preVP22a protein to homo-oligomerise. The partial procapsids subsequently enlarge to form closed spherical procapsids. Procapsids purified from Vero cells infected with *ts*ProtA (a HSV-1 mutant containing an identical *ts* lesion in the UL26 gene to that of *ts*1201) at the NPT have been shown to contain the UL6, UL15, and UL28 DNA cleavage and packaging proteins which were present in lower

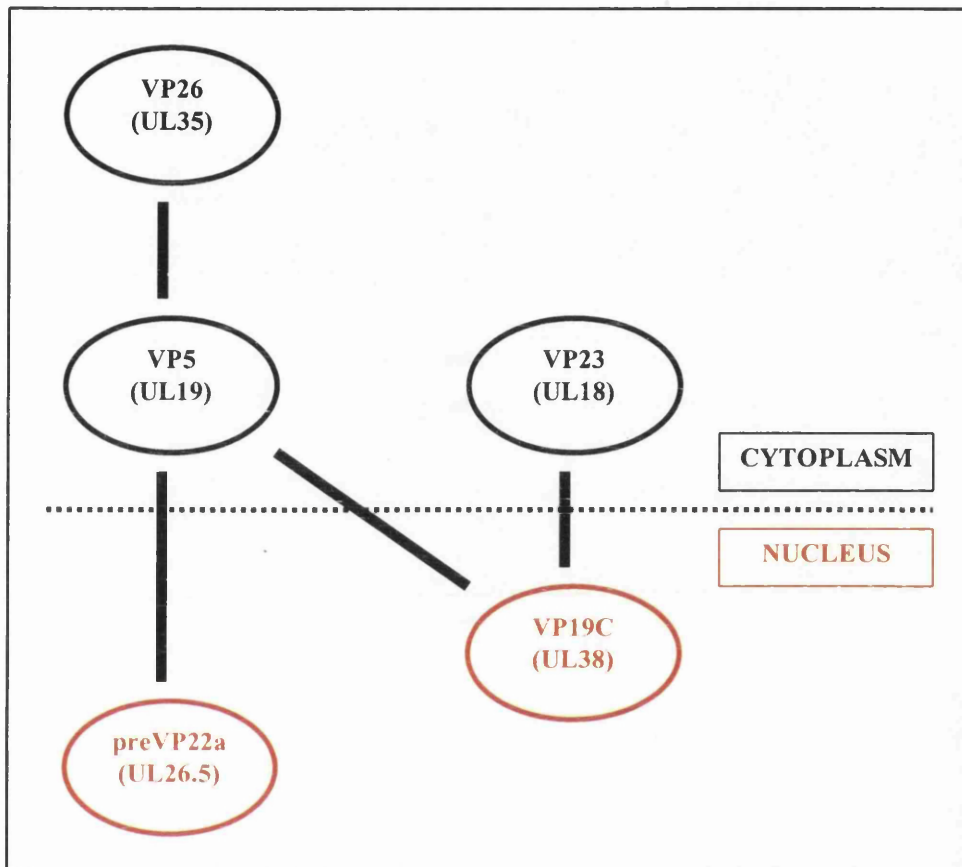


Figure 1.11 Protein-Protein Interactions Involving the HSV-1 Capsid Proteins.

The HSV-1 capsid proteins are illustrated above with the gene encoding each protein in brackets. Protein-protein interactions are shown as solid black lines and the dotted line represents the nuclear membrane. Proteins coloured red have an intrinsic capacity to localise to the nucleus.

amounts than in B and C capsids (Sheaffer *et al.*, 2001). However, it is not known at what stage the DNA cleavage and packaging proteins are incorporated into the procapsid and the nature of this association is also unknown. Newly replicated concatemeric viral DNA is then cleaved and packaged into the procapsid (section 1.2.6) (step 8, Figure 1.10). The interior protein scaffold is cleaved by the VP24 protease and removed from the procapsid which angularises to form a mature DNA-containing polyhedral capsid. Unlike the other capsid proteins, the VP26 protein is not required for the formation of procapsids and is only recruited to intranuclear sites of capsid assembly once procapsid maturation has begun (Chi & Wilson, 2000). This indicates that VP26 binds to the hexons either during, or after angularisation of the procapsid.

1.2.4.7 Tegument Acquisition, Envelopment and Virion Egress.

Following viral DNA cleavage and packaging, DNA-containing capsids leave the nucleus and acquire tegument and envelope layers before exiting the cell via the exocytic pathway, reviewed by Steven & Spear, (1997) and Rixon, (1993) (steps 9-13, Figure 1.10). The exact mechanism by which this is achieved by the virus is unknown and two popular theories exist to describe this stage of the HSV-1 lytic cycle. The first model, the luminal pathway, proposes that capsids acquire tegument and envelope structures by budding through patches in the nuclear membranes containing viral proteins. The newly enveloped capsids are delivered to the Golgi apparatus by a transport vesicle where the tegument proteins and glycoproteins are modified as part of the virion (step 11, Figure 1.10). The second model, the envelopment, deenvelopment, reenvelopment (EDR) pathway, suggests that capsids are enveloped by budding through the inner nuclear membrane into the perinuclear space but are deenveloped at the outer nuclear membrane and released into the cytoplasm of the infected cell (step 10, Figure 1.10). Capsids then acquire tegument proteins in the cytoplasm of the host cell whilst on route to the Golgi apparatus where they are reenveloped and gain viral-encoded glycoproteins. In both cases, the mature virions then leave the cell from the Golgi apparatus through the exocytic pathway (step 12, Figure 1.10).

Naked capsids and vesicle-enclosed enveloped capsids are observed in the cytoplasm of an HSV-1 infected cell analysed by electron microscopy at a late stage in the lytic cycle (Campadelli-Fiume *et al.*, 1991, Rixon, 1993), thus providing evidence in support of both the

luminal and EDR pathways. However, subsequent studies have provided additional evidence in favour the EDR pathway of virion egress. For example, in cells infected with a recombinant virus in which the expression of the essential glycoprotein, gH, was restricted to the endoplasmic reticulum-inner nuclear membrane by means of an endoplasmic reticulum retention motif, progeny virus demonstrated 100-fold less infectivity than virus released from wt virus-infected cells (Browne *et al.*, 1996). The virions released from cells infected with the recombinant virus did not contain detectable levels of gH and these findings were consistent with a model of virus exit whereby naked DNA-containing capsids in the cytoplasm acquire their final envelope from a subcellular compartment other than the endoplasmic reticulum-inner nuclear membrane. These experiments have been repeated using a HSV-1 mutant which encoded endoplasmic reticulum-retrieved glycoprotein D (Skepper *et al.*, 2001). The results from this study were similar to those obtained using the gH recombinant virus and also supported an EDR model for nucleocapsid maturation.

There is also some controversy regarding the intracellular localisation of the HSV-1 tegument proteins during wt virus-infection of cells and the cellular site of tegument acquisition by DNA-containing capsids has yet to be identified. Some investigators have shown that VP22 and VP16 localise to the cytoplasm of HSV-1-infected cells (Elliott *et al.*, 1995, Elliott & O'Hare, 1999) while others demonstrate these proteins are nuclear during HSV-1 infection (Ward *et al.*, 1996, Morrison *et al.*, 1998). Whatever the outcome regarding these two proteins, it is likely that at least some tegument proteins, such as the US11 protein (Ward *et al.*, 1996), associate with DNA-containing capsids within the nuclei of HSV-1 infected cells before they reach the cytoplasm.

1.2.5 HSV-1 Latency: An Overview.

HSV-1 latency has been reviewed extensively (Wagner & Bloom, 1997, Preston, 2000), and the following is a brief account concerning the main issues of this phenomenon. After infection of a human or experimental animal with HSV-1, virus replication occurs at the site of infection. Virus then enter the nerve termini and are transported intra-axonally to sensory ganglia, particularly trigeminal ganglia, where infected neurons initially support virus replication. Within a few days, however, no free virus can be detected and a latent state of infection is established which persists for the duration of the host's life (Stevens & Cook,

1971). Approximately 10-100 copies of the HSV-1 genome are present in each latently infected neuron and they exist within the nucleus as circular episomes (Mellerick & Fraser, 1987). During latency, the genes necessary for lytic replication are switched off and are not expressed until the signals which induce reactivation are received. Although the mechanism of reactivation is poorly understood, the signals that can trigger this process include tissue damage, UV radiation and immunosuppression and cause stress either to the animal as a whole or to the individual neuron. Reactivation results in the production of infectious progeny virus but does not destroy the neuron (Gominak *et al.*, 1990). Additionally, repeated reactivation does not normally appear to have a detrimental effect on the function or physiology of the trigeminal ganglia (Wagner & Bloom, 1997).

Prior lytic gene expression is not required for the formation of a latent state within a HSV-1 infected neuron. Therefore, latency and lytic infection are believed to be alternative and separate outcomes following infection of these cells. Once the virus has entered a neuron, latency is believed to result from insufficient or repressed HSV-1 IE gene expression. Within HSV-1 infected neurones, VP16 may be incapable of transactivating IE gene expression either because its function is inhibited or the protein cannot enter the nucleus. In sensory neurons Oct-1 is present at low abundance and other proteins of the Oct family are expressed preferentially (He *et al.*, 1989). Since many members of the Oct family can bind the TAATGARAT element within IE gene promoters, but only Oct-1 is known to interact with VP16, other Oct proteins could act as competitors to prevent the formation of the VP16/Oct-1/HCF transactivation complex. In support of this hypothesis, Oct-2 has been shown to repress HSV-1 IE gene expression in cell lines derived from sensory neurons (Lillicrop *et al.*, 1991, Lillicrop *et al.*, 1994). HCF has an important role in transporting VP16 to the nuclei of HSV-1-infected cells and in many cell types, HCF localises to both the cytoplasm and the nucleus (Kristie *et al.*, 1995, La Boissière *et al.*, 1999). However, this protein is retained almost exclusively in the cytoplasm of sensory neurones and, therefore, may be incapable of transporting VP16 to the nuclei of these cells resulting in the inefficient transcription of IE genes (Kristie *et al.*, 1999).

During the latent state, viral gene expression is restricted to a set of transcripts known as latency-associated transcripts (LATs) that accumulate to high levels predominantly within the nuclei of latently infected neurons (Stevens *et al.*, 1987). LATs are viral RNAs transcribed

anti-sense to, and partially complementary to the coding sequences of Vmw110 (ICP0). Their exact function is unknown and they are not absolutely required to establish or maintain a latent state of infection. Since LATs are partially complementary to Vmw110 coding regions, they may act as anti-sense inhibitors of this protein (Farrell *et al.*, 1991). The Vmw110 protein can specifically enhance IE gene expression and therefore, LATs may also function to repress IE gene activation.

1.2.6 HSV-1 DNA Cleavage and Packaging.

1.2.6.1 Introduction.

The HSV-1 DNA cleavage and packaging process is essential and no infectious progeny are generated in its absence. HSV-1 DNA replication results in the production of head-tail concatemers of genomic-length viral DNA which are cleaved at specific sites within the genome and packaged into preformed procapsids by tightly linked mechanisms in the nuclei of infected cells. Cleavage of the viral genome also appears to be linked with capsid formation since HSV-1 mutants that fail to assemble capsids due to the deletion of either the UL18 or UL19 genes also fail to cleave replicated concatemeric DNA (Desai *et al.*, 1993). This probably reflects the fact that the majority of the HSV-1 cleavage and packaging proteins are associated with the capsid structure (Table 1.4). The DNA cleavage and packaging process of the icosahedral dsDNA bacteriophages and HSV-1 have many similarities. However, while the components of the DNA cleavage and packaging machinery from icosahedral dsDNA bacteriophages, such as lambda, have been identified and characterised in detail (Catalano *et al.*, 1995), relatively little is known about this area of the HSV-1 lytic-cycle. Through the characterisation of various HSV-1 mutants, several HSV-1 encoded proteins that function in DNA cleavage and packaging have been identified (Table 1.4 and section 1.2.6.5), although their precise role in this process requires further investigation. This section aims to review the current knowledge concerning the signals, factors and mechanisms involved in HSV-1 DNA cleavage and packaging.

Gene / Protein	Size (kDa)	Association with Capsid Type				Required For	
		Procapsid	A	B	C	Cleavage	Packaging
UL6	74.1	+	+	+ *44±13	+	Yes	Yes
UL12	85	?	-	-	-	No	No
UL12.5	60	?	?	+	+	No	No
UL15	80.9	+	+	+	±	Yes	Yes
UL17	74.6	?	?	+	+	Yes	Yes
UL25	62.7	±	++	+ *42±17	++	No	Yes
UL28	85.6	+	+	+	-	Yes	Yes
UL31	34	?	-	-	-	No	No
UL32	63.9	?	?	-	-	Yes	Yes
UL33	14.4	?	?	-	-	Yes	Yes

* Protein copy number per B capsid, taken from Ogasawara et al. (2001).

Table 1.4 The HSV-1 DNA Cleavage and Packaging Proteins.

The above table summarises the properties of the HSV-1 proteins essential for viral DNA cleavage and packaging (UL6, UL15, UL17, UL25, UL28, UL32 and UL33). The remaining proteins (UL12, UL12.5 and UL31) are believed to have a more indirect role in this process. ± and ++ represents an decrease or an increase in the protein copy number respectively.

1.2.6.2 HSV-1 DNA Cleavage and Packaging Signals.

Cleavage of concatemeric HSV-1 DNA is a site-specific event controlled by *cis*-acting sequences located at the L-S junctions. Stow *et al.* (1983) demonstrated that DNA fragments from both the L and S termini of the HSV-1 genome contained all the *cis*-acting elements necessary to direct both cleavage and packaging of an HSV-1 amplicon. Since the *a* sequence was common to both these fragments the authors concluded that this sequence contained the specific signals recognised by the HSV-1 DNA cleavage and packaging machinery (the structure of the *a* sequence is discussed in section 1.2.1.2). The HSV-1 L and S genomic termini both end in partial copies of the 20 bp DR1 component of the *a* sequence (Davison & Wilkie, 1981, Mocarski & Roizman, 1982). Whereas single *a* sequences are flanked by separate DR1 repeats, tandemly repeated *a* sequences share the intervening DR1 repeat and the site at which concatemeric DNA is cleaved to generate the genomic termini lies within the shared DR1 repeat (Mocarski & Roizman, 1982).

Several observations have suggested that the process of HSV-1 genome maturation is complex. Firstly, although the cleavage site is within the DR1 element, this sequence is not required for genome maturation (Varmuza & Smiley, 1985, Deiss & Frenkel, 1986). This has led to the hypothesis that cleavage occurs at a fixed distance from separate cleavage signals. Secondly, sequences within both the u_b and u_c elements appear to be critical for the HSV-1 DNA cleavage and packaging process (Varmuza & Smiley, 1985, Deiss *et al.*, 1986, Deiss & Frenkel, 1986). Lastly, single *a* sequences predominate in replicating concatemeric HSV-1 DNA, however, mature progeny molecules have at least one *a* sequence at each end (Locker & Frenkel, 1979, Mocarski & Roizman, 1981). To account for these findings several mechanisms have been proposed which are discussed in section 1.2.6.3 (Varmuza & Smiley, 1985, Deiss & Frenkel, 1986).

A critical role for the *pac1* and *pac2* homology elements in HSV-1 DNA cleavage and packaging was identified in 1988 (Nasseri & Mocarski, 1988). This group demonstrated that all the *cis*-acting signals required for the cleavage and packaging of a HSV-1 amplicon were contained within a 179 bp DNA fragment which spanned two tandemly repeated *a* sequences from HSV-1 strain F and represents the minimal cleavage and packaging signal identified to date. This fragment contained both the *pac1* and *pac2* elements, situated within the u_b and u_c regions of the *a* sequence respectively, separated by a single DR1 sequence and can be

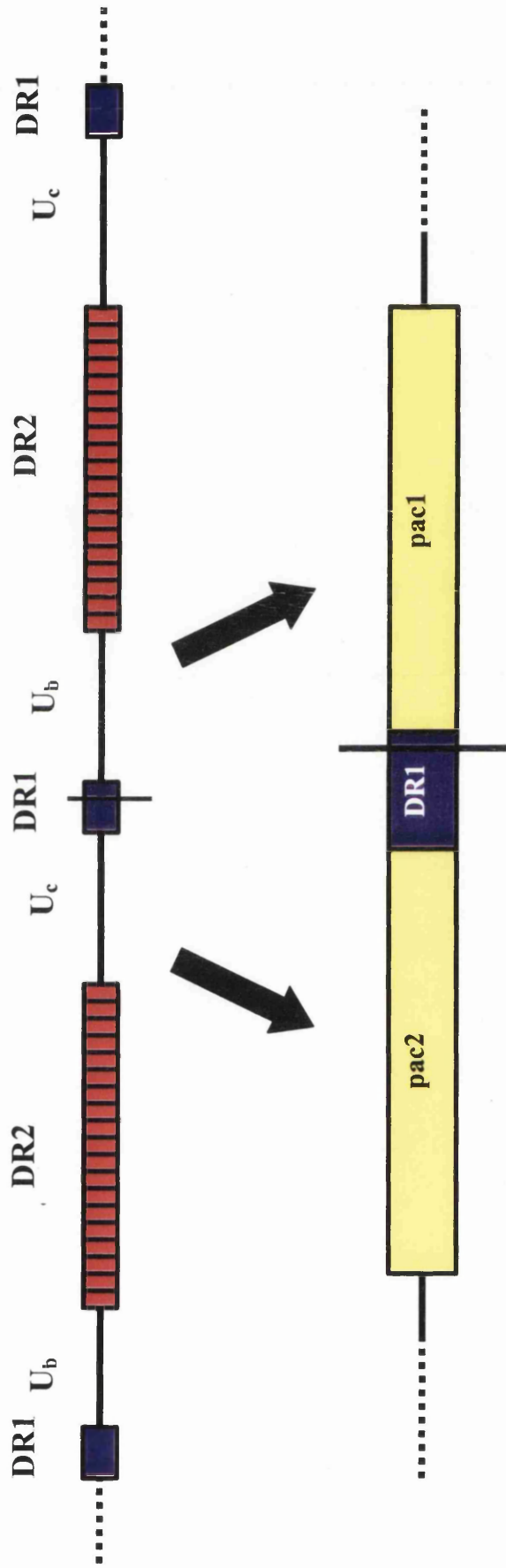
represented thus [DR4]_{0.6}-u_c-DR1-u_b-[DR2]₁. The nature of this fragment indicated that the cleavage signal was located at a novel junction between two *a* sequences and that cleavage at a single *a* sequence would only be possible following an *a* sequence duplication event. The cleavage signal between tandemly repeated *a* sequences is also the only arrangement in which the *pac1* and *pac2* sequences are brought into close proximity. In a single *a* sequence, these elements are as much as 400 bp apart. An interesting, although unrepeated, observation resulting from these experiments was that cleavage and packaging of the HSV-1 amplicon did not require prior replication of the plasmid and this finding suggested that concatemeric DNA was not the sole substrate for the HSV-1 DNA cleavage and packaging machinery.

Although much is known about the cleavage and packaging signals of HSV-1, the preferred arrangement of the signals required by the virus for this process to occur *in vivo* remain unknown. However, since both genomic termini end with at least one *a* sequence and have single-base 3' extensions from the DR1 repeat that can only be produced by cleavage and, when aligned, re-generate a complete 20 bp DR1 sequence (Mocarski & Roizman, 1982); the last step in the genome maturation process is likely to be a specific cleavage at the DR1 element situated between tandemly repeated *a* sequences (Figure 1.12).

The genomes of all herpesviruses carry signals located near the genomic termini that are required *in cis* for encapsidating progeny DNA and these signals appear to be structurally conserved. The *pac1* and *pac2* homology elements are located at the ends of a variety of herpesviruses and have been directly implicated in the DNA cleavage and packaging process of HCMV (Spaete & Mocarski, 1985), EBV (Zimmermann & Hammerschmidt, 1995), MCMV (McVoy *et al.*, 1998), HHV-6 (Deng & Dewhurst, 1998) and GPCMV (McVoy *et al.*, 1997). The ability of the *a* sequence of HCMV to direct cleavage and packaging of defective HSV-1 genomes demonstrated that the cleavage and packaging signal from at least two divergent herpesviruses are functionally conserved (Spaete & Mocarski, 1985).

1.2.6.3 The Production of Genomic-Length DNA Molecules from Concatemeric DNA.

Several models have been proposed to address the question of how the two genomic termini, each bearing at least one copy of the *a* sequence, are generated from concatemeric DNA containing predominantly single copies of this sequence. Straight-forward dsDNA cleavage at the DR1 element of a single *a* sequence within concatemeric DNA would produce



Site of HSV-1 DNA Cleavage

Figure 1.12 Sequence Arrangement in Adjacent HSV-1 *a* Sequences.

The cleavage of concatemeric HSV-1 DNA is believed to occur within the DR1 element located between tandemly repeated *a* sequences. The *pac1* and *pac2* sequences, located within the *u_b* and *u_c* regions of the *a* sequence respectively, are critical for DNA cleavage and are brought into close proximity in the arrangement shown above. Cleavage within the DR1 element generates 3' single-base overhangs which are present at incomplete DR1 sequences found at each end of the viral genome.

genomic termini composed of incomplete *a* sequences. However, as described previously, this is not the sequence observed at the ends of virion DNA (Wadsworth *et al.*, 1975, Locker & Frenkel, 1979, Mocarski & Roizman, 1981). The HSV-1 DNA cleavage models discussed below help to explain much of the experimental data collected to date, although none are entirely satisfactory, and the actual mechanism used by the virus in infected cells remains unknown.

a). Staggered Nick-Repair Model (Varmuza & Smiley, 1985).

This model (also known as the *a* sequence duplication model) proposes that the genomic termini arise by two ss nicks, rather than ds cleavages. For cleavage within a single *a* sequence, the S and L recognition complexes (presumably components of the DNA cleavage and packaging machinery) bind to signals in u_b and u_c respectively and one strand is nicked at the future L terminus and the other strand is nicked at the S terminus. Each terminus would then have a 5' overhang the length of the *a* sequence. Repair synthesis then ensues across the staggered cleavages, producing the two termini, each bearing a single *a* sequence. In the junctions of two or more *a* sequences, the u_b and u_c regions are brought into close proximity and could be processed by the co-operative action of the cleavage complexes producing a ds break generating ends with a protruding 3' nucleotide.

b). The Theft Model (Varmuza & Smiley, 1985).

The theft model suggests that the genomic termini are generated by two separate ds cleavage events, one creating an L terminus, the other, an S terminus. At any given L-S junction composed of a single *a* sequence, a dsDNA cleavage generates an L terminus ending with a single *a* sequence and an S terminus lacking an *a* sequence. Packaging of the genome with the *a* sequence-containing L terminus then occurs until the next L-S junction in the same orientation is encountered. Here the process is reversed, dsDNA cleavage generates an S terminus with an *a* sequence and an L terminus without one, producing a packaged genome with an *a* sequence at each end. The model essentially proposes that whenever junctions composed of a single *a* sequence are used as cleavage sites, the *a* sequence is 'stolen' from the adjacent genome in the concatemer. This model predicts that at least some of the dsDNA cleavages result in the formation of protruding 3' single-base extensions at the termini.

According to this model, a large number of genomic termini lacking an *a* sequence would be generated in the nuclei of HSV-1-infected cells. Such termini have not been detected and raises the possibility they are rapidly degraded (Deiss & Frenkel, 1986). However, neither of the above models can explain why the L termini end with a variable number of *a* sequences while the S termini have only one.

c). The Directional Cleavage Model (Modified Theft Model) (Deiss *et al.*, 1986).

The directional cleavage model modifies the theft model (Varmuza & Smiley, 1985) to incorporate polarity in the cleavage and packaging reaction. This model postulates the packaging complex binds anywhere within the L or S segments of the genome and traverses along the genome in either direction (random walk) until a junction containing a u_c signal is encountered. Cleavage then occurs at the DR1 element proximal to this u_c signal (creating a 3' single-base overhang) to form the L terminus while the S terminus is degraded. Packaging begins in an L-S direction and continues until a directly repeated junction is reached. A second cleavage (also generating a 3' single-base extension) then occurs proximal to the u_b element. This model can account for the distribution of *a* sequences at the L and S termini but, as with the theft model proposed by Varmuza and Smiley (1985), also predicts the formation of termini lacking *a* sequences, which have not been detected.

1.2.6.4 Translocation of DNA Into the Capsid.

Although nothing is known about the mechanism by which DNA is translocated into the HSV-1 procapsid, this process is thought to require the presence of ATP (Dasgupta & Wilson, 1999). Additionally, several observations suggest DNA enters the procapsid at the icosahedral vertices and, specifically, through the penton axial-channel. Firstly, HSV-1 genomic DNA can be extruded from C capsids following treatment with 0.5 M GuHCl (Newcomb & Brown, 1994). These workers found that DNA appeared to exit the capsid at the icosahedral vertices and no DNA was observed leaving the capsid via the icosahedral facets. Secondly, DNA packaging is associated with a conformational change of the penton channel. In procapsids, the channel is large enough to allow the passage of duplex DNA (Trus *et al.*, 1996), but in C capsids the penton channel appears either closed or blocked (Zhou *et al.*, 1999). Lastly, through the use of immunogold staining techniques to detect capsid-bound anti-UL25

antibodies, Ogasawara *et al.* (2001), tentatively suggested that the UL25 DNA packaging protein may be located at the icosahedral vertices although the location of the remaining capsid-associated DNA cleavage and packaging proteins remains unknown. It is also not known whether HSV-1 DNA is packaged at any icosahedral vertex or if packaging can only occur at a unique vertex, as seen in the icosahedral dsDNA bacteriophages.

In icosahedral ds DNA bacteriophages, a single multimeric portal complex (or connector) is located at the unique head-tail junction vertex (Bazinet & King, 1982). Image processing of electron micrographs of purified portal complexes from T4, ϕ 29, lambda, T3 and P22 indicates this component of the bacteriophage head has a ring structure that exhibits 12-fold rotational symmetry with a central tube through which the phage genome is believed to enter the prohead (Valpuesta & Carracosa, 1994). The portal complex of bacteriophage SPP1 is slightly different and appears to display 13-fold rotational symmetry (Dube *et al.*, 1993). The three-dimensional structure of the portal complexes from bacteriophages T3 and ϕ 29 has been elucidated and reveals that the portal complex is a cone shaped object divided into three, approximately cylindrical regions: the narrow end, the central part and the wide end (Figure 1.13) (Valpuesta *et al.*, 1992, Simpson *et al.*, 2000). The ϕ 29 DNA packaging process is absolutely dependent on the presence of an 174 nucleotide RNA species, termed pRNA (packaging RNA), which exists as a pentameric ring structure bound to the narrow end of the portal complex on the prohead exterior (Zhang *et al.*, 1998, Guo *et al.*, 1998, Simpson *et al.*, 2000). The pRNA is completely absent from mature phage heads and is considered an essential facilitator of the packaging event. This RNA species has only been identified in bacteriophage ϕ 29 and its closest relatives and it is unclear whether other icosahedral dsDNA bacteriophages also utilise RNA in their DNA packaging process.

Simpson *et al.* (2000) have determined the structure of portal complexes, isolated from bacteriophage ϕ 29 proheads in the process of packaging DNA, to a resolution of 3.2 Å by means of X-ray crystallography and found that, during packaging, DNA was translocated through the central channel of the portal complex into the bacteriophage prohead. This group proposed that the packaging machinery comprised a rotary motor with the prohead-pRNA-gp16 (the gp16 protein is an ATPase associated with the portal protein) complex acting as a stator, the DNA acting as a spindle and the portal complex acting as a ball-race. In their model, each monomeric subunit of the portal complex sequentially interacts with the base

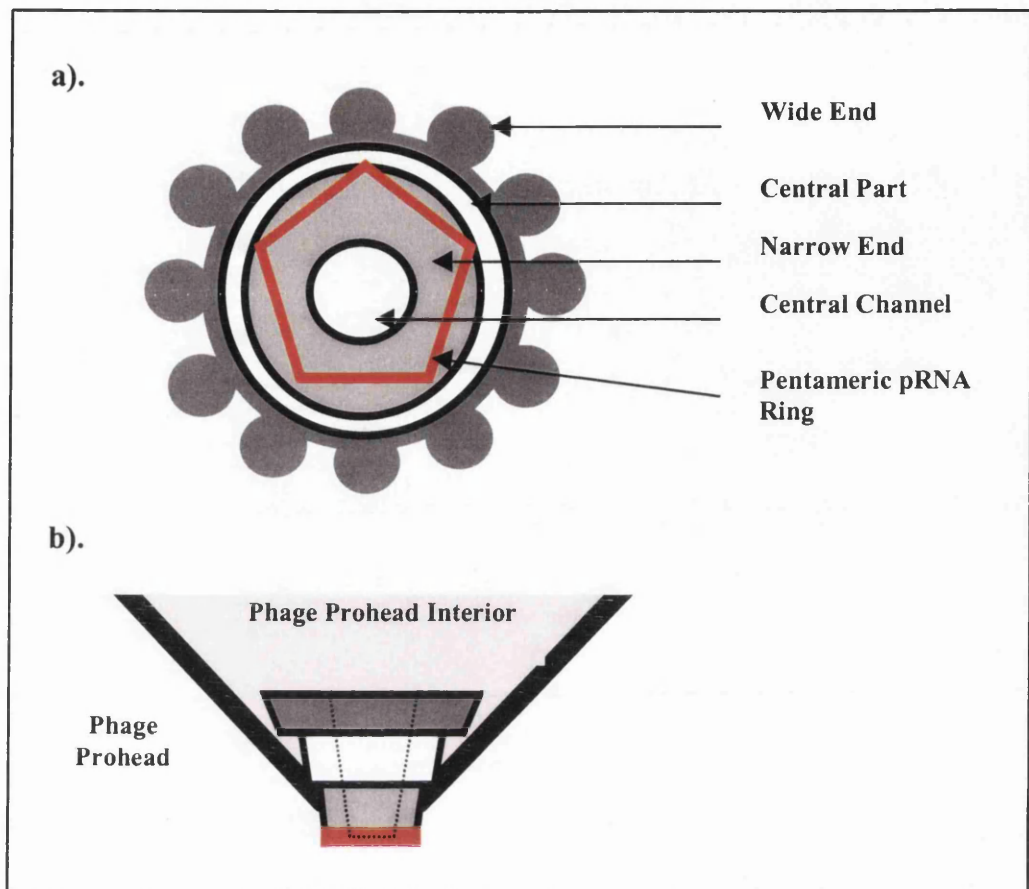


Figure 1.13 Structure of the Bacteriophage ϕ 29 Portal Complex (Simpson *et al.*, 2000).

The above figure is a schematic representation of the ϕ 29 portal protein complex showing **a)** the structure seen from the tail looking towards the head and, **b)** the same structure viewed within a cross-section of the phage prohead. The portal complex is composed of 12 monomeric subunits which form a conical structure made up of a narrow part, a central part and a wide end. The wide end is formed from 12 protruding protein domains (1 domain contributed per monomer) which imparts 12-fold rotational symmetry on the structure. A pentameric pRNA ring structure is associated with the narrow end of the portal complex situated on the prohead exterior. The portal protein complex is approximately 75 Å in length and has an internal channel with a diameter of about 36 Å at the narrow end increasing to 60 Å at the wide end.

components of the DNA helix using the energy released from ATP hydrolysis. The helical nature of the DNA converts the rotary motion of the portal complex into translocation of the DNA into the prohead in a similar manner to that proposed for bacteriophage SPP1 (Dube *et al.*, 1993). The model predicts that two base pairs of the DNA helix are packaged per ATP hydrolysis and this is consistent with the observed consumption of ATP during *in vitro* bacteriophage ϕ 29 DNA packaging (Guo *et al.*, 1987).

1.2.6.5 HSV-1 DNA Cleavage and Packaging Proteins.

a). UL6.

The UL6 protein is essential for HSV-1 DNA cleavage and packaging and is found associated with all capsid types, including procapsids (Patel & Maclean, 1995, Lamberti & Weller, 1996, Patel *et al.*, 1996, Sheaffer *et al.*, 2001). This protein is able to interact with B capsids in the absence of any other HSV-1 DNA cleavage and packaging proteins and this observation suggests the association of UL6 with the capsid may be mediated by an interaction with one or more of the capsid proteins listed in Table 1.2 (Patel *et al.*, 1996, Yu & Weller, 1998b). Approximately 44 copies of the UL6 protein are believed to associate with each B capsid and the level of this protein remains constant in all capsid types indicating UL6 may be an integral capsid-associated component of the HSV-1 DNA cleavage and packaging process (Ogasawara *et al.*, 2001, Sheaffer *et al.*, 2001).

The only capsid species assembled in the nuclei of cells infected with a UL6 null mutant virus were B capsids and the absence of A or C capsids is taken as evidence that cleavage and packaging was not even attempted in these cells (Patel *et al.*, 1996). These findings suggest that UL6 functions at a relatively early stage in the DNA cleavage and packaging process. The UL15 cleavage and packaging protein associates with B capsids lacking the UL6 protein less efficiently than with wt HSV-1 B capsids (Yu & Weller, 1998b). This observation indicated that the ability of UL15 to bind to the capsid may, in part, be facilitated by an interaction with the UL6 protein, although this remains speculation as an interaction between these two proteins has not been demonstrated. Additionally, proteolytic processing of full-length capsid-associated UL15 protein did not occur in non-complementing cells infected with a UL6 null mutant virus (Salmon & Baines, 1998). However, since this phenotype was not specific to the

UL6 null mutant virus (refer to page 39), it probably resulted from the absence of DNA cleavage and packaging within these cells.

Compared to wt virus-infected cells, the distribution of UL6 protein was altered in cells infected with a UL17 null mutant virus and this result indicated that the UL17 protein was necessary for the correct localisation of the UL6 protein in virus-infected cells (refer to page 40) (Taus *et al.*, 1998).

b). UL12.

The HSV-1 UL12 ORF encodes a non-capsid associated protein which exhibits deoxyribonuclease activity and is known as the alkaline nuclease since optimal enzyme activity requires alkaline pH conditions (Strobel-Fidler & Francke, 1980, Costa *et al.*, 1983). The alkaline nuclease displays strong exonuclease activity and degrades both single- and ds DNA in the 5'-3' direction (Knopf & Weissart, 1990). This enzyme also exhibits a weaker endonuclease function that has a preference for supercoiled substrates (Hoffmann & Cheng, 1979). The alkaline nuclease is known to be a heavily phosphorylated protein (Banks *et al.*, 1983) and is phosphorylated by the HSV-1 encoded serine threonine protein kinase, US3 (Daikoku *et al.*, 1995). The protein also contains a number of potential phosphorylation sites for host cell protein kinases such as protein kinase C and casein kinase II (Draper *et al.*, 1986, Shao *et al.*, 1993). Thus, it is possible that phosphorylation may represent a system by which the endo- and exonuclease functions of the protein are activated/regulated. Despite various biochemical analyses of purified UL12 enzyme, little is known about the role of the alkaline nuclease *in vivo*.

A viral mutant lacking most of the UL12 coding region, AN-1, has provided some insight into the role of this enzyme *in vivo* (Weller *et al.*, 1990). AN-1 is severely compromised for overall growth, producing infectious virions at only 0.1-1% the level of wt virus and the impaired replication of this virus has been directly attributed to the loss of the exonuclease activity of UL12 (Goldstein & Weller, 1998a). AN-1 synthesises wt levels of viral DNA and near wt levels of nuclear DNA-containing capsids (Shao *et al.*, 1993). The UL12 enzyme therefore has no direct function in HSV-1 DNA synthesis or cleavage and packaging.

In non-complementing cells infected with AN-1, the virus appears defective at the point of capsid egress from the nucleus. In contrast to wt virus-infected cells, in which both

cytoplasmic and nuclear DNA-containing capsids were observed, only nuclear DNA-containing capsids were seen in non-complementing cells infected with AN-1 (Shao *et al.*, 1993). Furthermore, non-complementing cells infected with AN-1 accumulated increased numbers of A capsids, which presumably reflect abortive DNA packaging events (Shao *et al.*, 1993). These observations suggest that the alkaline nuclease plays a role in the production of stable DNA-containing capsids which are competent for egress from the nucleus. Replicating HSV-1 exists in a complex nonlinear state and contains branched structures that arise from recombination between replicated concatemers. Presumably, genomic DNA must be resolved into linear concatemers prior to encapsidation and UL12 is proposed to function at nicks and gaps in replicating DNA to correctly repair or process the replicating genome into a form suitable for packaging into the procapsid (Martinez *et al.*, 1996a, Goldstein & Weller, 1998b). Genomes which are cleaved and packaged in the absence of functional alkaline nuclease may retain a certain level of complexity such as small branches. Capsids containing these nonlinear genomes would be unstable and unable to exit from the nucleus (Shao *et al.*, 1993, Martinez *et al.*, 1996a).

The UL12 protein has been identified as part of a protein complex (together with ICP1/UL36) that bound HSV-1 DNA in an *a* sequence-specific manner (Chou & Roizman, 1989). Therefore, it is possible that the endo- and exonuclease function of UL12 may also be involved in the rapid degradation of genomic termini lacking *a* sequences whose formation is predicted in several HSV-1 DNA cleavage models (described in section 1.2.6.3) (Weller *et al.*, 1990).

c). UL12.5.

The UL12.5 protein is translated from an internal methionine codon of the UL12 gene to generate a 60 kDa amino-truncated version of the alkaline nuclease lacking the 126 N-terminal amino acids present in the UL12 protein (Bronstein & Weber, 1996, Martinez *et al.*, 1996b). Although the UL12.5 protein exhibits enzymatic properties identical to that of the full length alkaline nuclease it cannot functionally replace the full-length UL12 protein (Martinez *et al.*, 1996b, Bronstein *et al.*, 1997). The UL12 protein is not a component of capsids but the UL12.5 protein is found associated with extracellular virions and viral capsids (Bronstein *et al.*, 1997). These observations suggest that the UL12.5 protein may have a separate and more

direct role in the HSV-1 DNA cleavage and packaging process compared to that of UL12. The true function or significance of the UL12.5 protein remains unknown.

d). UL15.

The UL15 gene of HSV-1 contains two exons separated by genes UL16 and UL17 and is one of the very few genes known to yield spliced RNAs (McGeoch *et al.*, 1988). A cDNA copy of the UL15 gene producing a single, unspliced RNA can replace UL15 exons 1 and 2 without affecting the capacity of the virus to replicate in cultured cells, suggesting that splicing does not have a physiological role (Baines & Roizman, 1992). Nevertheless, all herpesviruses characterised to date have a spliced UL15 transcript. The UL15 protein displays limited homology with the bacteriophage T4 terminase protein, gp17 (Davison, 1992). Both proteins contain a putative ATP-binding motif known as the Walker A and B boxes and the predicted ATP-binding site of UL15 has been shown to be essential for the correct function of this protein (Yu & Weller, 1998a). The T4 terminase protein is involved in cleaving concatemeric phage DNA into genomic-length molecules prior to encapsidation (Rao & Black, 1988) and the homology between the two proteins suggested UL15 may have an analogous role in the HSV-1 DNA cleavage and packaging process. The UL15 protein was shown to function in the HSV-1 DNA packaging process in 1993, following the characterisation of a HSV-1 mutant, *ts66.4*, which had a *ts* lesion in the UL15 gene (Poon & Roizman, 1993). In cells infected at the NPT, viral DNA was synthesised but was not encapsidated and no DNA-containing capsids were observed in the nuclei of these cells (Poon & Roizman, 1993). A subsequent study demonstrated that the viral DNA generated in cells infected with *ts66.4* at the NPT was in an endless (concatemeric) form and the UL15 protein was therefore proposed to function as a terminase, cleaving concatemeric DNA into unit-length molecules for packaging into procapsids (Baines *et al.*, 1994).

The UL15 gene contains within its second exon a novel ORF that is translated in frame and is coterminal with the UL15 protein (Baines *et al.*, 1997, Yu *et al.*, 1997). This second protein is designated UL15.5 and is approximately 35 kDa in size compared to the full-length 83 kDa UL15 protein (Baines *et al.*, 1997). The UL15.5 protein is expressed in the absence of the UL15 protein, indicating that it does not result from the proteolytic cleavage of the full-length UL15 protein (Baines *et al.*, 1997). The functional significance of the UL15.5 protein is

unknown and a plasmid encoding UL15, but not UL15.5, is able to complement a UL15/UL15.5 null mutant virus (Yu & Weller, 1998a). This result demonstrated the UL15.5 gene product was dispensable for virus replication in cultured cells. In cells infected with a UL15 null mutant of HSV-1 (that still expressed UL15.5) enveloped B capsids were observed in the cytoplasm, suggesting that in the absence of UL15, envelopment of capsids occurs independently of viral DNA cleavage or the presence of DNA within the capsid (Baines *et al.*, 1997, Yu *et al.*, 1997). It is possible that, in addition to the proposed terminase function, UL15 may also have a role in blocking the envelopment of particles lacking DNA; thus, in the absence of this protein, envelopment may occur indiscriminately.

The UL15 protein associates with all capsid types, including procapsids (Sheaffer *et al.*, 2001). The capsid-binding ability of UL15 is presumably facilitated through an interaction with the VP5 major capsid protein since a complex of the two proteins has been immunoprecipitated from HSV-1-infected cells (SmithKline Beecham Corporation, 1998). A 509 amino acid carboxyl-terminally truncated form of the UL15 protein has been demonstrated to bind capsids and the protein domain responsible for interacting with VP5 is therefore likely to reside within this region of the UL15 protein (Salmon *et al.*, 1999). Proteins of 83 kDa, 80 kDa and 79 kDa, which react with a UL15 specific polyclonal antibody, associate with B capsids isolated from wt HSV-1 infected cells but not with B capsids purified from cells infected with a UL15 null mutant (Salmon & Baines, 1998). The 80 kDa and 79 kDa proteins are believed to result from proteolytic cleavage of the amino terminus of the full-length UL15 protein (Salmon *et al.*, 1999). The full-length 83 kDa protein is the predominant UL15 species present in C capsids isolated from cells infected with wt HSV-1 and it is the only UL15 species present in B capsids purified from cells infected with viruses lacking the HSV-1 UL6, UL17, UL28, UL32 and UL33 genes, which are essential for cleavage of concatemeric HSV-1 DNA (Salmon & Baines, 1998, Salmon *et al.*, 1999). However, all three forms of the UL15 protein are detected in capsids lacking the UL25 protein which is not essential for viral cleavage (Salmon *et al.*, 1999). These observations suggested that the proteolytic cleavage of the full-length UL15 protein, which generated the 79 kDa and 80 kDa UL15 species, was tightly linked to the cleavage of viral DNA and that in the absence of viral DNA maturation, the full-length UL15 protein was not proteolytically processed.

The UL15 protein interacts with the UL28 protein and this interaction is necessary to localise UL28 to the nuclei of cells expressing these two proteins alone (Koslowski *et al.*, 1999, Abbotts *et al.*, 2000). The UL28 protein specifically binds to elements within the HSV-1 *a* sequence and UL28 and UL15 proteins are believed to form a terminase complex analogous to that of the bacteriophage terminases (Adelman *et al.*, 2001). The stoichiometry of the UL15-UL28 interaction is unknown but the UL15 protein is capable of self-interaction and the possibility exists that the terminase complex may form multimers (Abbotts *et al.*, 2000).

e). UL17.

The UL17 protein is found associated with the tegument in virions (Salmon *et al.*, 1998) and with B and C capsids (Goshima *et al.*, 2000). In non-complementing cells infected with a UL17 null mutant virus, viral DNA was synthesised but was neither cleaved nor encapsidated and only B capsids were assembled in the nuclei (Salmon *et al.*, 1998). These observations indicated the UL17 protein was essential for the HSV-1 DNA cleavage and packaging process. The intracellular localisation of the HSV-1 capsid proteins has been examined in cells infected with the UL17 null mutant virus to determine whether the lack of functional UL17 affected the distribution of these proteins (Taus *et al.*, 1998). In the absence of the UL17 protein, UL6 protein, VP5 and VP22a did not localise to replication compartments of HEp-2 cells as observed in wt virus-infection (Taus *et al.*, 1998). Furthermore, in HEp-2 cells infected with the UL17 null mutant virus, large aggregates of capsids were detected surrounding the nuclear periphery as opposed to a more general, diffuse localisation seen in wt virus-infected cells (Taus *et al.*, 1998). These results led to the conclusion that the UL17 gene was required for correct targetting of capsids and major and minor capsid proteins to the DNA replication compartments of HEp-2 cells and that, in the absence of this function, viral DNA was not cleaved or packaged. Consistent with this idea is the observation that in wt HSV-1-infected Vero cells, UL17 colocalised with VP5 and VP22a in the nuclei (Goshima *et al.*, 2000).

f). UL25.

The UL25 protein is classed as a leaky-late gene and is found associated with all capsid types, including procapsids (Ali *et al.*, 1996, McNab *et al.*, 1998, Sheaffer *et al.*, 2001). The involvement of this protein in the HSV-1 DNA cleavage and packaging process was first

demonstrated in 1984 through the characterisation of *ts1204* and *ts1208*, two HSV-1 mutants that carry *ts* lesions in the UL25 gene (Addison *et al.*, 1984). In cells infected at the NPT, *ts1204* appeared incapable of penetrating the host cell plasma membrane (Addison *et al.*, 1984). This defect could be relieved through a brief incubation at the PT before shifting the temperature up to the NPT. Under these conditions, it was discovered that *ts1204* also had a defect in capsid assembly and DNA packaging. Following a shift-up to the NPT, *ts1204* assembled fewer capsids in the nuclei of infected cells than wt virus and no DNA-containing capsids were produced (Addison *et al.*, 1984). The *ts1208* virus did not exhibit an early defect but was also impaired in capsid assembly and DNA packaging (Addison *et al.*, 1984). Although the UL25 protein is now firmly believed to function in the HSV-1 DNA packaging process, no additional evidence exists to support a role in cellular penetration.

In non-complementing cells infected with KUL25NS, a UL25 null mutant virus, viral DNA was replicated and cleaved but was not packaged (McNab *et al.*, 1998). The UL25 protein is therefore unique amongst the HSV-1 DNA cleavage and packaging proteins since its function is not absolutely required for viral DNA cleavage. Additionally, the nuclei of KUL25NS-infected non-complementing cells contained a large amount of A capsids. This observation led to the suggestion that, in the absence of the UL25 protein, DNA is cleaved and packaged but not retained in the capsid, hence the large numbers of empty capsids seen in the nuclei of these cells (McNab *et al.*, 1998). The terminase proteins, UL15 and UL28, were found in higher amounts in B capsids isolated from cells infected with KUL25NS compared to B capsids purified from cells infected with wt virus (Yu & Weller, 1998b). This finding raised the possibility that in addition to retaining newly packaged DNA within the capsid, the UL25 protein may also function to enhance the turnover rate of the terminase by disassociating it from capsids.

In 2001 Ogasawara *et al.* (2001) published several observations concerning the biological properties of the UL25 protein. Using far-Western blot analysis of denatured capsid samples, these workers demonstrated that the UL25 protein was capable of interacting with both the VP5 and the VP19C proteins. On the basis of results obtained using immunogold labelling techniques to detect the location of capsid-bound anti-UL25 antibodies, Ogasawara *et al.* (2001) suggested that the UL25 protein associated with the capsid vertices and the capsid-binding property of UL25 was facilitated through an interaction with VP5 and/or VP19C. This

group went on to present data which indicated that the VP19C protein could translocate the UL25 protein to the nuclei of cells expressing these two viral proteins alone and this result provided further evidence for an interaction between UL25 and VP19C. Gel mobility shift analysis experiments indicated that the UL25 protein could bind HSV-1 DNA. However, since full-length genomic HSV-1 DNA was used to test the DNA-binding properties of UL25, it is not known whether this association was sequence-specific. An indirect observation resulting from the DNA-binding experiments was that the amino-terminal portion of the UL25 protein was not only capable of binding HSV-1 DNA but also formed homo-oligomers. Based on their observations, Ogasawara *et al.* (2001) concluded that the UL25 protein functioned to anchor the packaged viral genome within the capsid through a direct interaction with the DNA. Although some of the data presented by this group was consistent with the proposed function of UL25, these findings require further clarification and much of the data conflicted with that of previous studies.

The amount of UL25 protein associated with the capsid is not constant and varies within the different capsid types. Procapsids contain reduced amounts of UL25 protein relative to that in B capsids (4-6-fold less) (Sheaffer *et al.*, 2001). Moreover, C capsids contain the most UL25 protein and have levels 15-fold higher than that in procapsids (and 3-4-fold more than in B capsids) (Sheaffer *et al.*, 2001). The scaffold may have a role in regulating the amount of UL25 that can bind to the capsid since capsids formed in the absence of preVP22a contain significantly higher levels of UL25 than capsids assembled in the presence of preVP22a (Sheaffer *et al.*, 2000). These observations have led to the suggestion that during the DNA packaging process, the loss of the scaffold mediates the binding of additional UL25 to the capsid. This extra UL25 protein is then proposed to retain the DNA within the capsid. The gp4, gp10 and gp26 proteins of phage P22 have a similar function in the phage DNA packaging process and bind to the portal protein complex after the phage genome has been packaged to seal the DNA within the phage head by blocking the portal complex channel (Poteete & King, 1977, Strauss & King, 1984). The phenotype of mutants defective in these gene products is similar to that of KUL25NS; in infected bacterial cells the DNA-containing phage heads of the mutants were unable to retain their DNA and this resulted in the accumulation of empty phage heads (Poteete & King, 1977, Strauss & King, 1984). It is

possible that UL25 may retain packaged HSV-1 DNA within the capsid in an analogous manner, blocking or sealing the route of DNA entry.

The PRV UL25 homologue appears to exhibit some interesting biological properties and has been shown to bind specifically to the microtubule component of the cellular cytoskeletal structure (Kaelin *et al.*, 2000). At least a part of the PRV UL25 protein is also located on the capsid surface and since infecting HSV-1 capsids are believed to utilise the microtubule network in order to reach the nucleus (Sodeik *et al.*, 1997), these findings raise the possibility that UL25 may play a role in the intracellular transport of capsids. However, this hypothesis remains unproven.

g). UL28.

In cells infected at the NPT with *ts1203*, a HSV-1 mutant containing a *ts* defect in the UL28 gene, viral DNA was replicated but was neither cleaved nor packaged and only B capsids were observed in the nuclei (Addison *et al.*, 1990). These findings indicated the function encoded by the UL28 gene was essential for the HSV-1 cleavage and packaging reaction. The UL28 protein is present in all capsid types, including procapsids (Taus & Baines, 1998, Yu & Weller, 1998b, Sheaffer *et al.*, 2001). However, the amount of UL28 protein is reduced in DNA-containing capsids and is absent from virions, suggesting that the association of this protein with the capsid is only transient and is linked to the cleavage and packaging process (Taus & Baines, 1998, Yu & Weller, 1998b). The UL28 protein is capable of binding to B capsids lacking the UL6, UL15 or UL25 proteins although it is not known whether the absence of UL17 protein can affect the capsid-binding property of UL28 (Taus & Baines, 1998, Yu & Weller, 1998b).

As mentioned in section 1.2.6.6d, the UL28 and UL15 proteins directly interact with each other and this interaction results in the translocation of UL28 to the nuclei of cells expressing these two proteins alone (Koslowski *et al.*, 1999, Abbotts *et al.*, 2000). The terminase of icosahedral dsDNA bacteriophages is composed of two subunits and, in light of the homology between UL15 and the large subunit of the T4 terminase, it is likely that the UL28 protein is the second subunit of the HSV-1 terminase, especially since the HCMV UL28 homologue has been shown to bind the DNA cleavage and packaging signals of this virus (Bogner *et al.*, 1998). This hypothesis was reinforced recently by the finding that the HSV-1 UL28 bound to

the *pac1* homology element of the *a* sequence from the HSV-1 genome in a sequence- and structure-specific manner (Adelman *et al.*, 2001). DNA fragments containing the *pac1* motif were induced by heat treatment to form novel, non-duplex DNA structures which were high-affinity substrates for the UL28 protein (Adelman *et al.*, 2001). The protein did not bind to dsDNA of identical sequence composition and it was also discovered that only one DNA strand of the *pac1* motif was responsible for the formation of novel DNA structures to which UL28 specifically bound (Adelman *et al.*, 2001). The way in which UL28 is proposed to bind DNA is similar to the mechanism by which the UL9 protein interacts with the HSV-1 *oriS*. High-affinity binding of UL9 to *oriS* involves the formation of novel DNA structures in which parts of the *oriS* are extruded as single strands. The separate strands adopt different structures, only one of which is bound tightly by UL9 (Aslani *et al.*, 2000). The exact conformation which the novel *pac1* structures adopt following heat treatment and whether these novel structures pre-exist within newly replicated viral DNA, or are induced to form during the cleavage and packaging reaction, are currently unknown.

h). UL31.

The UL31 protein is a non-capsid associated phosphoprotein which has been found to associate with the nuclear matrix (Chang & Roizman, 1993). In non-complementing cells infected with a UL31 null mutant, viral DNA is replicated, cleaved and packaged but both the yields of viral DNA synthesis and the extent of concatemer cleavage are reduced compared to wt virus-infected cells (Chang *et al.*, 1997). These results have led to the suggestion that, although the UL31 gene product is not directly involved in the HSV-1 DNA cleavage and packaging process, its function is to form a network to which the viral proteins involved in DNA replication and/or cleavage and packaging are anchored within the nucleus (Chang *et al.*, 1997). This hypothesis is supported by the observation that UL31 interacts with the UL34 gene product, which is believed to be involved in the intracellular transport of capsids (Ye *et al.*, 2000, Reynolds *et al.*, 2001). The UL34 protein localises to the nuclear membranes and it is therefore possible that at the nuclear membrane, the UL34 protein anchors a nuclear network containing UL31 which, in turn, enables efficient packaging of DNA into procapsids (Ye *et al.*, 2000).

i). UL32.

The UL32 protein is a non-capsid associated protein essential for HSV-1 DNA cleavage and packaging (Schaffer *et al.*, 1973). The amino acid sequence of the UL32 protein contains potential N-linked glycosylation sites and sequences that are conserved in aspartyl proteases and in zinc-binding proteins (Chang *et al.*, 1996). However, no UL32 specific proteolytic activity has been demonstrated and the corresponding sequences are dispensable for virus replication in tissue culture cells (Chang *et al.*, 1996). In non-complementing cells infected with *hr64*, a UL32 insertion mutant, HSV-1 DNA was replicated to wt virus levels but was not cleaved or packaged and only B capsids were observed in the nuclei (Lamberti & Weller, 1998). Furthermore, the capsids were more diffusely distributed throughout the nuclei and were not restricted to replication compartments as seen in wt virus-infected cells (Lamberti & Weller, 1998). These results suggest that UL32 may function to localise preassembled capsids to the nuclear sites where DNA cleavage and packaging occur. Although the proposed role of UL32 does not involve a direct association with the cleavage and packaging machinery its presence is, nevertheless, essential for this process to take place.

j). UL33.

Consistent with the phenotype of other HSV-1 DNA cleavage and packaging mutants, in cells infected with the UL33 *ts* mutant, *ts1233*, replicated viral DNA was neither cleaved nor packaged and only B capsids were observed in the nuclei, indicating the UL33 protein is essential for the HSV-1 DNA cleavage and packaging process (Al-kobaisi *et al.*, 1991). The UL33 protein does not associate with capsids and localises to nuclear replication compartments during wt virus-infection (Reynolds *et al.*, 2000). This may be a consequence of an interaction with the UL14 protein which has been shown to affect the intracellular localisation of a number of HSV-1 encoded proteins (Yamauchi *et al.*, 2001). Nothing further is known about the function of UL33 and the absence of UL31, UL32 and UL33 cleavage and packaging proteins from the HSV-1 capsid suggest they play very different roles from those of the minor capsid-associated cleavage and packaging proteins. Possible functions include steps in the cleavage and packaging process that only require a transient association with the capsid, chaperone-like functions to ensure the correct assembly of the cleavage and packaging machinery or intracellular transport of the DNA cleavage and packaging components.

CHAPTER 2

MATERIALS AND METHODS

2.1 Materials.

2.1.1 Chemicals and Reagents.

The majority of analytical grade chemicals and reagents were obtained from Sigma Chemical Co. Ltd. and BDH Laboratory Supplies. The exceptions are tabulated below :

Table 2.1 Chemicals and Reagents.

CHEMICAL/REAGENT	SUPPLIER
Ethanol 100%	Joseph Mills (denaturants) Ltd
Acetic Acid	PROLABO
30% (w/v) Acrylamide : 0.8% Bis-Acrylamide Stock Solution (37.5:1)	National Diagnostics
Ammonium Persulphate	BIO-RAD
Amylose Resin	New England Biolabs
Benzyl dimethylamine (BDMA)	Agar Aids
Chloroform	PROLABO
Dried Skimmed Milk	Marvel
Electron Microscopy Grade 25% Glutaraldehyde	Agar Scientific Ltd
EN ³ HANCE	NEN Life Science Products
Glycerol	PROLABO
LipofectAMINE	Gibco BRL
Medium Grade Electron Microscopy Resin and Hardener	TAAB Laboratories
Methanol	PROLABO
Mowiol 4-88	Hoechst
Ni-NTA Agarose	Qiagen
Osmium Tetroxide	TAAB Laboratories
Propan-2-ol	PROLABO
Protease Inhibitor Cocktail Tablets	Boehringer Mannheim
SeaPlaque Agarose	Flowgen Instruments Ltd
Sodium Chloride	PROLABO

2.1.2 Additional Materials.

Additional materials and their suppliers are tabulated below :

Table 2.2 Additional Materials.

ADDITIONAL MATERIAL	SUPPLIER
10 ml Columns for Protein Purification	BIO-RAD
Dialysis Tubing	Medicell International Ltd.
Fibracel Disks	Bibby Sterilin Ltd.
Hybond-XL Membrane	AmershamPharmacia Biotech
Hybond-ECL Membrane	AmershamPharmacia Biotech
Phosphorimager Screen and Cassette	BIO-RAD
500 ml Spinner Culture Vessel	New Brunswick Scientific
250 ml 0.22 μ m Stericup Filter	Millipore
X-Omat UV Film	Kodak

2.1.3 Solutions.

Table 2.3 Solutions.

SOLUTION	COMPOSITION
Alkaline Transfer Solution	400 mM NaOH, 600 mM NaCl.
Amylose Resin Column Buffer	20 mM Tris.HCl pH 7.5, 200 mM NaCl, 1 mM EDTA.
Denatured Calf Thymus DNA	5 mg.ml ⁻¹ in TE, phenol/chloroform extracted, quantitated by UV absorbance, incubated at 100°C for 10 minutes.
2x CLB (Cell Lysis Buffer)	20 mM Tris.HCl pH 7.5, 2 mM EDTA, 1.2% w/v SDS.
Coomassie Blue Stain	0.2% w/v Coomassie blue in polyacrylamide gel fix.
CSK Buffer	10 mM PIPES pH 6.8, 100 mM KCl, 300 mM sucrose, 2.5 mM MgCl ₂
DNase Storage Buffer	20 mM Tris.HCl pH 7.6, 50 mM NaCl, 1 mM DTT, 50% v/v Glycerol, 0.1 mg.ml ⁻¹ BSA.
Formyl Dye Solution	0.1% w/v bromophenol blue, 0.1% w/v xylene-cyanol, 20 mM Na ₂ EDTA in deionised formamide.
5x HEPES Buffered Saline	680 mM NaCl, 25 mM KCl, 3.5 mM Na ₂ HPO ₄ , 28 mM D-glucose, 100 mM HEPES pH 7.05
His-UL25 Harvest / Binding Buffer	20 mM Tris.HCl pH 7.0, 5 mM imidazole, 10 mM CHAPS, 10% v/v glycerol, 10% v/v DMSO, 1M NaCl.
His-UL25 Elution Buffer	20 mM Tris.HCl pH 7.0, 1 M imidazole,

	10 mM CHAPS, 10% v/v glycerol, 10% v/v DMSO, 1M NaCl.
His-UL25 Wash Buffer	20 mM Tris.HCl pH 7.0, 60 mM imidazole, 10 mM CHAPS, 10% v/v glycerol, 10% v/v DMSO, 1M NaCl.
IF Fixing Solution	5% v/v formaldehyde, 2% w/v sucrose in PBSA.
IF Permeabilisation Solution	0.5% v/v NP40, 10% w/v sucrose in PBSA.
IP Buffer	25 mM Tris.HCl pH 7.5, 25 mM NaCl, 0.5% (v/v) NP40
3% LGT Agarose	3% w/v SeaPlaque agarose in H ₂ O.
Lysis Buffer	10 mM Tris.HCl pH 7.5, 10 mM NaCl, 2 mM MgCl ₂ , 0.5% (v/v) NP-40.
MAB Elution Buffer	100 mM glycine.HCl pH 2.7.
MAB Neutralisation Buffer	1 M Tris.HCl pH 9.0.
MAB Start Buffer	10 mM Na ₂ HPO ₄ , 10 mM NaH ₂ PO ₄ , pH 7.0.
Methyl Cellulose	3% w/v carboxymethylcellulose sodium salt in H ₂ O.
Membrane Wash Buffer	0.2x SSC, 0.1% w/v SDS.
Mowiol	100 mM Tris.HCl pH 8.5, 10% w/v Mowiol 4-88, 25% v/v glycerol, 2.5% v/v 1,4-diazobicyclo-[2.2.2]-octane.
NaCl / EDTA Mix	4 M NaCl, 50 mM EDTA pH 8.0.
Neutralising solution	500 mM Tris.HCl pH 7.0, 1 M NaCl.
NTE (purification of HSV-1 capsids)	20 mM Tris.HCl pH 8.0, 500 mM NaCl, 1 mM EDTA.
NTE (production of HSV-1 DNA)	10 mM Tris.HCl pH 7.6, 100 mM NaCl, 1 mM EDTA.
Oligonucleotide Gel Elution Buffer	20 mM Tris.HCl pH 7.5, 0.5 M CH ₃ COONH ₄ (pH 7.0), 2 mM EDTA, 0.1% (w/v) SDS.
PBS Complete	170 mM NaCl, 3.4 mM KCl, 10 mM Na ₂ HPO ₄ , 6.8 mM CaCl ₂ , 4.9 mM MgCl ₂ .
Phenol / Chloroform / Isoamylalcohol	TE saturated phenol : chloroform : isoamylalcohol 25:24:1.
Polyacrylamide Gel Destain	5% v/v methanol, 7% v/v acetic acid in H ₂ O.
Polyacrylamide Gel Fix	50% v/v methanol, 7% v/v acetic acid in H ₂ O.
PGEB (Polyacrylamide Gel Electrophoresis Buffer)	50 mM Tris base, 35 mM glycine, 0.1% w/v SDS.
PGSB (Polyacrylamide Gel Sample Buffer)	125 mM Tris.HCl pH 6.8, 20% glycerol, 4% w/v SDS, 5% v/v 2-mercaptoethanol, 0.01% w/v bromophenol blue.
RSB	10 mM Tris.HCl pH 7.5, 10 mM KCl, 1.5

	mM MgCl ₂ .
4x RGB (Running Gel Buffer)	1.5 M Tris.HCl pH 8.8, 0.4% w/v SDS.
4x SGB (Spacer Gel Buffer)	500 mM Tris.HCl pH 6.8, 0.4% w/v SDS.
0.8 M Sodium Phosphate Buffer	700 mM Na ₂ HPO ₄ , 100 mM NaH ₂ PO ₄ , pH 7.4.
Southern Hybridisation Buffer	500 mM sodium phosphate buffer pH 7.4, 7% w/v SDS.
Southern Pre-Hybridisation Buffer	500 mM sodium phosphate buffer pH 7.4, 7% w/v SDS, 100 µg.ml ⁻¹ denatured calf thymus DNA (sheared).
20x SSC	3 M NaCl, 300 mM tri-sodium citrate.
STET Buffer	8% w/v sucrose, 5% v/v Triton X-100, 50 mM EDTA, 50 mM Tris.HCl pH 8.0.
Sucrose Buffer	10 mM Tris.HCl pH 7.5, 10 mM NaCl, 2 mM MgCl ₂ , 10% (w/v) sucrose.
1x T4 DNA Ligase Buffer	50 mM Tris.HCl pH 7.5, 10 mM MgCl ₂ , 10 mM dithiothreitol, 1 mM ATP, 25 µg.ml ⁻¹ bovine serum albumin.
1x TAE	40 mM Tris.acetate, 1 mM EDTA.
1x TBE	90 mM Tris base, 89 mM boric acid, 1 mM EDTA.
TE	10 mM Tris.HCl pH 7.5, 1 mM EDTA.
TER	TE + 20 µg.ml ⁻¹ RNase A
Tris Saline	20 mM Tris.HCl pH 7.5, 500 mM NaCl
Trypsin	0.25% w/v trypsin in Tris saline.
Versene	0.6 mM EDTA, 0.02% phenol red in PBS lacking MgCl ₂ and CaCl ₂ .

2.1.4 Enzymes.

Restriction endonuclease enzymes and buffers were supplied by New England Biolabs or Boehringer Mannheim. Other enzymes and their suppliers are tabulated below :

Table 2.4 Enzymes.

ENZYME	SUPPLIER
Dnase 1	Sigma Chemical Co. Ltd.
Lysozyme (from chicken egg whites)	
Protease XIV (pronase from <i>S.griseus</i>)	
Proteinase K	
Rnase A	
<i>Staphylococcus aureus</i> Protein-A - Horseradish Peroxidase Conjugate	
Calf Intestinal Phosphatase	Boehringer Mannheim
T4 DNA Ligase	New England Biolabs

2.1.5 Radiochemicals.

^{35}S L-Methionine at $1175 \text{ Ci.mmol}^{-1}$ ($10 \mu\text{Ci. } \mu\text{l}^{-1}$) and $5'$ [α - ^{32}P] deoxyribonucleoside triphosphates at $3000 \text{ Ci.mmol}^{-1}$ ($10 \mu\text{Ci. } \mu\text{l}^{-1}$) were supplied by NEN Radiochemicals.

2.1.6 Immunological Reagents.

Table 2.5 Immunological Reagents.

NAME	REAGENT	SPECIFICITY	SUPPLIER / REFERENCE
DM165	Mouse monoclonal antibody	HSV-1 VP5	Dr F.J. Rixon
MCA406	Mouse monoclonal antibody	HSV-1 UL26.5 Gene Product	Serotec
NC1	Rabbit polyclonal antibody	HSV-1 VP5	Dr G. Cohen
NC2	Rabbit polyclonal antibody	HSV-1 VP19C	Dr G. Cohen
166	Mouse monoclonal antibody	HSV-1 UL25 Gene Product	Produced by S. Graham and P. Targett-Adams
184	Rabbit polyclonal antibody	HSV-1 VP5	Dr F.J. Rixon
186	Rabbit polyclonal antibody	HSV-1 VP23	Dr F.J. Rixon
335	Rabbit polyclonal antibody	HSV-1 UL25 Gene Product	Dr V.G. Preston
Anti mouse-FITC	Goat polyclonal antibody – fluorochrome conjugate	Mouse Immunoglobulin G	Sigma Chemical Co. Ltd
Anti rabbit-FITC	Goat polyclonal antibody – fluorochrome conjugate	Rabbit Immunoglobulin G	Sigma Chemical Co. Ltd
Anti rabbit-Texas Red	Goat polyclonal antibody – fluorochrome conjugate	Rabbit Immunoglobulin G	Sigma Chemical Co. Ltd
Anti rabbit-Cy5	Goat polyclonal antibody – fluorochrome conjugate	Rabbit Immunoglobulin G	Amersham-Pharmacia Biotech
<i>Staphylococcus aureus</i> Protein-A immobilised on sepharose beads	Immunoglobulin binding protein-sepharose conjugate	Non-species specific Immunoglobulin G	Sigma Chemical Co. Ltd

2.1.7 Plasmids.

Table 2.6 Plasmids.

PLASMID	DESCRIPTION	REFERENCE / SUPPLIER
pAcCL29.1	Baculovirus transfer vector.	Livingstone & Jones, 1989
pAT153	Probe for the detection of pSA1 in Southern blot hybridisation.	Twigg & Sherratt, 1980
pCMV10	Mammalian transient protein expression vector.	White & Cipriani, 1989, Stow <i>et al.</i> , 1993
pMAL-c2	Maltose binding protein fusion vector.	New England Biolabs
pSA1	pAT153 containing HSV-1 $O_{r}S$ replication and u_{c} -DR1- u_{b} packaging sequence.	Dr N. Stow
pPTA3	pMAL-c2 containing HSV-1 UL25 ORF, encoding MBP-UL25 fusion protein.	Generated by Paul Targett-Adams
pPTA5	pUC19 containing HSV-1 UL25 ORF.	Generated by Paul Targett-Adams
pPTA8/76	pUC19 containing polyhistidine-tagged UL25 ORF.	Generated by Paul Targett-Adams
pPTA10/9	pAcCL29.1 baculovirus transfer vector containing polyhistidine-tagged UL25 ORF.	Generated by Paul Targett-Adams
pUC19	Vector for the manipulation of cloned DNA.	New England Biolabs

2.1.8 Bacterial Strains and Culture Media.

Plasmids were manipulated and propagated in *E. coli* strain DH5 α . Recombinant proteins were expressed in *E. coli* strains BL21 and BL21(DE3). All bacteria were grown in L-broth supplemented with 50 $\mu\text{g.ml}^{-1}$ of ampicillin, and 100 $\mu\text{g.ml}^{-1}$ of chloramphenicol when appropriate. Bacterial stocks containing plasmids were stored at -70°C in growth media containing 7.5% DMSO.

2.1.9 Cell Lines.

Baby hamster kidney (BHK) 21 clone 13 cells (MacPherson & Stocker, 1962), Vero cells (Rhim & Schell, 1967) and Sf21 (Vaughn *et al.*, 1977) cells were obtained from Dr V.G. Preston and routinely used during the course of this study. G5-11 cells were used to complement the K23Z null mutant virus and 8-1 cells were used to complement the K25NS null mutant virus. Both complementing cell lines were kindly supplied by S. Person (Desai *et al.*, 1993). A HSV-1 UL19 transformed rabbit skin cell line (generated by Dr V.G. Preston) was used to complement the K5 Δ Z null mutant virus. Hybridoma cell lines were constructed by Susan Graham at the Institute of Virology.

2.1.10 Cell Culture Media.

All cell culture media were supplied by Gibco BRL. BHK21 C13 cells were maintained in Glasgow modified Eagle's medium (GMEM) supplemented with 10% (v/v) newborn calf serum, 10% (v/v) tryptose phosphate broth, 100 units.ml⁻¹ of penicillin, 100 μ g.ml⁻¹ of streptomycin, 0.25% (v/v) sodium bicarbonate and 2 mM L-glutamine. Fully supplemented GMEM was designated as EC10.

Vero cells were maintained in Dulbecco's modified Eagle's media (DMEM) supplemented with 10% (v/v) foetal bovine serum, 100 units.ml⁻¹ of penicillin, 100 μ g.ml⁻¹ of streptomycin and 2 mM L-glutamine. Fully supplemented DMEM was designated as DC10.

Sf21 cells were maintained in TC100 media supplemented with 5% (v/v) foetal bovine serum, 100 units.ml⁻¹ of penicillin and 100 μ g.ml⁻¹ of streptomycin. Fully supplemented TC100 was designated as TC5.

G5-11 and 8-1 cells were constructed from Vero cells and were therefore maintained in DC10.

Hybridoma cell lines were maintained in DMEM supplemented with 1x HAT medium (a 50x solution from Sigma Chemical Co. Ltd. contained 5 mM hypoxanthine, 50 μ M aminopterin and 800 μ M thymidine), 10% (v/v) foetal bovine serum, 100 units.ml⁻¹ of penicillin, 100 μ g.ml⁻¹ of streptomycin and 1 mM L-glutamine. Fully supplemented hybridoma medium was designated HATc.

2.1.11 Viruses.

HSV-1 strains 17⁺ (McGeoch *et al.*, 1985, McGeoch *et al.*, 1988), 17 syn (Brown *et al.*, 1973) and KOS (Holland *et al.*, 1983) were obtained from the Institute of Virology stocks. The HSV-1 *ts* mutants of strain 17⁺ used in this investigation were *ts*1204 and *ts*1208 (Addison *et al.*, 1984) and were obtained from Dr V.G. Preston. *Ts*2 (Pertuiset *et al.*, 1989), a *ts* mutant of the syncytial strain A44, was also supplied by Dr V.G. Preston. A *ts*⁺ marker rescue virus of *ts*2 was constructed and termed *ts*2/Hindk MR#6. The HSV-1 null mutants of strain KOS used in this investigation were KUL25NS (UL25 null mutant) (McNab *et al.*, 1998), K5 ΔZ (UL19 null mutant), K23Z (UL18 null mutant) (Desai *et al.*, 1993) and K Δ 19C (UL38 null mutant) (Person & Desai, 1998). These viruses were kindly supplied by S. Person. A UL28 null mutant of strain KOS was also used (Tengelsen *et al.*, 1993). A recombinant baculovirus expressing a polyhistidine tagged HSV-1 UL25 protein, referred to as PTA10bac#14, was generated. Other recombinant baculoviruses used in this investigation were Ac26.5/19/38, which expressed the HSV-1 UL26.5, UL19 and UL38 genes; Ac26/18/35, which expressed the HSV-1 UL26, UL18 and UL35 genes (both constructed by J. McVicar, Institute of Virology); AcUL25, which expressed the HSV-1 UL25 gene (constructed by Dr V.G. Preston, Institute of Virology) and Ac19/38 which expressed the HSV-1 UL19 and UL38 genes (obtained from Dr F.J. Rixon, Institute of Virology).

2.2 Methods.

2.2.1 Tissue Culture.

2.2.1.1 Serial Passage of Cells.

BHK, Vero, G5-11, 8-1 and hybridoma cell lines were incubated at 37°C in an atmosphere supplemented with 5% CO₂. Sf21 cells were incubated at 28°C in an unsupplemented atmosphere. The various cell lines were passaged in the appropriate media as described in section 2.1.2

Tissue culture flasks (175 cm²) were seeded with 1-2 x 10⁶ cells. Confluent BHK, Vero and G5-11 monolayers were washed with 20 ml of versene followed by a 40 ml wash with trypsin:versene (1:1 v/v) and the trypsinised cells were resuspended in 10 ml of the appropriate medium. Hybridoma and Sf21 cell monolayers were disrupted by agitation and resuspended in 10 ml of appropriate medium. An aliquot of the resuspended cells was used to seed another 175 cm² tissue culture flask. BHK cells were discarded after 10 passages, other cell lines were discarded after approximately 30 passages.

2.2.1.2 Storage of Cells.

The cells from confluent 175 cm² tissue culture flasks were harvested as previously described, pelleted by centrifugation at 1500 rpm in a Sorvall RT6000B centrifuge for 5 minutes at 4°C and resuspended in the appropriate medium containing 10% (v/v) DMSO. Cells were stored in 2 ml vials at a concentration of approximately 1 x 10⁷ cells.ml⁻¹. The vials were cooled slowly to -70°C and then transferred to liquid nitrogen storage (-140°C).

The cells were recovered from storage by thawing the contents of the vial and transferring the cells to 9 ml of the appropriate medium (without DMSO). The cells were pelleted by centrifugation at 1500 rpm in a Sorvall RT6000B centrifuge for 5 minutes at 4°C and resuspended in 10 ml of the appropriate medium prior to seeding a 175 cm² tissue culture flask.

2.2.2 Virus Culture and Purification.

2.2.2.1 Production of HSV-1 Stocks.

Stocks of wt HSV-1 strain 17 and *ts* mutants were produced in BHK cells. K23Z null mutant virus was propagated in G5-11 cells, K5 Δ Z was grown in UL19 transformed rabbit skin cells and K25NS was cultivated in 8-1 cells.

A confluent monolayer of the appropriate cell type in a 850 cm² plastic roller bottle was infected with virus at a moi of 0.003 pfu per cell in 20 ml of cell culture medium. After an adsorption period of 1 hour at 37°C, 50 ml of fresh medium was added to the virus-infected cells and incubation continued at 31°C for 3-4 days until extensive cpe had developed. The virus-infected cells were harvested into the medium by agitation and pelleted by centrifugation at 1500 rpm in a Sorvall RT6000B centrifuge for 10 minutes at 4°C. Cell-associated virus was prepared by sonicating the virus-infected cell pellet in a small amount of medium in a sonicating waterbath until the sample was homogenous. Cellular debris was removed by centrifugation as before and the cell-associated virus stock was divided into aliquots and stored at -70°C.

The clarified culture medium was centrifuged at 12,000 rpm in a Sorvall SLA1500 rotor for 2 hours at 4°C to pellet cell-released virus. The cell-released virus was resuspended in GMEM supplemented with 20% (v/v) newborn calf serum and stored at -70°C in 100 μ l aliquots.

2.2.2.2 Preparation of High Titre Recombinant Baculovirus Stock.

Plastic roller bottles (850 cm²) were seeded with 6 x 10⁷ Sf21 cells in 300 ml of TC5 and incubated at 28°C. When a density of 5 x 10⁵ cells.ml⁻¹ was reached, the cells were infected with recombinant baculovirus at a moi of 0.1 pfu per cell and incubation was continued at 28°C. At 6 days pi the virus-infected cells were removed from the medium by centrifugation at 3000 rpm in a Sorvall SLA3000 rotor for 5 minutes at 4°C and the clarified medium was centrifuged at 12,000 rpm in a Sorvall SLA1500 rotor for 2 hours at 4°C. Each virus pellet was resuspended in 2 ml of TC5, transferred to a sterile glass universal bottle and sonicated using a sonicating waterbath to disperse the virus. The virus was stored at -70°C in 1 ml aliquots.

2.2.2.3 Sterility of Viral Stocks.

The sterility of viral stocks was checked by streaking a sample onto blood agar plate. The plates were incubated at 31°C for up to 5 days and any viral stocks containing bacterial contamination were discarded.

2.2.2.4 Titration of HSV-1.

Tissue culture dishes (35 mm) were seeded with 8×10^5 cells per dish in 2 ml of growth medium. The following day the medium was removed and the cells were infected with 100 μ l of virus serially diluted 10-fold in growth medium (or PBS complete containing 5% newborn calf serum). Titrations of wt virus and the null mutant viruses used in this study were carried out at 37°C. Titrations of the *ts* mutant viruses used in this study were performed at 31°C, the PT, and 39.2°C, the NPT, with the exception of *ts1208* which was incubated at a NPT of 39.5°C. After a 1 hour adsorption period at the appropriate temperature the virus inoculum was removed and 2 ml of medium containing 5% human serum was added to the virus-infected cells to prevent secondary plaque formation. Incubation was continued at the appropriate temperature until plaques were clearly visible. The monolayers were fixed and stained with Giemsa stain for 10 minutes at room temperature. The stain was removed with running water and the plaques were counted using a dissecting microscope.

2.2.2.5 Titration of Recombinant Baculovirus (Brown & Faulkner, 1977).

Tissue culture dishes (35 mm) were seeded with 1×10^6 Sf21 cells per dish in 2 ml of TC5. The following day the medium was removed and the cells were infected with 100 μ l of recombinant baculovirus serially diluted 10-fold in TC5. After a 1 hour adsorption period at room temperature the virus inoculum was removed and 1.5 ml of 3% LGT agarose:TC5 (1:1, v/v) at 45°C was added to the virus-infected cells. When the agarose had set 1.5 ml of TC5 was added to each of the dishes which were then incubated at 28°C. At 4 or 5 days pi, the liquid overlay was removed and replaced with 1 ml of TC5 containing 0.5% neutral red and 250 μ g.ml⁻¹ of X-gal. After 3-4 hours incubation at 28°C, the stain was removed and the dishes were left at 28°C overnight in an inverted position. The following day plaques were counted if a viral titre was required or picked into 1 ml of TC5 for plaque purification.

2.2.2.6 Purification of HSV-1 Virions (wt and *ts* mutants).

Confluent monolayers of BHK cells in 850 cm² plastic roller bottles were infected with HSV-1 at a moi of 0.002 pfu per cell in 20 ml of EC10. After the virus had been adsorbed to the cells for 1 hour at 37°C, 50 ml of fresh EC10 was added and incubation was continued at 31°C for 5 days until extensive cpe had developed. The virus-infected cells were harvested into the medium by agitation and pelleted by centrifugation at 3000 rpm in a Sorvall RT6000B centrifuge for 10 minutes at 4°C. The supernatants were pooled and centrifuged at 12,000 rpm in a Sorvall SLA1500 rotor for 2 hours at 4°C and the resulting pellet was resuspended in 1 ml of EC10 by sonication in a sonicating water bath. A 5-15% w/v ficoll gradient in 1x Eagles without phenol red was prepared in a Beckman 25 x 89 mm centrifuge tube using a Biocomp Gradient Master and the resuspended pellet was gently layered on top. The gradient was centrifuged at 12,000 rpm in a Sorvall AH629 rotor for 2 hours at 4°C. Virion bands were visualised by light scattering and harvested by puncturing the centrifuge tube just below the virion band with an 18G syringe needle attached to a 5 ml syringe. The virions were transferred to a fresh Beckman 25 x 89 mm centrifuge tube, diluted with 1x Eagles (without phenol red) and pelleted by centrifugation at 20,000 rpm in a Sorvall AH629 rotor for 1 hour at 4°C. The virion pellet was resuspended in 1x Eagles (without phenol red) supplemented with 20% (v/v) foetal bovine serum by sonication as before, divided into aliquots and stored at -70°C.

2.2.2.7 Purification of HSV-1 Capsids.

a). Purification of HSV-1 Capsids from Wt Virus-Infected Cells.

Confluent monolayers of BHK cells in 850 cm² plastic roller bottles were infected with HSV-1 17 at a moi of 5 pfu per cell in 20 ml of EC10. After the virus was adsorbed for 1 hour at 37°C, 50 ml of fresh EC10 was added to the cells and incubation was continued at 37°C for 14–18 hours. The virus-infected cells were harvested by washing with NTE containing 1% NP40 in a final volume of 100 ml and pelleted by centrifugation at 3000 rpm in a Sorvall RT6000B centrifuge for 10 minutes at 4°C. The resulting pellet (nuclei) was washed with 50 ml of NTE complete containing 1% NP40, centrifuged as before and resuspended in 50 ml of NTE containing 1% NP40. The nuclei were disrupted by sonication using a probe sonicator and the debris was removed by centrifugation. The supernatant was layered on to a 5 ml 40% (w/v) sucrose cushion (in NTE) in a Beckman 25 x 89 mm centrifuge tube and the sample was centrifuged at 25,000 rpm in a Sorvall

AH629 rotor for 1 hour at 4°C. The resulting pellet was resuspended in 2 ml of NTE containing 1% NP40 and loaded onto 10-40% sucrose (w/w in NTE) gradients, prepared in Beckman 14 x 95 mm centrifuge tubes using a Biocomp Gradient Master, and centrifuged at 40,000 rpm in a Sorvall TST41.14 rotor for 20 minutes at 4°C. A, B and C capsid bands were visualised by light scattering and harvested separately by puncturing the centrifuge tube with 18G syringe needles attached to 5 ml syringes. The A, B and C capsid samples were each transferred to a fresh Beckman 14 x 95 mm centrifuge tube, diluted with NTE and pelleted by centrifugation at 25,000 rpm in a Sorvall TST41.14 rotor for 1.5 hours at 4°C. The capsid pellets were resuspended in 100 µl of NTE using a sonicating water bath and stored at -70°C.

b). Purification of Recombinant B Capsids from *Sf21* Cells Infected with Recombinant Baculoviruses.

Plastic roller bottles (850 cm²) were each seeded with 2×10^7 *Sf21* cells in 100 ml of TC5. The cells were incubated at 28°C for 2-3 days until a density of 1×10^6 cells.ml⁻¹ was reached. At this point, 200 ml of fresh TC5 medium was added to the roller bottles and incubation was continued at 28°C until a density of $0.8-1.0 \times 10^6$ cells.ml⁻¹ was reached (usually the next day). The cells were then infected with Ac26.5/19/38 and Ac26/18/35 recombinant baculoviruses at a moi of 5 pfu per cell of each virus (and on occasion with AcUL25 as well). At approximately 70 hours pi the virus-infected cells were pelleted by centrifugation at 3000 rpm in a Sorvall RT6000B centrifuge for 10 minutes at 4°C and resuspended in 30 ml of NTE containing 1% NP40. The cell extract was sonicated using a probe sonicator and capsids were purified in a similar manner to HSV-1 capsids from wt virus-infected cells. The purified capsids were centrifuged through a second sucrose gradient to remove non-capsid associated proteins, then harvested as before. In an alternative protocol, the second sucrose gradient was fractionated into 0.5 ml aliquots and the protein content of these fractions was examined by Western blot analysis.

c). Purification of VP5-19C Particles from *Sf21* Cells Infected with Recombinant Baculoviruses.

This protocol was identical to that of section 2.2.2.7b with the exception that Ac19/38 and, on occasion, AcUL25 were used to infect *Sf21* cells.

2.2.3 The Generation of a Polyhistidine-Tagged UL25 Expressing Recombinant baculovirus.

2.2.3.1 Overview of the Baculovirus Expression System.

To produce a recombinant baculovirus that expresses a gene of interest, the gene is first cloned into a baculovirus transfer vector. The baculovirus transfer vector used to generate the polyhistidine-tagged UL25 expressing recombinant baculovirus was the pAcCL29.1 plasmid (Livingstone & Jones, 1989) and is shown in Figure 2.1. This plasmid vector contains the baculovirus polyhedrin promoter followed by a multiple cloning site to facilitate foreign gene insertion. Once cloned into the pAcCL29.1 vector, the foreign gene is flanked both 5' and 3' by viral-specific sequences and the recombinant vector is then transfected along with PAK6 baculovirus DNA into insect cells. The baculovirus PAK6 DNA contains the β -galactosidase gene in place of the polyhedrin gene and in a homologous recombination event, the foreign gene contained within the pAcCL29.1 vector is inserted into the viral genome and the β -galactosidase gene is excised. Once a viral stock is obtained after cotransfection, recombinant virus is identified by plaque assay in the presence of X-gal. In the absence of a recombination event the β -galactosidase gene encoded by the PAK6 DNA reacts with the X-gal substrate resulting in the formation of a blue plaque. Since a successful homologous recombination event results in the excision of the β -galactosidase gene, plaques formed by recombinant viruses remain colourless. Colourless plaques are therefore isolated and the baculoviruses are screened for recombinant protein production prior to plaque assay purification and generation of a high-titre stock.

2.2.3.2 Preparation of PAK6 Baculovirus Vector DNA.

PAK6 baculovirus vector DNA (5 μ g) was digested with 30 units of *Bsu*361 enzyme for 3 hours at 37°C. The reaction mixture was then treated with 20 units of CIP and incubated at 37°C for a further 2 hours. The reaction mixture was subsequently treated with an additional 10 units of CIP and incubation was continued for a further 2 hours. The reaction was terminated by incubating the reaction mixture at 80°C for 20 minutes and the digested PAK6 DNA was stored at 4°C. Digestion of the PAK6 DNA with *Bsu*361 converts the baculovirus DNA into linear forms, increasing the frequency of homologous recombination with the baculovirus transfer vector (Kitts *et al.*, 1990). This digestion also

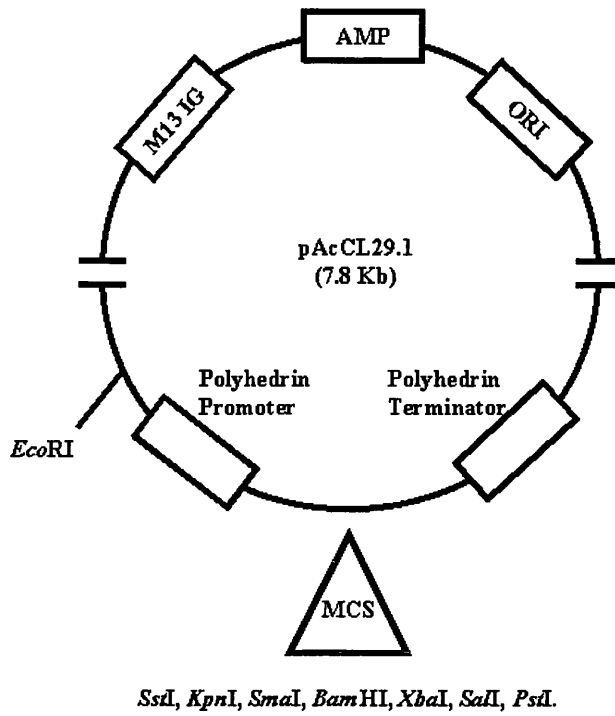


Figure 2.1 The Structure of Baculovirus Transfer Vector pAcCL29.1.

This vector contains the M13 intergenic region necessary for single strand production (M13 IG), the beta-lactamase gene (AMP), an origin of replication for propagation in bacteria (ORI) and baculovirus expression signals (polyhedrin promoter and terminator). The multiple cloning site (MCS) contains restriction endonuclease recognition sites for insertion of the foreign gene of interest.

deletes an essential portion of the 1629 ORF and results in the recovery of a high percentage of recombinant baculoviruses after cotransfection with a baculovirus transfer vector that can correct this deletion by replacing the deleted gene through homologous recombination (Kitts & Possee, 1993).

2.2.3.3 Cotransfection of Sf21 Cells with PAK6 Baculovirus Vector DNA and pPTA10/9.

Optimem medium (500 μ l) was used to dilute 1 μ g of *Bsu*361 digested PAK6 DNA and 2 μ g of pPTA10/9 DNA in a 15 ml Falcon tube (the construction of pPTA10/9 is described in section 3.2). In a separate 15 ml Falcon tube, 15 μ l of lipofectin was also diluted in 500 μ l of Optimem medium. The contents of both tubes were then gently mixed together and incubated for 15 minutes at room temperature. The transfection mixture was then added to Optimem washed Sf21 cells seeded in 35 mm tissue culture dishes (1×10^6 cells.dish⁻¹). The tissue culture dishes were incubated at 28°C in a sealed sandwich box containing a small piece of dry ice to maintain a slightly acidic environment optimal for the growth of Sf21 cells. At 5 hours post-transfection the mixture was removed from the cells, replaced with 2 ml of TC5 and the tissue culture dishes were incubated at 28°C. After 3 days incubation the medium from the cotransfected cells was transferred to 15 ml Falcon tubes and cells were removed by low-speed centrifugation. The resulting supernatant, containing potential recombinant baculovirus was stored at -70°C.

2.2.3.4 Selection of Recombinant Baculoviruses.

Putative recombinant baculoviruses in the supernatant from the cotransfected cells were titrated on Sf21 cells and the cells stained with neutral red in the presence of X-gal. Approximately 20 colourless plaques were each picked into 1 ml of TC5 and stored at -70°C.

A small scale virus stock of each plaque isolate was prepared. Tissue culture dishes (35 mm) seeded with 3×10^5 Sf21 cells per dish were infected with 200 μ l of the initial plaque isolate. After the virus had been adsorbed for 1 hour at room temperature, 2 ml of TC5 was added to the virus-infected cells and the samples were incubated at 28°C. At 3-4 days pi the medium from the virus-infected cells transferred to 15 ml Falcon tubes and the floating cells were removed by centrifugation at 1500 rpm in a Sorvall RT6000B centrifuge for 5 minutes at 4°C. The resulting small scale virus stock was stored at -70°C.

2.2.3.5 The Identification of Recombinant Baculoviruses Expressing the His-UL25 Protein.

A 24 well tissue culture dish was seeded with 2×10^5 Sf21 cells per well in 1 ml of TC5. The following day the medium was removed and the cells were infected with 200 μ l of the small scale virus stocks produced from plaque isolated virus. PAK6 virus and mock-infected cells were included as controls. After the virus was adsorbed at room temperature for 1 hour, 1 ml of TC5 was added to the virus-infected cells and the samples were then incubated at 28°C. At 30 hours pi the medium was replaced with 0.5 ml of methionine free TC100 containing 0.5% (v/v) foetal bovine serum, 1/10 the normal concentration of methionine and 20 μ l of ^{35}S L-methionine and incubation was continued at 28°C. After 16-20 hours incubation the radiolabelled cells were detached from the bottom of the wells by gentle pipetting into the TC5 medium and transferred to 1.5 ml Eppendorf tubes. The cells were concentrated by low speed centrifugation, washed with PBS complete and resuspended in 100 μ l of PGSB. The protein profile of the virus-infected cells was examined by SDS-PAGE and visualised by fluorography.

2.2.3.6 Plaque Purification of His-UL25 Expressing Baculovirus.

Selected virus isolates which expressed the His-UL25 protein were plaque purified as described previously. After the third plaque purification, small scale stocks of each virus isolate were prepared (as in section 2.2.3.4) and this small virus stock was used to produce a high titre recombinant baculovirus stock.

2.2.4 Isolation of HSV-1 Virion DNA.

2.2.4.1 Infection of Cells with Virus and Isolation of Cell-Released Virus and Cell-Associated Capsids.

Confluent monolayers of BHK cells in 850 cm² plastic roller bottles were each infected with 1×10^6 pfu HSV-1 in 20 ml of EC10. After the virus was adsorbed for 1 hour at 37°C, 50 ml of fresh EC10 was added to the virus-infected cells and incubation was continued at 31°C for 3-4 days until cpe had developed. The virus-infected cells were harvested into the medium by agitation and pelleted by centrifugation at 2000 rpm in a Sorvall RT6000B centrifuge for 10 minutes at 4°C. The resulting supernatant (cell-released virus) was centrifuged at 12,000 rpm in a Sorvall SLA1500 rotor for 2 hours at 4°C to concentrate the

virus particles. The cell pellet was resuspended in RSB containing 0.5% NP40 and incubated on ice for 10 minutes with occasional gentle agitation. The nuclei and cellular debris were pelleted by centrifugation at 2000 rpm in a Sorvall RT6000B centrifuge for 10 minutes at 4°C and the supernatant (de-enveloped cytoplasmic virions and capsid-tegment structures) was centrifuged at 12,000 rpm in a Sorvall SLA1500 rotor for 2 hours at 4°C. Both pellets were resuspended in 5 ml of NTE using a sonicating waterbath.

2.2.4.2 Extraction of Viral DNA.

SDS was added to the samples at a final concentration of 2% (w/v) and the samples were gently mixed by inverting the tubes. An equal volume of NTE saturated phenol was added to the samples which were incubated on a rocking platform for 20 minutes at room temperature. The samples were centrifuged at 3000 rpm in a Sorvall RT6000B centrifuge for 10 minutes at 4°C and the aqueous top layer containing the viral DNA was transferred to a fresh tube. Phenol extraction was carried out several times until there was a negligible amount of material (protein and SDS) at the interphase. An equal volume of chloroform was added to the DNA solution and the sample was incubated for 10 minutes on a rocking platform prior to centrifugation as before. The top layer was transferred to a clean tube, NaCl was added to a final concentration of 100 mM and the DNA was precipitated with 2.5 volumes of ethanol. DNA isolated from cell-released virus was pelleted by centrifugation as before, dried and gently resuspended in 2 ml of TE. DNA isolated from cell-associated virus was pelleted by centrifugation and resuspended in 10 ml of TE containing 100 mM NaCl, 1 mM MgCl₂ and 10 µg.ml⁻¹ of RNase A. After a 20 minute incubation at room temperature the DNA was extracted using 1:1 (v/v) unsaturated phenol/chloroform followed by an extraction with chloroform alone. The DNA was subsequently precipitated with ethanol, pelleted by centrifugation and gently resuspended in 2 ml of TE. The quality of both viral DNA samples was determined by electrophoresis of 1 µl of the viral DNA through a 0.5% TBE-agarose gel.

2.2.5 Preparation of Soluble/Insoluble Fractions from HSV-1 Infected Cells.

Tissue culture dishes (35 mm) were seeded with 8×10^5 Vero cells per dish in 2 ml of DC10 medium. The following day the medium was removed and the cells were infected with a 100 µl of HSV-1 in DC10 at a moi of 10 pfu per cell. After the virus had been adsorbed for 1 hour at the appropriate temperature, 2 ml of prewarmed DC10 medium

were added to the dishes and the cells were incubated at the appropriate temperature. At 10 hours pi the medium was removed and the cells were scraped gently into 1 ml of PBS complete and the cell suspension transferred to 1.5 ml Eppendorf tubes. The cells were pelleted by centrifugation at 6500 rpm in an MSE microfuge for 1 minute at room temperature and resuspended in 100 μ l of ice-cold lysis buffer. The cells were incubated on ice with occasional vortexing for 5 minutes and centrifuged at 6500 rpm in an MSE microfuge for 5 minutes. The soluble fraction (supernatant) was removed and combined with 50 μ l of 3x PGSB. The insoluble fraction (pellet) was resuspended in 1 ml of ice-cold sucrose buffer by vortexing and then centrifuged at 6500 rpm in an MSE microfuge for 5 minutes. The supernatant was removed and the insoluble pellet was resuspended in 150 μ l 1x PGSB. Both samples were then incubated in a waterbath set at 100°C for 10 minutes prior to analysis by SDS-PAGE.

2.2.6 Preparation of Plasmid DNA.

2.2.6.1 Large Scale Plasmid Preparation (CsCl banding).

Medium to low copy number plasmids were purified using the following method :

A 2 L flask containing 300 ml of L-broth supplemented with the relevant antibiotic was inoculated with a 5 ml overnight culture of bacteria and shaken overnight at 37°C. The bacteria were pelleted by centrifugation at 5000 rpm in a Sorvall SLA1500 rotor for 5 minutes at 4°C, resuspended in 20 ml of STET buffer, transferred to a 50 ml beaker and incubated for 1 minute at room temperature in the presence of 1 mg.ml⁻¹ of lysozyme. The mixture was brought to the boil with continuous stirring, using a Bunsen burner and transferred to a waterbath at 100°C for approximately 50 seconds. The now viscous mixture was centrifuged at 18,000 rpm in a Sorvall SS34 rotor for 45 minutes at 4°C. The supernatant was collected and combined with 0.9 volumes of isopropanol, mixed gently and centrifuged at 3000 rpm in a Sorvall RT6000B centrifuge for 5 minutes at 4°C. The resulting pellet was resuspended in TE and 200 μ l of ethidium bromide (from a 10 mg.ml⁻¹ stock) was added to give a total volume of 6.3 ml. The sample was incubated on ice for 10-15 minutes prior to the addition of 7 g of CsCl. After the CsCl had been dissolved the sample was centrifuged at 3000 rpm in a Sorvall RT6000B centrifuge for 10 minutes at 4°C to pellet any debris. The supernatant was transferred to 6 ml centrifuge tubes which were balanced, crimp sealed and centrifuged at 45,000 rpm in a Sorvall 65 V13 rotor for 16

hours (or overnight) at 15°C. The supercoiled plasmid DNA was harvested using a 2 ml syringe attached to a 18G syringe needle; the ethidium bromide was removed from the plasmid DNA solution by repeated butanol (saturated with TE) extraction and the CsCl was removed by dialysis for 2 hours against 2 L of TE. The plasmid DNA solution was treated with 100 µg.ml⁻¹ of RNase A for 1 hour at 65°C and then incubated at 37°C for 1 hour with 0.1% (v/v) SDS and 100 µg.ml⁻¹ of proteinase K. The plasmid DNA was phenol/chloroform extracted and precipitated by addition of 1/20 volumes of 5M NaCl and 2.5 volumes of ethanol followed by incubation at -20°C for 1 hour. The plasmid DNA was pelleted by centrifugation at 3000 rpm in a Sorvall RT6000B centrifuge for 10 minutes at 4°C, redissolved in 400 µl of H₂O, transferred to a 1.5 ml Eppendorf tube and precipitated as before. The DNA was pelleted by centrifugation at 13,000 rpm for 10 minutes in an MSE microfuge, washed in 70% ethanol and resuspended in 100-300 µl of H₂O depending on the size of the pellet. The concentration of the plasmid DNA was determined by measuring the UV absorbance at 260 nm (an absorbance reading of 1.0 corresponds to 50 µg.ml⁻¹ of dsDNA) and the quality of the plasmid DNA was established by electrophoresis of 0.5 µg of the plasmid DNA through a 0.8% agarose gel.

2.2.6.2 QIAGEN MIDI Plasmid Purification.

High copy number plasmids were routinely isolated from bacterial clones using a QIAGEN MIDI plasmid purification kit (QIAGEN) according to the manufacturer's instructions.

2.2.6.3 Small Scale Plasmid Preparation (miniprep) (Chowdhury, 1991).

To screen bacterial colonies for the presence of plasmid DNA, 2 ml of L-broth supplemented with the relevant antibiotic was inoculated with a single bacterial colony picked from an L-broth agar plate and shaken overnight at 37°C. Of this culture, 0.5 ml was mixed with 0.5 ml of phenol/chloroform/isoamylalcohol by vortexing the solutions together for 1 minute in a 1.5 ml Eppendorf tube. The mixture was then centrifuged at 13,000 rpm in an MSE microfuge for 1 minute. The upper aqueous phase was carefully removed, leaving the interphase undisturbed, and transferred to a fresh tube containing 0.5 ml of isopropanol. The solution was mixed thoroughly and centrifuged at 13,000 rpm in an MSE microfuge for 10 minutes. The resulting pellet was washed twice with 70% ethanol, vacuum dried and resuspended in 100 µl of TER.

2.2.7 Manipulation of DNA.

2.2.7.1 Synthesis and Purification of Oligonucleotides.

Oligonucleotides were synthesised within the Institute of Virology using a Cruachem PS250 synthesiser.

The newly synthesised oligonucleotides were supplied attached in their synthesis column. They were removed from the column with 1.5 ml of concentrated ammonia solution which was pushed through the column in 0.2 ml aliquots at 20 minute intervals. The oligonucleotides were deprotected for 5 hours at 55°C, vacuum dried overnight and resuspended in 90% (v/v) of deionised formamide in TBE.

The oligonucleotides were purified by PAGE. Briefly, for a 15-100 mer oligonucleotide, a 15% acrylamide gel with 4% cross-link was prepared and oligonucleotides were electrophoresed overnight. The oligonucleotides were visualised by fluorescence quenching under short wave UV, excised from the gel and incubated at 45°C overnight in oligonucleotide gel elution buffer. The next day the oligonucleotides were precipitated with ethanol, pelleted by centrifugation, washed in 70% ethanol and resuspended in 100 µl of TE. The purified oligonucleotide solution was quantitated by measuring the absorbance at 260 nm (an absorbance reading of 1.0 corresponds to 20 µg.ml⁻¹ of oligonucleotide).

Single stranded oligonucleotides were annealed by incubating 2 µg of each oligonucleotide in a water bath set at 100°C for 10 minutes followed by slow cooling. This resulted in the formation of 4 µg of double stranded oligonucleotide.

2.2.7.2 Gel Electrophoresis of DNA.

DNA was typically analysed by electrophoresis through a 0.8% non denaturing agarose gel using a BRL horizontal electrophoresis apparatus according to the manufacturer's instructions. Briefly, the agarose gel was prepared in TBE buffer which contained 0.5 µg.ml⁻¹ of ethidium bromide, immersed in TBE buffer prior to electrophoresis, and the samples in formyl dye solution were loaded into the wells of the gel. Electrophoresed DNA was visualised using a short wave UV light source. When it was necessary to purify DNA fragments, an agarose gel was prepared and electrophoresed in TAE buffer. The electrophoresed DNA was visualised using a long wave UV light source and agarose gel slices containing the DNA of interest were excised from the gel.

2.2.7.3 Southern Blotting and Hybridisation.

a). Southern Blot Transfer (Southern, 1975).

Prior to transfer, DNA restriction enzyme products were electrophoresed through a 0.8% non-denaturing agarose gel as described above. The DNA was denatured by gentle agitation in alkaline transfer buffer for 30 minutes and the gel was transferred onto 2 sheets of Whatman 3mm chromatography paper which were in contact with, but not immersed in, alkaline transfer buffer. A sheet of Hybond-XL membrane, the exact size of the gel, was soaked in alkaline transfer buffer and placed on top of the gel. Six sheets of Whatman 3mm chromatography paper, cut 2 mm smaller than the gel, were soaked in alkaline transfer buffer and placed on top of the membrane. Finally, a weighted stack of paper towels was laid on top of the Whatman paper. Approximately 17 hours later, the membrane was removed, neutralised by immersion in neutralisation solution with gentle agitation for 15 minutes and the DNA was cross-linked to the membrane using a Stratagene UV crosslinker (1200 Jcm²).

b). Preparation of Radio-Labelled Probe for Southern Blot Hybridisation.

Approximately 200 ng of purified DNA fragment was labelled with 50 µCi of [α ³²P] dNTP using an NEBlot kit (New England Biolabs) which is used to radio-label DNA in a reaction utilising random primers, dNTPs and Klenow enzyme. Radio-labelled probe was separated from unincorporated nucleotides using a G50 sephadex column. Prior to hybridisation the probe was denatured in a waterbath at 100°C for 5 minutes.

c). Southern Blot Hybridisation.

During the hybridisation procedure the temperature was kept constant at 65°C and the tubes were rotated in a hybridisation oven (Hybaid) The dried Hybond-XL membrane was placed in a hybridisation tube (Hybaid) with 50 ml of Southern pre-hybridisation buffer and incubated for 2 hours. The Southern pre-hybridisation buffer was then replaced with 10 ml of Southern hybridisation buffer prewarmed to 65°C and the membrane was incubated for a further 3 hours. The purified, denatured, radio-labelled probe was added and incubation continued for a further 16-20 hours. The membrane was washed once in 50 ml of Southern hybridisation buffer and once in 50 ml of membrane wash buffer, dried and exposed to either autoradiography film or a phosphorimager screen.

d). Quantitative Analysis.

Quantitative measurements of the amount of replicated or packaged DNA were made using the Quantity One software package (BIO-RAD). The Southern blot membrane was exposed to the phosphorimager screen and scanned into the computer using a Personal Molecular Imager FX phosphorimager (BIO-RAD). The scanned phosphorimage file was used for quantitation by volume analysis which sums the pixel values within a given object and subtracts the summed background pixel values. Identically sized rectangles were drawn around each of the objects for which intensities were to be calculated. An identically sized rectangle was also positioned somewhere on the image outwith the sample lanes to calculate the background volume. The volume contained within each of the rectangles was then calculated, subtracting the volume of the background.

2.2.7.4 Restriction Endonuclease Enzyme Digestion of DNA.

Restriction enzyme digestion of DNA was carried out using commercial enzymes and the buffers supplied. Typically, 1 µg of DNA was incubated with 10-20 units of enzyme for 3 hours at 37°C in a final reaction volume of 20-30 µl.

2.2.7.5 Purification of DNA Fragments.

DNA fragments of 70 bp to 10 kb were purified from agarose gel slices using a QIAquick Gel Extraction Kit according to the manufacturer's instructions. Typically, 50-60% of digested DNA was recovered using this method.

2.2.7.6 Ligation of DNA Fragments.

Prior to ligation of DNA fragments, the linearised plasmid backbone was treated with CIP to prevent recircularisation. The ligation reaction consisted of a 3:1 molar ratio of insert with respect to plasmid backbone together with 1 unit of T4 DNA ligase in 1x ligation buffer (and on occasion the reaction mixture also contained 5 ng of dsDNA oligonucleotide). The reaction mixture was incubated at 16°C overnight in a final reaction volume of 15-20 µl prior to transformation of competent *E. coli*.

2.2.8 Preparation and Transformation of Competent *E. coli*.

2.2.8.1 Preparation and Transformation of Competent BL21 *E. coli* (CaCl₂ Method).

L-broth (10 ml) was inoculated with a single bacterial colony picked from an L-broth agar plate and shaken overnight at 37°C. Of this culture, 0.5 ml was used to inoculate 50 ml of prewarmed L-broth which was shaken at 37°C until an optical density reading of 0.3 at 590 nm was reached. The bacterial culture was chilled on ice for 10 minutes and pelleted by centrifugation at 3000 rpm in a Sorvall RT6000B centrifuge for 15 minutes at 4°C. The resulting pellet was resuspended in 20 ml of 0.1 M CaCl₂ and incubated on ice for 1-2 hours. The bacterial cells were pelleted by centrifugation as before and resuspended in 3 ml of 0.1 M CaCl₂. The competent bacteria were stored at -70°C in 100 µl aliquots containing 7.5% (v/v) DMSO.

To transform the bacteria, 100 µl of competent cells was mixed with 1, 2 and 5 µl of ligation mix and incubated on ice for 1 hour. The cells were heat shocked at 42°C for 90 seconds, cooled on ice for 2-3 minutes and shaken for 1 hour at 37°C in 900 µl of L-broth containing 20 mM D-glucose. Finally, the cells were plated out on L-broth agar plates supplemented with the relevant antibiotic and incubated overnight at 37°C.

2.2.8.2 Preparation of Electrocompetent DH5α *E. coli*.

L-broth (50 ml) was inoculated with a sterile toothpick scraped on a frozen DH5α bacterial stock and shaken overnight at 37°C. This culture was used to inoculate 1 L of prewarmed L-broth in a 2 L flask and shaken at 37°C until an optical density reading of 0.5-0.6 at 550 nm was reached. The culture was transferred to pre-chilled 250 ml centrifuge tubes, incubated on ice for 30 minutes and pelleted by centrifugation at 3000 rpm in a Sorvall RT6000B for 15 minutes at 0°C. The cells were resuspended in a total of 1 L of sterile, pre-chilled H₂O, centrifuged as before and then resuspended in 500 ml of sterile, pre-chilled H₂O and centrifuged again. The cells were then resuspended in 40 ml of sterile, ice-cold 10% glycerol (v/v) in H₂O and transferred to ice-cold 50 ml centrifuge tubes and centrifuged at 6000 rpm in a Sorvall SS34 rotor for 15 minutes at 0°C. The supernatant was discarded and the pellet was resuspended in 2 ml of ice-cold 10% glycerol (v/v) in H₂O. The electrocompetent cells were divided into 80 µl aliquots, frozen rapidly on dry ice and stored at -70°C.

2.2.8.3 Transformation of Electrocompetent DH5 α *E. coli*.

Transformation of electrocompetent DH5 α *E. coli* was carried out using a BIO-RAD GenePulser according to the manufacturer's instructions. Briefly, 1-2 μ l of DNA (usually from a ligation reaction) was diluted with water to give a final volume of 20 μ l and mixed with an aliquot of electrocompetent DH5 α *E. coli*. The cells were transferred to BIO-RAD electroporation cuvettes and electroporated with the following settings, capacitance 25 μ FD, resistance 400 OHMS and voltage at 1.6 V. The cells were added to 1 ml of 2YT broth, incubated for 1 hour at 37°C with shaking and plated on L-broth agar plates supplemented with the appropriate antibiotic and incubated overnight at 37°C.

2.2.9 Generation of Monoclonal Antibodies Specific for the HSV-1 UL25 Protein.

2.2.9.1 Immunisation of Mice with MBP-UL25.

Female BALB/c mice, aged 6-8 weeks, were immunised sub-cutaneously with 20 μ g of purified MBP-UL25 in Freund's Complete Adjuvant and boosted sub-cutaneously three times, at two week intervals, with 20 μ g of purified MBP-UL25 in Freund's Incomplete Adjuvant. An analysis of the immunoreactivity in serum isolated from blood taken in a test bleed revealed a disproportionate immune response in favour of the MBP constituent of the MBP-UL25 fusion protein. Mice were therefore boosted with 20 μ g of purified His-UL25 in Freund's Incomplete Adjuvant to expand B lymphocyte populations secreting antibodies specific for the UL25 constituent of the MBP-UL25 fusion protein prior to harvesting the spleen of the mouse. Immunisations and test bleeds were performed by biological services technicians.

2.2.9.2 Fusion of Splenic Lymphocytes with Myeloma Cells.

Most of the work on the isolation of hybridoma cells secreting monoclonal antibodies specific for UL25 was carried out by Susan Graham at the Institute of Virology. Briefly, lymphocytes were harvested from the spleens of immunised mice and fused with Sp2/O-Ag 14 myeloma cells (Shulman *et al.*, 1978) in the presence of polyethylene glycol. Multiwell plates were seeded with the fused cells in HATc medium to select for hybridoma cells which result from the successful fusion of splenic lymphocytes with Sp2/O-Ag 14 myeloma cells. HATc medium consists of normal DC10 culture medium with three additives: hypoxanthine, aminopterin and thymidine. Aminopterin is an antibiotic which

effectively blocks the *de novo* nucleic acid biosynthesis pathway, forcing all cells to use the alternative 'salvage' nucleic acid biosynthesis pathway. This pathway is dependent on the enzyme HGPRT which utilises hypoxanthine and thymidine to synthesise purine and pyrimidine components of nucleic acids. If this enzyme is absent, as in the case with myeloma cells, purine and pyrimidine biosynthesis cannot occur and the cells will die. Hybrid cells of enzyme-deficient myeloma and enzyme-positive lymphocytes will be able to survive because they will have inherited the enzyme from the lymphocyte parent. Therefore after incubation for 10-14 days at 37°C in HATc medium, the only surviving cells in the fusion mixture will be myeloma/spleen hybrids as unfused spleen cells will eventually die.

2.2.9.3 Screening Hybridoma Cell Colonies for Production of Monoclonal Antibodies Specific for UL25.

Approximately 50 µl of medium was removed from wells containing single hybridoma cell colonies and was screened in an ELISA assay for UL25-specific antibodies using a cell extract from *Sf21* cells infected with AcUL25 as a source of antigen. Hybridoma cell colonies that tested positive in this assay were seeded on to 24 well tissue culture dishes and subsequently grown up in small tissue culture flasks. The medium from the tissue culture flasks was used to further characterise the monoclonal antibodies and the cells were stored at -140°C.

2.3.0 Protein Purification.

2.3.0.1 MBP-UL25 Purification.

a). Expression of MBP-UL25 Fusion Protein and Generation of Soluble Cell Extracts.

A 2 L flask containing 1 L of 2YT broth, 2 g of D-glucose and 100 µg.ml⁻¹ of ampicillin was inoculated with a 10 ml overnight culture of *E. coli* BL21 carrying the pPTA3 and shaken at 37°C until the bacterial culture had reached an optical density reading of 0.5-0.6 at 590 nm. The culture was incubated with shaking at 15°C for 20 minutes and a sample of uninduced cells was removed for subsequent analysis by SDS-PAGE (1 ml cells were pelleted by centrifugation and resuspended in 100 µl of PGSB). Expression of MBP-UL25 fusion protein was induced by the addition of IPTG to 0.1 mM

and the induced culture was incubated with shaking at 15°C for a further 6 hours. After incubation, a sample of induced cells was taken as before and the remaining bacteria were pelleted by centrifugation at 6000 rpm in a Sorvall SLA1500 rotor for 15 minutes at 4°C. The bacterial pellet was resuspended in 50 ml of amylose resin column buffer and frozen in a dry ice/ethanol bath. The cell extract was either thawed for immediate use or stored at -20°C for no longer than 1 month. The thawed extract was sonicated using a probe sonicator and centrifuged at 15,000 rpm in a Sorvall SS34 rotor for 20 minutes at 4°C. The supernatant (soluble protein extract) was collected and a sample was taken to ascertain whether the induction of the soluble fusion protein was successful. The supernatant was either used to purify MBP-UL25 immediately or stored at -20°C for no longer than 1 month. The pellet (insoluble protein) was resuspended in 25 ml of amylose resin column buffer and a sample was taken to determine the relative amount of insoluble fusion protein present in the sample.

b). Purification of MBP-UL25 Fusion Protein by Affinity Chromatography.

Amylose resin columns were prepared using five 10 ml protein purification columns (BIO-RAD), each containing 1 ml of amylose resin, and were washed with 8 ml of amylose resin column buffer prior to the addition of the soluble protein extract. The soluble protein extract was diluted 1:2 with amylose resin column buffer and allowed to percolate through the amylose resin by gravity flow. The columns were washed with 10 ml of amylose resin column buffer and then plugged with the sleeve provided (BIO-RAD). A volume of 500 µl of amylose resin column buffer containing 10 mM maltose was added to each plugged column and mixed into the resin by pipetting. The columns were incubated for 10 mins at room temperature with occasional mixing and the elutes were collected and pooled. A sample was taken for subsequent analysis and the purified protein was stored at -70°C.

2.3.0.2 Purification of His-UL25 from PTA10bac#14 Infected Sf21 Cells.

a). Preparation of Virus-Infected Cell Extracts.

Tissue culture flasks were seeded with 2×10^7 Sf21 cells in TC5. The following day the medium was removed and the cells were infected with PTA10bac#14 at an moi of 5 pfu.cell⁻¹. After an adsorption period of 1 hour at room temperature 40 ml of TC5 was

added to the virus-infected cells. After incubation at 28°C for 3 days, the cells were dislodged into the medium by agitation and pelleted by centrifugation at 3000 rpm in a Sorvall RT6000B centrifuge for 5 minutes at 4°C. The cells were washed in 5 ml of cold PBS complete, centrifuged as before and resuspended in 1 ml of PBS complete. The cells were pelleted for a final time in an MSE microfuge and resuspended in 0.5 ml of His-UL25 harvest buffer. DNase 1 and MgCl₂ were added to a final concentration of 20 µg.ml⁻¹ and 10 µg.ml⁻¹ respectively and the cells were incubated for 10 minutes at room temperature with occasional gentle mixing. The cell extract was sonicated using a sonicating waterbath and centrifuged at 13,000 rpm in an MSE microfuge for 5 minutes. Half of the resulting supernatant was transferred to a fresh 1.5 ml tube on ice and the pellet was sonicated as before in the remaining 250 µl of supernatant prior to centrifugation as before. This supernatant was pooled with the first supernatant and a sample of virus-infected cell extract was taken for subsequent analysis by SDS-PAGE. The virus-infected cell extract was used immediately to purify His-UL25 by affinity chromatography.

b). Purification of His-UL25 by Affinity Chromatography.

Ni-NTA agarose beads (0.5 ml) were washed once with 0.5 ml of distilled water and once with 0.5 ml of His-UL25 binding buffer. The agarose beads were added to the 0.5 ml of virus-infected cell extract and incubated for 1 hour in an end-over-end shaker at 4°C. The agarose beads were pelleted by centrifugation at 6500 rpm in an MSE microfuge for 1 minute and the supernatant was discarded. The agarose beads were then washed three times in 1 ml of His-UL25 binding buffer and three times in 1 ml of His-UL25 wash buffer and finally resuspended in 300 µl of His-UL25 elution buffer. The agarose beads were incubated for 10 minutes in an end-over-end shaker at 4°C and pelleted by centrifugation at 13,000 rpm in an MSE microfuge for 1 minute. The supernatant containing the purified His-UL25 protein was removed, stored at 4°C and a sample was taken for subsequent analysis.

2.3.0.3 Purification of Monoclonal Antibodies by Affinity Chromatography.

Fibracel disks (5g) were seeded with approximately 3-6 x 10⁷ hybridoma cells in a spinner culture vessel containing 500 ml of HATc medium buffered with 10 mM MOPS and incubated at 37°C with continuous stirring. After 4 days, half of the HATc medium was removed and stored at 4°C and 250 ml of fresh HATc medium was added to the

spinner culture vessel and incubation was continued as before. After a total of 8 days incubation at 37°C the HATc medium from the spinner culture vessel was collected and pooled with the previous batch of medium to give approximately 0.75 L of medium which contained monoclonal antibodies secreted by the cultured hybridoma cells. The HATc medium from the cultured hybridoma cells was filtered through a 0.22 µm membrane and dialysed against MAb start buffer. The monoclonal antibodies were purified from the HATc medium using a Hi-Trap Protein G column (PharmaciaBiotech) and an ÄKTA automated purifier (PharmaciaBiotech) according to the manufacturer's instructions. Using this method approximately 15 mg of purified monoclonal antibody per 0.75 L of HATc medium was recovered. The purified monoclonal antibody was dialysed against PBS complete, divided into aliquots and stored at -20°C.

2.3.1 Protein Analysis.

2.3.1.1 SDS-PAGE.

A 30% (w/v) acrylamide:0.8% bis-acrylamide stock solution (37.5:1) was used for analysis of proteins. The final concentration of polyacrylamide used depended on the molecular weights of the proteins to be examined but was generally between 8-12% (w/v) polyacrylamide in RGB. The polyacrylamide gel was assembled and protein samples were electrophoresed using a Mini Protean II gel kit (BIO-RAD) according to the manufacturer's instructions. Briefly, the polyacrylamide gel solution was polymerised by the addition of ammonium persulphate and TEMED at a final concentration of 0.1% (w/v) and 0.16% (v/v) respectively. A 5% (w/v) polyacrylamide solution in SGB was prepared, the polymerising agents added and the solution layered onto the solidified gel. Wells were formed with Teflon combs and protein samples in PGSB were denatured in a water bath at 100°C for 5 minutes prior to loading into the wells of the gel. Denatured proteins were separated by electrophoresis in freshly prepared PGEB.

2.3.1.2 Coomassie Blue Staining of Polyacrylamide Gels.

Electrophoresed proteins were stained by immersing the polyacrylamide gel in Coomassie Blue stain for 10 minutes with gentle agitation at room temperature. The stain was removed and protein bands were visualised by immersing the polyacrylamide gel in

polyacrylamide gel destain with gentle agitation for 2-3 hours at room temperature in the presence of rolled up tissue paper.

2.3.1.3 Fluorography.

Radiolabelled proteins were separated by electrophoresis as described above and the polyacrylamide gel was immersed in polyacrylamide gel fix for 1 hour with gentle agitation at room temperature. The gel was transferred to 5 gel volumes of EN³HANCE and agitation was continued for an additional hour. The gel was then rinsed thoroughly with deionised H₂O for 30 minutes. Finally, the gel was dried under vacuum at 80°C onto a sheet of Whatman 3 mm paper and placed in contact with autoradiography film for 20-48 hours at -70°C.

2.3.1.4 Western Blotting.

Proteins were separated by electrophoresis as described above and then transferred to Hybond-ECL membrane using a Mini Protean II blotting kit (BIO-RAD) according to the manufacturer's instructions. Non-specific protein binding sites on the membrane were blocked by immersing the membrane in PBSA containing 5% (w/v) dried skimmed milk powder and 0.05% (v/v) Tween-20 for 1 hour with gentle agitation at room temperature. The membrane was incubated with primary antibody diluted to the appropriate concentration in PBSA, containing 5% (w/v) dried skimmed milk powder and 0.05% (v/v) Tween-20, for 2 hours with gentle agitation at room temperature. Unbound primary antibody was removed by washing the membrane extensively with PBSA containing 0.05% (v/v) Tween-20. The membrane was then incubated with *Staphylococcus aureus* Protein-A-horseradish peroxidase conjugate, diluted at 1/1000 with PBSA containing 2% (w/v) dried skimmed milk powder and 0.05% (v/v) Tween-20, for 1 hour with gentle agitation at room temperature. Unbound Protein-A conjugate was removed by washing the membrane extensively with PBSA. Bound antibody was visualised using an ECL chemiluminescent kit (Amersham) according to the manufacturer's instructions and the membrane was exposed to film for usually no longer than 10 seconds.

2.3.1.5 Immunofluorescence.

Linbro wells, each containing a sterile 13 mm glass coverslip, were seeded with 7×10^4 Vero cells per well in DC10. The following day the medium was removed and the dishes were infected with 100 µl of virus at a moi of 10 pfu per cell in DC10. After a 1 hour

adsorption period at 37°C the virus inoculum was replaced with 1 ml of DC10 and incubation was continued at 37°C for 8-12 hours. The DC10 medium was removed from the wells and the cells were washed twice with PBSA prior to treatment with IF fixing solution for 10 minutes at room temperature. The cells were subsequently incubated with IF permeabilisation solution for 10 minutes at room temperature. Non-specific protein binding sites were blocked by incubating the permeabilised cells with PBSA containing 10% (v/v) human serum (or on occasion PBSA containing 10% (v/v) newborn calf serum) for 1 hour at room temperature. The cells were incubated with primary antibody, diluted to the appropriate concentration in PBSA containing 10% (v/v) newborn calf serum for 1-2 hours at room temperature. Unbound primary antibody was removed by washing the cells with PBSA containing 1% newborn calf serum. The cells were then incubated with a secondary antibody conjugated to an appropriate fluorochrome. Unbound secondary antibody was removed by washing the cells with PBSA and the coverslips were placed on a paper towel to dry prior to mounting onto glass slides using Mowiol mounting fluid. The samples were examined using a Zeiss Axioplan 2 LSM510 confocal microscope and the images obtained using the associated LSM510 software. The images were exported to Adobe Photoshop v4.0 to be arranged in a manner suitable for publication.

2.3.1.6 Immunofluorescent Detection of Incoming Capsids.

This experiment was carried out essentially as above with the exception cells were infected with purified virions at an moi of 50 pfu per cell in the presence of 100 µg.ml⁻¹ of cycloheximide at the NPT of 39.2°C. After 1 hour, virus inoculum was removed and replaced with 1 ml of DC10 containing 100 µg.ml⁻¹ of cycloheximide prewarmed to 42°C and the cells were incubated at the NPT for a further 1 hour prior to processing as in section 2.3.1.5.

2.3.1.7 Immunoprecipitation of HSV-1 Infected Cells.

Tissue culture dishes (24 well) were seeded with 3 x 10⁵ Vero cells per well in DC10. The following day the medium was removed and the dishes were infected with 100 µl of HSV-1 virus at a moi of 10 pfu per cell in DC10. After a 1 hour adsorption period at 37°C the virus inoculum was replaced with 1 ml of DC10 and incubation was continued at 37°C for 6 hours. The DC10 medium was removed from the wells and the cells were washed in unsupplemented methionine-minus Eagle's medium. The virus-infected cells were overlaid

with 500 µl of Eagle's medium containing 1/5 the normal concentration of methionine and 25 µCi of ³⁵S L-methionine per well and incubated overnight at 37°C. Alternatively, the virus-infected cells were incubated with 500 µl of methionine-free Eagle's medium containing 100 µCi of ³⁵S L-methionine per well for 2 hours at 37°C. The labelling medium was replaced with 500 µl of PBS complete and the cells were dislodged from the plastic well surface. The suspended cells were transferred to 1.5 ml Eppendorf tubes and pelleted by centrifugation at 6500 rpm in an MSE microfuge. The cells were washed in 500 µl of PBS complete and lysed in 150 µl of IP buffer. After the gentle agitation on ice for 15 minutes the cells were centrifuged at 13,000 rpm in an MSE microfuge for 10 minutes. The clarified virus-infected cell extract was transferred to a fresh tube, 10 µl of primary antibody (either polyclonal or purified monoclonal antibody) was added and immune complexes were allowed to form for 3-5 hours in an end-over-end shaker at 4°C. A volume of 50 µl of 50% (w/v) *Staphylococcus aureus* Protein-A (immobilised on sepharose beads) in IP buffer was added to the sample to bind any immune complexes and incubation was continued as before for a further 1 hour. The Protein-A beads were pelleted by centrifugation at 6500 rpm in an MSE microfuge for 1 minute and washed four times using 150 µl of IP buffer per wash. Before the final wash the beads were transferred to a fresh tube. The beads were finally resuspended in 50 µl of PGSB, incubated in a water bath at 100°C for 5 minutes to dissociate the immune complexes and proteins were separated by SDS-PAGE and visualised by fluorography.

2.3.2 Transient Transfection of Cells Using LipofectAMINE.

Tissue culture dishes (24 well) were seeded with 7×10^4 Vero cells per well in DC10. If transfected cells were to be examined by immunofluorescence cells were seeded on to sterile 13 mm glass coverslips placed within the wells (1 coverslip per well). The following day plasmid DNA (pCMV10 containing the ORF to be expressed) was diluted in Optimem. For single transfections, 1 µg of DNA was used in a final volume of 50 µl and for multiple transfections 0.5 µg of each plasmid in final volume of 50 µl was used. LipofectAMINE (3 µl) was diluted in 47 µl of Optimem, added to the diluted DNA and the sample was incubated at room temperature. After 45 minutes incubation, 400 µl of unsupplemented DMEM was added to the transfection mixture. Meanwhile, the DC10 medium was removed from the wells and the cells were washed twice with unsupplemented DMEM. The transfection mixture was then added to the washed cells

which were incubated at 37°C. After 5 hours incubation, 500 µl of DC10 containing 20% (v/v) foetal calf serum was added to the cells and incubation continued overnight at 37°C. The cells were ready for analysis the following day.

2.3.3 Detergent Extraction of Transiently Transfected Cells.

Tissue culture dishes (24 well) containing sterile 13 mm glass coverslips (1 coverslip per well) were seeded with 7×10^4 Vero cells per well in DC10. The following day the medium was removed and the cells on each coverslip were transfected with 1 µg of plasmid DNA as described in section 2.3.2. At 24 hours post-transfection the DC10 medium was removed from the wells and the cells were washed twice with CSK buffer. The cells were then incubated with CSK buffer containing 1% NP40 for 5 minutes on ice. The detergent-insoluble cell components were washed with CSK buffer and fixed with methanol for 5 minutes at -20°C. The cells were washed three times in PBSA containing 1% (v/v) newborn calf serum and then incubated with primary antibody diluted to the appropriate concentration in PBSA containing 10% (v/v) newborn calf serum for 1-2 hours at room temperature. Unbound primary antibody was removed by washing the cells with PBSA containing 1% (v/v) newborn calf serum. The cells were then incubated with a secondary antibody conjugated to an appropriate fluorochrome. Unbound secondary antibody was removed by washing the cells with PBSA and the coverslips were placed on a paper towel to dry prior to mounting onto glass slides using Mowiol mounting fluid. The samples were examined using a Zeiss Axioplan 2 LSM510 confocal microscope and the images obtained using the associated LSM510 software. The images were exported to Adobe Photoshop v4.0 to be arranged in a manner suitable for publication.

2.3.4 Analysis of Virus-Infected Cells by Electron Microscopy.

2.3.4.1 Virus Infection of Cells.

Tissue culture dishes (35 mm) were seeded with 8×10^5 Vero cells per dish in 2 ml of DC10 medium. The following day the medium was removed and the cells were infected with 100 µl of virus at an moi of 20 pfu per cell in DC10. An adsorption period of 2 hours at 36°C was used for cells infected with ts1249. The virus inoculum was then replaced with 2 ml of DC10 prewarmed to 42°C and incubation was continued for 16 hours pi at the NPT of 39.2°C. An adsorption period of 1 hour at the NPT of 39.5°C was used for cells infected

with ts1208. The virus inoculum was then replaced with 2 ml of DC10 prewarmed to 42°C and incubation was continued for 16 hours pi at the NPT. Marker rescue and wt virus were used as controls at the appropriate temperature.

2.3.4.2 Embedding Virus-Infected Cells in Epon Resin.

The DC10 medium was removed from the virus-infected cell monolayers and the cells were washed once with PBS complete. The cells were harvested into 0.5 ml of PBS complete, transferred to beam capsules and pelleted by centrifugation at 1500 rpm for 10 minutes at room temperature. The PBS was removed and the cells were fixed with 2.5 % (v/v) glutaraldehyde in PBS complete for up to 48 hours at 4°C. After a brief wash in PBSA the cell pellets were fixed with 1% (w/v) osmium tetroxide for 1 hour, washed with PBSA and dehydrated through a series of increasing ethanol concentrations (30, 50, 70, 90, 100% v/v in PBSA). The cell pellets were incubated overnight in epon resin containing 1.5% (v/v) BDMA which was replaced the following day with fresh epon resin containing BDMA. Polymerisation of the resin was achieved by incubating the samples at 65°C for 2 days.

2.3.4.3 Thin Sectioning.

Pelleted cells, embedded in polymerised epon resin, were sectioned with a diamond knife on an ultra-microtome (Ultracut E, Reichert-Jung), and thin sections were collected on parlodium-coated copper grids. Sections were stained with saturated uranyl acetate in 50% (v/v) ethanol for 1 hour, washed with deionised H₂O and counter-stained with lead citrate for 90 seconds. The sections were washed again, dried and examined at 80 KV in a Jeol 100S transmission electron microscope.

2.3.4.4 Negative Staining.

Recombinant HSV-1 capsids and VP5/19C particles were purified as described in sections 2.2.2.7b and c respectively. A 2 µl sample was applied to a parlodium-coated copper grid and incubated for 30 seconds at room temperature. The excess liquid was removed from the grid using filter paper and 5 µl of 1% phosphotungstic acid (PTA) was layered carefully onto the grid and incubated for 3-5 minutes at room temperature. The excess PTA was removed as before and the grids were dried and examined at 80 KV in a Jeol 100S transmission electron microscope.

2.3.5 HSV-1 DNA Packaging Assay.

2.3.5.1 Virus Infection of Cells.

Tissue culture dishes (60 mm) were seeded with 2×10^6 Vero cells per dish in 4 ml of DC10 medium. The following day the medium was removed and the cells were treated with 4 ml of DC10 containing $100 \mu\text{g}\cdot\text{ml}^{-1}$ of cycloheximide for 15 minutes at 36°C prior to virus infection. The medium was removed and the cells were infected with HSV-1 (wt virus, *ts1249*, *ts1208* and marker rescuant viruses) in $500 \mu\text{l}$ of DC10 containing $100 \mu\text{g}\cdot\text{ml}^{-1}$ of cycloheximide at an moi of 10 pfu per cell. After an adsorption period of 2 hours at 36°C the virus inoculum was removed and the cells were washed with 4 ml of 0.14 M NaCl and non-penetrated virus was inactivated by incubating the cells for 1 minute with 4 ml of 0.14 M NaCl/0.1 M glycine pH 3.0. The cycloheximide was removed from the cells with three, 90 second washes with 4 ml of DC10 prewarmed to 42°C . Samples were either harvested immediately (0 hour time point) or incubated at the NPT in 4 ml of DC10 for 24 hours pi.

2.3.5.2 Harvesting the Virus-Infected Cells.

The medium was removed and the virus-infected cells were harvested into 2.3 ml of PBS complete. The cells were transferred to a 10 ml tube, dispersed by gentle vortexing and divided into two, 1 ml samples. Packaged (DNase resistant) DNA was prepared from the first sample and total DNA was prepared from the second sample.

2.3.5.3 Preparation of HSV-1 Packaged DNA.

The virus-infected cells were pelleted by centrifugation at 6500 rpm in an MSE microfuge for 2 minutes and resuspended in $184 \mu\text{l}$ of RSB containing 0.5% (v/v) NP40 and $100 \mu\text{g}\cdot\text{ml}^{-1}$ of DNase 1. After the samples were incubated at 37°C for 1 hour with occasional mixing, $184 \mu\text{l}$ of 2x CLB containing $1 \text{ mg}\cdot\text{ml}^{-1}$ of Protease XIV was added to each preparation and incubation was continued at 37°C for a further 2 hours. Following the incubation, $35 \mu\text{l}$ of NaCl/EDTA mix was added and the nucleic acids were sequentially extracted with phenol/chloroform, precipitated with 2.5 volumes of ethanol and resuspended in $50 \mu\text{l}$ of 1x B buffer (Boehringer Mannheim) containing 20 units of BamH1 restriction endonuclease enzyme and $10 \mu\text{g}\cdot\text{ml}^{-1}$ of RNase A.

2.3.5.4 Preparation of Total DNA.

The virus-infected cells were pelleted by centrifugation at 6500 rpm in an MSE microfuge for 2 minutes and resuspended in 184 μ l of RSB containing 0.5% (v/v) NP40. The cells were placed on ice and 184 μ l of 2x CLB containing 1 mg.ml⁻¹ of Protease XIV was added to each preparation. After the samples had been incubated at 37°C for 3 hours, 35 μ l of NaCl/EDTA mix was added and the nucleic acids were sequentially extracted with phenol/chloroform, precipitated with 2.5 volumes of ethanol and resuspended in 50 μ l of 1x B buffer containing 20 units of BamH1 restriction endonuclease enzyme and 10 μ g.ml⁻¹ of RNase A.

2.3.5.5 Analysis of Total and HSV-1 Packaged DNA.

A 20 μ l portion of each sample was digested for an additional 3 hours at 37°C using 10 units of *BamH1* restriction endonuclease enzyme in 1x B buffer in a final reaction volume of 30 μ l. The samples were electrophoresed through a 0.8% TBE-agarose gel, transferred to a Hybond-XL membrane and hybridised to an [α ³²P] dGTP labelled HSV-1 specific probe.

2.3.6 HSV-1 Transient DNA Packaging Assay.

2.3.6.1 Transfection of Vero Cells with pSA1.

Tissue culture dishes (60 mm) were seeded with 1.4 x 10⁶ Vero cells per dish in 4 ml of DC10 medium. The following day 2 μ g of pSA1 plasmid was diluted in 250 μ l of DMEM containing 8 μ l of LipofectAMINE PLUS reagent (Gibco BRL) and incubated at room temperature. After 15 minutes, 12 μ l of LipofectAMINE was also diluted in DMEM to a final volume of 250 μ l and following a 15 minute incubation at room temperature the two solutions were mixed together. The cells were washed twice with DMEM prior to addition of the transfection mixture and were then incubated at 37°C. At 3 hours post-transfection 4 ml of DC10 was added to the cells and incubation was continued as before.

2.3.6.2 Superinfection of Vero Cells with HSV-1.

At 12 hours post-transfection the medium was removed and the cells were incubated with 4 ml of DC10 containing 100 μ g.ml⁻¹ of cycloheximide at 36°C prior to virus infection. After 15 minutes the medium was removed and the cells were infected with

HSV-1 (wt virus, *ts1249*, *ts1208* and marker rescuant viruses) at an moi of 10 pfu per cell in 500 µl of DC10 containing 100 µg.ml⁻¹ of cycloheximide. After an adsorption period of 2 hours at 36°C the virus inoculum was discarded and the cycloheximide was removed with three, 90 second washes with 4 ml of DC10 prewarmed to 42°C. The virus-infected cells were then incubated in 4 ml of DC10 at the NPT.

2.3.6.3 Detection of Replicated and Packaged Amplicon DNA.

At 21 hours pi the cells were harvested and total and DNase resistant DNA were prepared as described in section 2.3.5. The samples were digested with *EcoR1* and *Dpn1*, electrophoresed through an 0.8 % TBE-Agarose gel, transferred to Hybond-XL membrane and hybridised to [$\alpha^{32}\text{P}$] dGTP labelled pAT153 plasmid.

2.3.7 Marker Rescue of HSV-1 *Ts2* with Cloned wt HSV-1 *HindIII* k DNA Fragment.

2.3.7.1 Cotransfection of Cells with *Ts2* DNA and *HindIII* k DNA.

Tissue culture dishes (35 mm) were seeded with 8 x 10⁵ Vero cells per dish in 2 ml of DC10. The following day, a 436 µl transfection mixture containing 0.5 µg of DNA isolated from *ts2* virions, 1 µg of purified wt HSV-1 *HindIII* k DNA fragment and 2.4 µg of calf thymus carrier DNA (pre-optimised) was prepared in hepes buffered saline and mixed gently. A transfection mixture without the *HindIII* k DNA fragment was also included as a control to examine the reversion rate from *ts2* virus to *ts+* virus. The volume of the transfection mixture was increased to 500 µl using 1 M CaCl₂, mixed gently and incubated at room temperature for 5 minutes. The DC10 medium was removed from the tissue culture dishes and the cells were washed with serum free medium. Half the transfection mixture was added to each dish and the cells were incubated at 37°C. After 45 minutes, 2 ml of DC10 was added to each dish of cells and incubation was continued at 37°C. At 4 hours post-transfection the cells were washed once with fresh DC10 and incubated for 4 minutes with 25% (v/v) DMSO in hepes buffered saline at room temperature. The cells were then washed three times with DC10 and incubated at 31°C for 3 days.

2.3.7.2 Selection and Isolation of Marker Rescue Virus.

The transfected cells were harvested into the medium and sonicated with a sonicating water bath. The progeny virus was titrated at 31°C (the PT) and 39.2°C (the NPT) using

methyl cellulose (1:1 v/v) in DC10 as an overlay to prevent secondary plaque formation. Plaques formed at the NPT were isolated using a sterile glass Pasteur pipette and transferred to vials containing 0.5 ml of DC10. The virus was plaque purified three times before a high-titre stock was prepared. At this stage the plating efficiency of the virus at the PT and the NPT was examined to ensure the virus was exhibiting a phenotype close to that of wt virus and an isolate referred to as *ts2/Hindk* MR#6 was selected for use in subsequent experimentation.

CHAPTER 3

RESULTS

3.1 Sequence Analysis of the HSV-1 UL25 Protein.

3.1.1 Introduction

In the absence of any direct experimental information concerning the structure of a given protein it is often useful to utilise several of the many online bioinformatic software tools. These programs examine the primary amino acid sequence of a protein to produce multiple homology alignments and predictions of protein secondary structure. As there is no direct experimental data available concerning the structure of the HSV-1 UL25 protein, these bioinformatic tools were employed to examine the HSV-1 UL25 amino acid sequence.

3.1.2 Sequence Alignment of the HSV-1 UL25 Protein and its Homologues.

The HSV-1 17⁺ UL25 amino acid sequence was submitted to the JPRED sequence alignment program (Cuff *et al.*, 1998) and the results are shown in Figure 3.1. This program searches for and aligns homologous amino acid sequences and indicates areas of conservation between them. The results demonstrated a large degree of conservation between the homologues of the UL25 protein from alpha- beta- and gammaherpesviruses. The protein exhibited the highest degree of conservation within the C-terminal 200 amino acids whilst the N-terminal portion showed the least conservation within the protein. Furthermore, the UL25 amino acid sequence was exclusive to the herpesvirus family, displaying no significant homology with any other amino acid sequences of viral or non-viral origin.

3.1.3 Predicted Secondary Structure of the HSV-1 UL25 Protein.

3.1.3.1 PSIPRED and PHDsec Secondary Structure Predictions.

The HSV-1 UL25 17⁺ amino acid sequence was submitted to the PSIPRED protein secondary structure prediction program (Jones, 1999) and the results are shown in Figure 3.2. This program assigns an amino acid residue to a secondary structural element based upon the probability of that residue adopting a specific secondary structure within the context of its surrounding amino acid residues. This program predicted that the UL25 polypeptide chain adopted a predominantly helical secondary structure and this finding is consistent with the results from the PHDsec secondary structure prediction program (Rost

Figure 3.1 Sequence Alignment of the HSV-1 UL25 Protein and its Homologues.

The HSV-1 UL25 amino acid sequence was analysed using the JPRED sequence alignment programme which aligned UL25 amino acid sequences from alpha-, beta- and **gamma**herpesviruses. Heavy shading represents strongly conserved regions whereas lighter shading represents regions of lesser conservation. The viruses used in this alignment were **HSV-1**, herpes simplex virus type 1; **HSV-2**, herpes simplex virus type 2; **BHV-1**, bovine herpesvirus type 1; **EHV-4**, equine herpesvirus type 4; **GHV-1**, gallid herpesvirus type 1; **GHV-2**, gallid herpesvirus type 2; **ILTV**, infectious laryngotracheitis virus; **PRV**, pseudorabies virus; **VZV**, varicella zoster virus; **HCMV**, human cytomegalovirus; **HHV6**, human herpesvirus type 6; **HHV7**, human herpesvirus type 7; **ALCELAPHINE HV-1**, Alcelaphine herpesvirus type 1; **ATELINE HV-3**, Ateline herpesvirus type 3; **EBV**, Epstein-Barr virus; **EHV-2**, equine herpesvirus type 2; **KSHV**, Kaposi's sarcoma associated herpesvirus; **MHV-4** murid herpesvirus type 4 and **MMRV**, macaca mulatta rhadinovirus.

Virus

UL25 Amino Acid Sequence

HSV-1 1 MDPYCPFDA... DVWEHRRRFIVADS... N... TPEF... RDRDFWMS... FNLPRETAAEQVV... LQAQRT
 HSV-2 1 MDPYCPFDA... DVWEHRRRFIVADS... S... TPEF... RDRDFWMLP... FNI PRETAAERAA... LQAQRT
 BHV-1 1 MALGRLEFACLG... DIHAVADV... VPDE... N... APAF... B... LRFWDEP... LRGIGDADAPARE... AAARA
 EHV-4 1 MAEYVDYVFGS... YVCDTARTIPTDV... K... I... APPF... B... LNFWSAPTFTASSNPRADPTK... VAARH
 GHV-1 1 MASFAWDARILTDPGPS... HPADV... N... APPW... LHFWRPE... FSGNLGDAERQLA... VKARNS
 GHV-2 1 MANFIWDARILTDGGM... PADV... N... APPW... IEFWKEP... FTSNRANMERQLA... ITARNN
 ILTV 1 MFRPRPEPMN... DSNKPSMTVLADRLN... SCAEGSSKYASK... FEGTLIDAEIMAR... EDLER
 PRV 1 MDRAWFAFEAAAI PGSAR... H... E... APPF... VGFWARPGFSEGLDAR... LA... AHANA
 VZV 1 MTARYGFGS... SFPNKCGI... LSTT... N... APNFE... IHYWTAPAFELRGRMNPDLKNTLTLKN
 HCMV 1 MSLLHTFWRLPVAF... EPHEE... V... RCPERVRLLEDAATMRGGWREDEV... LMDRVR
 HHV6 1 MAQC... EFYQYPTITILEGHV... ILICTEKVEKQSSLLRREK... IDQHRDKLL
 HHV7 1 MTQLS... EFYQFP... IQI... EGHV... TLICTEEDMQQLON... GIRKLRKE... KEETQKNKIL
 ALCELPAPHINE HV-1 1 MWVGVSSYTRACS... VORWPKRCY... APSQ... V... EINPHRFQESRRSAALYRKHV... VESKLNLIK
 ATELINE HV-3 1 MLKLEKNYISAPKQKLTHTGIF... WTPHQ... S... L... FIDKELLIETKRNSAVYRSHL... INVETDQIK
 EBV 1 MALSGHVLIDPAR... PRDTGPEM... WAPSLRNS... LRV... SPEALAEAREARSER... WDRCAQVLIK
 EHV-2 1 MQAARKRWPPSVF... WSPSP... KHY... VRDRDSL... RETR... LASSLRNA... LAARVARVK
 KSHV 1 MLTSERSYLRYPKNRRWTEAGFWAPHEN... V... F... HK... TMEETRR... VALGLRSL... VRNRERKTK
 MHV-4 1 MFYLNPNP... KNTLRIDAEAL... TETRR... LAARAWDLK... YQMTKQGMH
 MMRV 1 MRTSEKCMRYPRKPARQITAFWAPHNN... V... F... HK... PSLIEERRNFAVVRNQ... LALRVHTLR

HSV-1 61 AAA... PA... L... NAAMQAAELPVD... ERR... P... P... R... N... HEIAGAT... EAL... STAAAAA... E... ADAARGDEPA
 HSV-2 61 AAA... AA... L... NAALQAAELPVD... ERR... P... P... Q... O... Q... HHIADA... EAL... STAAAAA... E... ADAARDAEAE
 BHV-1 61 AAA... AA... AD... NLAKQRAAGAE... DAR... P... P... SAR... A... EVAAV... AD... LA... EAARRAE... E... ADA... A... ESARR
 EHV-4 61 AAA... AA... AD... TL... BAOSQYSSAN... DAL... P... P... ER... Q... AKVADA... AA... L... DA... A... A... A... A... A... ADAATPOVN
 GHV-1 60 AA... I... AA... L... S... D... DR... TL... I... AVE... ER... R... P... EDK... EQIATT... AD... L... RA... A... S... A... A... E... L... ADA... A... A... DEAOV
 GHV-2 60 AA... T... AA... L... W... D... GH... T... DS... IA... IE... D... RR... L... P... EEK... EYIATA... AD... S... H... A... A... A... A... A... E... L... ADA... A... A... MDIAV
 ILTV 61 AA... K... AA... L... B... L... EN... MSATVPVH... SSAL... OT... EYP... ETVIDV... DD... JAQR... AVQEK... D... IVGSYKTI
 PRV 51 AAA... AA... L... DN... MA... A... GAR... LEAE... DE... Q... L... P... ER... Q... ERVAEA... L... V... ETARA... A... E... E... ADA... A... A... A... E... E
 VZV 61 AA... V... AA... L... DN... R... GE... T... I... L... P... TE... D... RR... L... P... ER... Q... TRMAKV... DS... ST... AA... A... A... E... E... ADA... A... Q... SEECTE
 HCMV 57 Y... R... Q... R... E... GHRVQTYCED... EGR... V... SEA... L... AL... N... Q... CELY... SR... H... DA... ITGVVAP... S... VAASAAA
 HHV6 55 R... K... T... A... A... Q... KM... Q... K... D... SDV... N... SH... A... TA... DA... L... ENQ... K... I... IPS... THSVL...
 HHV7 55 L... L... K... T... A... V... QAHVQTECKNTN... D... I... NA... L... ENQ... K... I... IPS... THSVL...
 ALCELPAPHINE HV-1 58 L... L... K... A... E... L... DN... V... Q... T... NLANSQA... L... TDY... L... T... L... EDLAN... ILVDRAQQ... PASSNQC... GAR... P... Q... T...
 ATELINE HV-3 58 M... W... NY... E... L... D... K... E... MR... D... HL... K... R... S... N... I... TR... D... L... E... I... EN... M... V... D... K... L... Q... D... T... K... T... P... P... Y... S... Q... P... P... L... S... P... T... T...
 EBV 58 L... R... V... E... L... D... G... I... MR... D... HL... R... A... B... E... T... R... O... D... L... D... A... V... A... F... S... D... G... L... E... S... M... Q... V... R... S... T... G... R... S... A... P... A... P... P... S... P...
 EHV-2 53 M... F... R... A... E... L... G... N... S... Q... L... QA... H... A... H... G... V... L... A... D... L... A... R... L... E... Q... A... T... A... L... H... V... A... G... D... G... R... G... NP... P... T... S... P... C... Q... G... H... P... L... S...
 KSHV 58 L... L... S... L... E... L... D... R... L... V... Q... H... D... S... R... V... R... V... T... I... N... A... D... I... D... A... N... K... O... M... T... G... N... I... D... M... P... Q... S... R... S... H... E... P... P... L... V...
 MHV-4 43 M... F... R... A... E... L... DN... L... E... I... L... ER... G... H... S... A... A... F... T... T... N... S... L... E... A... N... V... L... D... O... P... A... P... P... D... P... T... Q... G... E... K... G... L... P... P... S... S...
 MMRV 58 L... R... L... E... L... DN... V... L... Q... H... Q... R... E... T... E... V... M... R... D... L... E... T... I... O... N... M... V... G... D... I... R... S... P... G... R... E... T... A... N... A... Q... T... S... L... N... P... Q... P... .

HSV-1 GGGDGGAPPLAVAEMEVQIVRNDPPPIRVDNINLPWLLHMVYAGRGATGSSGVVFGIWIYR
 HSV-2 GAADGAAPSGPAAAEVMEVQIVRNDPPPIRVDNINLPWLLHMVYAGRGAAAGSSGVVFGIWIYR
 BHV-1 AAADAEEGLEAVRARRVQIAKNDPPELEKDTTAAALLLAMVYTARAGGGSAGIVFGIWIYR
 BHV-4 .DSDQRDNN.VAQSLSSEIQIAKNDVPEFQINLAVELTITVIVFVGRAAGGSGVIVFGIWIYR
 GHV-1 D.SNECQKN..SAASREVQIVRNDPSIRVDNINLWVLLINIIYASRG.AANSQVAVFGIWIYR
 GHV-2 EKSQGHKED..ITSAREIQIVKNDPLRVDNINLWVLLINIIYASRG.AANSQVAVFGIWIYR
 ILLTV .APGE.....DVPANVIMIKNGEPTINIFQVQFLITTSYAIAG...NGLRGFGSMWR
 PRV 111 ATAAADEGR.....EVLAKNDVALAKANLSSIFLAMVYAAAR...GAASGVLFGIWIYA
 VZV 121 IIRNESIHP.....EVLAKNDAPQVQANFQVQFLITVILGRAGNNSPGIVFGPWIYR
 HCMV 117 AERPL.....PGNVPSYFGTQV...FIRHIDFRGEVANTMFENAS...TTFSS...I...Y
 HHV6 106 .KSPE.....KLEKFNQVATPL...FIRTDIFRGEVINTFENNAQ...MNFY...S...FY
 HHV7 103 .EESL.....QAKTVQVITQID...AIHFTLFRPEMIKTFNNTQ...M...SYT...G...AMY
 ALCELAPHINE HV-1 111 .HVPQAPAPPKENTTIVIIAPGDSGYTFSTINFLREFLSGLYATSA...SWLPSYGPWFY
 ATELINE HV-3 110 .TLSN....AKPNVYITVAPGDPGFTVEANFKLELVSSLYTNQQ...QWLPYSGPWIYS
 EBV 111 .AQPFTR..LTGNAQYAVSISPTDPIVMAGSLAQTLNLYGNIN...QWVPSFSGPWIYR
 EHV-2 107 .NSDSHGGGGGELLITISPDGPTFSVKDDFRTEFISGLYTRQS...QWLPFYGPWIYA
 KSHV 111 .SPPQ....ASHRNFTVAIVPGDPHFSVDRDLRGLMPTLYMNQN...QWLPYSGPWFY
 MHV-4 95 .VES.....RTEGVYTVVYPGDPAPEIQDSLPOKIWPMLYLHQQ...RWLPYSGPWHI
 MMRV 110 .IAPQ.....THGDAFVVTIAPGDPGFTVNDLRLLELLPSLYMNQN...QWLPQYGPWIYS

HSV-1 IQDRTITFFLITRSADFRDGRMSKTFMIALLSIQCGRLVQVQRYSAFECVAVLCIY
 HSV-2 IQDRTIAFFLITRSADFRDGRMSKTFMIALLSIQCGRLVQVQRYSAFECVAVLCIY
 BHV-1 IQDRLIARFLATRIMDYRDGRMSRTFMAAAALQSSGRMYSZRAYSAFECVAVLCIYH
 EHV-4 AIQDRLVTRPVATRSIDYRDGRMSKTFMATAVALQSCGRLVQVQRYSAFECVAVLCIYH
 GHV-1 IIQNSLVAENSAARKIDYRDGRMSRTFMATAVALQSCGRLVQVQRYSAFECVAVLCIY
 GHV-2 IIQNALVAFVPSVARKIDYHGGRMSRTFMATAVALQSCGRLVQVQRYSAFECVAVLCIY
 ILLTV 169 AIQTLQLDNNAIARVLNVMGDTRISGRFMKTAALRARSAMEIATITROYSGFEATVLCIY
 PRV 162 IIOATLIAARPOVSRMIDSRDGRMSRTFMGVTTTALQSCGRLVQVQRYSAFECVAVLCIYH
 VZV 174 IQOERLILRFPVAARVQVCKDGRISRTFMNTTITCLQVAGRMVYEDRAYSAFECVAVLCIY
 HCMV 169 RIKRGLYQPKVYVLAQMDNFSIQOELILGVNAENVTVYPTY..CV...LE...A...
 HHV6 157 KIKRVFYNPRALILTNVDSLITIKELAVTINAEQATVYPIFG.SEM...LE...A...
 HHV7 154 KIKRAFFTISKAMLLTYVDSLITIQOELISISINAEQITIYPIH..NL...LE...A...
 ALCELAPHINE HV-1 167 AMTANAWORRPEKELKGTANLKNSTSLKLI TEVITVVASINVDYTDLRNLSDFNAAALCII
 ATELINE HV-3 161 SLTDIAWORRPEKELKGLNLFQNSTLKLMLHAVITTISSATEDFYSDVRHLSLDTNAAALVIL
 EBV 165 IWSANAWORRPEKOLRGNLNFQNSVSLKMLTEVAVLEGATQDFSDVRHLPDLOALILS
 EHV-2 163 AMTDSAWORRPEKELKGNVNFQNSTLKLMLTGLLEVLASATEDFYTI GRNLSLVNAAALCII
 KSHV 162 SLITDNAWORRPEKELKCVNFQNSTLKLISHTLITVASTADFFAIARHLITIQAAALCLV
 MHV-4 145 RFTSSAWORRPEKIRCOANFQNSMSLKITALTVDVLSRISLDFYSDLRHLSLDTMSALCII
 MMRV 161 SLITDNAWORRPRDIRGTNFQNSTLKLMSAVISTAAASITQDFYADVVRNVSLITQAAALCII

HSV-1 SRGHNFIMWEDQTLIHTATANTITGTRQILANVADLNNRIQLIMIPGAVPSEA
 HSV-2 RFGHNFIMWEDQTLIHTATANTITLAIIRLIANVADLNNRIQLIMIPGAVPAEA
 BHV-1 PRAQNFIAEDOSLHAATDTITALETRLIANVADLRNNFQITLPGAAAPGD
 EHV-4 VRAQNFITEDOTLHASTINTITALLTRLIANVADLRNNFOLAVENLSVALG
 GHV-1 GHAQPFIMEDOTLHAATDTIVLILRALIMNTNSAVKNCQFOLAFPGVPPDLT
 GHV-2 GHAQPFIMEDQPLHASTDTITLILRHLDIMNTNSAVKNIIFOLAFPGIVPDLT
 ILTV PERTIPIHEDDPLHIVDSLSLITQILFNSNVTSIHLNRFOPSAFFELPLGTQS
 PRV SRQNFIFGEDAPLHAATNTITLILRLHNNVGDLRNNFOLAFENAPPP...
 VZV BRAQNFIMEDQTLIHTDTITLILRLHNNVGDLRNNFOLAFSEATGPTI
 HCMV SDVVEVH.EQY.SLITCLAGLWKVINADS.PA.PRTGATADLGSDAVAGG
 HHV6 NNVEIPIH.CHYRSELVA.ESEFMRI.NSESLFN.RVGRSLTISIF.....
 HHV7 KEVILPVH.QOY.SIVA.ESEYMQINSESLFG.KRTGKEYTITIF.....
 ALCELPAPHINE HV-1 334 SDNIPPEGN.YQLNLRSGIKGVEYLILAVLTLANAQLS.KPDGRILHLKALIGAAFEH...
 ATELINE HV-3 322 GEDVPPFSS.HQWNLFVGLAALEALMLVYTL CETANIA.EAATRRLHLSLIPQAMQRK
 EBV 329 GENVPPFIT.YCLNLFITGKALELLIVVYIVIENAHVOHNTVNRRLQIPALIGDOYKR...
 EHV-2 327 GSDIPPFSA.YQWNLFAGHVALEVFILAVGILLEFGOVARGHPNRRLLNLSLIGPKFQP...
 KSHV 302 CDNIPPFAA.YQWNLFSGHKAESLILLLFLLDVNVPA..TSNKRLHLEALIGESYSK...
 MHV-4 325 SEDVPPFOA.YQWNLFAGLSAGLCLVLYVYVLELELAQITPRSPHRRLLNLSLIGGRFSK...
 MMRV

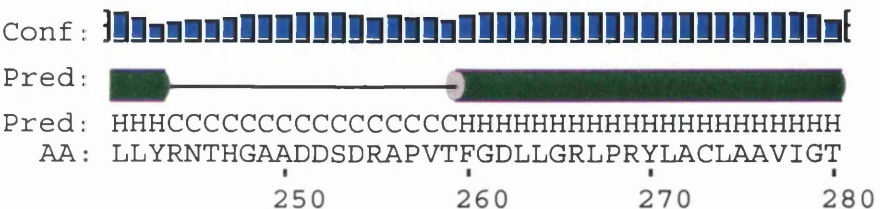
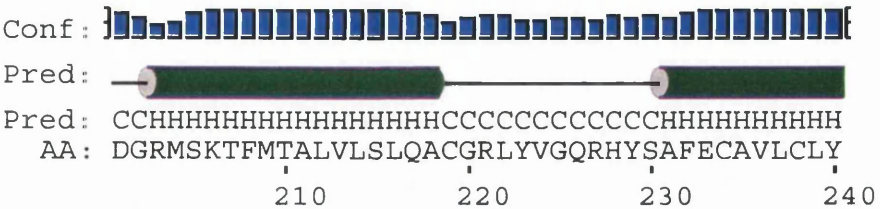
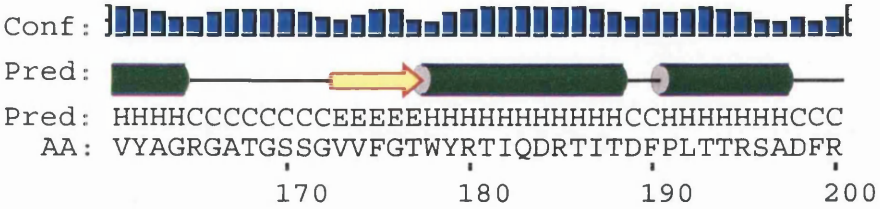
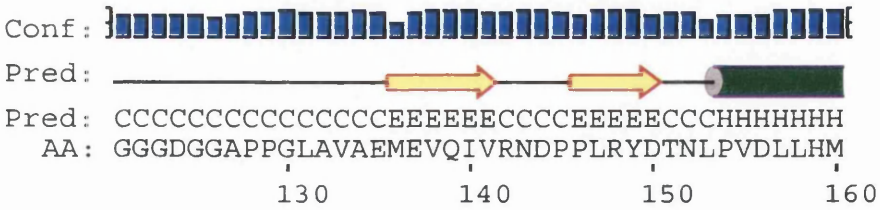
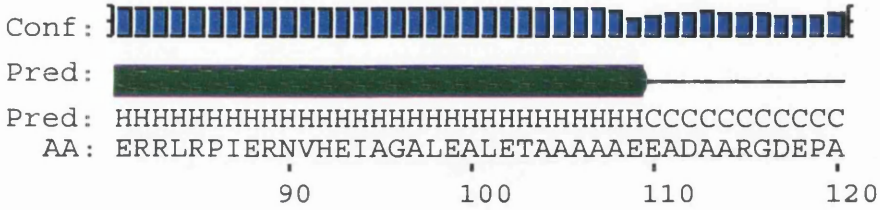
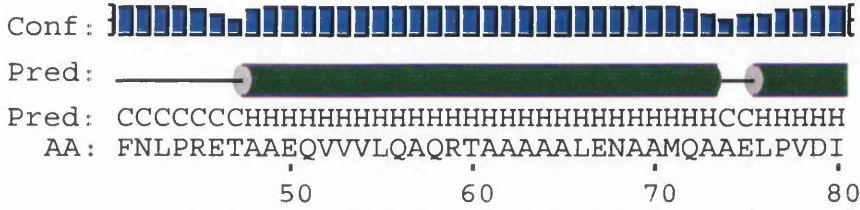
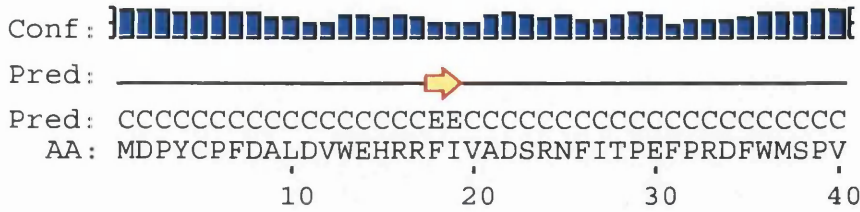
HSV-1 IARGASGSDSGAKSGDINLEAICANVYFIRADEAENICDFPGLAALCLIAQAGRVP
 HSV-2 IARGASGLDSGAKSGDINLEACVNVYFIRYADETNEICLPPGLAALCLIAQAGRPL
 BHV-1 VTRGADGGDGAVGARSQDANLJTEICAVXVARVEACEBENTCLPPGAALALALAPRSA
 EHV-4 NARGAIGASAMVRSRGNHHTPCSNVSEVLANTENETCLPPGLAALCLIAQOTGARN
 GHV-1 411 ..VZASVTIPGDVTKSDGRNLTIRLFPQXVYFVSVVVKGENTCLPPGLVAILCLVPPFSDST
 GHV-2 412 ..VZASVTIPGDIKSDGRNLMELFQXVYFVYDNRCEVTEGFPGLAALCLVPLFSSH
 ILTV SRPQATADNGQDAASRDNNLFRIFEXVYFVYVADERTETCLPPGLAALALIAHSAH...
 PRV 386 ..RZASGD.APASRSGDGNLRTLLAVYVAVRADERTETCLPPGLAALALIAHSAH...
 VZV 411 ILRGAIG.FDGKFKSGMNFQICEYLAFTLNRTEETETFPGLVAILCLIAHTQLSR
 HCMV 405 GLPRAEYGGRHGRVREAVRYIGWARDATILSOYVAGALAVTESVRSS.
 HHV6 383 ..QLENVNNFEAGN..IPEBEMHVEVEMNLQNDISITPFGHVCNESVRL...
 HHV7 380 ..HVNAETEFSN..IPEBEMKNVETLANNESTSTPFGHISVNESVRLN.
 ALCELPAPHINE HV-1 390 ...SS....KVQFKRDEVFTFLMKEVYVPLLSHNNNTISTEFLGNALAALEVGNQIN.
 ATELINE HV-3 379 ...SST.EPNKIYKKGQVSELSKNNVPLTINNENNPISFLFFGVTLIALESLAGP...
 EBV 394 PAMASAGYPVQTFRHGELFRFIAHVRPITVAADPOASISSLFFGLVLIJALEKLMDS.
 EHV-2 386 ...PAAQQPAAFKKGFLEFSVYKNNVYVPLTRR.POTPASSLFFGAVLIJALETADAAGS
 KSHV 384 ...GAL.DPNAPMLKRGOLFSEHVIIPILQANPNAPVSEFFGIIJLAALEARSTVP.
 MHV-4 357 ...GSR.RRTGPLEDAGGSVSEFLMENVLPTLLHRPTTNMSALFFIGLVIJOLEFSSGA...
 MMRV 382 ...VED.SGSKQYLKKGOLFDFLTENYISPLSRADPTSTLFFPGAYLAALEAKAIST.

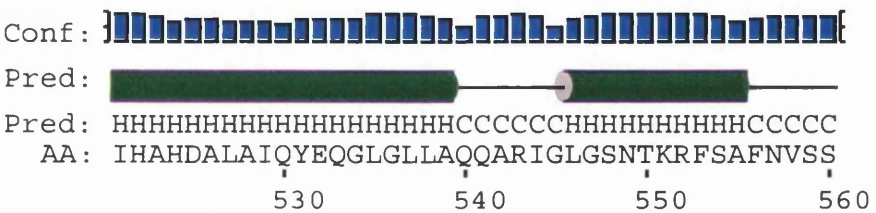
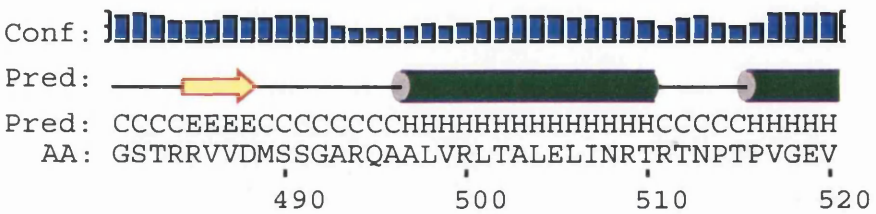
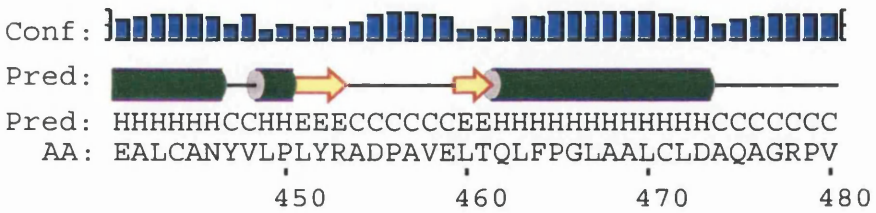
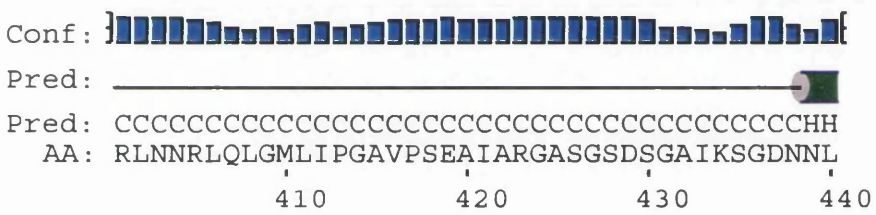
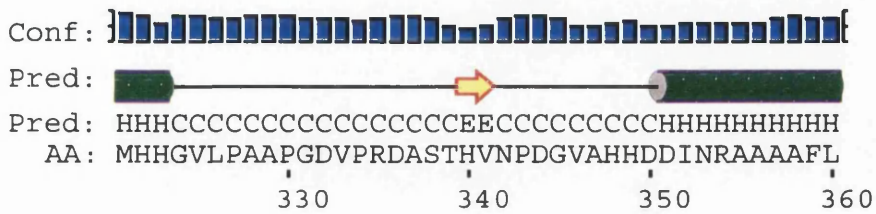
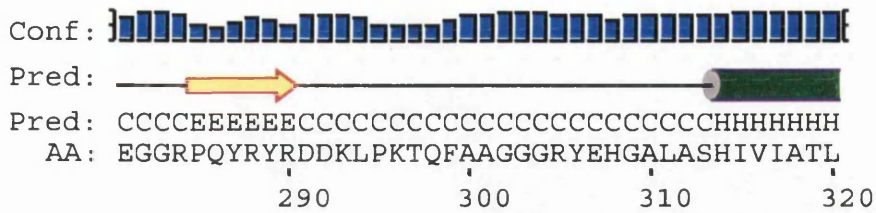
HSV-1 481 GSTRV DMSGAPAAVRITALEINRTRINPTVGEVSHAHDAIAQVCSLGLAQ
 HSV-2 481 ASTRV DMSGAPAAVRITALEINRTRINPTVGEVSHAHDAIAQVCSLGLAQ
 BHV-1 477 AGAPAA SGGGHHGGLRVALEENRRAAPAVVEVAHADAAIQVBRGIGLQ
 EHV-4 474 HPHHA NMTGNITNTRIGIEENRKTAPAPINEVAHADAAIQVBRGIGLQ
 GHV-1 469 RIPSII DLSLSTGASVKLISLEONRSRANVVSCEVTHHLLTQVBRGIESLQ
 GHV-2 470 RAPSIV DLSLSTGASVKLISLEENRANVVSCEVTHHLLTQVBRGIESLQ
 ILTV 464 IPTAIR . GEYSSCNIELDKRTSHG . . SGAAA RAVHDSITGDVEEGRSLIE
 PRV 439 RARVOHLNVRVALEONRQVTV . APVNEVAHADAAIQVBRGIGLQ
 VZV 470 GSLRTV DSGQEDRISIALEENRQVTSPIAARSHSMMQVBRGIGLQAH
 HCMV 464 REDSAGGSIPVADYFAQSSKQYGD LRRLEVVA LFHYHSGRVS
 HHV6 437 KCAGAPSDSEPFVEYRAQ . MEQQAD VALIEK CILFHLN NNTS
 HHV7 435 QNTITQNTKDNPFVEYRSQ . EETAET LAVIEK KILFHN NNTS
ALCELAPHINE HV-1 442 KEFVMEAGTKETKIFNVINQK . IMFKDV RELVAKSELRVALENGLFATIN
ATELINE HV-3 433 PFINTIGNRFODIFEIINQK . FTFKDP ESLMAAHTAFRLKVEHGLGNLIS
EBV 453 HYAINLIGQKEDTLFEIINQK . LLFEDP AAMIARTQIRLAFEDGVCVAVIG
KSHV 443 GQTGELINLSGKKYDQLFDVINQK . LTFRDV QGLIGAQTALRITLERGINLIS
MHV-4 439 GPFVNLGSRNEIFEIINQK . LTFRDP LALLQARTALRLATEEGLDVLLS
MMRV 411 IAHLLDDVKRRDIFNILLVQS . NVFQDS QELIRAKQSLRVSCETGSGNLLIE
 437 RPFVNLGSRNEIFDIINQK . LTFRDA GSLIQAQTSRLRTAEGLAATIS

HSV-1 541 QARIGLGNTRKFSANVSSDYIMLYFLCLGTFPOYLSAN
 HSV-2 541 QARIGLASNTRKRAFNVGSDYILLYFLCLGTFPOYLSVA
 BHV-1 537 QPRLRRALERRLSQFNVASDYILLYFLCLGTFPLFTSAN
 EHV-4 534 KPRLAASFEKRLGQFNVASDYILLYFLCLGTFPSFTSAN
 GHV-1 529 VQRFTRFFKKAALAFNVVETDYILLYFLCLGTFERSVSAS
 GHV-2 530 IQRPSRIFKKAALAFNVVETDYILLYFLCLGTFPKLISTI
 ILTV 517 VFDALKAFERJEDIORGV
 PRV 492 QPHLNAADK . RLGQFGVSSDYDLYFLCLGTFPOFAAAA .
 VZV 530 QPRVAAALERRLAQFNVNSDYDLYFLCLGTFPOFASTP
 HCMV 515 VTLRHRVSTGSSLNILLYSSVDFLVSVAVL .
 HHV6 487 FTLRORIFAMASSLNNITFTVDFLIPAVI .
 HHV7 485 LALRHRIFAMASSLNNITFTVDFLIPAVI .
ALCELAPHINE HV-1 492 SIAPVNAVVEVIQKQGGDDYRLYFLVLCGLPVTVAVV
ATELINE HV-3 482 NPSPTTFATEIHKHQGGEDNYITLYFTVLCGLPIAWAAV
EBV 503 RPSPLAAREILERQFSASDDYRLYFLTLGXLASPVAPS
EHV-2 496 KPSPLTSATEVISTQFGGDDXISLYFLILGCLPVTMAVV
KSHV 489 HPSPTTLQEIISKQFGGDDXIRAFVFWLGLCPVWLAVV
MHV-4 460 SLSPGTTWRDIIRKEFMAQVYLYVFCVLCALPVTVAVV
MMRV 487 HPSPPGLAHEIMKSQFGVYDDYRLYFLVLCGLPVTVAISVV

Figure 3.2 PSIPRED Predicted Secondary Structure of the HSV-1 UL25 Protein.

The HSV-1 17⁺ UL25 amino acid sequence was analysed using the PSIPRED program which predicted the amino acid residues that were likely to form α -helices and β -sheets (strands) together with an indication of the confidence of that prediction.





& Sandler, 1993). The PHDsec program has been demonstrated to have an accuracy of over 70% when compared to experimentally derived data and predicted that 47.4% of the UL25 protein was composed of α -helices, 5.9% was composed of β sheets and 46.7% was composed of non-specific coiled loops.

3.1.3.2 ISREC COILS Secondary Structure Prediction.

The HSV-1 17⁺ UL25 amino acid sequence and homologous UL25 amino acid sequences from alpha-, beta- and gammaherpesviruses were submitted to the ISREC COILS protein secondary structure prediction program (Lupas *et al.*, 1991) and the results are shown in Figure 3.3. COILS is a program that calculates the probability of an amino acid sequence adopting an α -helical coiled-coil structure which is formed when two parallel α -helical subunits coil around each other. The program compares an amino acid sequence to a database of known parallel two-stranded coiled-coils and derives a similarity score. By comparing this score to the distribution of scores in globular and coiled-coil proteins, the program then calculates the probability that the sequence will adopt a coiled-coil conformation. The program strongly predicted the presence of an α -helical coiled-coil region within the first 120 amino acids of the N-terminus of the HSV-1 17⁺ UL25 protein (Figure 3.3a) which was also identified in the homologous region of pseudorabies virus, another alphaherpesvirus (Figure 3.3b), human herpesvirus 7, a betaherpesvirus (Figure 3.3c) and to a lesser extent in Epstein-Barr virus, a gammaherpesviruses (Figure 3.3d). This is not an exhaustive list of the UL25 homologues examined and in all amino acid sequences submitted to the ISREC COILS program an α -helical coiled-coil region was predicted within the first 120 amino acids of the N-terminus of the UL25 protein homologues. Furthermore, additional coiled-coil prediction programs such as COILSCAN from the genetic computer group (GCG) also predicted the presence of an α -helical coiled-coil structure within this region of the UL25 homologues (data not shown).

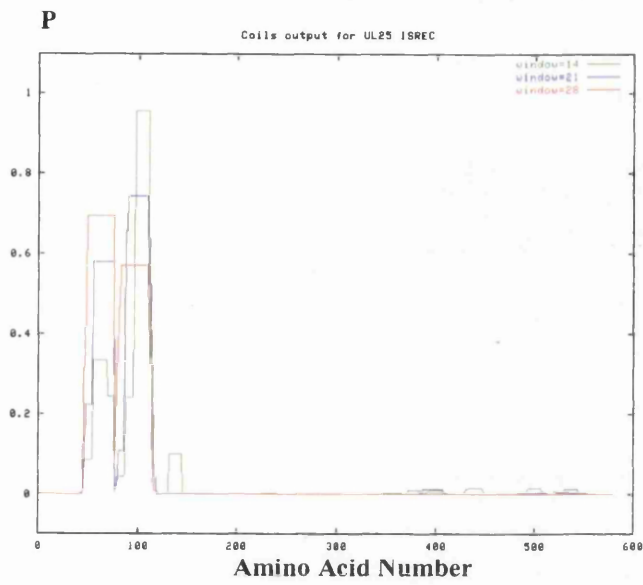
3.1.4 Discussion.

The large degree of homology within the UL25 protein of the herpesviruses suggested a highly conserved function. Bioinformatic analysis of the UL25 protein failed to detect any characterised protein domains such as zinc finger regions and it is likely that the UL25 protein performs a function that is not associated with a specific protein domain or motif. Although a PROSITE motif search (Bairoch *et al.*, 1997) revealed the presence of a

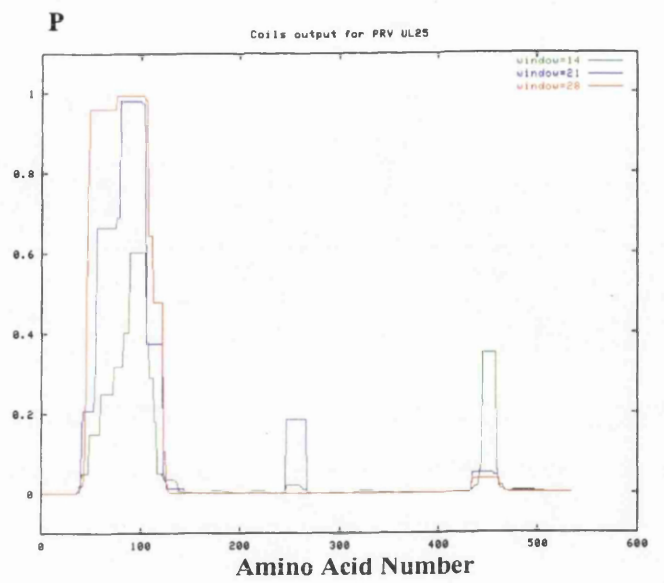
Figure 3.3 ISREC COILS Analysis of the HSV-1 17⁺ UL25 Amino Acid Sequence and its Homologues.

Herpesvirus UL25 amino acid sequences were analysed using the ISREC COILS program which plotted the probability (**P**) of each amino acid residue forming an α -helical coiled-coil against the amino acid number in the primary sequence. The window size indicates that the program analysed the full primary amino acid sequence, sequentially, in groups of 14, 21 and 28 amino acids. **a).** HSV-1 17⁺ UL25 (alphaherpesvirus), **b).** Pseudorabies virus UL25 (alphaherpesvirus), **c).** Human herpesvirus 7 VP U50 (UL25) (betaherpesvirus) and **d).** Epstein-Barr BVRF1 (UL25) (gammaherpesvirus).

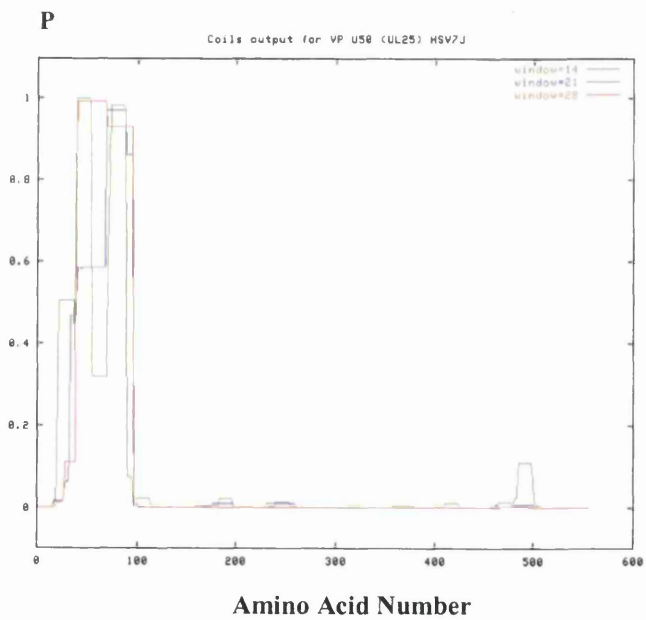
a).



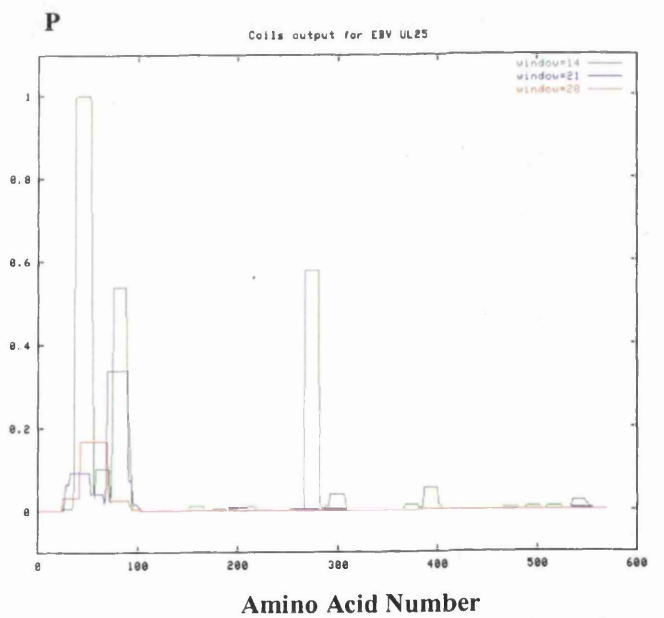
b).



c).



d).



myristylation, a glycosylation and several phosphorylation sites within the primary amino acid sequence of the UL25 protein, it is unlikely that the UL25 protein is post-translationally modified because there do not appear to be multiple high molecular weight forms of the protein.

The UL25 polypeptide was predicted to fold into a protein with a secondary structure composed largely of α -helices which is typical of globular proteins. The α -helix is predominantly a structural motif and is also associated with portions of transmembranal proteins that cross lipid bilayers although there is no evidence to suggest that the UL25 protein is associated with viral or cellular lipid bilayers. The UL25 protein was also predicted to contain an α -helical coiled-coil region near the N-terminus. This structural feature was conserved throughout the herpesviruses even though the sequence alignment data suggested that the N-terminus was not as highly conserved as the C-terminus. This was probably due to the nature of the coiled-coil motif which consists of a heptad repeat of hydrophilic and hydrophobic amino acid residues and not necessarily a repeat of specific amino acid residues. Amino acid positions within the heptad repeat are designated *a* to *g* and the coiled-coil is characterised by hydrophobic residues at positions *a* and *d* and hydrophilic residues at positions *b*, *c*, *e*, *f* and *g*. The hydrophobic residues constitute the helix interface and are evident as a 4-3 repeat in the primary amino acid sequence. Coiled-coil regions are known to mediate a variety of interactions including protein heterodimerisation (Krammerer *et al.*, 1999) and homo-oligomerisation (Procopio *et al.*, 1999). These regions are also known to facilitate the DNA binding properties of some proteins (Akhmedov *et al.*, 1999) and the possibility exists that the predicted coiled-coil region of the UL25 protein is involved in similar interactions.

3.2 Generation and Characterisation of Reagents Used in This Study.

3.2.1 The Generation of a Polyhistidine-Tagged UL25 Expressing Recombinant Baculovirus.

3.2.1.1 Introduction.

The most widely used baculovirus expression system utilises a lytic virus known as *Autographa californica* nuclear polyhedrosis virus (hereafter referred to as baculovirus). This virus forms proteinaceous viral occlusions called polyhedra within the nuclei of infected cells; the major protein component of these occlusion bodies is the baculovirus-encoded polyhedrin protein. Although the polyhedrin protein is essential for survival of the virus in nature, it is dispensable for virus propagation and viability in tissue culture cells and recombinant baculoviruses have been generated by replacing the polyhedrin gene with a foreign gene through homologous recombination.

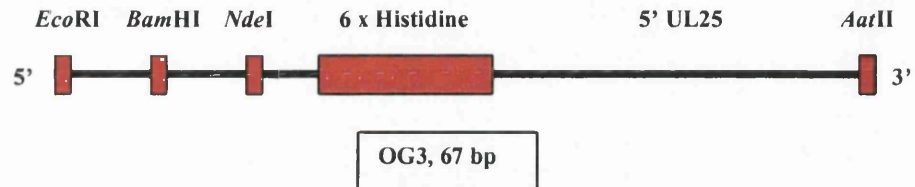
Initially, the pET expression system (Novagen) was used to generate and express a polyhistidine-tagged UL25 protein in *E. coli*. However, despite thorough investigation into the conditions of protein production and purification, the recombinant protein remained predominantly insoluble. Since recombinant proteins produced in the baculovirus system are often more soluble than proteins synthesised in bacterial expression systems, the aim of the work described in this section was to utilise the baculovirus system to produce high levels of a soluble polyhistidine-tagged UL25 protein. The polyhistidine tag functions as a metal-binding domain to enable purification of the recombinant protein by affinity chromatography using a column composed of nickel-agarose. Purified recombinant protein was to be used as an immunogen in the production of monoclonal antibodies specific for the UL25 protein. Provided a sufficient amount of soluble recombinant protein could be purified to near homogeneity, an additional goal was to examine the properties of the protein using biochemical techniques.

3.2.1.2 The Generation of Oligonucleotide OG3.

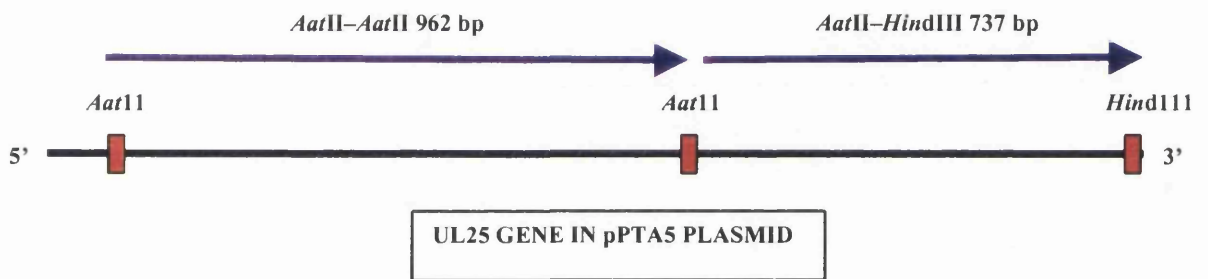
A dsDNA oligonucleotide was designed for the purpose of engineering a polyhistidine tag onto the N-terminal portion of the UL25 protein. This oligonucleotide was termed OG3 and was formed by annealing single stranded DNA oligonucleotides VP226 and VP227 (Figure 3.4 and step 1 of Figure 3.5). The OG3 oligonucleotide contained *EcoRI* and

Figure 3.5 An Outline of the Cloning Strategy used to Generate the pPTA10 Plasmid (pAcCL29.1 Baculovirus Transfer Vector Encoding the Polyhistidine Tagged UL25 Protein).

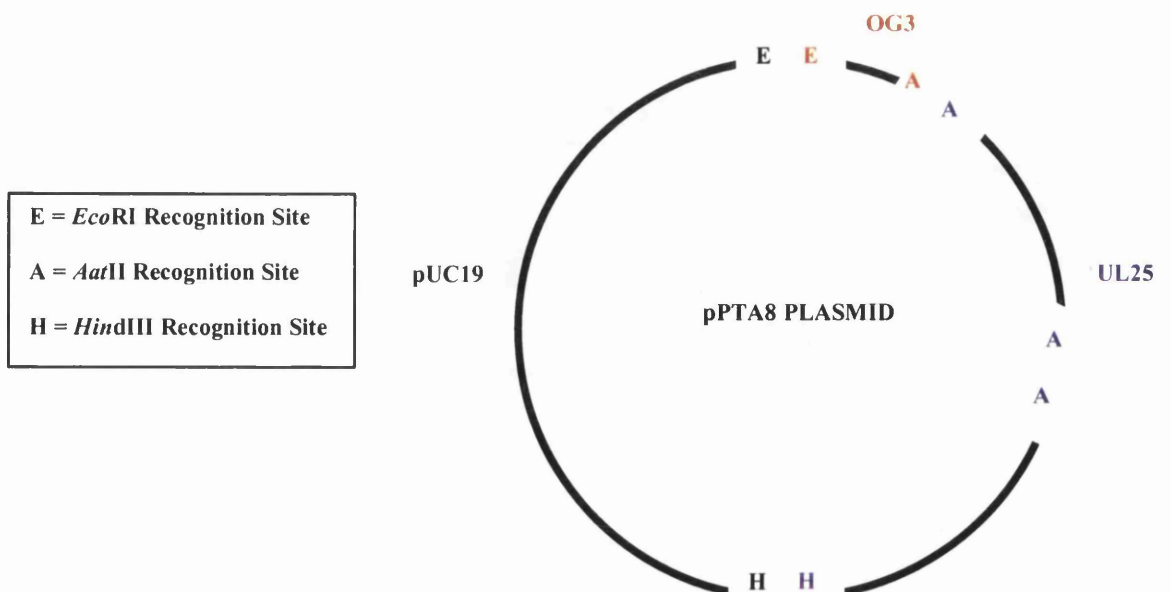
1. Oligonucleotide OG3 was constructed and purified.



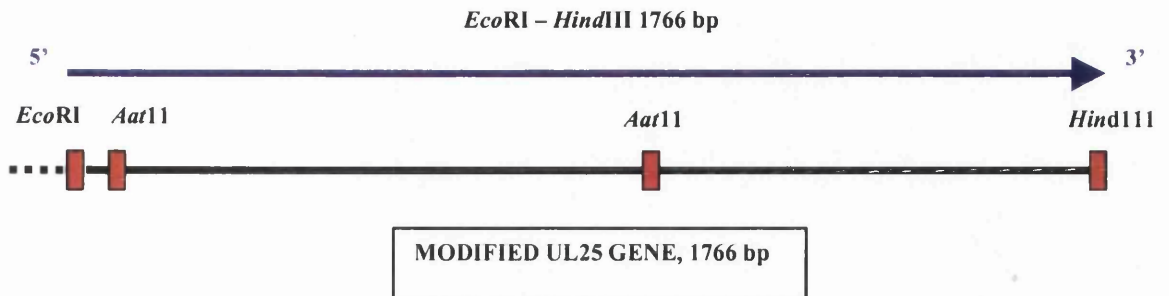
2. The UL25 gene DNA fragments were isolated and purified.



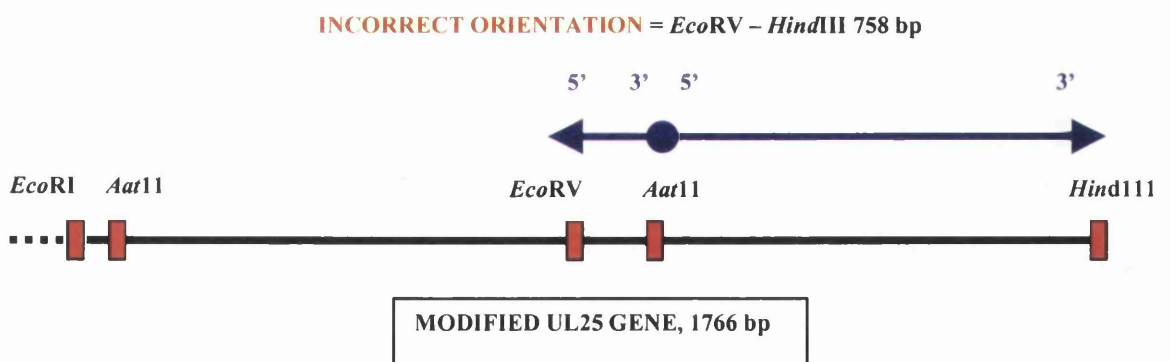
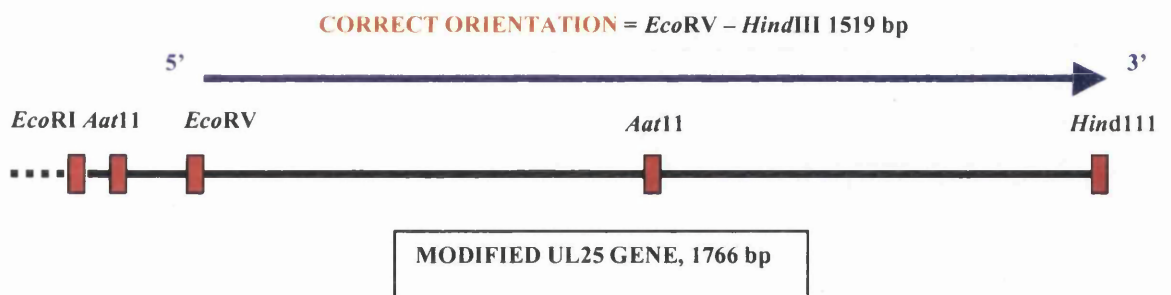
3. The OG3 oligonucleotide and the UL25 DNA fragments were ligated to *EcoRI/HindIII* linearised pUC19 plasmid to create the pPTA8 plasmid.



4. An *EcoRI/HindIII* screen was used to identify constructs in which the pUC19 plasmid backbone and all three HSV-1 DNA fragments had ligated successfully to form the pPTA8 plasmid.

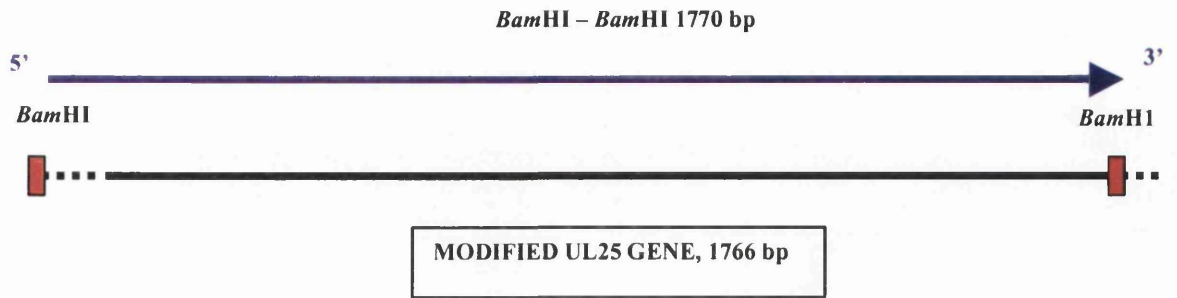


5. An *EcoRV/HindIII* screen was used to identify constructs containing the UL25 *AatII–AatII* DNA fragment in the correct orientation within the pPTA8 plasmid.

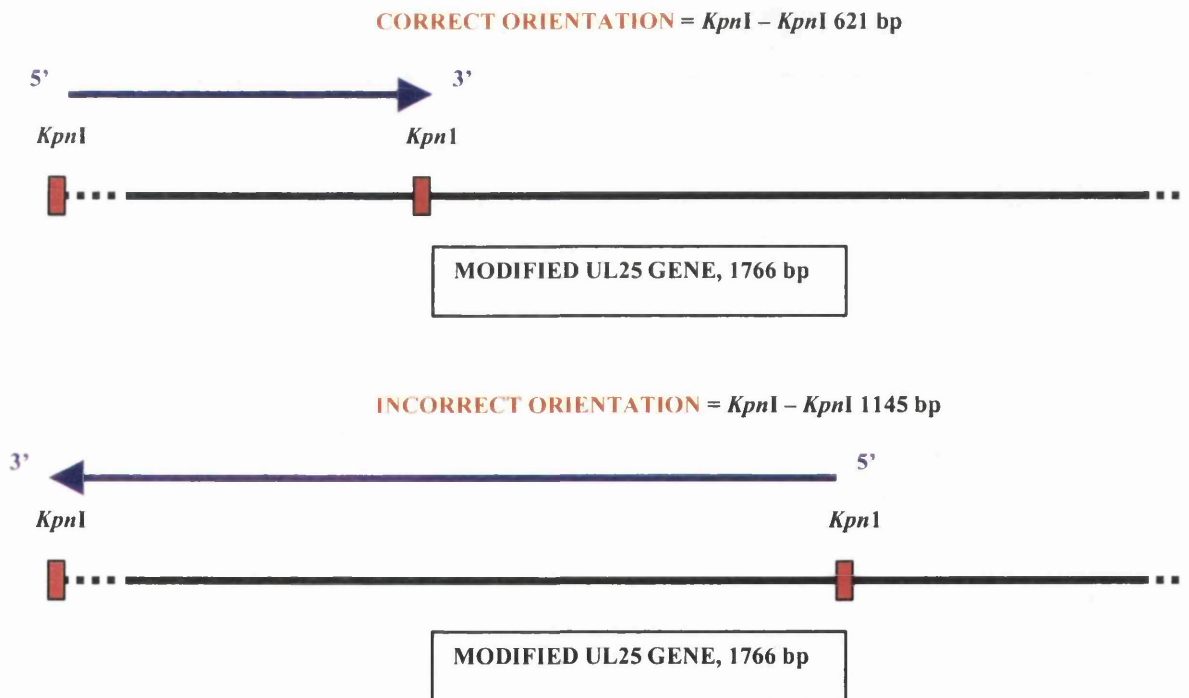


6. The modified UL25 gene was excised from the pPTA8 plasmid as a *BamHI* fragment and ligated to *BamHI* linearised pAcCL29.1 baculovirus transfer vector to generate the pPTA10 plasmid.

7. A *Bam*HI screen was used to plasmids in which the pAcCL29.1 plasmid and the modified UL25 gene had ligated successfully to form the pPTA10 plasmid.



8. A *Kpn*I screen was used to identify constructs containing the modified UL25 gene in the correct orientation within the pPTA10 plasmid.



*Bam*HI restriction endonuclease recognition sites at the 5' terminus to facilitate cloning, and an *Nde*I site to provide an ATG translational start signal. Sequences specifying a hexahistidine motif were incorporated downstream of the *Nde*I recognition site at the 5' portion of the UL25 gene. The natural start ATG codon of the UL25 gene was removed to ensure translation resulted only in the production of a polyhistidine tagged protein. The UL25 gene contains an *Aat*II restriction endonuclease recognition site between nucleotides 31-36 (inclusive) and the OG3 oligonucleotide was designed to contain the 5' portion of the UL25 gene up to and including this site.

3.2.1.3 Purification of UL25 Gene Fragments and Linearised pUC19 Plasmid.

In order to generate the UL25 gene fragments necessary for the cloning procedure, the pPTA5 plasmid (the HSV-1 UL25 gene in a pUC19 plasmid vector) was digested with *Aat*II and separately with *Aat*II and *Hind*III enzymes. At the same time, the pUC19 plasmid was digested with *Eco*RI and *Hind*III enzymes. The digested DNA samples were electrophoresed through a 0.8% agarose-TBE gel containing 0.5 $\mu\text{g}\cdot\text{ml}^{-1}$ ethidium bromide and the DNA was visualised using a long wave UV source. The 962 bp *Aat*II-*Aat*II UL25 gene fragment, the 737 bp *Aat*II-*Hind*III UL25 gene fragment and the large *Eco*RI/*Hind*III fragment from the pUC19 plasmid were excised from the gel and purified using a QIAquick gel extraction kit (step 2 Figure 3.5). A small amount of each DNA fragment were electrophoresed through a 0.8% agarose-TBE gel containing 0.5 $\mu\text{g}\cdot\text{ml}^{-1}$ ethidium bromide and the DNA was visualised using a short-wave UV source. The concentration of each DNA fragment was estimated by comparing the intensity of the fluorescent band with 50 ng and 100 ng of λ DNA run on the same gel. The DNA fragments were purified to a sufficient quantity to allow the preparation a ligation reaction.

3.2.1.4 Ligation of the OG3 Oligonucleotide and UL25 Gene Fragments to the Linearised pUC19 Plasmid.

The OG3 ligation reaction (step 3 Figure 3.5) was prepared as described in section 2.2.7.6 and electrocompetent *E. coli* were transformed with the reaction mixture as described in section 2.2.8.3.

3.2.1.5 An *EcoRI/HindIII* Screen was Used to Identify Plasmids Containing the Full-Length UL25 ORF Modified at the 5' End.

One hundred ampicillin resistant bacterial colonies were selected and used to produce small scale DNA samples which were screened using an *EcoRI/HindIII* DNA digestion to determine whether all three DNA fragments had been ligated into the pUC19 plasmid backbone (step 4 Figure 3.5). Due to the nature of the ligation reaction there were two possible end products. The first would be the pUC19 plasmid backbone containing only the OG3 oligonucleotide and the 737 bp *AatII-HindIII* UL25 gene fragment and would produce a DNA fragment of 804 bp as a result of *EcoRI/HindIII* digestion. The second and desirable end product would be the pUC19 plasmid backbone containing the OG3 oligonucleotide and both the 962 bp *AatII-AatII* and the 737 bp *AatII-HindIII* UL25 gene fragments and would produce a DNA fragment of 1766 bp as a result of *EcoRI/HindIII* digestion. Figure 3.6 shows the results of the *EcoRI/HindIII* screen using bacterial clones 92-100 and demonstrates that clones 93, 97 and 99 produced the desired 1766 bp fragment as a result of the *EcoRI/HindIII* digestion. Out of the 100 bacterial clones screened only five cultures, derived from numbers 76, 91, 93, 97 and 99, contained a plasmid which had the *EcoRI/HindIII* fragment of 1766 bp. The plasmid contained within these clones was termed pPTA8.

3.2.1.6 An *EcoRV/HindIII* Screen was Used to Identify Constructs Containing the UL25 *AatII-AatII* DNA Fragment in the Correct Orientation Within the pPTA8 Plasmid.

Since the 962 bp *AatII-AatII* UL25 gene fragment within the pPTA8 plasmid of bacterial clones 76, 91, 93, 97 and 99 may have been present in either the correct or the incorrect orientation, the small scale DNA samples from these clones were screened using an *EcoRV/HindIII* DNA digestion (step 5 Figure 3.5). The UL25 *AatII-AatII* gene fragment contains an *EcoRV* site 180 bp downstream from the 5' terminus and if this fragment was present in the correct orientation, *EcoRV/HindIII* digestion of the pPTA8 plasmid would result in the production of a 1519 bp DNA fragment. If the UL25 *AatII-AatII* gene fragment was present in the incorrect orientation, *EcoRV/HindIII* digestion of the pPTA8 plasmid would generate a 917 bp DNA fragment. Figure 3.7 demonstrates that the pPTA8 plasmid of bacterial clone numbers 76, 93 and 99 contained the UL25 *AatII-AatII* gene fragment in the correct orientation whereas clones 91 and 97 contained this fragment in the incorrect orientation. A large culture of clone number 76 was grown up and

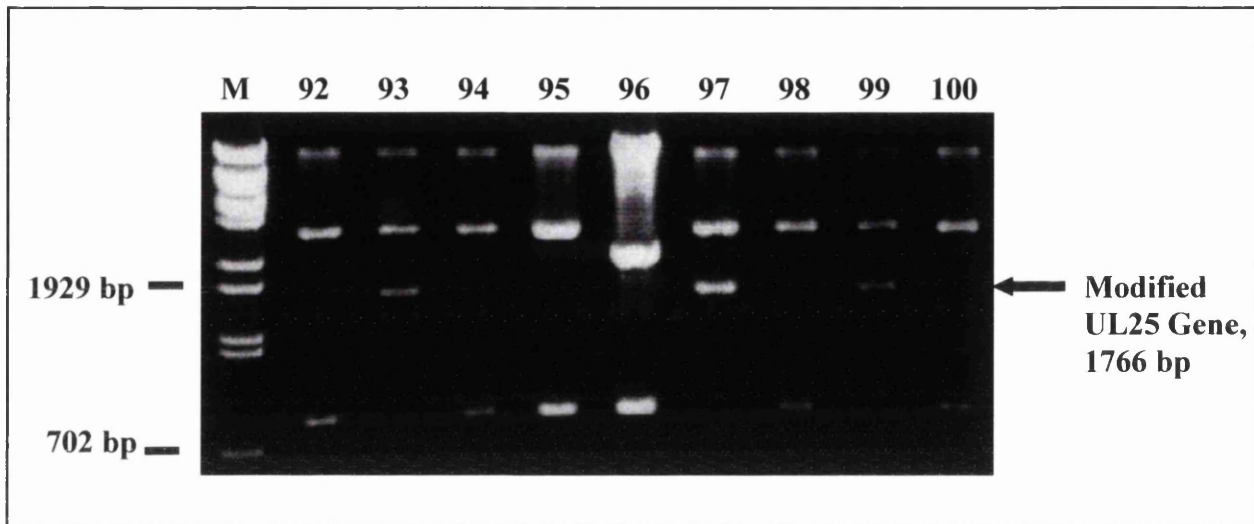


Figure 3.6 An *EcoRI/HindIII* Screen was Used to Identify Constructs in which the Modified UL25 Gene had been Introduced Into the pUC19 Plasmid Backbone to Form the pPTA8 Plasmid.

Electrocompetent *E.coli* DH5 α were transformed with the ligation reaction containing the OG3 oligonucleotide and plated on L-broth agar plates containing 50 $\mu\text{g.ml}^{-1}$ ampicillin to select for transformed bacteria. One hundred bacterial colonies were isolated and small scale DNA samples prepared. The *EcoRI/HindIII* digested DNA fragments were separated by electrophoresis through a 0.8% agarose-TBE gel containing 0.5 $\mu\text{g.ml}^{-1}$ ethidium bromide and the DNA was visualised using a short-wave UV source. The above figure illustrates the results of this screen using bacterial clones 92-100. The presence of the full-length modified UL25 gene containing the OG3 oligonucleotide and both the UL25 gene fragments would result in the formation of a DNA fragment of 1766 bp as exemplified by clones **93, 97** and **99**. A DNA fragment of 804 bp would be generated in the absence of the 962 bp UL25 *AatII-AatII* gene fragment and this is exemplified by clones **92, 94, 95, 98** and **100**. *BstEII* digested λ DNA was used as marker DNA (**M**).

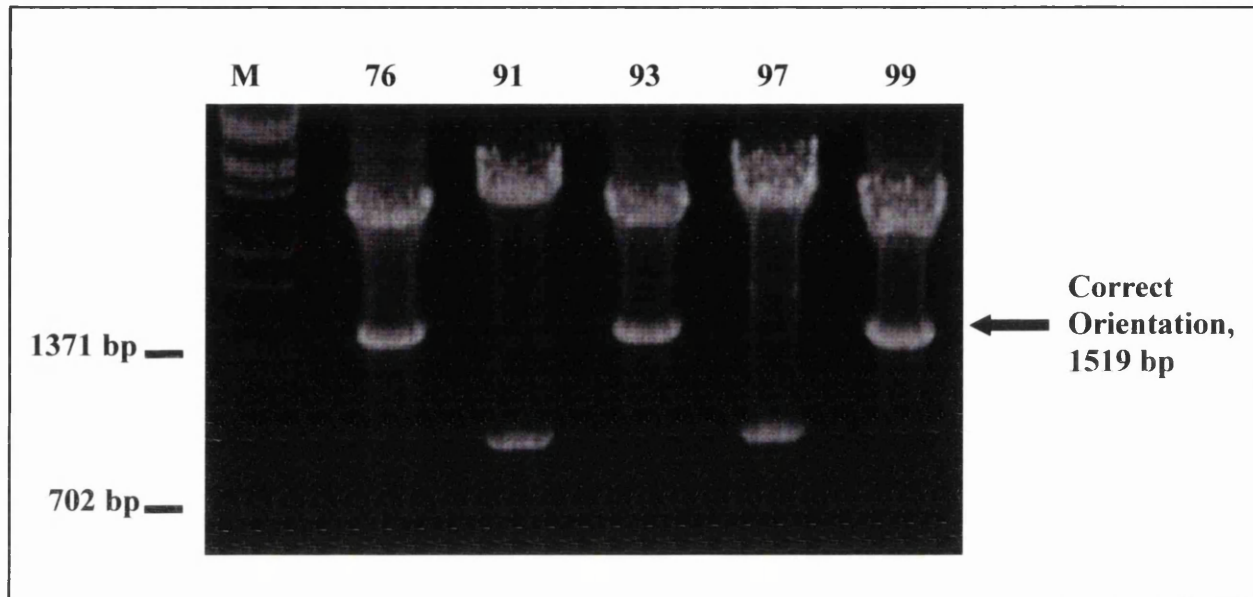


Figure 3.7 An *EcoRV/HindIII* Screen was Used to Identify Plasmids Containing the UL25 *AatII-AatII* DNA Fragment in the Correct Orientation Within the pPTA8 Plasmid.

The bacterial clones that contained the pPTA8 plasmid were screened using an *EcoRV/HindIII* DNA digest to determine whether the UL25 *AatII-AatII* gene fragment was present in the correct orientation. Digested small scale DNA was electrophoresed through a 0.8% agarose-TBE gel containing $0.5 \mu\text{g}\cdot\text{ml}^{-1}$ ethidium bromide and the DNA was visualised using a short-wave UV source. The presence of the UL25 *AatII-AatII* gene fragment in the correct orientation would result in the formation of a 1519 bp DNA fragment as exemplified by clones **76**, **93** and **99**. The presence of the UL25 *AatII-AatII* gene fragment in the incorrect orientation would result in the formation of a 758 bp DNA fragment as exemplified by clones **91** and **97**. *BstEII* digested λ DNA was used as marker DNA (**M**).

plasmid DNA was purified using a QIAGEN MIDI plasmid purification kit and termed pPTA8/76.

3.2.1.7 The Cloning of the Modified UL25 Gene Into Baculovirus Transfer Vector pAcCL29.1 to Generate the pPTA10 Plasmid.

The modified UL25 gene was isolated by *Bam*HI digestion of pPTA8/76. At the same time, the pAcCL29.1 baculovirus transfer vector was linearised with *Bam*HI and treated with CIP (step 6 Figure 3.5). The digested DNA fragments were isolated and purified as described in section 3.2.1.3. The two DNA fragments were ligated together plasmid as described in section 2.2.7.6 and electrocompetent *E. coli* were transformed with the reaction mixture as described in section 2.2.8.3.

3.2.1.8 A *Bam*HI Screen was Used to Identify Plasmids in Which the Modified UL25 Gene had Ligated Successfully into pAcCL29.1.

Small scale DNA samples were prepared from twenty-four ampicillin resistant bacterial colonies and screened using *Bam*HI DNA digestion to determine whether the modified UL25 gene had ligated into the pAcCL29 plasmid (step 7 Figure 3.5). Figure 3.8 demonstrates that all 24 bacterial clones screened produced the desired 1770 bp DNA fragment as a result of the *Bam*HI digestion. The plasmid contained within these clones was named pPTA10.

3.2.1.9 A *Kpn*I Screen was Used to Identify Plasmids Containing the Modified UL25 Gene in the Correct Orientation Within the pPTA10 Plasmid.

To determine the orientation of the HSV-1 fragment within the pAcCL29.1 plasmid, the small scale DNA samples were digested with *Kpn*I (step 8 Figure 3.5). If the modified UL25 gene was present in the correct orientation, *Kpn*I digestion of pPTA10 would produce a 621 bp DNA fragment. If the modified UL25 gene was present in the incorrect orientation, *Kpn*I digestion of pPTA10 would generate a 1145 bp DNA fragment. Figure 3.9 demonstrates that clone numbers 5, 7, 9, 10, 11, 13, 14, 15, 16, 20 and 22 contain a plasmid which had a *Kpn*I DNA fragment of 621 bp. A large culture of the bacterial clone number 9 was grown up and plasmid DNA was purified using a QIAGEN MIDI plasmid purification kit and was referred to as pPTA10/9.

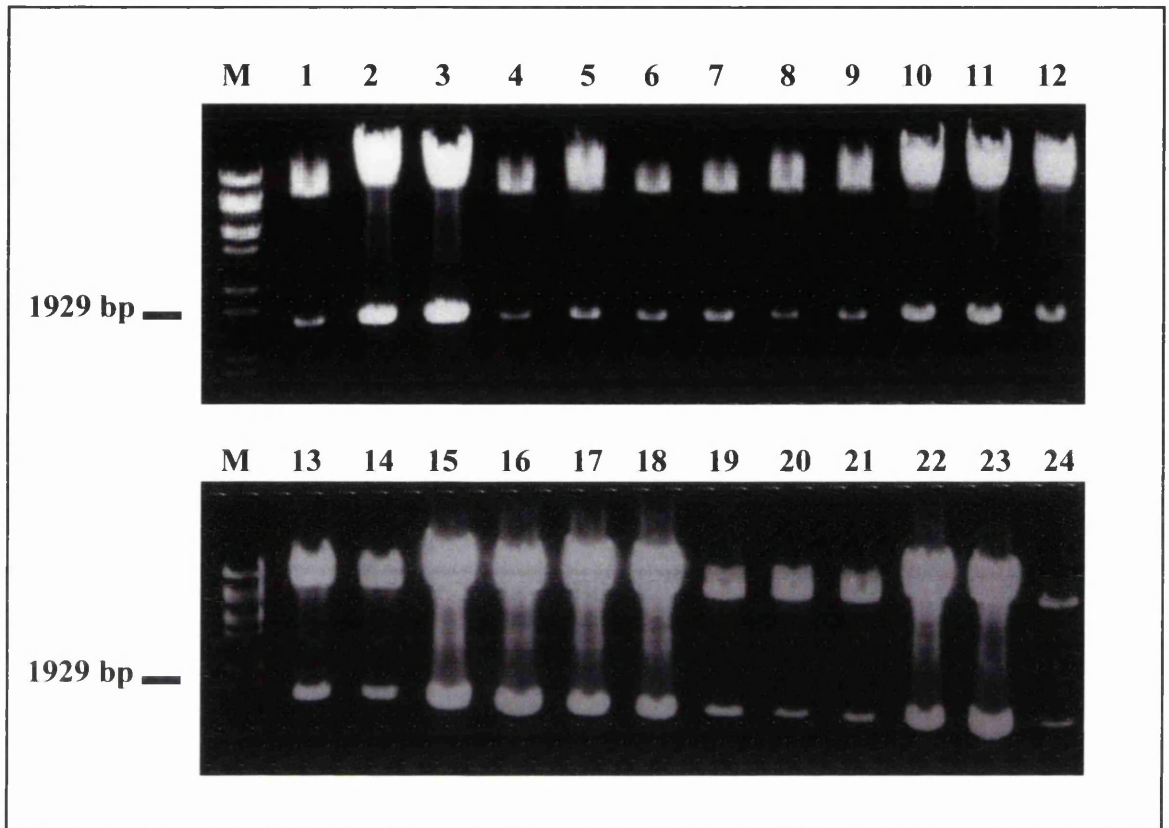


Figure 3.8 A *Bam*HI Screen was Used to Identify Constructs in which the pAcCL29.1 Plasmid and the Modified UL25 Gene had Ligated Successfully to Form the pPTA10 Plasmid.

Electrocompetent *E.coli* DH5 α were transformed with the ligation reaction mixture containing the linearised pAcCL29.1 plasmid and the modified UL25 gene and plated on L-broth agar plates containing 50 $\mu\text{g}\cdot\text{ml}^{-1}$ ampicillin. Small scale DNA samples were prepared from twenty-four of the resulting colonies and the samples digested with *Bam*HI. The digested DNAs were electrophoresed through a 0.8% agarose-TBE gel containing 0.5 $\mu\text{g}\cdot\text{ml}^{-1}$ ethidium bromide and the DNA was visualised using a short-wave UV source. The presence of the full-length modified UL25 gene would result in the formation of a DNA fragment of 1770 bp and all the 24 bacterial clones tested contained this DNA fragment. *Bst*EII digested λ DNA was used as marker DNA (M).

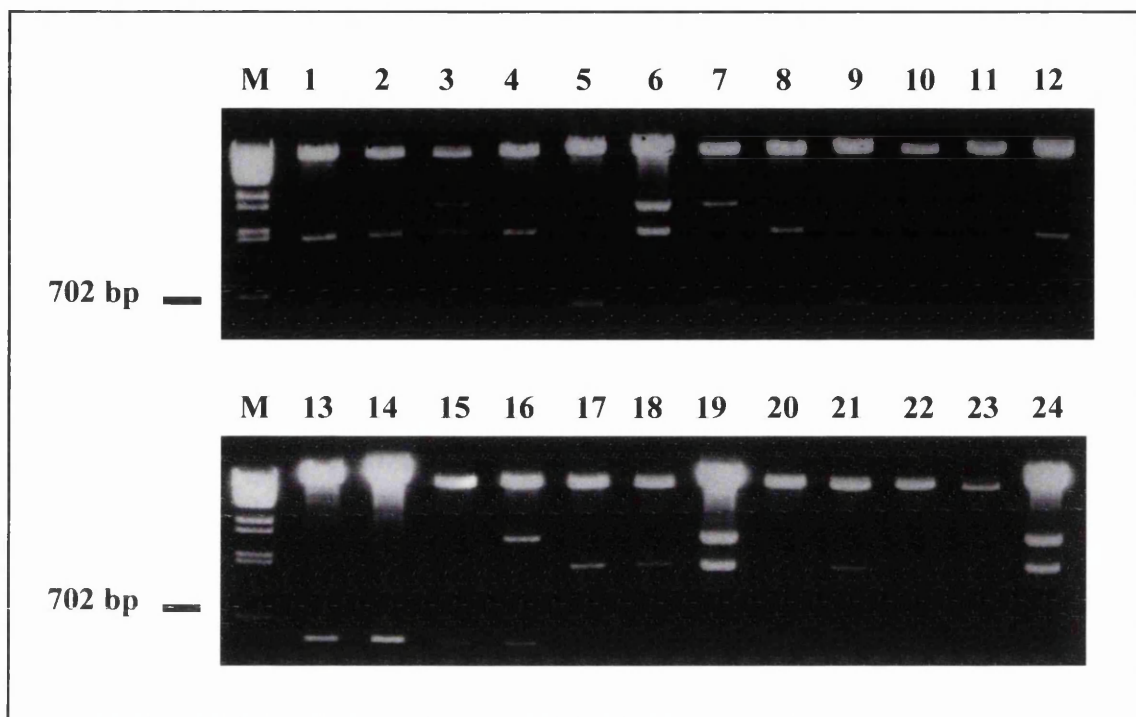


Figure 3.9 A *KpnI* Screen was Used to Identify Constructs Containing the Modified UL25 Gene in the Correct Orientation Within the pPTA10 Plasmid.

The bacterial clones that contained the pPTA10 plasmid were screened using an *KpnI* DNA digest to determine whether the modified UL25 gene was present in the correct orientation. The digested DNA was electrophoresed through a 0.8% agarose-TBE gel containing $0.5 \mu\text{g}\cdot\text{ml}^{-1}$ ethidium bromide and the DNA was visualised using a short-wave UV source. The presence of the modified UL25 gene in the correct orientation would result in the formation of a 621 bp DNA fragment as exemplified by clones **5, 7, 9, 10, 11, 13, 14, 15, 20 and 22**. The presence of the modified UL25 gene in the incorrect orientation would result in the formation of a 1145 bp DNA fragment as exemplified by clones **1, 2, 4, 8, 12, 17, 18 and 21**. *BstEII* digested λ DNA was used as marker DNA (M).

3.2.1.10 The Isolation of PTA10bac#14: A His-UL25 Expressing Recombinant Baculovirus.

Sf21 cells were cotransfected with PAK6 and pPTA10/9 DNA and recombinant baculoviruses were isolated and screened for the ability to synthesise the His-UL25 protein in virus-infected cells as described in sections 2.2.3.2 to 2.2.3.5. Figure 3.10 demonstrates that, with the exception of isolate number 8, all baculovirus isolates synthesised a large amount of the 62 kDa His-UL25 protein which was not present in mock- or PAK6-infected *Sf21* cells.

Baculovirus isolates 3 and 14, whose small scale virus stocks demonstrated good expression of the His-UL25 protein, were plaque purified as described previously. After the third plaque purification small scale virus stocks were prepared. A high titre recombinant baculovirus stock was produced from a small scale virus stock originating from isolate number 14. This recombinant baculovirus expressing the His-UL25 protein was termed PTA10bac#14.

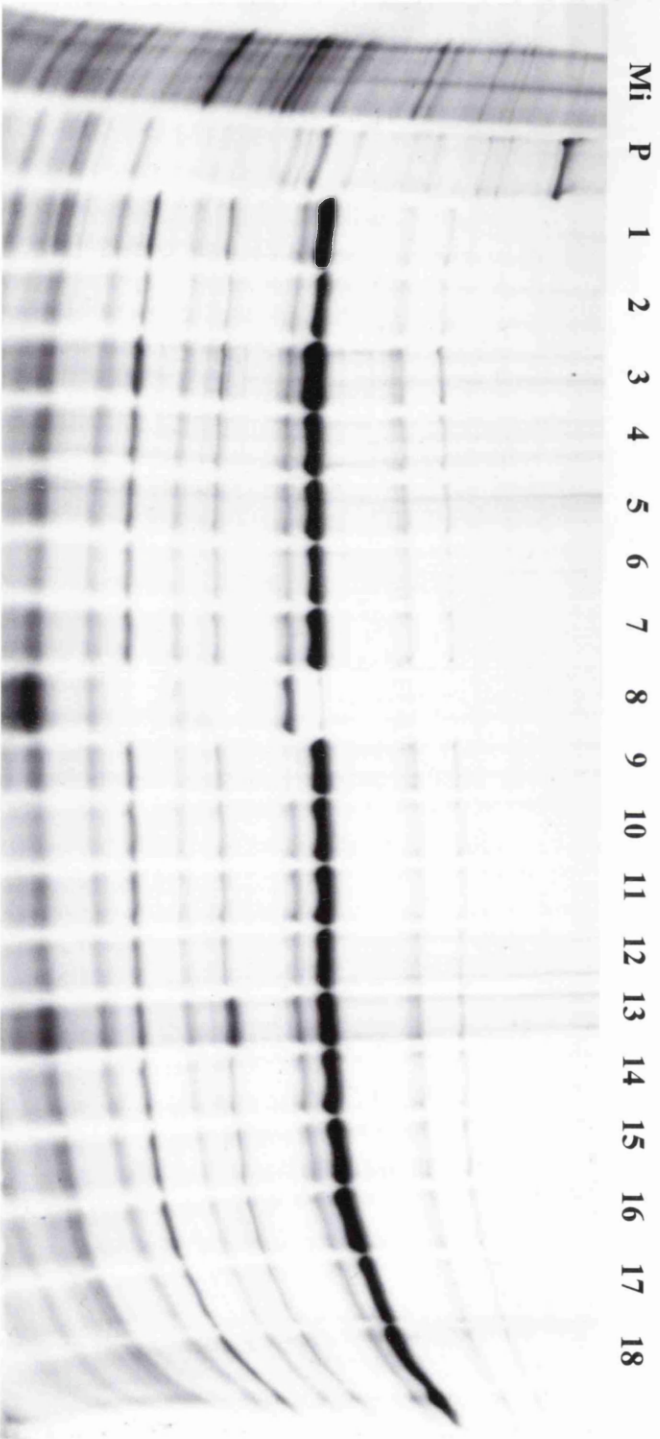
3.2.2 The Generation of a MBP-UL25 Fusion Protein Expressing Bacterial Clone.

The pMAL-c2 plasmid contains the *malE* gene of *E. coli* which encodes maltose-binding protein (MBP) and is used to express a gene of interest fused to this protein. Since MBP is soluble in *E. coli*, foreign proteins are often less insoluble in bacteria when fused to MBP (Maina *et al.*, 1988). Additionally, MBP binds amylose with high affinity and MBP-fusion proteins can be purified by chromatography with a column composed of amylose resin. The HSV-1 UL25 gene was cloned into the pMAL-c2 plasmid with a view to obtaining soluble, purified MBP-UL25 fusion protein for use as an antigen in the production of monoclonal antibodies.

The UL25 ORF was isolated by *Bam*HI digestion of pPTA5 and ligated to *Bam*HI linearised, and CIP treated, pMAL-c2 plasmid vector. Competent BL21 *E. coli* were transformed with the ligated DNA and ampicillin resistant bacterial clones were isolated. To establish that the UL25 ORF had ligated to the pMAL-c2 plasmid, small scale DNA samples were prepared from the ampicillin resistant bacterial clones and digested with *Bam*HI. The correct orientation of the UL25 ORF within the pMAL-c2 plasmid was determined by digesting the small scale DNA samples with *Kpn*I and *Xba*I. The plasmid that contained the UL25 ORF in the correct orientation was termed pPTA3 and bacterial clones that carried this plasmid were named PTA3.

Figure 3.10 His-UL25 Recombinant Protein Screen of Plaque Isolated Small Scale Virus Stocks.

Radiolabelled virus-infected *Sf21* cells were prepared from small scale virus stocks as described in section 2.2.3.5. PAK6 virus (**P**) and mock-infected (**Mi**) cells were included as controls. Samples of radiolabelled virus-infected cell extracts were resolved on an 8% SDS polyacrylamide gel and the protein profile was visualised by fluorography. The lane numbers are equivalent to the original plaque isolates from which the small scale virus stocks were produced.



66 K ●

Mi P 1 2 3 4 5 6 7 8 9 10 11 12 13 14 15 16 17 18

His-UL25

3.2.3 The Generation and Characterisation of Monoclonal Antibodies Specific for the HSV-1 UL25 Protein.

3.2.3.1 Introduction.

There are no commercially available antibodies specific for the HSV-1 UL25 protein and a polyclonal antiserum specific for UL25 demonstrated non-specific activity in indirect immunofluorescent analysis of wt HSV-1-infected cells. Additionally, the UL25 specific polyclonal antiserum did not appear to bind to the UL25 polypeptide with a high affinity in these types of experiments. Thus, the aim of the work described in this section was to generate highly specific monoclonal antibodies against the HSV-1 UL25 protein, primarily for use in indirect immunofluorescent assays. Furthermore, the isolation of UL25 specific monoclonal antibodies would enable dual labelling of virus-infected cells for the detection of two HSV-1 antigens in colocalisation studies. Following the protocol outlined in section 2.2.9, 12 hybridoma cell lines that produced monoclonal antibodies specific for UL25 as judged by ELISA were isolated as a result of two spleen fusion experiments. Hybridoma cell lines secrete monoclonal antibodies into their growth medium and the HATc medium from each of the cultured hybridoma cell lines was harvested and analysed for specific immunoreactivity in Western blot, immunoprecipitation and indirect immunofluorescent assays.

3.2.3.2 Purification of MBP-UL25 and His-UL25 Proteins.

3.2.3.3 Purification of MBP-UL25 Protein for Immunisation of BALB/c Mice.

A clarified cell extract from IPTG-induced PTA3 bacteria was used as a source of MBP-UL25 protein for purification by affinity chromatography with a resin composed of amylose immobilised to agarose beads as described in section 2.3.0. A sample of purified protein was resolved by SDS-PAGE and visualised by Coomassie blue staining and the result is shown in Figure 3.11. Approximately 1 mg of MBP-UL25 protein per litre of induced PTA3 bacterial culture was recovered with a purity of 60-70%. This purified protein sample was used directly as a source of antigen for immunisation of 4 BALB/c mice.

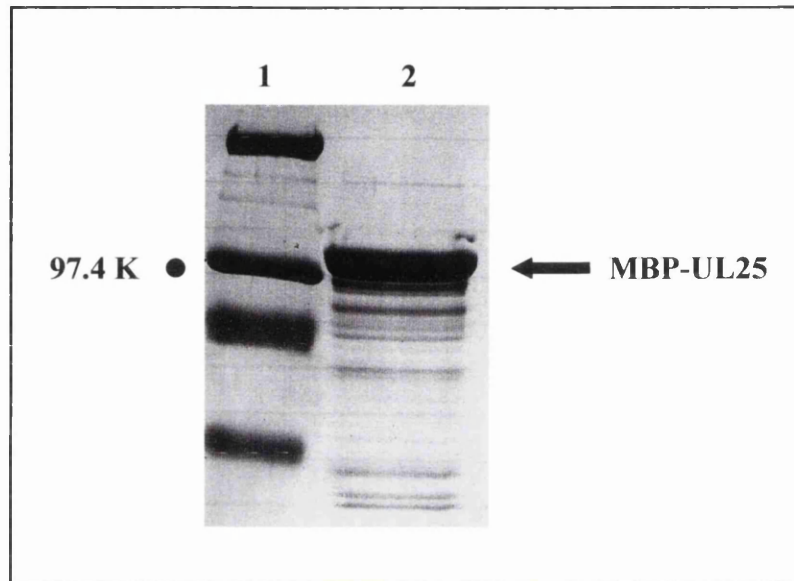


Figure 3.11 Purification of MBP-UL25 from IPTG Induced PTA3 Bacteria Carrying pPTA3.

A clarified cell extract from a culture of IPTG-induced PTA3 bacteria was used as a source of MBP-UL25 protein for purification by affinity chromatography with amylose resin. A sample of purified MBP-UL25 protein (**lane 2**) was resolved on an 8% SDS polyacrylamide gel and visualised by Coomassie blue staining. **Lane 1** represents molecular weight markers (5 μg of each marker).

3.2.3.4 Purification of His-UL25 Protein for Boosting Immunised BALB/c Mice.

An analysis of the specific immunoreactivity in serum isolated from blood taken in a test bleed from MBP-UL25 immunised mice revealed a disproportionate immune response in favour of the MBP constituent of the MBP-UL25 fusion protein (Figure 3.12). The immunised mice were therefore boosted with His-UL25 protein in an attempt to expand the population of immune cells secreting antibodies specific for the UL25 constituent of the MBP-UL25 protein prior to the preparation of a spleen fusion experiment.

A clarified cell extract from PTA10bac#14-infected *Sf21* cells was used as a source of soluble His-UL25 protein for purification by affinity chromatography with a resin composed of nickel ions immobilised to agarose beads (Ni-NTA) as described in section 2.3.0. A sample of purified protein was resolved by SDS-PAGE and visualised by Coomassie blue staining. These results are shown in Figure 3.13. Approximately 75-100 µg of His-UL25 protein with a purity of 80-90% was recovered from each 175 cm² flask of *Sf21* cells infected with PTA10bac#14. This purified protein sample was used directly as a source of antigen for boosting the 3 surviving BALB/c mice immunised with MBP-UL25.

3.2.3.5 The Reactivity of Monoclonal Antibodies Specific for the UL25 Protein in a Western Blot Assay.

The monoclonal antibodies were screened for their ability to react with UL25 in a Western blot assay as described in section 2.3.1.4 and a typical positive result is shown in Figure 3.14. The antibodies were screened against an AcUL25-infected *Sf21* cell extract which contained the unmodified UL25 protein as an antigen. Samples of purified MBP-UL25 and MBP alone were also included as controls together with a sample of PAK6-infected *Sf21* cells. The proteins within each sample were separated by SDS-PAGE, transferred to Hybond-ECL membrane and probed with HATc medium collected from the hybridoma cell lines. Seven of the twelve monoclonal antibodies isolated bound the UL25 protein in this assay and the data are summarised in Table 3.1, together with an indication of the affinity each monoclonal antibody had for the UL25 antigen. However, as the concentration of the antibodies in the HATc medium was not established this may not represent a true indication of the affinity each monoclonal antibody had for the UL25 antigen in this assay.

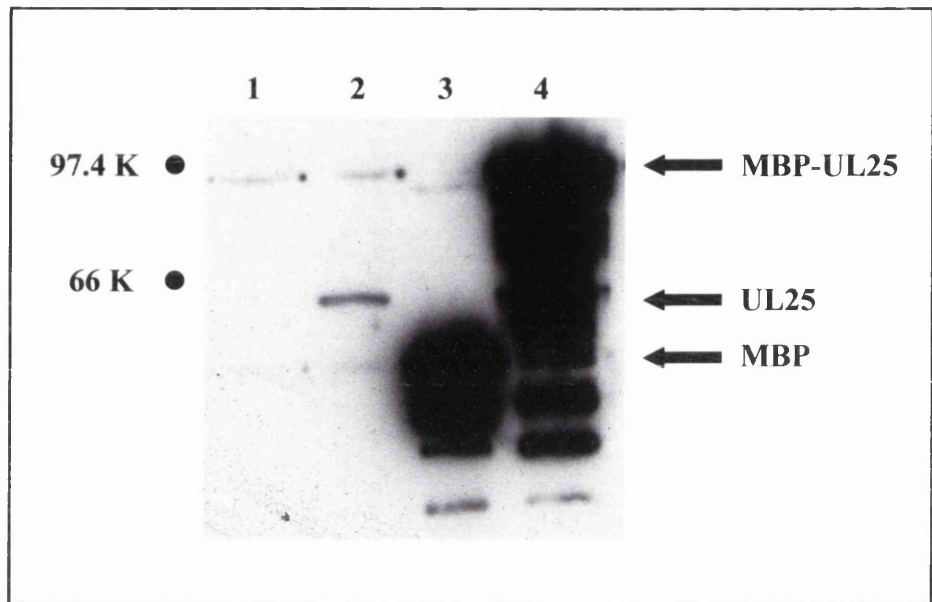


Figure 3.12 Western blot Analysis of the Specific Immunoreactivity in Serum from Blood Taken in a Test Bleed from MBP-UL25 Immunised Mice.

A 20 μ l sample of blood was taken from the tail of each immunised mouse and the serum was used as a source of primary antibody in a Western blot assay. The above figure is typical of the result achieved using each of the four serum samples. Protein samples were resolved on an 8% SDS polyacrylamide gel and transferred to Hybond-ECL membrane. In the above case, serum from mouse number 3 diluted to a concentration of 1/500 was used to probe the membrane. **Lane 1**, PAK6-infected *Sf21* cell extract; **lane 2**, Ac25-infected *Sf21* cell extract; **lane 3**, 2 μ g MBP; **lane 4**, 2 μ g MBP-UL25.

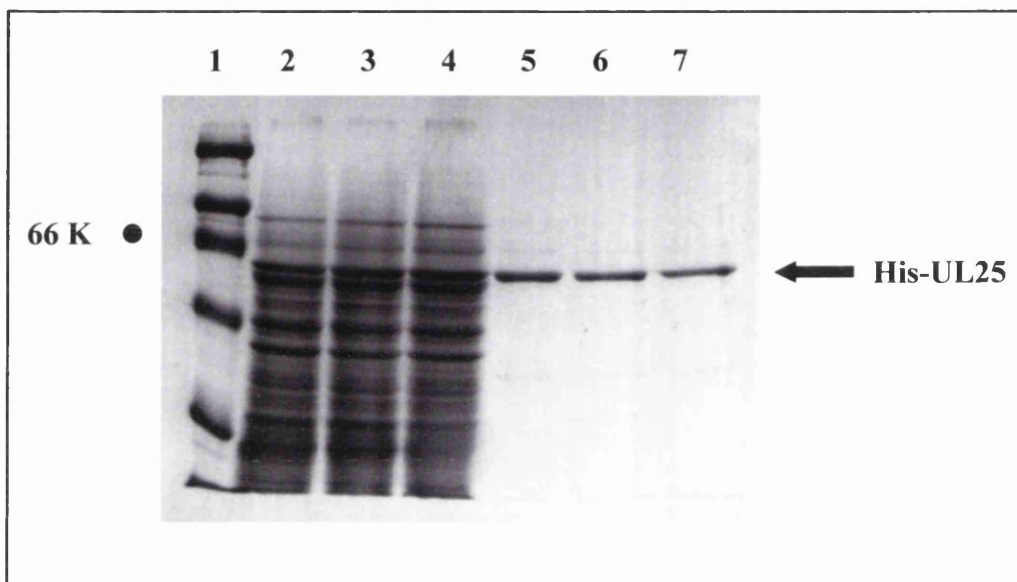


Figure 3.13 Purification of His-UL25 from *Sf21* Cells Infected with PTA10bac#14.

A clarified cell extract from *Sf21* cells infected with PTA10bac#14 was used as a source of soluble His-UL25 protein for purification by affinity chromatography with Ni-NTA resin. Clarified infected-cell extract from three preparations (**lanes 2, 3, 4**) and purified protein (**lanes 5, 6, 7**) was resolved on a 10% SDS polyacrylamide gel and visualised by Coomassie blue staining. **Lane 1** represents molecular weight markers (5 μ g of each marker).

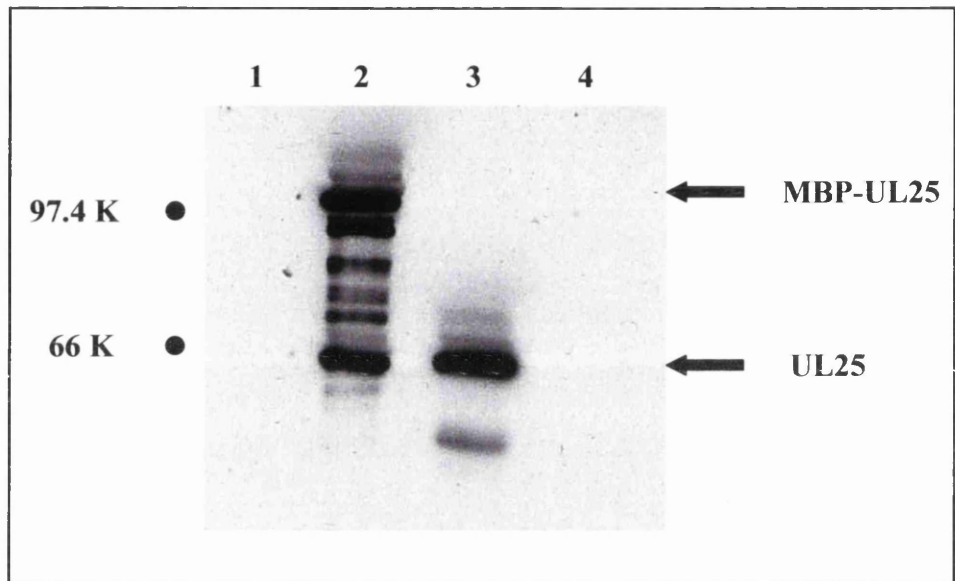


Figure 3.14 Monoclonal Antibody 166 Functions in a Western blot Assay.

The monoclonal antibodies were tested for their ability to react with UL25 in a Western blot assay. Protein samples were resolved on an 8% SDS polyacrylamide gel, transferred to Hybond-ECL membrane and probed using 10 ml of undiluted HATc medium from hybridoma cell lines as a source of primary antibody. The above figure is typical of a positive result and was achieved using medium from hybridoma cell line number 166. **Lane 1**, 1 μ g MBP; **lane 2**, 1 μ g MBP-UL25; **lane 3**, Ac25-infected *Sf21* cell extract; **lane 4**, PAK6-infected *Sf21* cell extract.

Monoclonal Antibody	WB	IP	IF
116	-	-	-
126	++	-	-
162	+	+	-
166	+++	+++	++++
174	+	-	-
195	++	+	++
220	-	++++	++
230	+++	-	++
439	+	-	-
453	-	-	-
485	-	-	++
526	-	-	-

Table 3.1 Summary of the Characterisation of Monoclonal Antibodies Specific for the HSV-1 UL25 Protein.

The above table indicates the affinity of the monoclonal antibodies for the UL25 protein in each of the immunoassays used. **WB**, Western blot; **IP**, immunoprecipitation; **IF**, immunofluorescence.

3.2.3.6 The Reactivity of Monoclonal Antibodies Specific for the UL25 Protein in an Immunoprecipitation Assay.

The UL25 specific monoclonal antibodies were tested for their ability to function in an immunoprecipitation assay as described in section 2.3.1.7 and a typical positive result is shown in Figure 3.15. The antibodies were screened against an HSV-1 17⁺-infected Vero cell extract which contained the unmodified UL25 protein as an antigen. A sample from a mock-infected Vero cell extract was also included as a control. Four of the twelve monoclonal antibodies isolated bound the UL25 protein in this assay and the data are summarised in Table 3.1 together with an indication of the affinity each monoclonal antibody had for the UL25 antigen. However, as before, this may not represent a true indication of the affinity each monoclonal antibody had for the UL25 antigen in this assay.

3.2.3.7 The Reactivity of Monoclonal Antibodies Specific for the UL25 Protein in Indirect Immunofluorescence Assays.

The monoclonal antibodies were screened for their ability to react with the UL25 polypeptide in an indirect immunofluorescence assay. Vero cells were transfected as described in section 2.3.2 with the pCMV10-UL25 plasmid which expressed the unmodified UL25 protein and mock-transfected Vero cells were included as a control. Five of the twelve monoclonal antibodies isolated bound the UL25 protein in this assay and the data are summarised in Table 3.1 together with an indication of the affinity each monoclonal antibody had for the UL25 antigen. Again, this may not represent a true indication of the affinity each monoclonal antibody had for the UL25 antigen in this assay.

A similar indirect immunofluorescent assay was also employed to examine whether the monoclonal antibodies could also react with the UL25 polypeptide in HSV-1-infected cells as described in section 2.3.1.5. Vero cells were either mock-infected or infected with HSV-1 17⁺. At 10 hours pi the cells were fixed, permeabilised and probed with HATc medium from the hybridoma cell lines. The specific reactivity of the monoclonal antibodies with HSV-1-infected cells and pCMV10-UL25 transfected cells was similar and the same five antibodies bound the UL25 protein in both assays although a slightly higher level of non-specific activity was observed in HSV-1 infected cells.

3.2.4 Discussion.

The polyhistidine-tagged UL25 expressing recombinant baculovirus proved to be a valuable reagent for the isolation of monoclonal antibodies specific for UL25. In *Sf21* cells

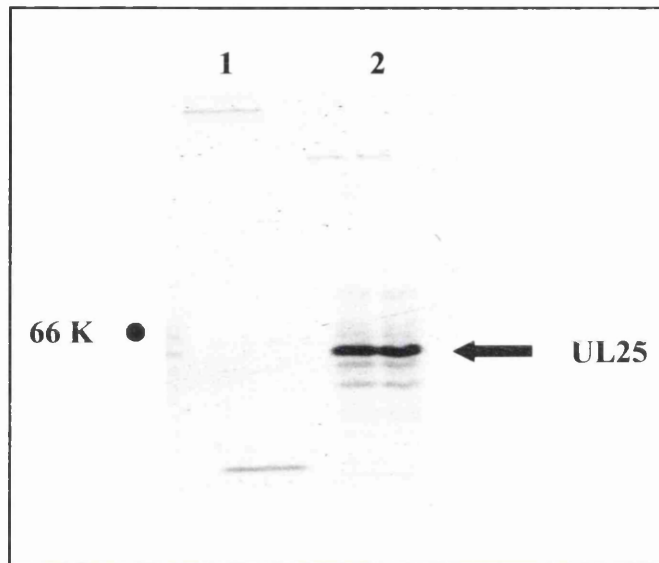


Figure 3.15 Monoclonal Antibody 220 Functions in an Immunoprecipitation Assay.

The monoclonal antibodies were tested for their ability to immunoprecipitate the UL25 polypeptide using 50 μ l of undiluted HATc medium from hybridoma cell lines as a source of primary antibody. The protein samples were resolved on an 8% SDS polyacrylamide gel and visualised by fluorography. The above figure is typical of a positive result and was achieved using medium from hybridoma cell line number 220. **Lane 1**, Mock infected Vero cells; **lane 2**, HSV-1 17⁺ infected Vero cells.

infected with PTA10bac#14 the His-UL25 protein was expressed in large amounts and was predominantly soluble. To purify a sufficient quantity of soluble His-UL25 protein necessary for the immunisation of mice, the purification protocol had to be modified extensively. In the first instance, the solubility of the His-UL25 protein in *Sf21* cells infected with PTA10bac#14 was examined over a period of 96 hours pi. The highest level of soluble His-UL25 protein had accumulated by 72 hours pi and therefore, *Sf21* cells infected with PTA10bac#14 for the purpose of protein purification were subsequently never incubated longer than 72 hours pi. Additionally, purified His-UL25 protein was unstable and would precipitate out of solution when stored in a buffer containing only Tris.HCl and NaCl. Therefore, to increase the solubility of the purified protein, the composition and pH of the purification buffer was investigated thoroughly. The final purification buffer (pH 7.5) contained CHAPS, NaCl, DMSO and glycerol (refer to Table 2.3, His-UL25 Harvest / Binding Buffer) and purified His-UL25 protein stored in this buffer at 4°C remained soluble for up to 8 weeks. Unfortunately, purified His-UL25 protein was insoluble above a concentration of 250 $\mu\text{g.ml}^{-1}$ under the conditions used and could not be purified to a concentration of 1 mg.ml^{-1} necessary for many of the procedures involved in the biochemical analysis of proteins.

As a consequence of two spleen fusion experiments using BALB/c mice immunised with the purified MBP-UL25 and His-UL25 proteins, 12 hybridoma cell lines secreting monoclonal antibodies specific for the HSV-1 UL25 protein were isolated. These antibodies were characterised using a variety of immunoassays and the results are summarised in Table 3.1.

The results identified nine monoclonal antibodies that reacted with the UL25 protein in one or more of the three assays used. From the pattern of reactivity of the monoclonal antibodies in the immunoassays it was clear that each of the monoclonal antibodies was directed against one of at least six epitopes on the UL25 protein. Three antibodies, 116, 453 and 526 did not recognise the UL25 protein in Western blot, immunoprecipitation or immunofluorescent assays and it is likely that these antibodies either recognised the protein by ELISA only or that the concentration of antibody in the HATc medium was below that required to elicit a positive result. Monoclonal antibody 166 demonstrated a strong affinity for the UL25 protein in each of the immunoassays used and was purified by affinity chromatography using a Hi-Trap Protein G column and an ÄTKA automated purifier primarily for use in subsequent experimentation involving indirect immunofluorescent

analysis. At this stage in the project there was no need to identify the exact epitope of the UL25 protein to which each of the monoclonal antibodies bound and priority was given to more pressing experiments.

3.3 A Study of the Factor(s) Required for the Nuclear Localisation of the UL25 Protein in Cells Infected with HSV-1.

3.3.1 Introduction.

Protein-protein interactions are important for transporting certain HSV-1 proteins within the cell, for example, the VP5 and VP23 capsid proteins. In both these cases, an interaction in the cytoplasm of HSV-1 infected cells with the VP19C protein, which contains a nuclear localisation signal, results in the translocation of these proteins to the nucleus (Rixon *et al.*, 1996). In a similar manner, the localisation of the VP5 protein to the cell nucleus requires the presence of the VP22a scaffolding protein (Nicholson *et al.*, 1994). In the absence of any other viral proteins the UL25 protein localised almost exclusively to the cellular cytoplasm (Figure 3.16). However, during wt HSV-1 infection the UL25 protein exhibited a predominantly nuclear localisation (Figure 3.17). Thus, the aim of the work described in this section was to ascertain which proteins were involved in directing or retaining the UL25 protein to the nuclei of HSV-1 infected cells and to investigate whether the capsid assembly process was necessary for the nuclear retention of the UL25 protein.

3.3.2 The Intracellular Localisation of the UL25 Protein in Non-Complementing Cells Infected with K23Z, K5ΔZ and KΔ19C.

To determine whether capsid assembly was required for the nuclear localisation of the UL25 protein in cells infected with wt virus, the intracellular localisation of the UL25 protein was examined in non-complementing cells infected with K23Z by indirect immunofluorescent analysis. K23Z is a UL18 null mutant of HSV-1 strain KOS and does not synthesise VP23 or assemble capsids in infected non-complementing cells. The UL25 protein co-localised with the VP19C protein in the nuclei of Vero cells infected with K23Z (Figure 3.18). This indicated that neither capsid assembly nor the VP23 protein was required for the nuclear localisation of the UL25 protein in non-complementing cells infected with this virus.

The intracellular localisation of the UL25 protein was also examined in non-complementing cells infected with K5ΔZ, a UL19 null mutant of HSV-1 strain KOS, by indirect immunofluorescent analysis. This mutant does not synthesise VP5 or assemble capsids in infected non-complementing cells. The UL25 protein co-localised with the

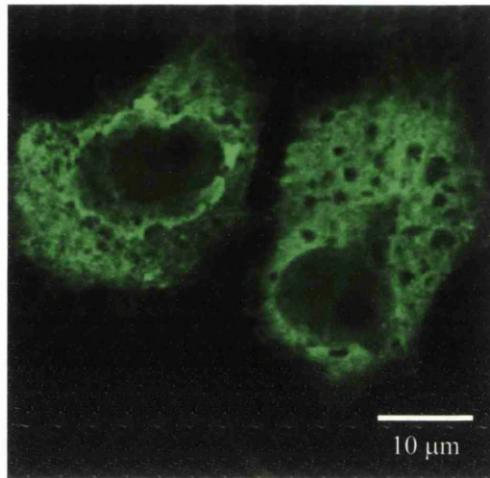


Figure 3.16 In the Absence of Other Viral Proteins the UL25 Protein Localises to the Cellular Cytoplasm.

Vero cells were transfected with 1 μg of pCMV10-UL25 (refer to section 2.3.2). At 24 hours post-transfection the cells were fixed with 5% formaldehyde and permeabilised with 0.5% NP40. The transfected cells were incubated with UL25 protein specific monoclonal antibody 166 diluted to a concentration of 1/100 for 1 hour followed by a 30 minute incubation with an anti mouse-FITC conjugated secondary antibody. The cells were then examined by confocal microscopy.

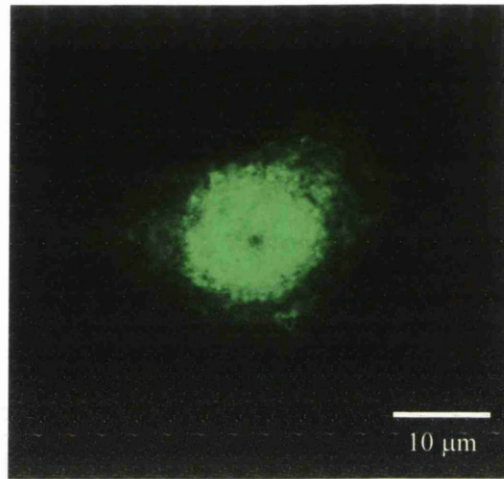


Figure 3.17 The UL25 Protein Localises Primarily to the Nucleus During Wt HSV-1 Infection.

Vero cells were infected with HSV-1 *ts⁺ 17⁺* using a moi of 10 pfu.cell⁻¹. At 10 hours post-infection the cells were fixed with 5% formaldehyde and permeabilised with 0.5% NP40. The infected cells were incubated with UL25 protein specific monoclonal antibody 166 diluted to a concentration of 1/100 for 1 hour followed by a 30 minute incubation with an anti mouse-FITC conjugated secondary antibody. The cells were then examined by confocal microscopy.

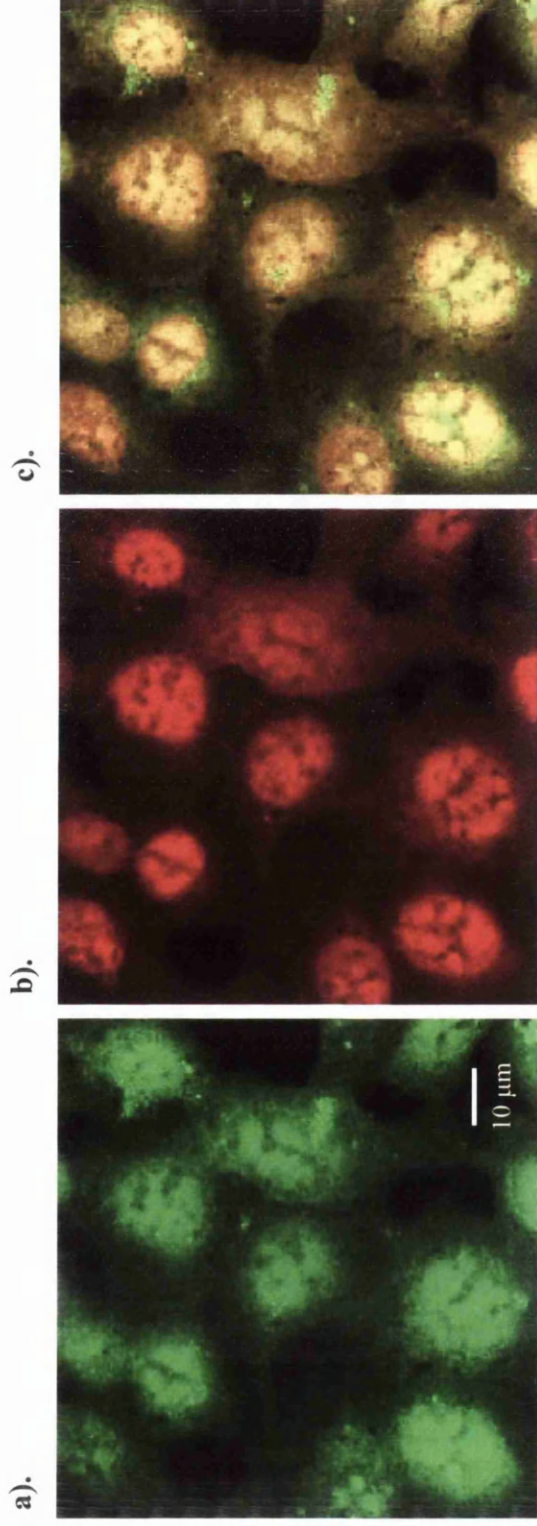


Figure 3.18 The UL25 Protein Co-Localises with the VP19C Protein in the Nuclei of Non-Complementing Cells Infected with K23Z.

Vero cells were infected with K23Z using a moi of 10 pfu.cell^{-1} . At 12 hours post-infection the cells were fixed with 5% formaldehyde and permeabilised with 0.5% NP40. The infected cells were incubated with monoclonal antibody 166, specific for the UL25 polypeptide, and polyclonal antibody NC2, specific for VP19C, diluted to a concentration of 1/100 for 1 hour followed by a 30 minute incubation with anti mouse-FITC and anti rabbit-CY5 conjugated secondary antibodies. The cells were then examined by confocal microscopy. Image **a)**. UL25; **b)**. VP19C; **c)**. Merge.

VP23 protein in the nuclei of Vero cells infected with K5 Δ Z (Figure 3.19). This confirmed that capsid assembly was not required for the nuclear localisation of the UL25 protein and also indicated that the VP5 protein was not required for the nuclear localisation of the UL25 protein in non-complementing cells infected with this virus.

To investigate whether the nuclear localisation of the UL25 protein during wt virus infection was dependent on the presence of VP19C protein, the intracellular localisation of the UL25 protein was examined in non-complementing cells infected with K Δ 19C, a UL38 null mutant of HSV-1 strain KOS, by indirect immunofluorescent analysis (data not shown). However, this virus appeared to have an early replication defect in non-complementing cells since it synthesised reduced levels of UL25 and the capsid shell proteins in comparison to wt virus. It is therefore likely that this virus contained at least one additional mutation. The low level of UL25 protein produced in these cells resulted in the inability to conclusively identify the intracellular location of the UL25 protein under these conditions and no further information was obtained through the use of this virus.

3.3.3 The Intracellular Localisation of the UL25 and Capsid Proteins in Cells Infected with *Ts2*.

To determine if the VP19C protein was necessary for the nuclear localisation of the UL25 protein during wt HSV-1 infection, the intracellular distribution of UL25 protein was examined in cells infected with *ts2* at the NPT. The *ts2* virus used in this study was derived from a *ts* mutant of HSV-1 strain A44, *ts2* syn, and contains a *ts* lesion in the VP19C protein encoded by the UL38 gene (Pertuiset *et al.*, 1989). As previously mentioned, the VP19C protein interacts with the VP23 protein, to form the triplex component of the capsid and also associates with the major capsid protein VP5. In cells infected with *ts2* at the NPT capsids are not assembled (Pertuiset *et al.*, 1989). As expected, in Vero cells infected with *ts2* at the PT, the UL25, VP19C, VP23 and VP5 proteins all localised to the nuclei, typical of the intracellular localisation of these proteins during wt virus infection (Figure 3.20). However, in Vero cells infected with *ts2* at the NPT, the UL25 protein was found exclusively in the cytoplasm, characteristically surrounding the nuclear periphery and strongly colocalised with the VP23 protein (Figure 3.21). The UL25 protein colocalised to a lesser extent with the VP19C protein which was also present in the cytoplasm, but in contrast to UL25 protein, a small proportion of VP19C was distributed in the nucleus (Figure 3.22). The VP5 protein displayed a similar

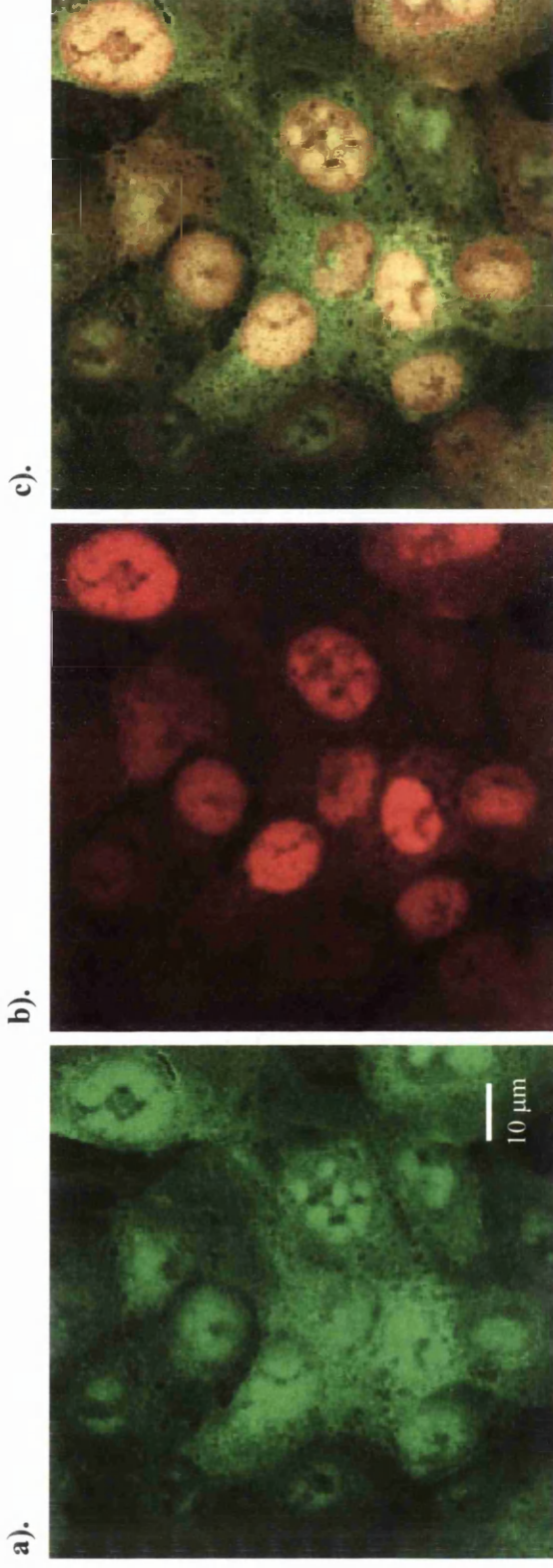


Figure 3.19 The UL25 Protein Co-Localises with the VP23 Protein in the Nuclei of Non-Complementing Cells Infected with K5ΔZ.

Vero cells were infected with K5ΔZ using a moi of 10 pfu.cell⁻¹. At 12 hours post-infection the cells were fixed with 5% formaldehyde and permeabilised with 0.5% NP40. The infected cells were incubated with UL25 polypeptide specific monoclonal antibody 166, diluted to a concentration of 1/100, and polyclonal antibody 186, specific for the VP23 protein, diluted to a concentration of 1/500 for 1 hour followed by a 30 minute incubation with anti mouse-FITC and anti rabbit-CY5 conjugated secondary antibodies. The cells were then examined by confocal microscopy. Image a). UL25; b). VP23; c). Merge.

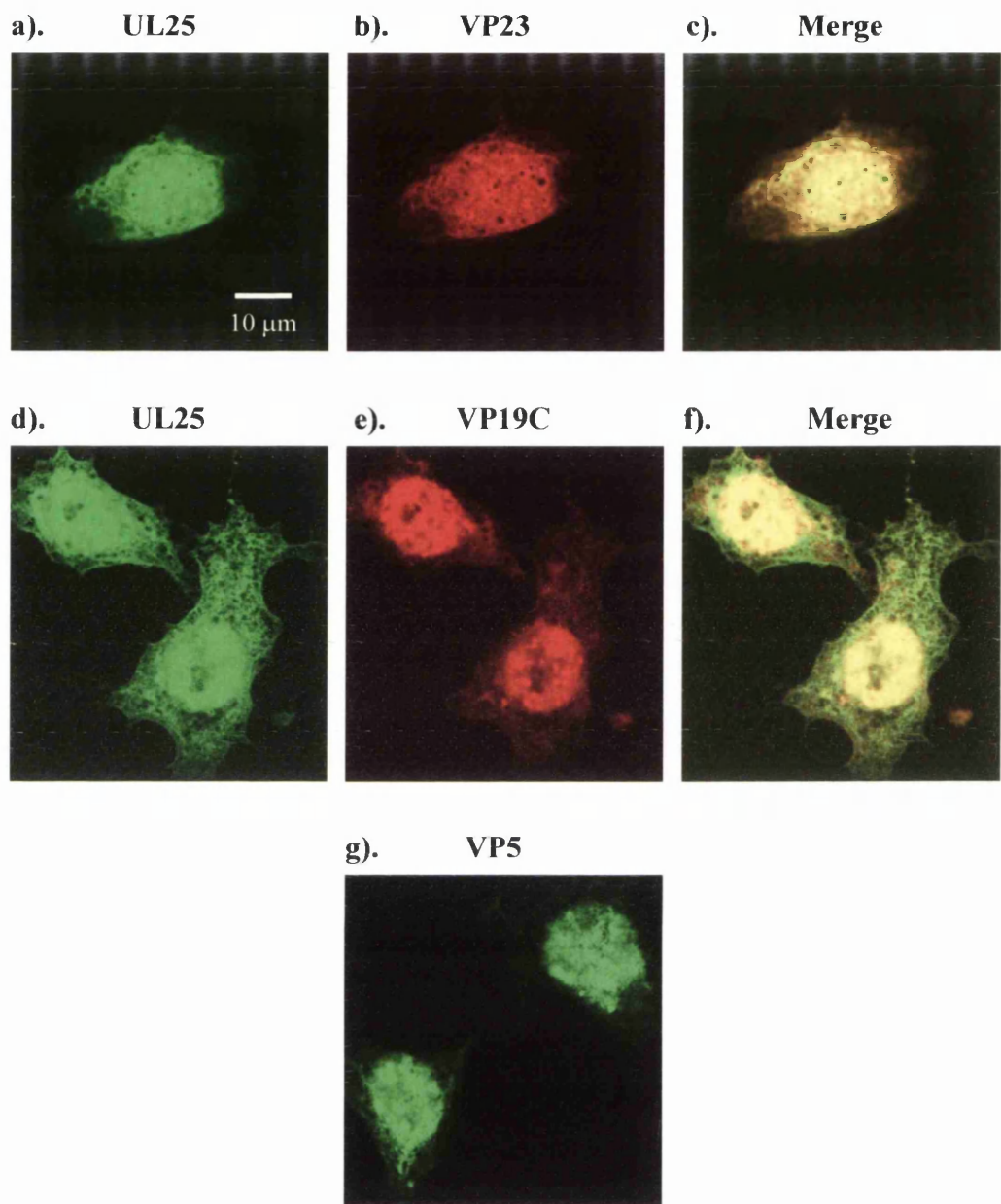


Figure 3.20 The Intracellular Localisation of the UL25 and Capsid Proteins in Cells Infected with *Ts2* at the PT.

Vero cells were infected with *ts2* at the PT using a moi of 10 pfu.cell^{-1} . At 10 hours post-infection the cells were fixed with 5% formaldehyde and permeabilised with 0.5% NP40. The infected cells were incubated with primary antibodies 166 **a)** and **d)**, 186 **b)**, NC2 **e)** and DM165 **g)** specific for UL25, VP23, VP19C and VP5 respectively, for 1 hour. After a 30 minute incubation with the appropriate secondary antibodies, the cells were washed and examined by confocal microscopy.

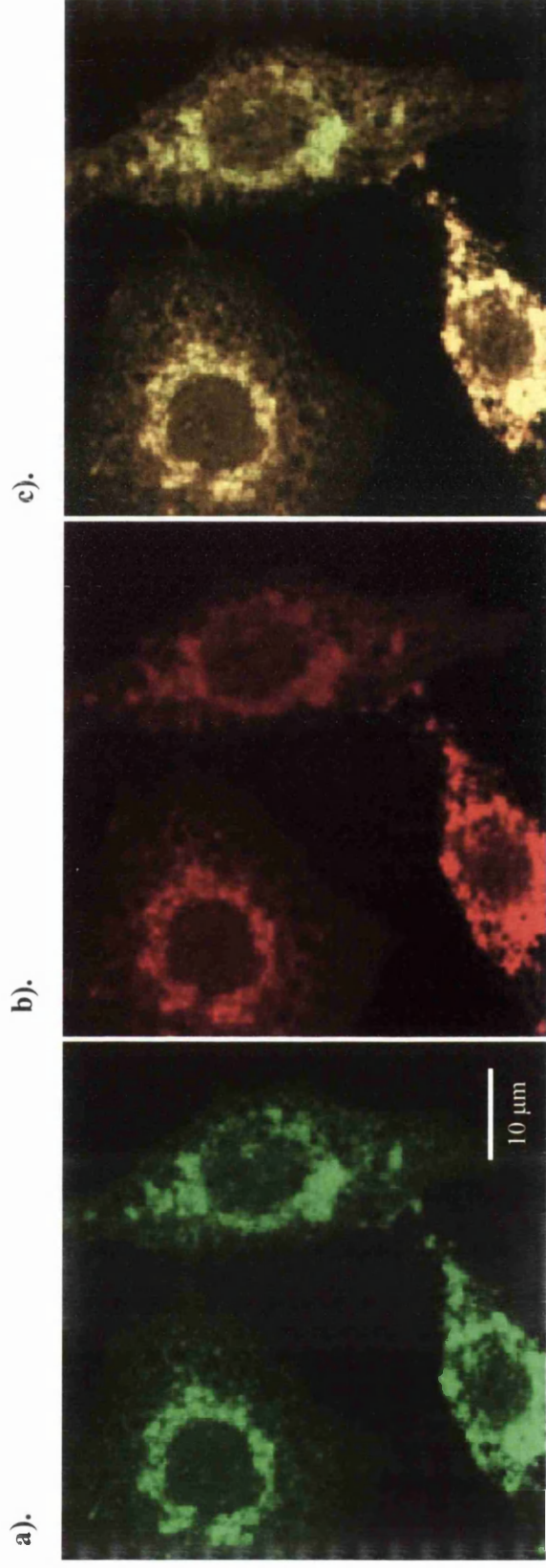


Figure 3.21 The UL25 Protein Co-Localises with the VP23 Protein at the Perinuclear Region of Cells Infected with *Ts2* at the NPT.

Vero cells were infected at the NPT with *ts2* using a moi of 10 pfu.cell⁻¹. At 10 hours post-infection the cells were fixed with 5% formaldehyde and permeabilised with 0.5% NP40. The infected cells were incubated with UL25 polypeptide specific monoclonal antibody 166, diluted to a concentration of 1/100, and polyclonal antibody 186, specific for VP23, diluted to a concentration of 1/500, for 1 hour followed by a 30 minute incubation with anti mouse-FITC and anti rabbit-CY5 conjugated secondary antibodies. The cells were then examined by confocal microscopy. Image **a).** UL25; **b).** VP23; **c).** Merge.

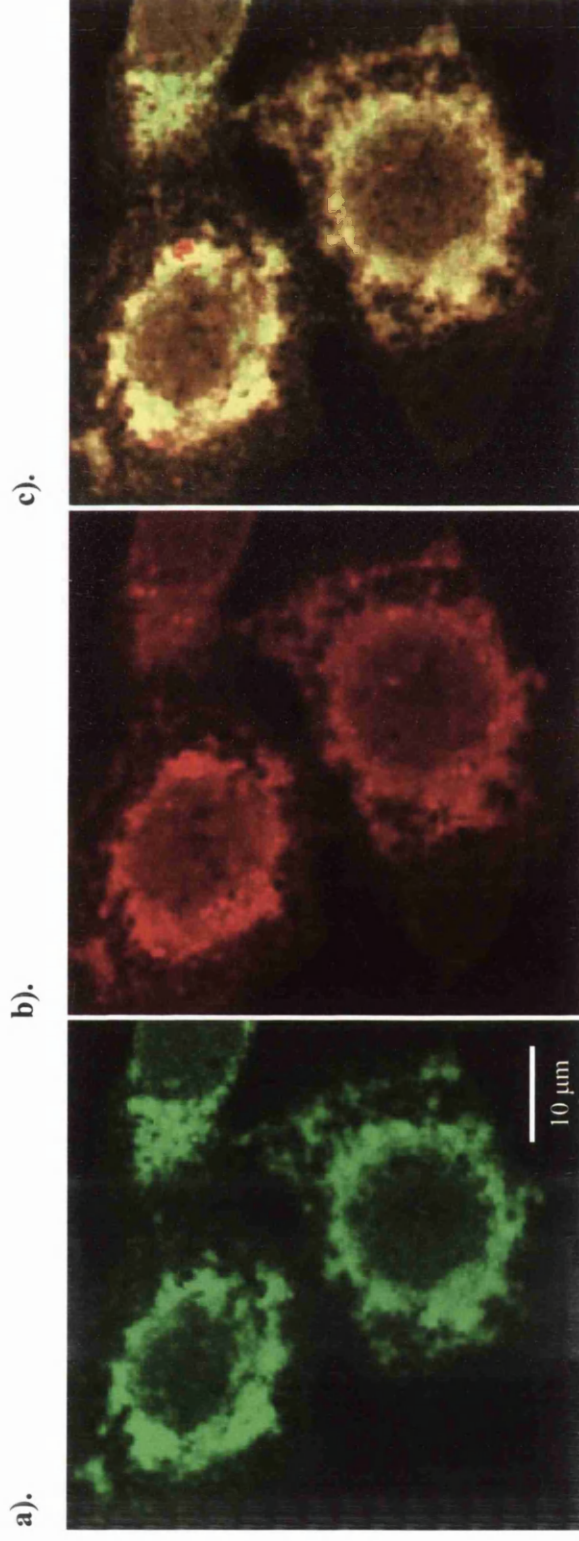


Figure 3.22 The UL25 Protein Co-Localises with the VP19C Protein at the Perinuclear Region of Cells Infected with *ts2* at the NPT.

Vero cells were infected at the NPT with *ts2* using a moi of 10 pfu.cell⁻¹. At 10 hours post-infection the cells were fixed with 5% formaldehyde and permeabilised with 0.5% NP40. The infected cells were incubated with UL25 specific monoclonal antibody 166 and polyclonal antibody NC2, specific for the VP19C protein, for 1 hour at a concentration of 1/100 followed by a 30 minute incubation with anti mouse-FITC and anti rabbit-CY5 conjugated secondary antibodies. The cells were then examined by confocal microscopy. Image a). **UL25; b). VP19C; c). Merge.**

intracellular distribution to that of the VP19C protein localising primarily to the perinuclear region of cells infected with *ts2* at the NPT with a small proportion located in the nucleus (Figure 3.23). To confirm that the UL25 protein was perinuclear in cells infected with *ts2* at the NPT, *ts2*-infected Vero cells were probed with monoclonal antibody 166 specific for the UL25 protein and then stained with propidium iodide which binds to nucleic acids and autofluoresces at a wavelength of 543 nm. Figure 3.24 demonstrates that in cells infected with *ts2* at the NPT, the UL25 protein was localised to the perinuclear region, with little if any protein localised to the nuclei.

Western blot analysis revealed that a larger proportion of UL25 and VP23 protein was insoluble in cells infected with *ts2* at the NPT compared to cells infected with wt virus (Figure 3.25). This finding suggested that, as the VP19C protein co-localised with the insoluble UL25 and VP23 proteins at the perinuclear region, it too was likely to be insoluble in cells infected with *ts2* at the NPT. This result combined with the data from indirect immunofluorescent analysis of *ts2*-infected cells indicated that the *ts* mutation of *ts2* altered the conformation of the VP19C protein such that the triplex became insoluble and was unable to enter nuclei of virus-infected cells. This also resulted in the failure of the VP5 protein to enter the nuclei and it too localised to the perinuclear region of cells infected with *ts2* at the NPT. The evidence suggested that the cessation of capsid assembly in cells infected with *ts2* at the NPT was a consequence of the altered solubility and intracellular localisation of the triplex and the VP5 proteins. This also resulted in the altered intracellular localisation of the UL25 protein which indicated that the nuclear localisation of the UL25 protein during wt virus-infection of cells was dependent on the presence of functional triplex complexes. Additionally, the data indicated a potential interaction between the UL25 protein and the VP23 and/or the VP19C protein.

3.3.4 The Construction of *Ts2Hindk* MR#6, a *Ts2* Marker Rescue Virus.

To ensure that the altered intracellular localisation of the UL25 protein in cells infected with *ts2* at the NPT was due to the *ts2* lesion, a marker rescue virus of *ts2* was constructed as described in section 2.3.7. Cloned wt virus *HindIII* k DNA fragment, containing the UL38 gene, was recombined with *ts2* viral DNA by calcium-phosphate transfection of both DNA species into Vero cells (Stow & Wilkie, 1976). After extensive cpe had developed the progeny viruses were harvested and screened for the ability to form plaques on Vero cell monolayers infected at the NPT of 39.2°C. A *ts*⁺ virus was isolated, plaque purified and used to produce a high titre stock of marker rescue virus which was termed *ts2Hindk*

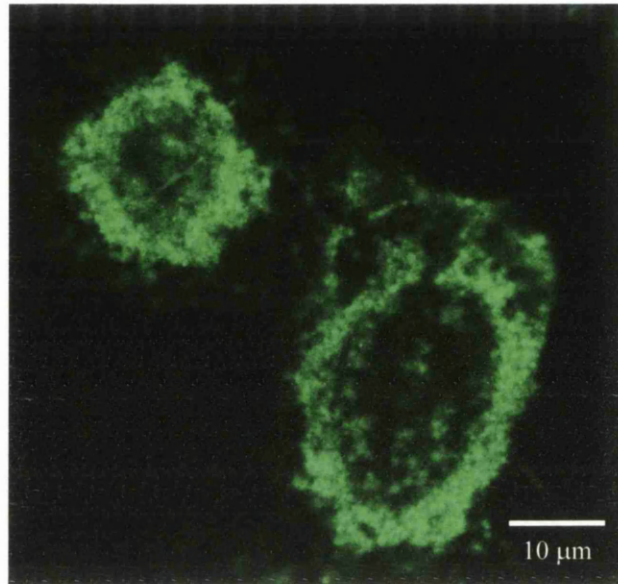


Figure 3.23 The Intracellular Localisation of the VP5 Protein in Cells Infected with *Ts2* at the NPT.

Vero cells were infected with *ts2* using a moi of 10 pfu.cell⁻¹. At 10 hours post-infection the cells were fixed with 5% formaldehyde and permeabilised with 0.5% NP40. The infected cells were incubated with VP5 specific monoclonal antibody DM165 diluted to a concentration of 1/500 for 1 hour followed by a 30 minute incubation with an anti mouse-FITC conjugated secondary antibody. The cells were then examined by confocal microscopy.

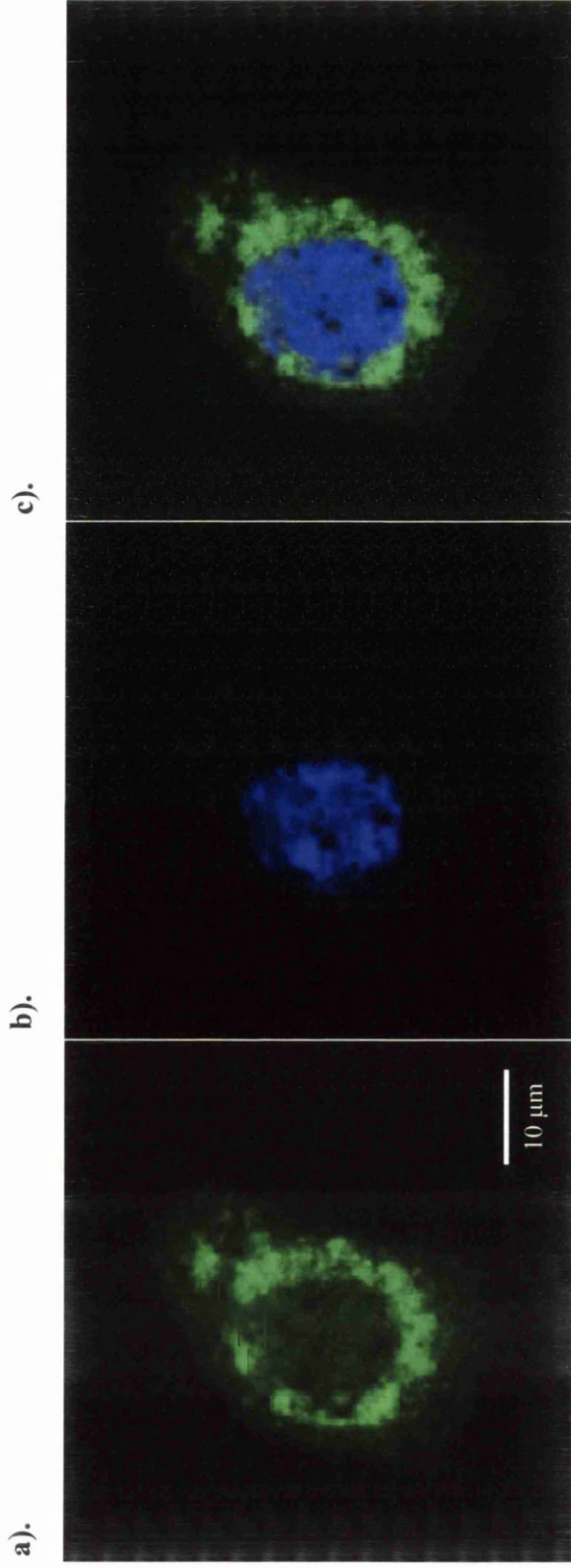


Figure 3.24 Confirmation of the Perinuclear Localisation of the UL25 Protein in Cells Infected with *ts2* at the NPT.

Vero cells were infected at the NPT with *ts2* using a moi of 10 pfu.cell⁻¹. At 10 hours post-infection the cells were fixed with 5% formaldehyde and permeabilised with 0.5% NP40. The infected cells were incubated with UL25 specific monoclonal antibody 166, diluted to a concentration of 1/100, for 1 hour followed by a 30 minute incubation with an anti mouse-FITC conjugated secondary antibody. The cells were then incubated with 0.5 µg.ml⁻¹ propidium iodide for 20 seconds, washed and examined by confocal microscopy. Image a). **UL25; b). Propidium Iodide; c). Merge.**

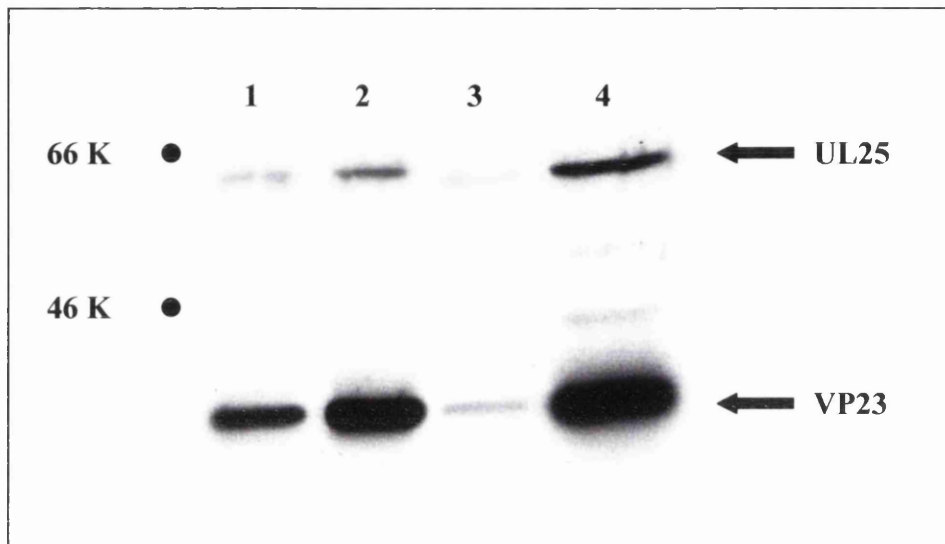


Figure 3.25 An Analysis of the Solubility of the UL25 and VP23 Proteins in Cells Infected with *Ts2* at the NPT.

Vero cells were infected with HSV-1 *ts*⁺ 17⁺ (**lanes 1, 2**) or *ts2* (**lanes 3, 4**) at a moi of 10 pfu.cell⁻¹ and incubated at the NPT. At 10 hours pi the cells were harvested, lysed in a buffer containing 0.5% NP40 and then centrifuged at 6500 rpm (refer to section 2.2.5). A sample of the soluble fraction (**lanes 1, 3**) and the insoluble fraction (**lanes 2, 4**) was resolved on a 10% SDS polyacrylamide gel, transferred to Hybond-ECL membrane and probed with polyclonal antibody 335 and 186, specific for UL25 and VP23 proteins respectively. The membrane was washed extensively and bound antibody was visualised using an ECL chemiluminescent kit (Amersham) as described in section 2.3.1.4.

MR#6. The plating efficiency of this virus at the PT and the NPT was compared to that of wt virus to ensure that *ts2Hindk* MR#6 exhibited a wt virus phenotype. Table 3.2 demonstrates that *ts2Hindk* MR#6 formed plaques on Vero cell monolayers with approximately the same efficiency as wt virus at the PT and the NPT and this marker rescue virus of *ts2* was therefore used for subsequent analysis.

3.3.5 The Intracellular Localisation of the UL25 and Capsid Proteins in Cells Infected with *Ts2Hindk* MR#6.

Indirect immunofluorescent analysis demonstrated that replacement of the defective UL38 gene of *ts2* with the wt UL38 gene resulted in the ability of the VP23 (Figure 3.26), VP19C (Figure 3.27) and VP5 (Figure 3.28) proteins to localise to the nucleus of cells infected with *ts2Hindk* MR#6 at the NPT. However, as Figures 3.26 and 3.27 also demonstrate, most of the UL25 protein was still unable to enter the nuclei of cells infected with *ts2Hindk* MR#6 at the NPT and remained localised to the perinuclear region of these cells. Clearly a sufficient proportion of UL25 protein must have been directed to the nuclei of cells infected with *ts2Hindk* MR#6 at the NPT since this virus did not appear to have a growth defect at the higher temperature (Table 3.2). In cells infected with *ts2Hindk* MR#6 at the PT the UL25 protein was concentrated in the nuclei and co-localised with the VP23 protein and the VP19C protein (Figure 3.29). These findings indicated that an unidentified *ts* lesion(s) was responsible for the altered intracellular localisation of the UL25 protein in cells infected with *ts2* at the NPT.

3.3.6 The Intracellular Localisation of the UL25 Protein in Cells Infected with *Ts*⁺ A44.

To determine whether the altered intracellular localisation of the UL25 protein in cells infected with *ts2Hindk* MR#6 at the NPT was the result of mutation(s) acquired during the construction and selection of the *ts2* marker rescue virus, the distribution of the UL25 protein in cells infected with the syncytial strain HSV-1 *ts*⁺ A44, the parental virus of *ts2* syn, was examined by indirect immunofluorescence. The original *ts2* syn virus formed large syncytia in infected cells and was crossed with HSV-1 *ts*⁺ 17 syn⁺ to generate the virus that was used in this study. This isolate retained the *ts2* defect but had a reduced capacity to form syncytia in infected cells and therefore grew better than the original *ts2* syn virus at the PT. In cells infected with this virus at the PT the UL25 protein was found almost exclusively in the nuclei (Figure 3.30a.). However, in cells infected with *ts*⁺ A44 at

Virus	Titre at the Permissive Temperature (31°C)	Titre at the Non-Permissive Temperature (39.2°C)	Efficiency of Plating
Wild-Type (HSV-1 <i>ts</i> ⁺ 17 ⁺)	3.3 x 10 ⁸ pfu.ml ⁻¹	2.5 x 10 ⁸ pfu.ml ⁻¹	0.76
<i>ts</i> 2Hindk MR#6	4.9 x 10 ⁸ pfu.ml ⁻¹	5 x 10 ⁸ pfu.ml ⁻¹	1.02

Table 3.2 The Plating Efficiency of *Ts*2Hindk MR#6 and Wt Virus at the PT and the NPT.

Samples of both viruses were diluted to a concentration of approximately 5 x 10⁸ pfu.ml⁻¹ and titrated on Vero cells at the PT and the NPT. When plaques became visible, the cells were fixed with Giemsa stain and plaques were counted using a dissecting microscope. The efficiency of plating was derived by dividing the titre at the NPT over the titre at the PT.

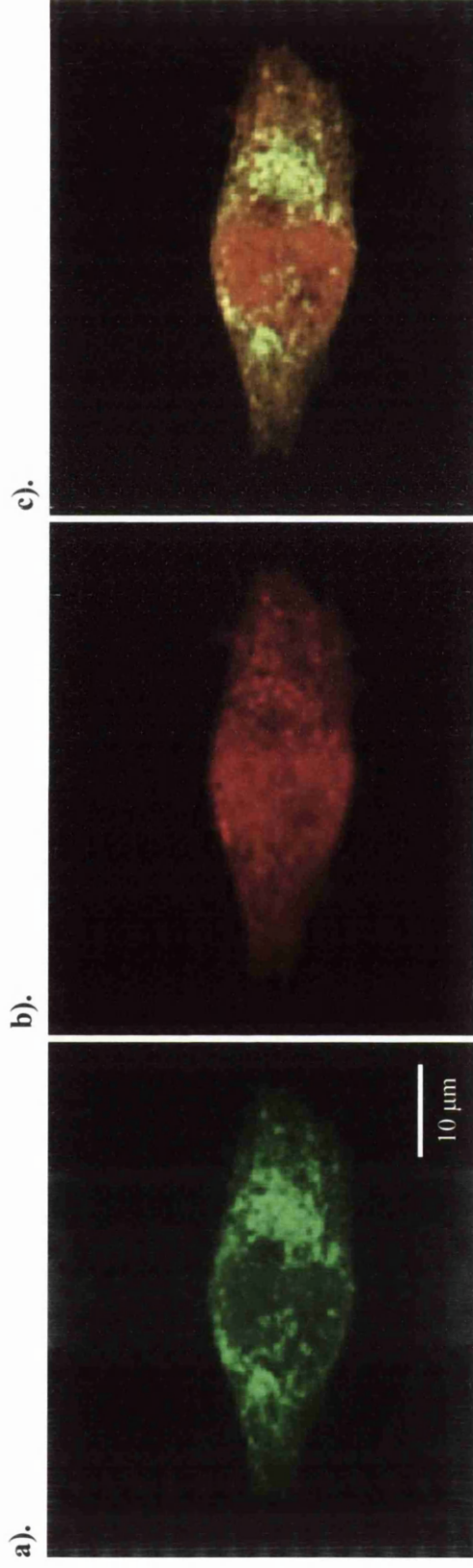


Figure 3.26 The UL25 Protein Does Not Co-Localise with the VP23 Protein in the Nuclei of Cells Infected with *Ts2Hindk MR#6* at the NPT.

Vero cells were infected at the NPT with *ts2Hindk MR#6* using a moi of 10 pfu.cell⁻¹. At 10 hours post-infection the cells were fixed with 5% formaldehyde and permeabilised with 0.5% NP40. The infected cells were incubated with UL25 protein specific monoclonal antibody 166, diluted to a concentration of 1/100, and VP23 protein specific polyclonal antibody 186, diluted to a concentration of 1/500, for 1 hour followed by a 30 minute incubation with anti mouse-FITC and anti rabbit-CY5 conjugated secondary antibodies. The cells were then examined by confocal microscopy. Image a). UL25; b). VP23; c). Merge.

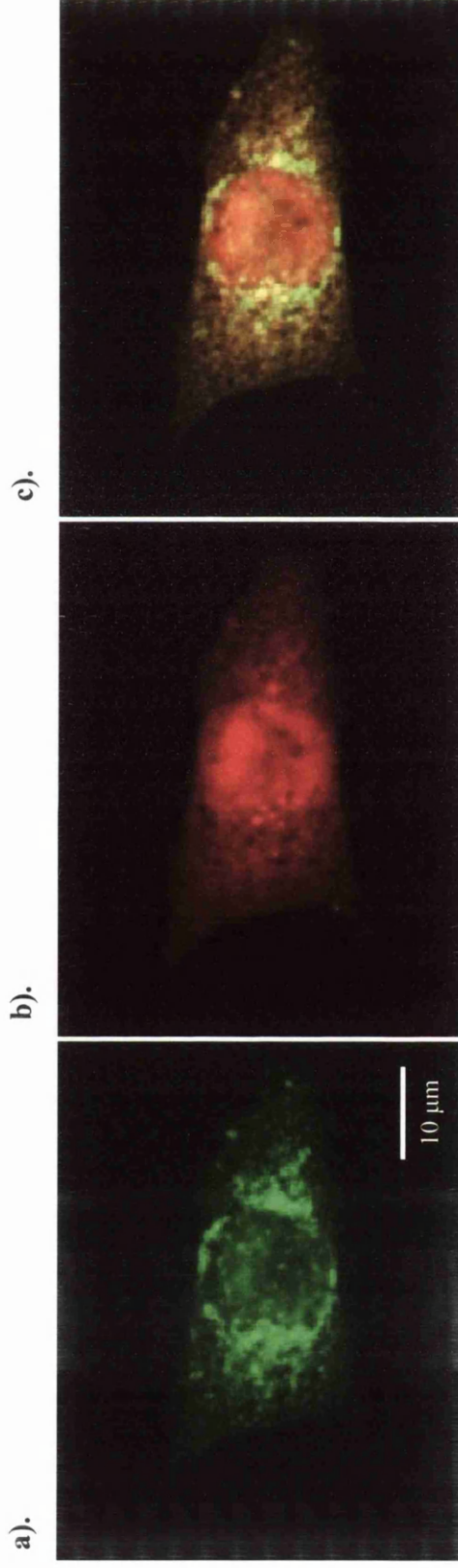


Figure 3.27 The UL25 Protein Does Not Co-Localise with the VP19C Protein in the Nuclei of Cells Infected with *Ts2Hindk MR#6* at the NPT.

Vero cells were infected at the NPT with *ts2Hindk MR#6* using a moi of 10 pfu.cell⁻¹. At 10 hours post-infection the cells were fixed with 5% formaldehyde and permeabilised with 0.5% NP40. The infected cells were incubated with monoclonal antibody 166 specific for the UL25 protein and VP19C protein specific polyclonal antibody NC2, diluted to a concentration of 1/100, for 1 hour followed by a 30 minute incubation with anti mouse-FITC and anti rabbit-CY5 conjugated secondary antibodies. The cells were then examined by confocal microscopy. Image **a)**. **UL25; b)**. **VP19C; c)**. **Merge.**

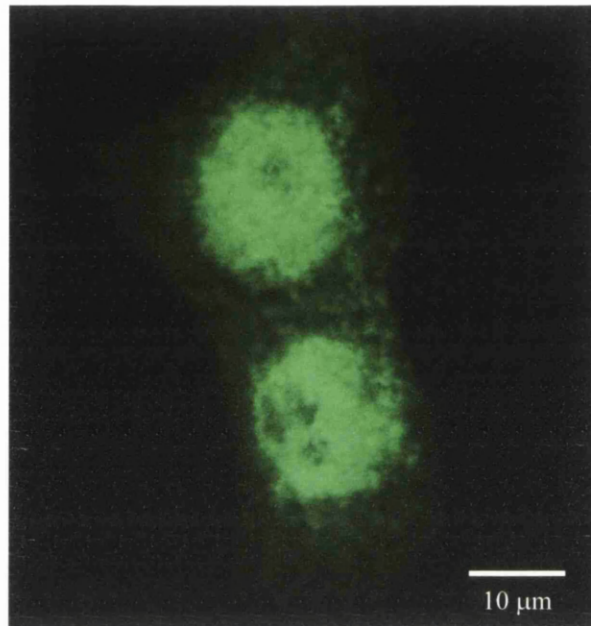


Figure 3.28 The Intracellular Localisation of the VP5 Protein in Cells Infected with *Ts2Hindk* MR#6 at the NPT.

Vero cells were infected with *ts2Hindk* MR#6 using a moi of 10 pfu.cell⁻¹. At 10 hours post-infection the cells were fixed with 5% formaldehyde and permeabilised with 0.5% NP40. The infected cells were incubated with VP5 specific monoclonal antibody DM165, diluted to a concentration of 1/500, for 1 hour followed by a 30 minute incubation with an anti mouse-FITC conjugated secondary antibody. The cells were then examined by confocal microscopy.

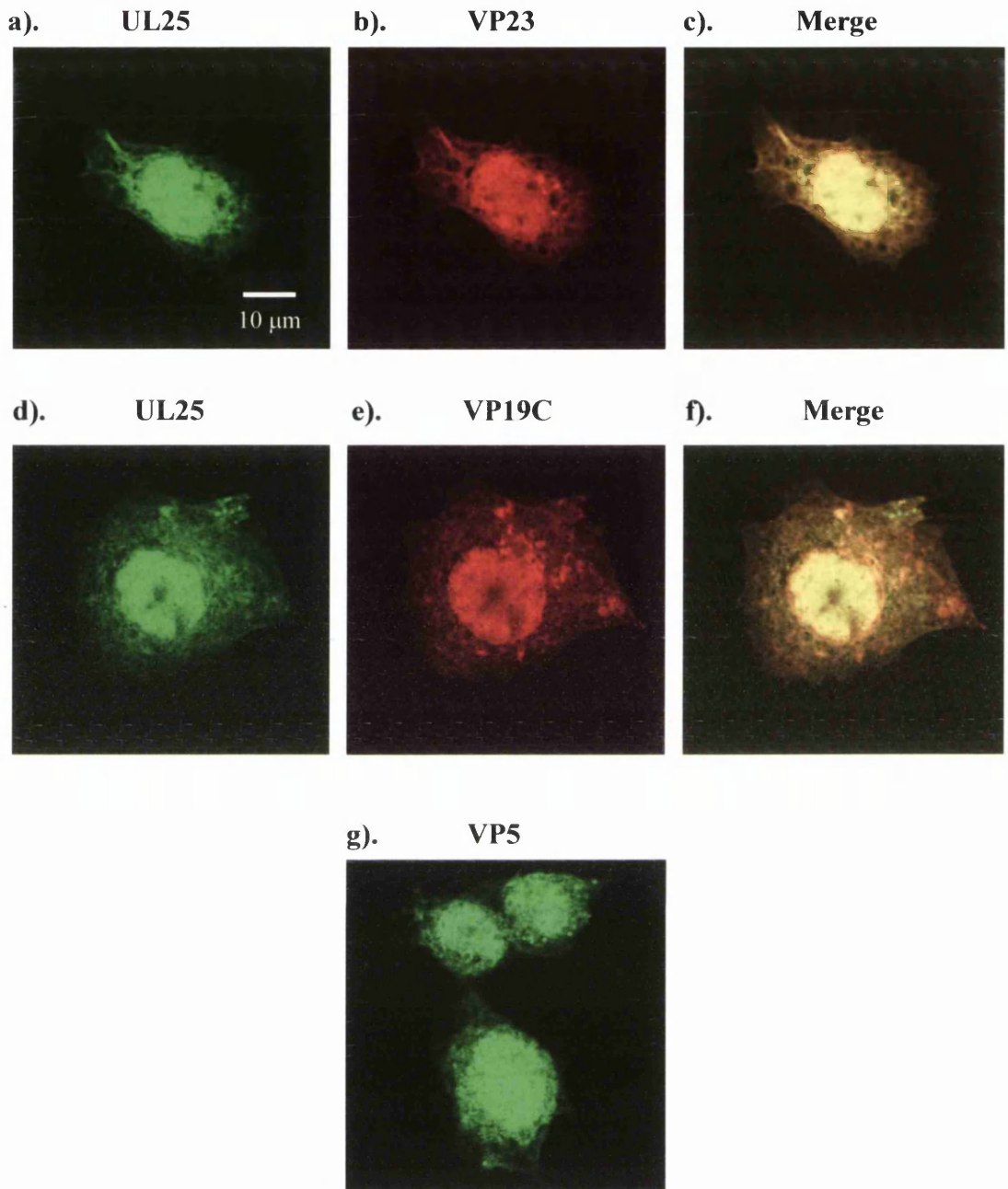
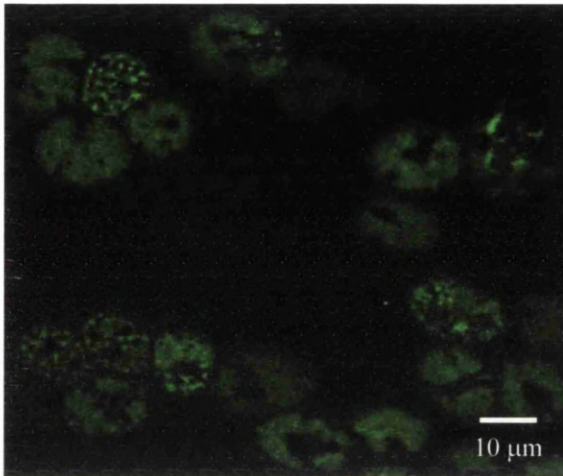


Figure 3.29 The Intracellular Localisation of the UL25 and Capsid Proteins in Cells Infected with *Ts2Hindk* MR#6 at the PT.

Vero cells were infected with *ts2Hindk* MR#6 at the PT using a moi of 10 pfu.cell^{-1} . At 10 hours post-infection the cells were fixed with 5% formaldehyde and permeabilised with 0.5% NP40. The infected cells were incubated with primary antibodies 166 **a)** and **d)**, 186 **b)**, NC2 **e)** and DM165 **g)** specific for UL25, VP23, VP19C and VP5 respectively for 1 hour. After a 30 minute incubation with the appropriate secondary antibodies, the cells were washed and examined by confocal microscopy.

a).



b).

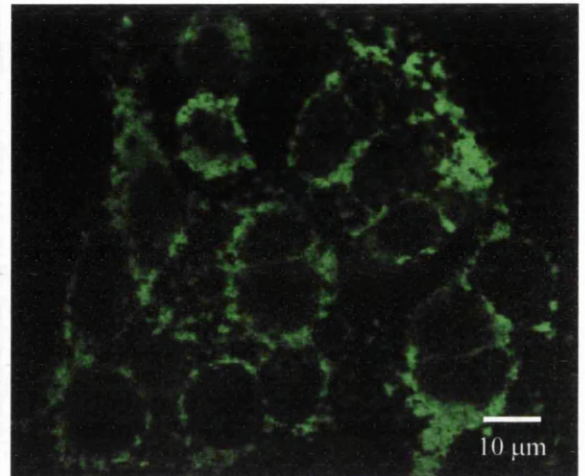


Figure 3.30 The Altered Intracellular Localisation of the UL25 Protein in Cells Infected with HSV-1 *Ts*⁺ A44 at the NPT.

Vero cells were infected HSV-1 *ts*⁺ A44 using a moi of 10 pfu.cell⁻¹. At 10 hours post-infection the cells were fixed with 5% formaldehyde and permeabilised with 0.5% NP40. The infected cells were incubated with UL25 protein specific monoclonal antibody 166, diluted to a concentration of 1/100, for 1 hour followed by a 30 minute incubation with an anti mouse-FITC conjugated secondary antibody. The cells were then examined by confocal microscopy. Image a). UL25 PT; b). UL25 NPT.

the NPT the UL25 protein localised to the perinuclear region with little protein found in the nuclei (Figure 3.30b). This strongly suggested that the altered intracellular distribution of the UL25 protein in cells infected with *ts2* at the NPT was due to an additional *ts* mutation(s) present in *ts2* and was not connected to the lesion in the UL38 gene found in the *ts2* virus. Interestingly, both *ts*⁺ A44 and *ts2* used in this study displayed a *ts* syncytial phenotype whereby the virus induced the formation of syncytia in cells infected at the NPT to a considerably larger degree compared to cells infected at the PT. It is tempting to speculate that the formation of syncytia in cells infected with these viruses at the NPT was connected to the drastic alteration of the intracellular localisation of the UL25 protein. To examine whether the intracellular localisation of the UL25 protein was altered by the formation of syncytia, HSV-1 *ts*⁺ 17 syn infected cells were examined by indirect immunofluorescence. HSV-1 *ts*⁺ 17 syn is a strain of HSV-1 that induces the formation of syncytia in infected cells and Figure 3.31a shows that the UL25 protein localised to the nuclei of cells infected with HSV-1 17 syn at the NPT in a similar manner to cells infected with *ts*⁺ 17 syn⁺ (Figure 3.31b). This indicated that the formation of syncytia in itself did not alter the subcellular localisation of the UL25 protein and it appeared likely that an unidentified *ts* mutation(s) was responsible for the different intracellular distribution of UL25 in cells infected with *ts2* at the NPT. Surprisingly, this did not affect the viral replication cycle in as much as *ts2*/Hindk MR#6 grew to titres similar to those of *ts*⁺ 17 syn⁺ and formed plaques with the same efficiency as *ts*⁺ 17 syn⁺ in cells infected at the NPT (Table 3.2).

3.3.7 Discussion.

Since UL25 is a capsid-associated protein, the distribution of UL25 protein was examined in cells infected with HSV-1 mutants which fail to express the VP5, VP23 or VP19C capsid shell proteins to investigate whether these proteins were required for the nuclear localisation of UL25 in HSV-1-infected cells. The analysis of non-complementing cells infected with either K23Z or K5ΔZ null mutants indicated that neither capsid assembly nor the VP23 and VP5 proteins were necessary for the nuclear localisation of the UL25 protein. Although capsid assembly was not required for the nuclear distribution of the UL25 protein it is clear that at least one viral protein was responsible for this localisation. Transient transfection assays coupled to indirect immunofluorescent analysis demonstrated that neither the VP19C, VP5, VP23 or VP22a proteins alone or in

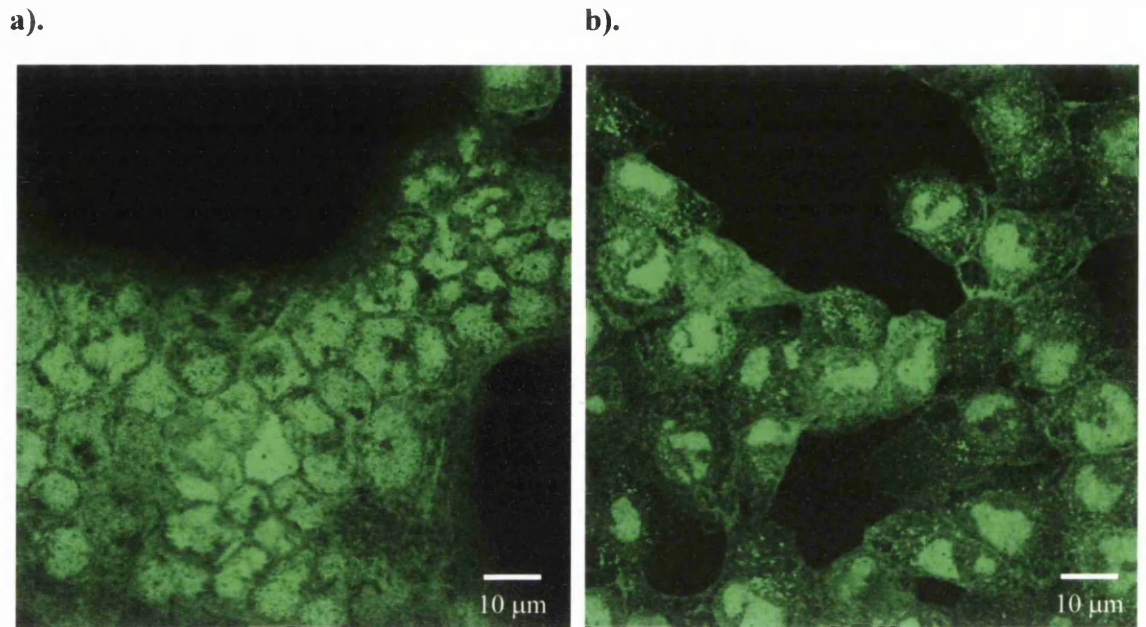


Figure 3.31 The Intracellular Localisation of the UL25 Protein in Cells Infected with HSV-1 *Ts*⁺ 17 *syn* and *Ts*⁺ 17 *syn*⁺ at the NPT.

Vero cells were infected with HSV-1 *ts*⁺ 17 *syn* (a) or HSV-1 *ts*⁺ 17 *syn*⁺ (b) using a moi of 10 pfu.cell⁻¹. At 10 hours post-infection the cells were fixed with 5% formaldehyde and permeabilised with 0.5% NP40. The infected cells were incubated with monoclonal antibody 166, specific for the UL25 polypeptide, diluted to a concentration of 1/100 for 1 hour followed by a 30 minute incubation with an anti mouse-FITC conjugated secondary antibody. The cells were then examined by confocal microscopy.

combination could translocate the UL25 protein into the nucleus (data not shown). This suggested that the nuclear localisation of the UL25 protein during wt virus (HSV-1 *ts*⁺ 17 *syn*⁺) infection either did not depend on the presence of these proteins or required additional, as yet unidentified, protein factors.

Experiments using a UL38 null mutant virus, KΔ19C, yielded no further information regarding the viral factors necessary to direct the UL25 protein to the nuclei of HSV-1-infected cells. Therefore, the intracellular localisation of the UL25 protein was examined in cells infected with *ts2* at the NPT. This virus contained a *ts* lesion in the UL38 gene and failed to assemble capsids in cells infected at the NPT. Indirect immunofluorescent analysis of cells infected with *ts2* at the PT revealed that the UL25 protein and the capsid shell proteins, VP5, VP19C and VP23 were all localised to the nuclei in a manner expected of wt virus infection (Rixon *et al.*, 1996). However, infection of cells with *ts2* at the NPT resulted in a drastic alteration of the intracellular localisation of these proteins which colocalised to the nuclear periphery and were unable to enter the nuclei. Western blot analysis revealed that at least the UL25 and the VP23 proteins were largely insoluble in cells infected with *ts2* at the NPT. Thus, in cells infected with *ts2* at the NPT the *ts* lesion within the UL38 gene resulted in the formation of an insoluble triplex complex which altered the intracellular localisation patterns of the triplex proteins and the VP5 protein. The end result of this was the failure to assemble capsids. The inability of the UL25 protein to enter the nuclei of cells infected with *ts2* at the NPT indicated that the nuclear localisation of the UL25 protein during wt virus infection was dependent on the presence of functional triplex complexes. Additionally, the colocalisation of the UL25 and triplex proteins in cells infected with *ts2* at the NPT suggested a potential interaction between these proteins. However, the characterisation of a *ts2* marker rescue virus indicated that the altered intracellular localisation of the UL25 protein in cells infected with *ts2* at the NPT was not a consequence of the *ts* lesion within the UL38 gene of *ts2* and was related to an unidentified *ts* lesion(s). Examination of cells infected with *ts*⁺ A44 at the NPT revealed a similar phenotype to that of *ts2*Hindk MR#6 infected cells at the NPT. This finding suggested that in addition to the *ts* lesion in the UL38 gene, *ts2* contained a further *ts* mutation(s) which was responsible for the altered intracellular distribution of the UL25 protein in cells infected at the NPT. Although these viruses formed syncytia to a larger degree in cells infected at the NPT compared to cells infected at the PT, no additional evidence was found to link the intracellular distribution of the UL25 protein with the

formation of syncytia. However, the formation of syncytia in HSV-1-infected cells has been linked to several different genes (Raucina *et al.*, 1984, Goodman & Engel, 1991, Dolter *et al.*, 1994, Wilson *et al.*, 1994) and the genes involved in the formation of syncytia in cells infected with *ts*⁺ A44 at the NPT may be different from those of HSV-1 *ts*⁺ 17 syn. Therefore, it remained possible that the formation of syncytia in cells infected with *ts*⁺ A44 at the NPT resulted in the altered intracellular localisation of the UL25 protein. Although the *ts2* virus used in this study did not form syncytia in infected cells to the same extent as *ts*⁺ A44, it nevertheless retained the *ts* lesion of A44 which was also present in the *ts2* marker rescue virus. Unfortunately, the mapping of the additional lesion(s) within these viruses would be hindered by the lack of any selectable marker. The *ts2* marker rescue virus contained the additional defect(s) but grew to titres similar to that of wt virus and no difference was detected in plaque morphology or plating efficiency. The identification of the additional defect(s) of *ts2* therefore remained unresolved.

3.4 Protein-Protein Interactions Involving the UL25 Protein.

3.4.1 Introduction.

Protein-protein interactions involving the HSV-1 capsid shell proteins have been identified and have contributed to a basic understanding of the capsid assembly process (Desai & Person, 1996, Rixon *et al.*, 1996). Initial interactions involving these proteins results in the formation of unstable spherical procapsids. The transformation of the procapsid requires the extensive re-modelling of these interactions to form a stable, angularised capsid with a defined capsid floor layer not present in the procapsid. In contrast to the information obtained about capsid protein association, little is known about the protein-protein interactions involving the HSV-1 DNA cleavage and packaging proteins. The UL6, UL15, UL17, UL25 and UL28 DNA cleavage and packaging proteins have been shown to associate with different types of HSV-1 capsids (Patel & Maclean, 1995, McNab *et al.*, 1998, Yu & Weller, 1998, Goshima *et al.*, 2000, Sheaffer *et al.*, 2001). The putative HSV-1 terminase is a heterodimeric complex composed of the UL15 and UL28 proteins and appears to transiently interact with the capsid. The levels of UL15 and UL28 present in C capsids are diminished compared to those bound to either A or B capsids and it is believed that the terminase is removed from the capsid after DNA encapsidation. The UL6 and UL25 proteins bind to A, B and C capsids and the UL17 protein interacts with B and C capsids but it is not known whether this protein is also found in A capsids. Although the amount of UL6 protein remains constant in all capsid types examined, the level of UL25 varies within different capsid types with the most UL25 protein being associated with C capsids (Sheaffer *et al.*, 2001). This observation has led to the suggestion that additional copies of UL25 bind to the capsid following DNA packaging to seal the genome within the capsid.

When the present study was initiated the interactions which mediated the binding of the cleavage and packaging proteins to the HSV-1 capsid had not been identified. In 1998, the UL15 protein was shown to associate with the VP5 major capsid protein and presumably this interaction facilitates the capsid-binding property of the UL15 protein (SmithKline Beecham corporation, 1998). As mentioned above, the UL15 and UL28 DNA cleavage and packaging proteins interact to form the putative terminase complex (Koslowski *et al.*, 1999, Abbotts *et al.*, 2000). However, no other interactions involving the capsid-associated HSV-1 DNA cleavage and packaging proteins have been identified. Thus, the aim of the

work described in this section was to identify any protein-protein interactions involving the UL25 protein to elucidate the nature by which the UL25 protein associates with the HSV-1 capsid. Additionally, the identification of any protein-protein interactions involving the UL25 protein may provide clues about its role in the HSV-1 DNA cleavage and packaging process.

3.4.2 The Association of the His-UL25 Protein with Recombinant HSV-1 Capsids.

It has been previously demonstrated that the UL25 protein associates with A, B and C capsids purified from wt virus-infected cells and with B capsids produced from co-infection of insect cells with recombinant baculoviruses expressing the major capsid proteins (McNab *et al.*, 1998). In order to establish that the His-UL25 protein was able to be incorporated into capsids, *Sf21* cells were multiply-infected with recombinant baculoviruses expressing the VP5, VP23, VP19C, VP22a, VP24, VP21, VP26 and His-UL25 proteins. The recombinant B capsids were purified by centrifugation through two successive sucrose gradients and the second gradient was fractionated. Samples from the fractions were analysed by Western blotting and probed with antibodies 184 and 335, specific for VP5 and UL25 protein respectively. The result shown in Figure 3.32 demonstrates that the recombinant B capsids were located in fractions 5 - 8 as judged by the levels of VP5 protein contained within these fractions. The highest levels of the His-UL25 protein were also located in fractions 5 - 8. This result indicated that the His-UL25 protein associated with the recombinant B capsids and therefore appeared to be associated with B capsids. This finding also indicated that no other cleavage and packaging proteins were necessary for the ability of the His-UL25 protein to interact with B capsids produced in this system.

3.4.3 The Association of the His-UL25 Protein with VP5/19C Particles.

Virus-like particles termed VP5/19C particles can be purified from *Sf21* cells infected with recombinant baculoviruses expressing only the HSV-1 VP5 and VP19C proteins (Saad *et al.*, 1999). A negatively stained preparation of VP5/19C particles viewed by transmission electron microscopy is shown in Figure 3.34a and a sample of recombinant HSV-1 B capsids prepared in a similar manner is shown in Figure 3.34b for comparison. The VP5/19C particles appear spherical rather than icosahedral in shape and are smaller, with a diameter of 88 nm compared to a diameter of 125 nm exhibited by HSV-1 capsids. Using electron cryomicroscopy and computer reconstruction, Saad *et al.* (1999),

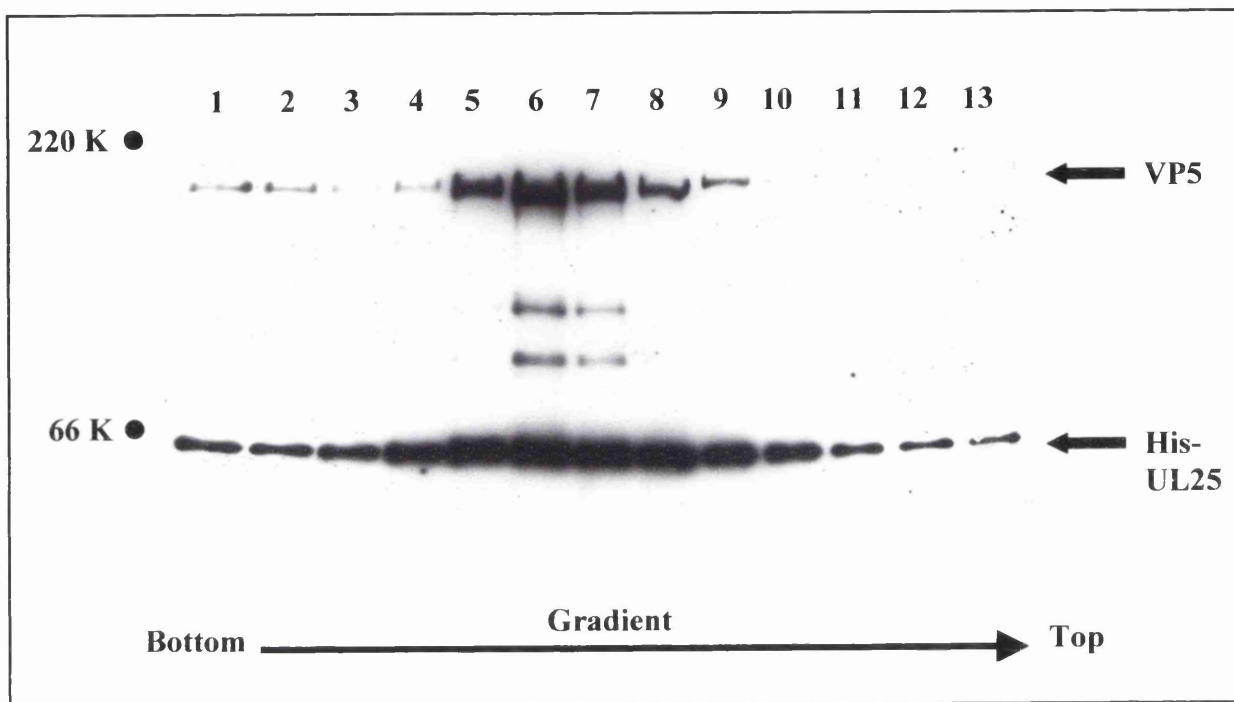


Figure 3.32 His-UL25 Co-Migrates with B Capsids Generated from Co-Infection of *Sf21* Cells with Recombinant Baculoviruses Expressing the HSV-1 Capsid Proteins.

Sf21 cells were infected with recombinant baculoviruses expressing the VP5, VP23, VP19C, VP22a, VP24, VP21, VP26 and His-UL25 proteins using a moi of 5 pfu.cell⁻¹ of each virus. After 3 days incubation at 28°C the cells were lysed and the cell extract layered on a 40% w/v sucrose cushion and centrifuged at 25,000 rpm. The pellet was resuspended in a small volume of NTE and centrifuged through a 10-40% w/w sucrose gradient. The capsid band was visualised by light scattering and harvested. The capsids were pelleted by centrifugation and purified further through a second 10-40% w/w sucrose gradient. Approximately 20 0.5 ml fractions were sequentially collected from the gradient and the protein content within a sample of each fraction was resolved on a 10% SDS polyacrylamide gel and Western blot analysis carried out. The proteins were transferred to Hybond-ECL membrane and probed with polyclonal antibodies 335, specific for UL25 protein, and 184, specific for VP5, both diluted to a concentration of 1/500. **Lanes 1-13** represent the sequential fractions collected from the gradient starting from the bottom of the gradient.

demonstrated that the VP5/19C particles exhibit T=7 icosahedral symmetry as opposed to T=16 icosahedral symmetry exhibited by HSV-1 capsids. This group also showed that the VP5/19C particles have a poorly defined capsid floor and the structure as a whole is generally more porous (Saad *et al.*, 1999). To determine whether the UL25 protein was able to associate with VP5/19C particles, Sf21 cells were infected with recombinant baculoviruses expressing the VP5, VP19C and His-UL25 proteins. The VP5/19C particles were purified and analysed according to section 3.4.2. The result shown in Figure 3.33 demonstrates that the VP5/19C particles were located in fractions 6 - 11 as judged by the levels of VP5 protein contained within these fractions. To confirm this, the material contained within fraction number 9 was pelleted by centrifugation and resuspended in a small volume of PBS. A 2 µl sample was stained with 1% phosphotungstic acid as described in section 2.3.4.4 and examined using a transmission electron microscope and Figure 3.34a shows that VP5/19C particles were present in this fraction. The His-UL25 protein co-migrated with the VP5 protein on the sucrose gradient, with the highest levels of His-UL25 also located in fractions 6 – 11. This finding indicated that the His-UL25 protein associated with the VP5/19C particles and suggested that the association of the UL25 protein with the HSV-1 capsid was mediated through an interaction with the VP5 protein and/or the VP19C protein.

3.4.4 Is the UL25 Protein Located on the External Surface of the HSV-1 Capsid?

To determine whether the UL25 protein, or at least a portion of the protein, was located on the external surface of the HSV-1 capsid, Vero cells at a very early stage of HSV-1 infection were examined for the presence of the UL25 protein on incoming viral capsids using indirect immunofluorescent analysis. Vero cells were infected with wt HSV-1 and at 1 hour pi the virus-infected cells were fixed, permeabilised and then probed with antibodies DM165 and 335, specific for VP5 and UL25 protein respectively. After addition of the appropriate secondary antibodies the cells were examined using confocal microscopy and the result is shown in Figure 3.35. The incoming viral capsids were clearly detectable in the cytoplasm of virus-infected cells probed with DM165 (Figure 3.35a) and 335 (Figure 3.35b). The co-localisation of the two fluorescent signals in Figure 3.35c indicated that at least one epitope of the UL25 protein recognised by the 335 polyclonal antibody was located on the external surface of the incoming viral capsids. No fluorescent signal was detected in mock-infected cells and prolonged infection periods resulted in the

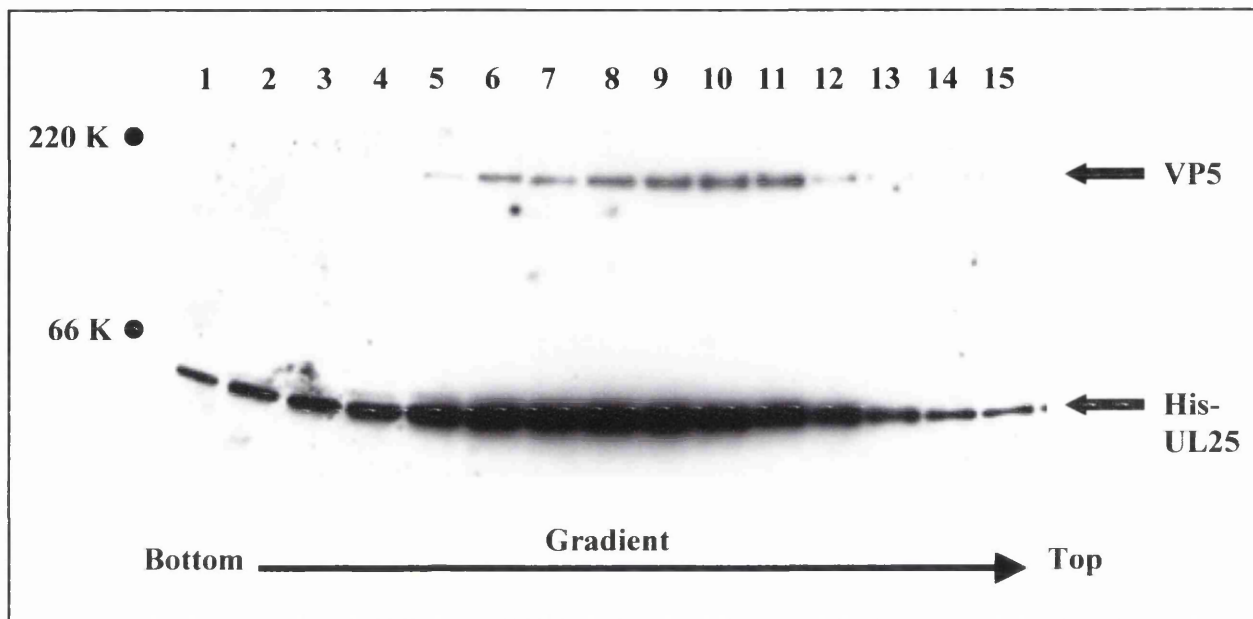


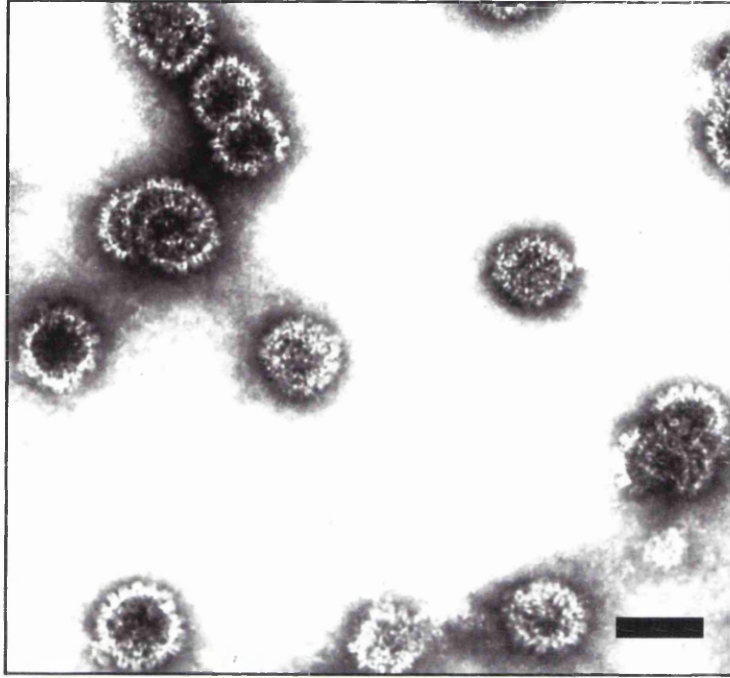
Figure 3.33 His-UL25 Co-Migrates with VP5/19C Particles Generated in *Sf21* Cells Multiply-Infected with Recombinant Baculoviruses Expressing the HSV-1 VP5 and VP19C Capsid Proteins and the His-UL25 Protein.

Sf21 cells were infected with recombinant baculoviruses expressing the VP5, VP19C and His-UL25 proteins each at a moi of 5 pfu.cell⁻¹. VP5/19C particles were purified exactly as described in Figure 3.32. Approximately 20 0.5 ml fractions were sequentially collected from the second sucrose gradient and the protein content in a sample of each fraction was resolved on a 10% SDS polyacrylamide gel. The proteins were transferred to Hybond-ECL membrane and Western blot analysis carried out. The membrane was probed with polyclonal antibodies 335 and 184, specific for UL25 and VP5 protein respectively, both diluted to a concentration of 1/500. **Lanes 1-15** represent the sequential fractions collected from the centrifuge tube starting from the bottom of the gradient.

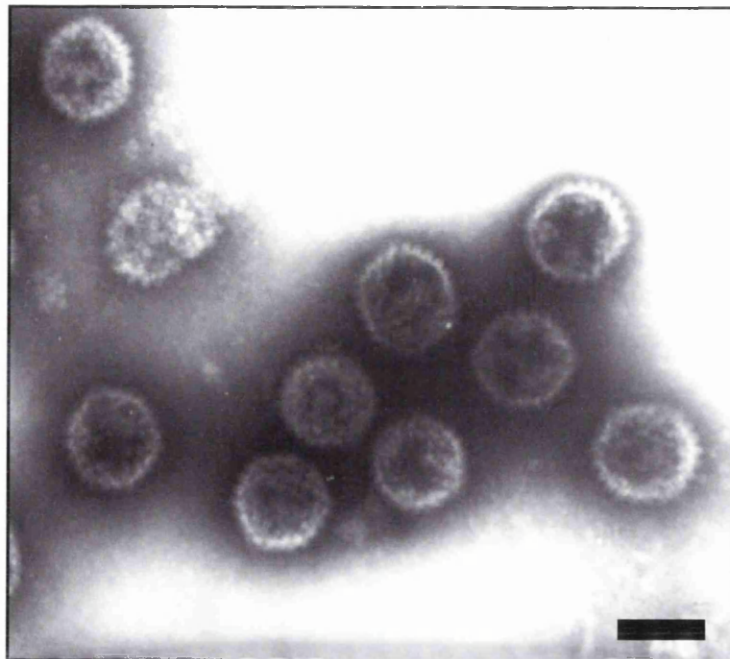
Figure 3.34 Negatively Stained VP5/19C Particles and Recombinant HSV-1 Capsids.

Sf21 cells were infected with recombinant baculoviruses expressing either the VP5, VP19C and UL25 proteins alone (a) or the VP5, VP23, VP19C, VP22a, VP24, VP21 and VP26 proteins (b) using a moi of 5 pfu.cell⁻¹ for each virus. The contents of fraction number 9 from the 10-40% sucrose gradient described in Figure 3.33 were pelleted by centrifugation at 25,00 rpm and resuspended in a small volume of PBS. The VP5/VP19C particles contained within a sample of this fraction were visualised by negative staining (refer to section 2.3.4.4) under a transmission electron microscope (a). Recombinant capsids were purified as described in section 2.2.2.7b and examined as before (b). Recombinant capsid image supplied by F. Rixon taken from Rixon *et al*, 1996. Bar markers represent 100 nm.

a).



b).



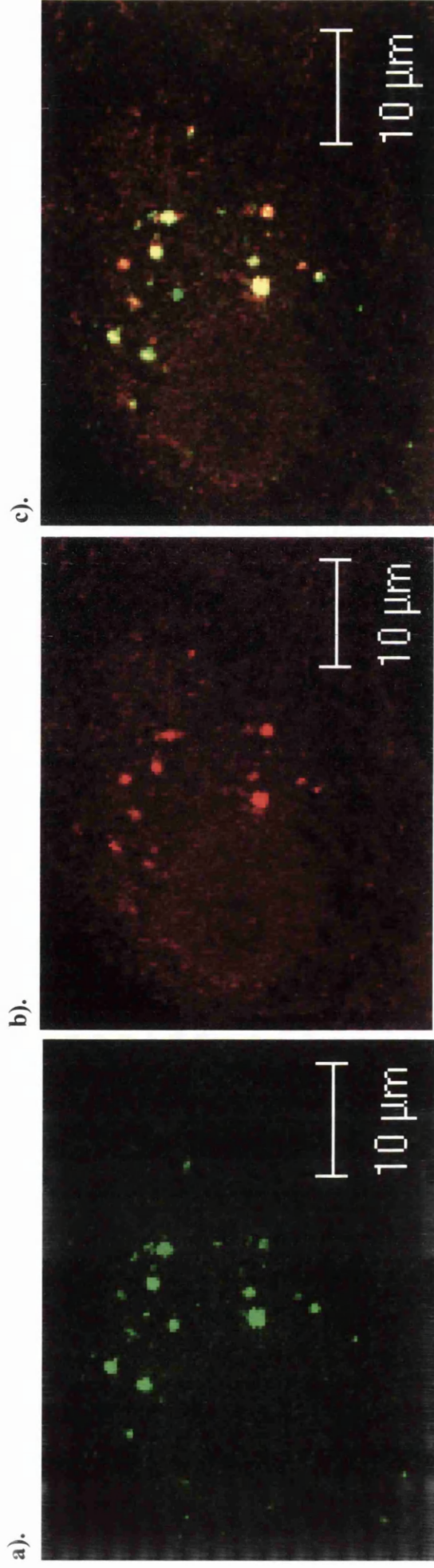


Figure 3.35 At Least Part of the UL25 Protein is Located on the External Surface of the HSV-1 Capsid.

Vero cells were infected HSV-1 17⁺ at a moi of 50 pfu.cell⁻¹. At 1 hour pi the cells were fixed with 5% formaldehyde and permeabilised with 0.5% NP40. The infected cells were incubated for 1 hour with monoclonal antibody DM165 and polyclonal antibody 335, both diluted to a concentration of 1/500, followed by a 30 minute incubation with anti mouse-FITC and anti rabbit-Cy5 conjugated secondary antibodies. The cells were then examined by confocal microscopy. Image a). VP5; b). UL25; c). Merge.

migration of the capsids to the nuclear periphery as described by Sodeik *et al.* (1997). This suggested that genuine incoming viral capsids were observed and that the fluorescent signal seen in virus-infected cells was not due to spurious non-specific binding of the antibodies. No other available antibody specific for the UL25 protein that tested positive in indirect immunofluorescent assays was able to recognise the UL25 protein in the context of the incoming capsid, including a mouse polyclonal antibody and monoclonal antibodies 166, 195, 220, 230 and 485 (data not shown).

3.4.5 An Estimation of the Copy Number of the UL25 Protein in the HSV-1 Capsid.

3.4.5.1 Elevated Levels of the UL25 Protein are Found in Recombinant Capsids Compared to Wt HSV-1 Capsids.

Recombinant B capsids were isolated from *Sf21* cells multiply-infected with recombinant baculoviruses expressing the VP5, VP23, VP19C, VP22a, VP24, VP21, VP26 and UL25 proteins as described in section 2.2.2.7b and HSV-1 B capsids were purified from BHK cells infected with wt HSV-1 according to section 2.2.2.7a. Western blot analysis was used to compare the level of UL25 protein associated with HSV-1 B capsids with the amount of UL25 protein present in recombinant B capsids. Figure 3.36 demonstrates that when two approximately equal samples of purified capsids were examined, as judged by the levels of VP23 protein, there was substantially more UL25 protein associated with the recombinant capsids compared to the wt capsids. The experiment was repeated using new preparations of both HSV-1 B capsids and recombinant capsids and the UL25 protein was consistently found to be present in levels approximately eight-fold higher in the recombinant B capsids compared to the wt B capsids.

3.4.5.2 The UL25 Protein Found in Recombinant Capsids is Resistant to 2 M GuHCl Treatment.

Samples of recombinant capsids made in *Sf21* cells were treated with GuHCl to determine whether the additional levels of the UL25 protein in these capsids were stably incorporated or whether the elevated levels of the protein simply represented UL25 protein aggregates that copurified with the recombinant B capsids. Treatment of purified HSV-1 capsids with 2 M GuHCl leads to the selective removal of some capsid proteins without altering the icosahedral nature of the capsid shell (Newcomb & Brown, 1991). The interior

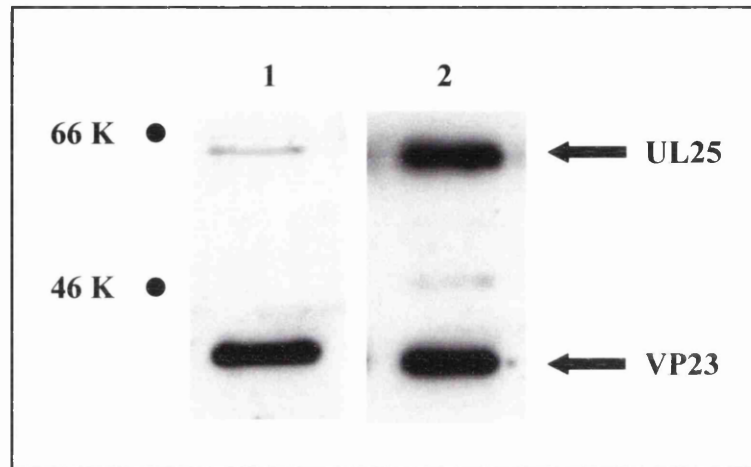


Figure 3.36 Approximately Eight-Fold More UL25 Protein is Found in Recombinant Capsids Compared to Wt HSV-1 Capsids.

The level of the UL25 protein associated with the capsid was examined by Western blot analysis using B capsids purified from wt virus-infected cells and recombinant B capsids purified from recombinant baculovirus-infected *Sf21* cells. The capsid proteins were resolved on a 10% SDS polyacrylamide gel, transferred to Hybond-ECL membrane and probed with polyclonal antibodies 335 and 186, specific for UL25 and VP23 protein respectively, both diluted to a concentration of 1/500. Approximately equal amounts of capsid preparation were compared as judged by the level of the VP23 protein in each sample. **Lane 1**, Wt B capsids; **lane 2**, recombinant B capsids.

VP21, VP22a and VP24 proteins, together with the exterior 12 pentons, penton-associated triplexes and VP26 decorating protein, are lost from the capsid (Newcomb & Brown, 1991). Figure 3.37 demonstrates that treatment of recombinant B capsids with 2 M GuHCl did not result in the total removal of the VP22a scaffolding protein. Approximately 50% of VP22a remained associated with recombinant capsids treated in this manner (Table 3.3). However, no significant loss of UL25 protein was observed and, compared to untreated capsids, 87% of UL25 protein was retained in recombinant capsids under these conditions (Table 3.3). This indicated that the elevated levels of the UL25 protein associated with the recombinant B capsids were stable and unlikely to represent insoluble aggregates of the protein that copurified with the capsids. The UL25 protein associated with HSV-1 B capsids was less stable than that associated with recombinant capsids and compared to untreated capsids, only 37% of UL25 protein was retained in HSV-1 capsids treated with 2 M GuHCl.

3.4.5.3 The Additional Levels of the UL25 Protein Found in Recombinant Capsids Allow an Estimation of the Copy Number of the UL25 Protein in HSV-1 Capsids.

Samples of purified recombinant B capsids and purified wt HSV-1 B capsids were resolved on a 10% SDS polyacrylamide gel and the protein content was visualised by Coomassie blue staining (Figure 3.38). This technique was unable to detect the UL25 protein in the sample of purified wt HSV-1 B capsids, however, the additional levels of the UL25 protein associated with the recombinant B capsids was clearly visible. Moreover, the amount of protein in the bands representing the VP23 and UL25 proteins was very similar. There are 640 copies of the VP23 protein the HSV-1 B capsid (Newcomb *et al.*, 1993) and, since the UL25 protein is roughly twice as large as the VP23 protein (62 kDa as opposed to 34 kDa), this indicated that in the recombinant B capsids the copy number of the UL25 protein was approximately 320. The work described in section 3.4.5.1 demonstrated that there was approximately eight-fold more UL25 protein associated with recombinant B capsids than with wt HSV-1 B capsids. Therefore, the approximate copy number of the UL25 protein in wt HSV-1 B capsids is 40. This figure is consistent with data presented by Ogasawara *et al.* (2001), who predicted that 42 ± 17 copies of UL25 protein were present in each HSV-1 B capsid.

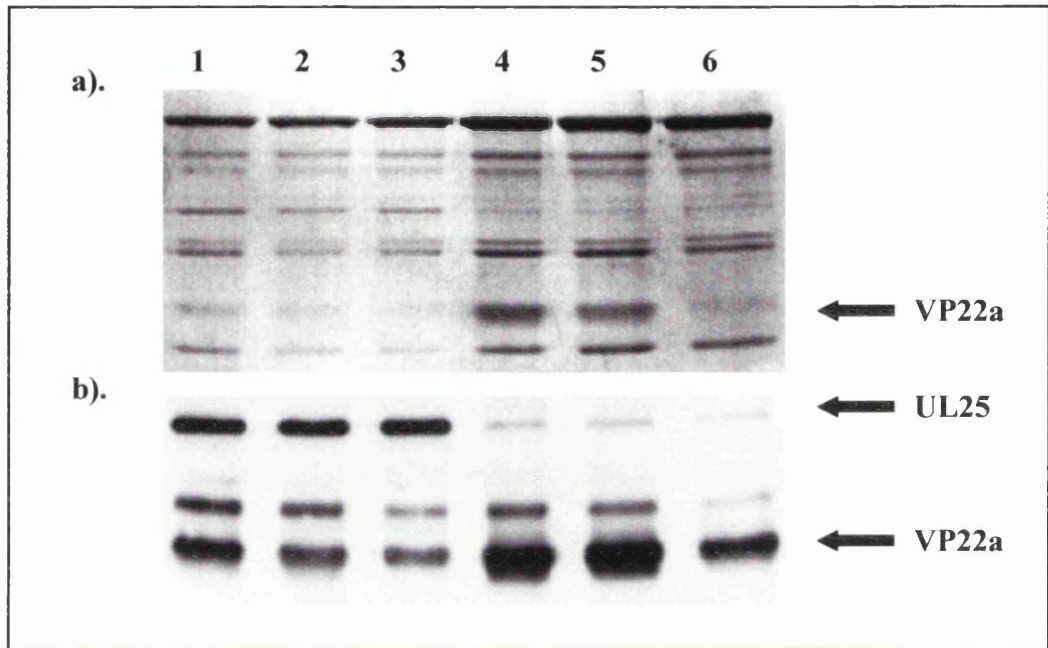


Figure 3.37 The Elevated Levels of the UL25 Protein Associated with Recombinant Capsids are Resistant to 2 M GuHCl Treatment.

Samples of recombinant capsids (**lanes 1-3**) and wt HSV-1 B capsids (**lanes 4-6**) were treated with 0 M (**lanes 1, 4**), 1 M (**lanes 2, 5**) and 2 M (**lanes 3, 6**) GuHCl for 20 minutes with occasional mixing. The capsids were pelleted by centrifugation, resuspended in PBS complete and the protein content was examined on a 10% SDS polyacrylamide gel (**a**) and Western blot analysis using UL25 protein specific polyclonal antibody 335 and monoclonal antibody 406, specific for the HSV-1 UL26.5 gene product carried out (**b**).

Capsid Sample	Protein	Guanidine Hydrochloride Concentration (M)		
		0	1	2
HSV-1	VP22a	100 %	113 %	66 %
	UL25	100 %	97 %	37 %
Recombinant	VP22a	100 %	77 %	50 %
	UL25	100 %	91 %	87 %

Table 3.3 The Effect of GuHCl Concentration on the Levels of UL25 and VP22a Protein in HSV-1 Capsids and Capsids Generated Using Recombinant Baculoviruses.

The relative amounts of UL25 and VP22a proteins detected by Western blot analysis of capsid samples treated with different concentrations of GuHCl shown in Figure 3.37 were quantified using the Quantity One software package (BIO-RAD). The level of UL25 and VP22a protein remaining in capsids treated with 1 and 2 M GuHCl is expressed as a percentage of the protein present in untreated capsid samples.

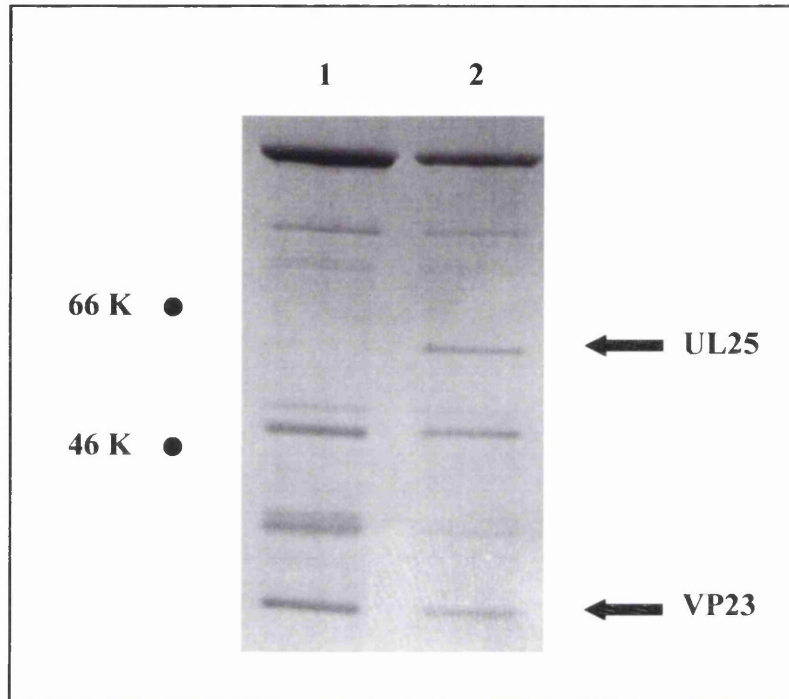


Figure 3.38 An Estimation of the Copy Number of the UL25 Protein in the HSV-1 Capsid.

The protein content in samples of wt HSV-1 B capsids (**lane 1**) and recombinant B capsids (**lane 2**) was resolved on a 10 % SDS polyacrylamide gel and visualised by Coomassie blue staining. To estimate the copy number of UL25 in the HSV-1 capsid, the indicated bands were quantified using the Quantity One software package (BIO-RAD). The ratio of VP23 protein to UL25 protein in the recombinant capsid sample was 1:0.96.

3.4.6 The Analysis of Protein-Protein Interactions Involving the UL25 Protein in HSV-1 *ts*⁺ 17 *syn*⁺ Infected Cells Using an Immunoprecipitation Assay with Monoclonal Antibody 166.

Vero cells were either mock-infected or infected with KUL25NS or HSV-1 *ts*⁺ 17 *syn*⁺ and incubated at 37°C. At 6 hours pi the cells were washed with methionine-free Eagle's medium and incubated for a further 2 hours in identical medium containing ³⁵S-methionine. Radiolabelled mock- and virus-infected cell extracts were prepared as described in section 2.3.1.7 and incubated with monoclonal antibody 166, specific for the UL25 protein, for 3 hours at 4°C with continuous agitation. Immunocomplexes were isolated from the reaction mixture by the addition of Protein A immobilised to sepharose beads followed by low-speed centrifugation. In order to assess the affinity of the protein-protein interactions identified, the stringency of the washes in the immunoprecipitation assay was varied with respect to the concentration of NaCl which ranged from 25 mM to 100 mM. Figure 3.39 demonstrates that in the presence of 50 mM or 75 mM NaCl an unknown protein of approximately 55 kDa was co-immunoprecipitated with the UL25 protein from cells infected with HSV-1 but was not immunoprecipitated from mock- or KUL25NS-infected cells. This indicated that the presence of the UL25 protein was necessary for the association of the unknown protein with the 166 antibody. When the cells were radiolabelled prior to infection, the 55 kDa protein was no longer detectable upon immunoprecipitation analysis using monoclonal antibody 166, indicating that this protein was either of viral origin or was a cellular protein that was induced upon viral infection (data not shown). Table 3.4 lists the potential HSV-1 candidates for this protein based upon a molecular weight of approximately 55 kDa. The most interesting of these candidates is the VP19C protein since the apparent association of the His-UL25 protein with VP5/19C particles indicated a potential interaction between the UL25, VP19C and/or the VP5 proteins. However, due to the lack of a VP19C-specific antibody the possibility that the unknown 55 kDa protein was the VP19C protein remained speculation.

3.4.7 The UL25 Protein Associates with the Cellular Cytoskeleton.

To express the functions encoded in the HSV-1 genome, the virus releases the capsid-tegument structure into the cellular cytoplasm following receptor-mediated fusion of the HSV-1 envelope with the cellular plasma membrane. The capsid-tegument structure is transported along the microtubule network to the nuclear pore where the viral genome is released into the nucleus (Sodeik *et al.*, 1997). The HSV-1 UL34 virion protein has been

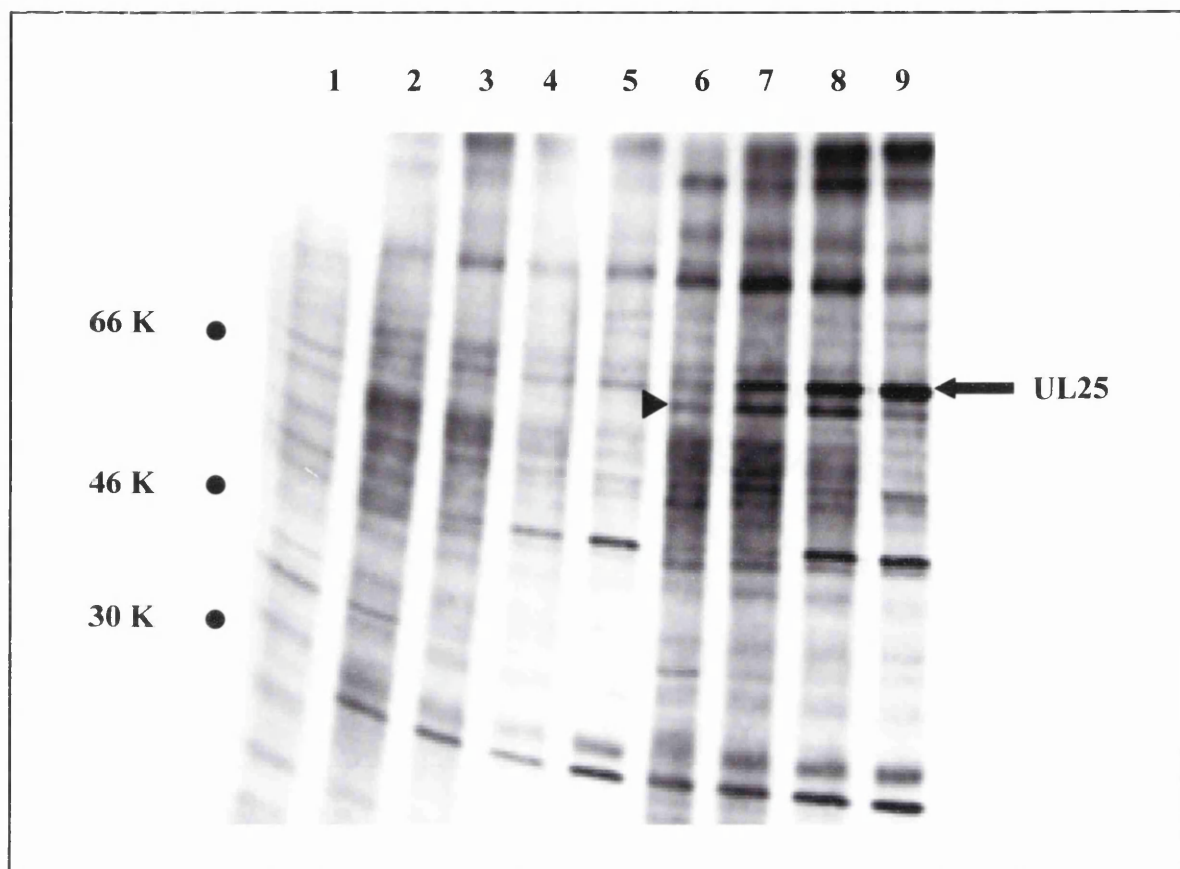


Figure 3.39 Monoclonal Antibody 166 Co-Immunoprecipitates the UL25 Protein and an Unknown Protein of Approximately 55 kDa from Wt Virus-Infected Cells.

Vero cells were either mock-infected (**lane 1**) or infected with KUL25NS (**lanes 2-5**) and HSV-1 17⁺ (**lanes 6-9**) using a moi of 10 pfu.cell⁻¹. At 6 hours pi the cells were labelled for 2 hours with ³⁵S-methionine and then harvested. Radiolabelled virus-infected cell extracts were prepared by incubating the cells with 0.5% NP40 and pelleting the cellular debris by centrifugation as described in section 2.3.1.7. The supernatant was harvested, incubated with monoclonal antibody 166, specific for the UL25 protein, and immunocomplexes were precipitated using Protein A immobilised on sepharose beads. The beads were washed extensively with buffers containing 25 mM NaCl (**lanes 2,6**), 50 mM NaCl (**lanes 3,7**), 75 mM NaCl (**lanes 4,8**) and 100 mM NaCl (**lanes 5,9**) and were finally resuspended in 1x PGSB. The protein content was resolved on a 10% SDS polyacrylamide gel and proteins were visualised by fluorography. The arrowhead indicates the position of the unknown protein with a molecular weight of approximately 55 kDa that co-immunoprecipitated with the UL25 protein.

Gene	Mr (kDa)	Protein / Function	Reference
UL10	51	Glycoprotein M.	Baines & Roizman, 1993
UL13	57	VP18.8 Tegument Protein, Protein Kinase.	Overton <i>et al.</i> , 1992
UL21	57	Virion Protein.	Baines <i>et al.</i> , 1994
UL38	50	VP19C, Triplex Protein.	Rixon <i>et al.</i> , 1990
UL41	55	Virion Associated Host Shut Off Protein.	Smibert <i>et al.</i> , 1992
UL42	51	DNA Polymerase Subunit.	Johnson <i>et al.</i> , 1991
UL48	54	α -TIF, Tegument Protein.	Batterson & Roizman, 1983
UL54	55	Vmw63, Gene Regulation.	McMahan & Schaffer, 1990
US3	52	Protein Kinase.	Purves <i>et al.</i> , 1991

Table 3.4 Potential HSV-1 Protein Candidates for Interaction with the UL25 Protein.

shown to interact with the cytoplasmic dynein intermediate polypeptide chain (Ye *et al.*, 2000). The cytoplasmic dynein protein is a microtubule-associated motor protein involved in intracellular transport. The UL34 protein is believed to facilitate retrograde transport of the capsid-tegment structure to the nuclear pore by anchoring the capsid-tegment to the microtubule network through an interaction with this protein.

The UL25 protein homologue of pseudorabies virus (PRV) has been shown to associate with the microtubule network in cells transiently transfected with PRV UL25 (Kaelin *et al.*, 2000). To determine whether the HSV-1 homologue of the PRV UL25 protein exhibited a similar phenotype, the ability of the HSV-1 UL25 protein to associate with the cellular cytoskeleton was examined. Vero cells were transfected with a plasmid containing either the HSV-1 UL25 gene or as a control, the HSV-1 UL18 gene, under the regulation of the CMV immediate-early promoter. At 24 hours post-transfection the cells were either treated with 1% NP40 to remove the plasma membrane and the cytoplasm and fixed in methanol (section 2.3.3), or fixed with formaldehyde and permeabilised with NP40 as usual (section 2.3.1.5). The cells were then probed with antibodies 166 and 186 and, after addition of an appropriate secondary antibody, the cells were examined using confocal microscopy. Figure 3.40 demonstrates that detergent extraction of UL18 transfected cells resulted in the formation of small aggregates of the VP23 protein in the cytoplasm. In detergent treated UL25 transfected cells the UL25 protein localised to a fibrous network surrounding the nucleus, typical of the cytoskeletal structure which indicated that, as with the PRV UL25 protein, the HSV-1 UL25 protein associated with the cytoskeletal structure.

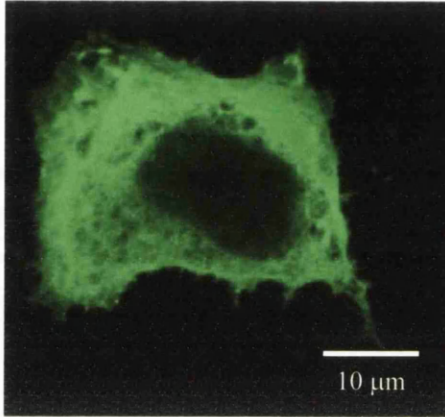
3.4.8 Discussion.

The UL25 protein associated with recombinant capsids in the absence of any other cleavage and packaging proteins. This suggested that UL25 was interacting with at least one of the capsid proteins. The ability of the UL25 protein to associate with capsid-like particles composed of only the VP5 and VP19C proteins indicated that the UL25 protein was binding to either one or both of these proteins. It is therefore likely that an interaction between the UL25 protein and the VP5 and/or the VP19C protein resulted in the ability of the UL25 protein to associate with recombinant capsids in the absence of other cleavage and packaging proteins. These results were consistent with data presented by Ogasawara *et al.*, 2001, who demonstrated that the UL25 protein is capable of interacting with VP19C and VP5. However, it should be noted that these findings do not rule out the possibility that the His-UL25 protein formed aggregates that copurified with recombinant capsids and

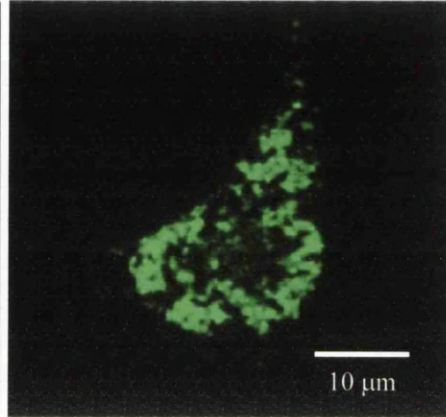
Figure 3.40. The UL25 Protein Associates with the Cellular Cytoskeletal Structure.

Vero cells were transfected with 1 µg pCMV10-UL18 (**a, b**) or pCMV10-UL25 (**c, d**). At 24 hours post-transfection the cells were either detergent extracted with 1% NP40 and fixed in methanol (**b, d**) or fixed in formaldehyde and permeabilised with 0.5% NP40 (**a, c**). The cells were probed with polyclonal antibody 186, specific for VP23 protein, diluted to a concentration of 1/500 (**a, b**) or UL25 polypeptide specific monoclonal antibody 166 diluted to a concentration of 1/100 (**c, d**) for 1 hour followed by a 30 minute incubation with anti rabbit-FITC and anti mouse-FITC conjugated secondary antibodies respectively. The cells were then examined by confocal microscopy.

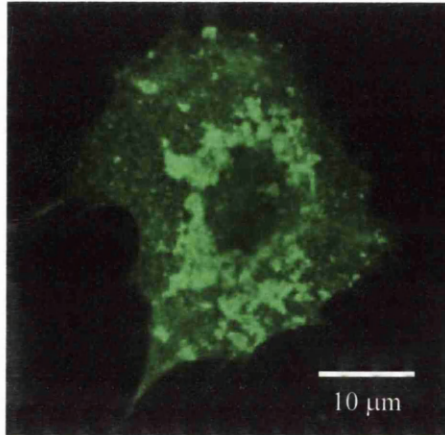
a).



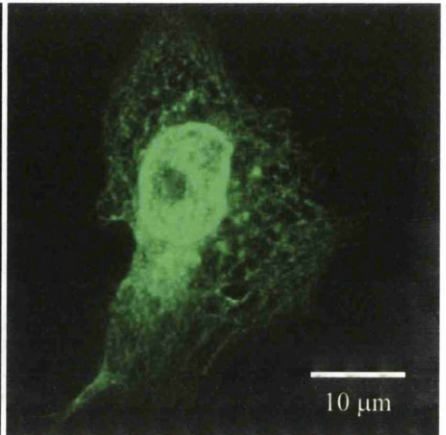
b).



c).



d).



VP5/19C particles generated in insect cells. McNab *et al.* (1998) demonstrated that insoluble aggregates of UL25 protein copurified with recombinant capsids but were solubilised using 2M GuHCl. No appreciable loss of His-UL25 protein was observed from recombinant capsids following treatment with 2M GuHCl (Table 3.3) which suggested that His-UL25 formed a tight association with these capsids. Since the icosahedral capsid structure of VP5/19C particles is generated and maintained through the interactions formed between only two of the HSV-1 capsid proteins, these structures are unlikely to be stable in the presence of denaturants such as GuHCl. Therefore, it is highly probable that VP5/19C particles would be disrupted during treatment with 2M GuHCl and this procedure was not used to test whether the His-UL25 protein bound specifically to these structures. In contrast to the findings with recombinant capsids, only 37% of UL25 protein was retained in HSV-1 B capsids after treatment with 2M GuHCl. This result suggested that the UL25 protein formed a stronger interaction with recombinant capsids and it is possible that the additional proteins present in B capsids isolated from wt virus-infected cells affected the affinity of the UL25 protein for these capsids.

Imunoprecipitation analysis of HSV-1 infected cells using a UL25 specific monoclonal antibody revealed an unknown protein of approximately 55 kDa associated with the UL25 protein. This protein was either a cellular protein induced in response to HSV-1 infection or a HSV-1 encoded protein and potential HSV-1 protein candidates based on a mass of 55 kDa are listed in Table 3.4. Proteins such as α -TIF, which is phosphorylated and gM, which is glycosylated, can be eliminated since the post-translational modification of these proteins *in vivo*, increases the mass of the protein to that above the predicted 55 kDa. Of the remaining candidates, the VP19C protein is the most obvious interaction partner for UL25 although the true identification of this protein remained unresolved. As mentioned in section 3.3, no interaction between UL25 and the capsid proteins was detected using transient transfection assays. It is possible that an interaction between UL25 and one or more of the capsid proteins only occurred in the context of the capsid structure and was dependent not on the presence of one protein alone but on a specific conformation formed by the capsid proteins within the icosahedral capsid shell.

The elevated level of the UL25 protein found in recombinant B capsids was an intriguing but not a unique phenomenon. B capsids formed in non-complementing cells infected with Δ ICP35, a null mutant of HSV-1 KOS that does not express the VP22a major scaffold protein, contain 2.8-4 fold more UL25 protein than B capsids formed during wt

virus-infection (Sheaffer *et al.*, 2000). Similarly, 3-4 fold more UL25 protein is associated with C capsids isolated from wt virus-infected cells compared to B capsids isolated from the same source (Sheaffer *et al.*, 2001). Sheaffer *et al.* (2000), suggested that the removal of the scaffold structure facilitated the addition of extra copies of the UL25 protein and this proposal may explain the presence of the additional levels of the protein associated with recombinant capsids. It is possible that the scaffold structure did not form correctly or was less stable in recombinant capsids which allowed additional levels of the UL25 protein to bind. The amount of UL25 protein in the recombinant capsids was consistently eight-fold higher than in HSV-1 B capsids. This allowed an estimation of the copy number of UL25 protein molecules associated with the HSV-1 B capsid. An approximate copy number of 40 immediately indicated that the UL25 protein is unlikely to be located at one site only within the capsid since 40 copies of a 62 kDa protein would represent a 2.5 MDa mass of protein which would be detectable by electron microscopy. It is far more likely that the UL25 protein is distributed over a number of sites within the HSV-1 capsid. Ogasawara *et al.* (2001) suggested that the UL25 protein interacted with the pentons of HSV-1 B capsids. The present study found that recombinant capsid-associated UL25 protein was resistant to 2 M GuHCl treatment which removes the VP26 decorating protein, the pentons, the peripentonal triplexes and the interior scaffold proteins, and it seemed likely that only a small proportion of the UL25 protein associated with these capsids was bound to the pentons. However, almost two thirds of UL25 protein was removed from HSV-1 B capsids following treatment with 2M GuHCl compared to untreated HSV-1 B capsids and may indicate that the majority of HSV-1 B capsid-associated UL25 protein interacted with the pentons of these capsids. With a copy number of only 40 it is impossible for the UL25 protein to associate with every hexon or every triplex in the HSV-1 capsid on a 1:1 basis. However, if the UL25 protein is distributed in a symmetrical manner within the HSV-1 capsid then a copy number of 40 may indicate that the UL25 protein associates with a subset of hexons or triplexes. The 150 hexomeric capsomeres of the HSV-1 capsid are composed of 60 P- and C-hexon capsomeres and 30 E-hexon capsomeres and the 320 triplex complexes are composed of 60 copies of subsets Ta, Tb, Tc, Td, Te and 20 of subset Tf (Zhou *et al.*, 1994). Figure 1.7 shows the arrangement of these capsid components in one of the 60 asymmetric units of the icosahedral capsid. It is possible that with a copy number of approximately 40, two copies of the UL25 protein could associate with each one of the 20 Tf triplex complexes. Since the level of UL25 protein associated with HSV-1 C capsids is approximately 3-4 fold higher than that associated with HSV-1 B

capsids (Sheaffer *et al.*, 2001), the predicted copy number of the UL25 protein in C capsids is 120-160. The additional level of UL25 protein found in C capsids could either interact with the UL25 protein already present or bind to other sites, presumably associated with hexon or triplex subsets. Data presented in this study suggested that the increased levels of UL25 protein that were associated with recombinant capsids were more stable than UL25 protein bound to HSV-1 B capsids. Although it is not known, it is also possible that the additional copies of UL25 protein present within C capsids are more stable than the UL25 protein contained within B capsids. The increased stability of the UL25 protein within DNA-containing capsids would presumably serve to retain the newly packaged viral DNA within the capsid.

The HSV-1 UL25 protein appeared to associate with the cellular cytoskeleton and in this respect exhibited similar biological properties to the PRV UL25 protein (Kaelin *et al.*, 2000). The cytoskeletal structure is composed of actin filaments and microtubule elements and through the use of drugs that specifically depolymerise these components of the cytoskeleton Kaelin *et al.* (2000), demonstrated that the PRV UL25 protein specifically associated with the microtubule component of the cytoskeleton. Although not proven it is reasonable to conclude that the association of the HSV-1 UL25 protein with the cytoskeleton is also mediated through the microtubule component. The functional significance of this association is unknown. No interaction between the UL25 protein and the UL34 protein or cytoplasmic dynein has been demonstrated but the possibility that UL25 is somehow involved in the transport of the capsid-tegument structure to the nuclear pore cannot be excluded at this stage. A role in the early events of the HSV-1 life cycle has been described for the UL25 protein (Addison *et al.*, 1984) and the finding that at least a portion of the UL25 protein was located on the external surface of the protein supported the idea that the UL25 protein may be involved in the intracellular transport of capsids. However, there is no additional evidence to support this hypothesis. It is clear that in HSV-1-infected cells the majority of UL25 is not bound to the cellular cytoskeleton since this protein appears to localise predominantly to the nuclei of cells under these conditions and it remains possible that the association of the UL25 protein with the cellular cytoskeleton in transiently transfected cells is simply an artefact.

3.5 The Characterisation of *Ts*1204 and *Ts*1208 Mutants.

3.5.1 Introduction.

Two HSV-1 mutants, *ts*1204 and *ts*1208, that have *ts* mutations in the UL25 gene have been previously characterised (Addison *et al.*, 1984). *Ts*1204 has two phenotypic defects at the NPT, a very early block in virus infection and another in the assembly of functional capsids. *Ts*1208 has a defect in virus assembly only. Initially, the early defect in *ts*1204 infection at the NPT was thought to be in the penetration of the virus into the host cell. This conclusion was based on two observations, first, infection of the mutant at high moi at the NPT prevented subsequent infection by wt HSV-1 but not wt HSV-2 and second, the early defect was overcome by treatment of the mutant-infected cells with polyethylene glycol, a membrane fusing agent. This latter finding was unable to be repeated and more recent work has shown that the UL25 protein is involved in DNA packaging and is associated with capsids in the cell nucleus (Ali *et al.*, 1996, McNab *et al.*, 1998). The defects in *ts*1204 and *ts*1208 have therefore been reassessed and the base pair changes responsible for these *ts* mutations have been determined.

3.5.2 Sequence Analysis of the *Ts*1204 and *Ts*1208 Mutations.

The alteration in the DNA sequence responsible for the UL25 temperature sensitive lesions in *ts*1204 and *ts*1208 was determined by dideoxy sequence analysis (this work was carried out by I.M. McDougall, Institute of Virology). Previous marker rescue studies using cloned wt virus DNA had mapped each of the mutations to a small region within the UL25 gene and the corresponding sequence in the cloned mutant DNAs was sequenced. The *ts*1204 phenotype resulted from a single base pair change in the UL25 gene leading to the substitution of glutamic acid residue 133 with a lysine. *Ts*1208 had an in-frame deletion of three base pairs in the coding sequences of the UL25 gene resulting in the loss of valine 161.

3.5.3 The Construction of *Ts*1249.

Ts⁺ virus isolated from cells transfected with *ts*1204 viral DNA and a cloned fragment containing the wt UL25 gene behaved like wt virus at the NPT of 38.5°C. On the basis of this finding it was concluded that *ts*1204 had a single *ts* lesion (Addison *et al.*, 1984). It was subsequently discovered that at a higher NPT of 39.5°C the marker rescuant of *ts*1204

formed plaques at a low efficiency compared with wt virus, and therefore had more than one *ts* defect. A virus with the UL25 lesion only, *ts*1249, was constructed by recombining the cloned *ts*1204 *Eco*RI f fragment containing UL25 gene into wt virus DNA (this work was carried out by Dr V.G. Preston, MRC Institute of Virology). The presence of the UL25 mutation in the *ts* virus was confirmed by the failure of *ts*1249 to recombine with *ts*1204. *Ts*⁺ marker rescuants of *ts*1249 (*ts*⁺1249MR), generated by recombining wt *Bam*HI u fragment into the *ts*1249 DNA, formed plaques at 39.5°C and the PT of 32°C with the same efficiency as wt virus. *Ts*1249 therefore contained a single *ts* lesion. *Ts*⁺ marker rescuants of *ts*1208 (*ts*⁺1208MR) behaved in a similar manner to wt virus at both temperatures, suggesting that this mutant had a single *ts* mutation.

3.5.4 The Protein Profile of *Ts*1249 and *Ts*1208 in Cells Infected at the NPT.

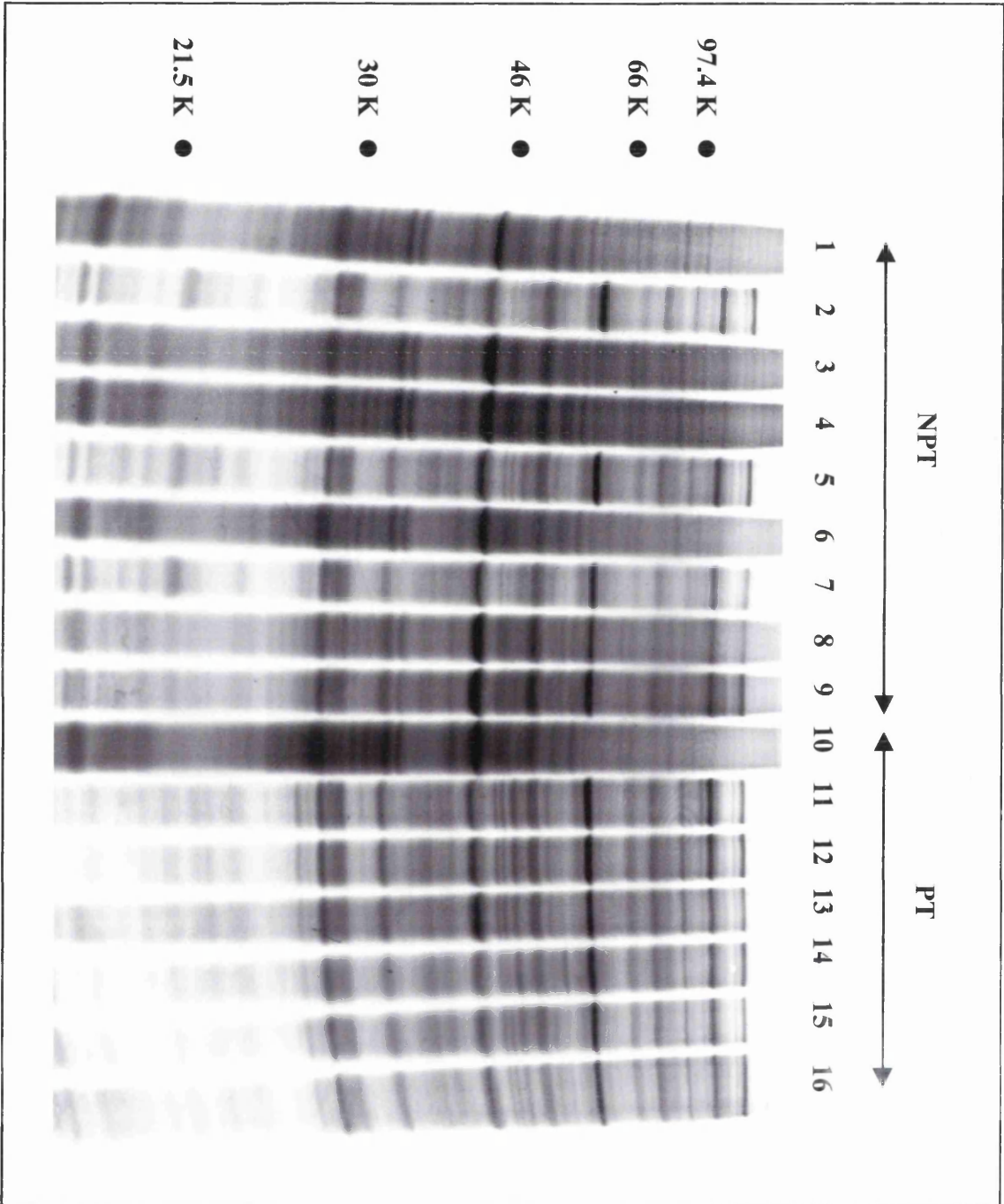
To examine the profile of viral polypeptide expression at the NPT, Vero cells were infected with wt virus, *ts*1249, *ts*1208 and marker rescuant viruses and labelled with ³⁵S-methionine. Mock-infected and *ts*1204-infected cells were also included as controls. At 20 hours pi the cells were harvested, the protein content analysed by SDS-PAGE and the protein profile was visualised using fluorography (Figure 3.41). *Ts*1249 and *ts*1204 failed to synthesise any detectable viral polypeptides in cells infected at the NPT and the mutant-infected polypeptide profiles resembled that of the mock-infected control. This suggested that the *ts* lesion in the UL25 gene of *ts*1204 was responsible for the lack of viral protein synthesis in cells infected with this virus at the NPT. This was supported by the finding that *ts*⁺1249MR produced similar levels of viral polypeptides to that of wt virus-infected cells at the NPT. *Ts*1208 synthesised similar levels of viral polypeptides in cells infected at the NPT compared to *ts*⁺1208MR and wt virus-infected cells at the NPT. All viruses produced similar levels of viral polypeptides in cells infected at the PT.

3.5.5 The Entry of *Ts*1249 Into Cells Infected at the NPT.

To determine whether *ts*1249 had an entry defect, an immunofluorescence assay was used to detect incoming capsids. Vero cells were infected with purified virions at a moi of 50 pfu.cell⁻¹ in the presence of cycloheximide to prevent *de novo* synthesis of viral polypeptides. At 1 hour pi the cells were fixed, permeabilised and probed with monoclonal antibody DM165. After incubation with an anti-mouse-FITC secondary antibody the cells were examined using the confocal microscope. *Ts*1249 and *ts*⁺1249MR capsids were clearly detected in the cytoplasm of Vero cells infected at the PT (Figure 3.42). Similarly,

Figure 3.41 The Protein Profile of *Ts1249* and *Ts1208* in Cells Infected at the NPT.

Vero cells were either mock-infected (**lanes 1, 6 and 10**) or infected with prewarmed wt virus (**lanes 2, 7 and 11**), *ts1204* (**lanes 3 and 12**), *ts1249* (**lanes 4 and 13**), *ts⁺1249MR* (**lanes 5 and 14**), *ts1208* (**lanes 8 and 15**) or *ts⁺1208MR* (**lanes 9 and 16**) viruses using a moi of 10 pfu.cell⁻¹. Virus was adsorbed at the PT of 36.5°C (**lanes 10-16**) or at the NPT of 39.2°C (**lanes 1-5**) or 39.5°C (**lanes 6-9**) for 1 hour. Prewarmed media was added and at 5 hours pi the plates were washed with prewarmed methionine-free media and prewarmed media containing ³⁵S-methionine was added. Incubation was then continued at the appropriate temperature and at approximately 20 hours pi the cells were harvested. A sample was resolved on a 10% SDS polyacrylamide gel and the protein profile was visualised by fluorography.



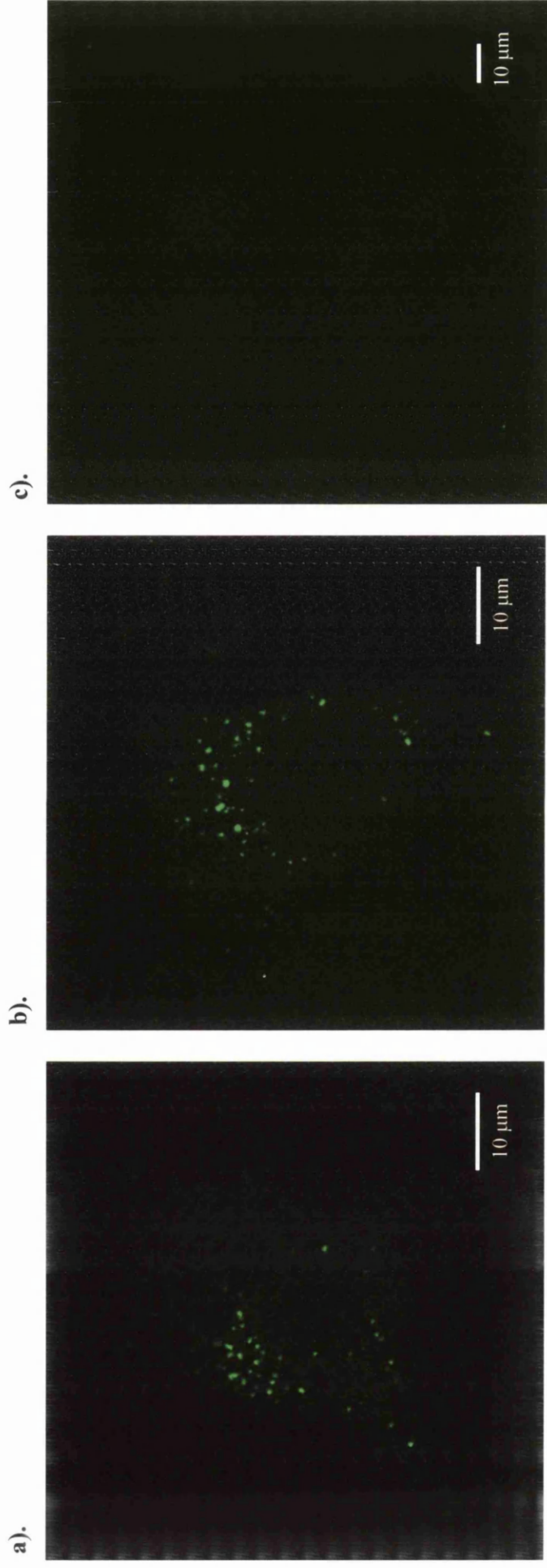


Figure 3.42 Entry of Ts1249 Into Cells Infected at the PT.

Vero cells were either mock-infected or infected with purified virions at a moi of 50 pfu.cell⁻¹. Virus was adsorbed at 36.5°C in the presence of cycloheximide for 1 hour. Medium containing cycloheximide was then added to the cells and incubation was continued for a further hour. The cells were fixed with 5% formaldehyde, permeabilised with 0.5% NP40 and incubated for 2 hours with monoclonal antibody DM165, specific for VP5 protein, diluted to a concentration of 1/250 followed by a 30 minute incubation with FITC conjugated secondary antibody. Image a). *ts*⁺1249MR, b). *ts*1249, c). Mock infected cells.

ts1249 capsids were observed in the cytoplasm of Vero cells infected at the NPT (Figure 3.43) and migrated to the nuclear periphery by 4 hours pi (data not shown). The behaviour of the mutant capsids was indistinguishable from that of the marker rescuant in this assay, suggesting that *ts1249* did not have a defect in cellular penetration or cytoplasmic transport of capsids to the nucleus.

3.5.6 Electron Microscopic Analysis of Mutant Virus-Infected Cells.

Vero cells, infected with *ts1249*, wt virus or *ts*⁺1249MR, were initially incubated for two hours at 31°C to allow the virus to enter cells and release its genome from the capsid. After this period the cells were transferred to 39.2°C. At 16 hours pi cells were harvested and thin sections were prepared for examination under the electron microscope. In the wt virus- and the marker rescuant-infected cells DNA-containing capsids were present in the cell nuclei and in vacuoles in the cytoplasm (Figure 3.44a and c). Enveloped capsids were also observed in the cytoplasm and between the inner and outer nuclear membrane. In cells infected with *ts1249* few DNA-containing capsids were detected in the nuclei of cells but no DNA-containing capsids were observed in the cytoplasm. Capsids lacking DNA were also present in the nuclei, most of which contained a scaffold but some empty capsids were evident (Figure 3.44b).

Vero cells infected with *ts1208*, wt virus or *ts*⁺1208MR were incubated for 16 hours at 39.5°C, harvested and thin sections prepared for electron microscopic analysis. Cells infected with *ts1208* did not contain as many capsids as those infected with wt or *ts*⁺1208MR virus (Figure 3.44d and e). The predominant capsid form was a capsid containing a cleaved internal scaffold, few DNA-containing capsids were observed and these and the other capsid forms were detected only in the cell nuclei. At the high NPT of 39.5°C, wt virus capsids package DNA less efficiently than at lower temperatures and fewer DNA-containing capsids were observed in wt virus-infected cells or *ts*⁺1208MR-infected cells at this temperature than at 39.2°C. Despite the reduction in efficiency of viral DNA encapsidation, it was clear that cells infected with the wt virus or *ts*⁺1208MR contained significantly more DNA-containing capsids than those infected with the mutant virus. In contrast to the findings with *ts1208*, enveloped DNA-containing capsids were observed in the cytoplasm, in vacuoles and between the inner and outer nuclear membranes in cells infected with *ts1208*MR or wt virus at the NPT.

Addison *et al.* (1984), previously found that at 6 hours post infection (pi) at the NPT both *ts1204* and *ts1208* produced low numbers of capsids in the nuclei of cells in

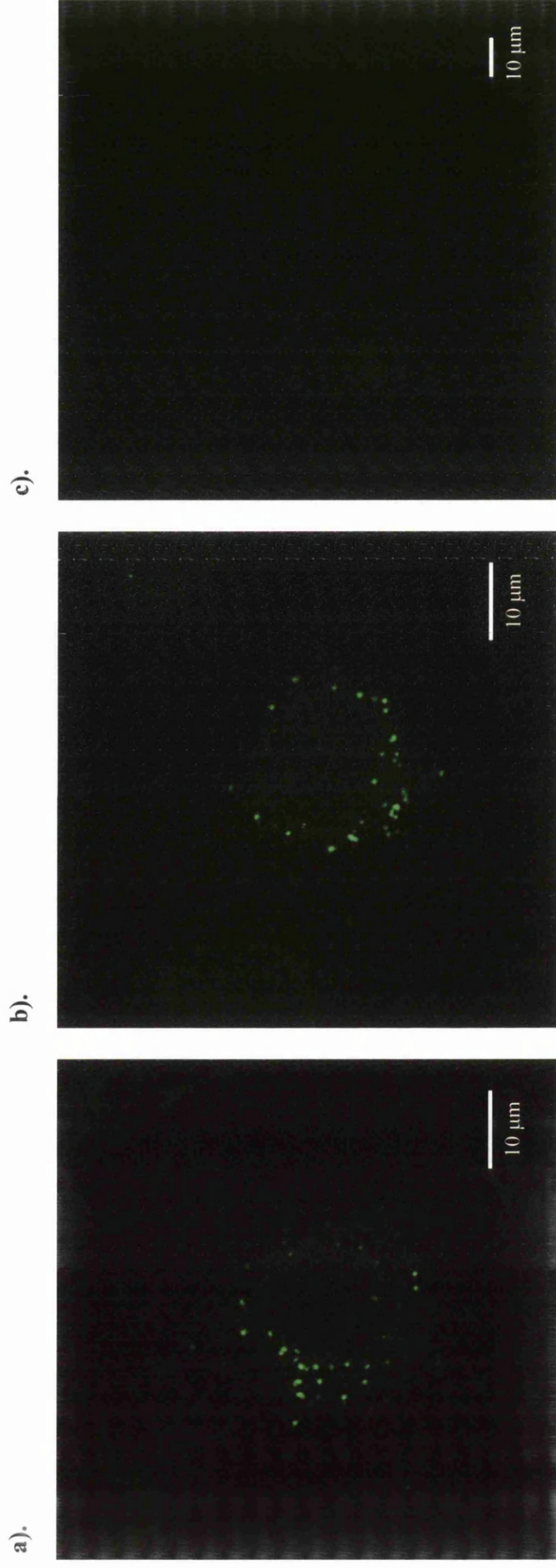


Figure 3.43 Entry of Ts1249 Into Cells Infected at the NPT.

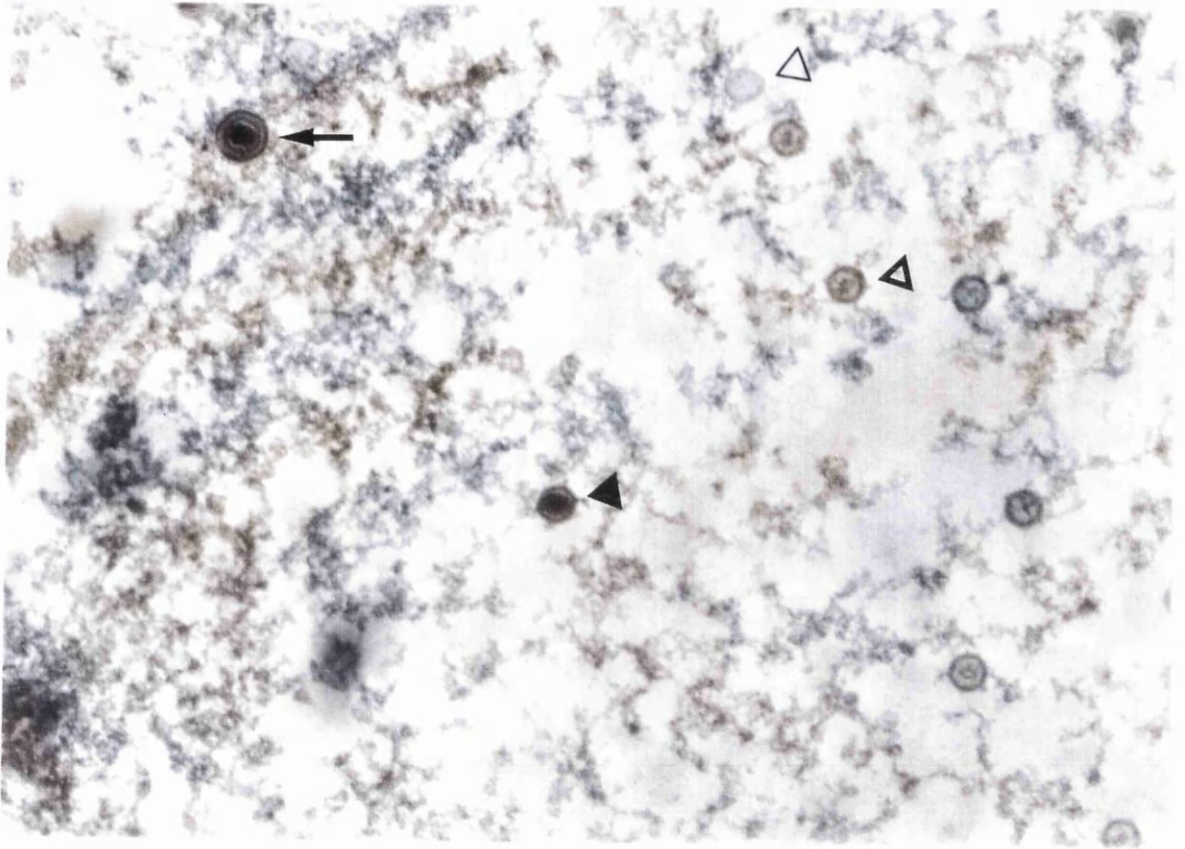
Vero cells were either mock-infected or infected with prewarmed purified virions at a moi of 50 pfu.cell⁻¹. Virus was adsorbed at 39.2°C in the presence of cycloheximide for 1 hour. Prewarmed medium containing cycloheximide was then added to the cells and incubation was continued for a further hour. The cells were fixed with 5% formaldehyde, permeabilised with 0.5% NP40 and incubated for 2 hours with VP5 polypeptide specific monoclonal antibody DM165 diluted to a concentration of 1/250 followed by a 30 minute incubation with FITC conjugated secondary antibody. Image a). *ts*⁺ 1249MR, b). *ts*1249, c). **Mock infected cells.**

Figure 3.44 Electron Microscopic Analysis of Mutant Virus-Infected Cells.

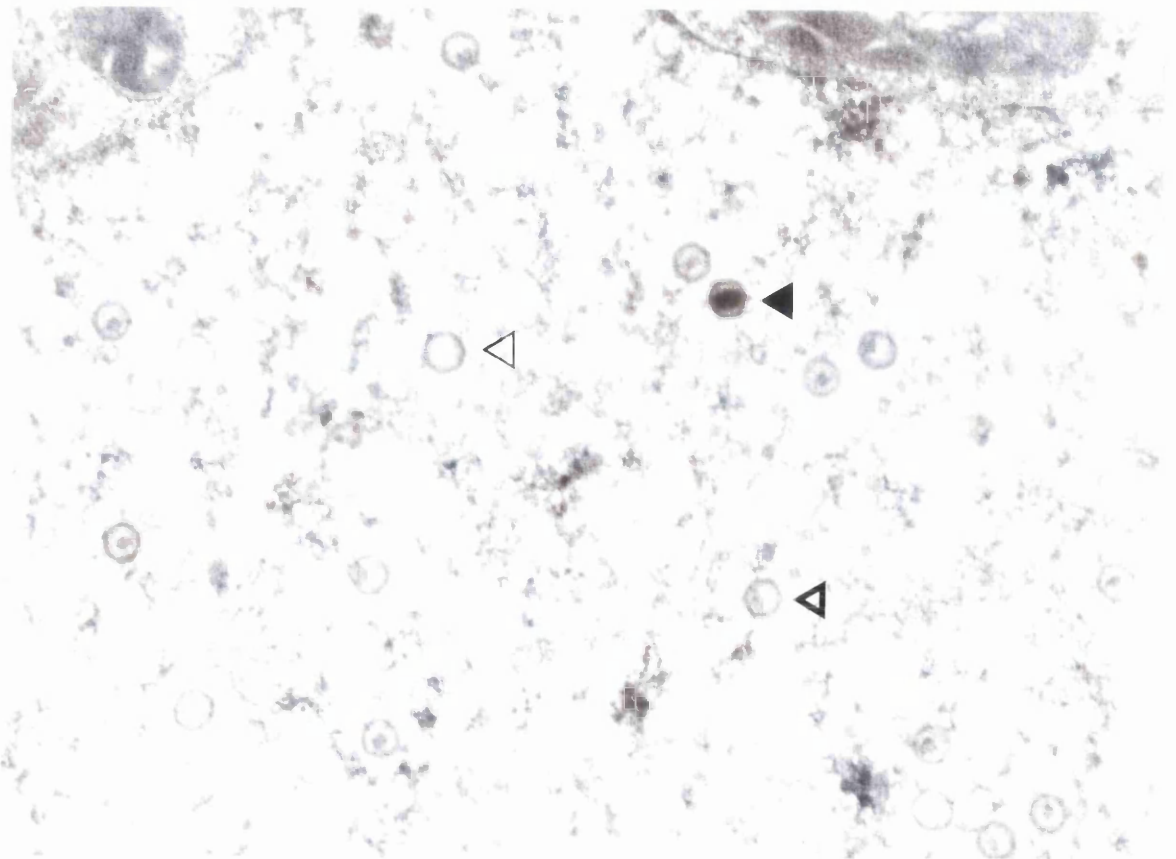
Vero cells were infected with prewarmed *ts1208*, *ts⁺1208MR* or wt virus at 39.5°C using a moi of 20 pfu.cell⁻¹ for each virus. Virus was adsorbed for 1 hour and cells incubated for 16 hours pi at the same temperature. *Ts1249* or *ts⁺1249MR* were adsorbed to Vero cells for 2 hours at 36.5°C, and DC10 media, prewarmed to 42°C, was added to the virus-infected cells which were transferred to 39.2°C for 16 hours pi. At 16 hours pi the cells were harvested and fixed in 2.5% glutaraldehyde. The cells were treated with osmium tetroxide and dehydrated by a series of alcohol washes before embedding in resin. Thin sections were prepared, stained with uranyl acetate and lead citrate and examined under the electron microscope. a). Wt virus, b). *ts1249*, c). *ts⁺1249MR*, d). *ts1208*, e). *ts⁺1208MR*.



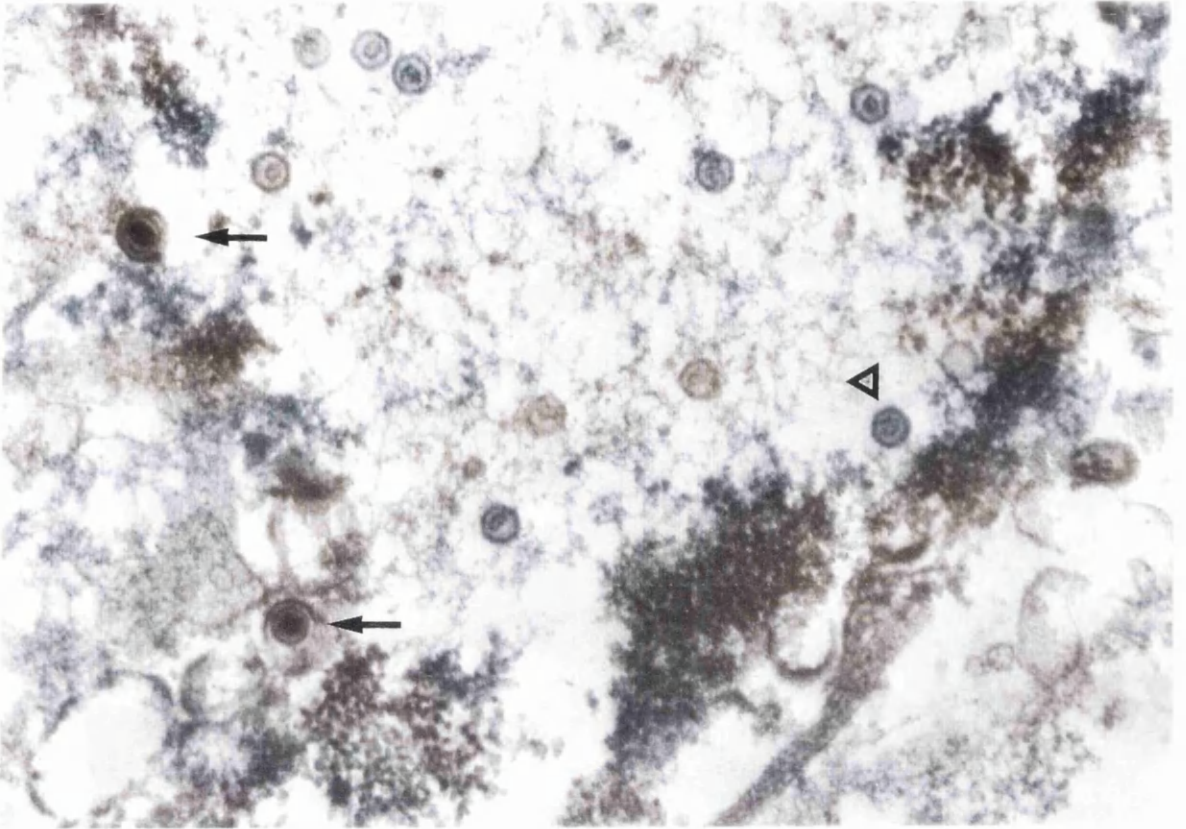
a).



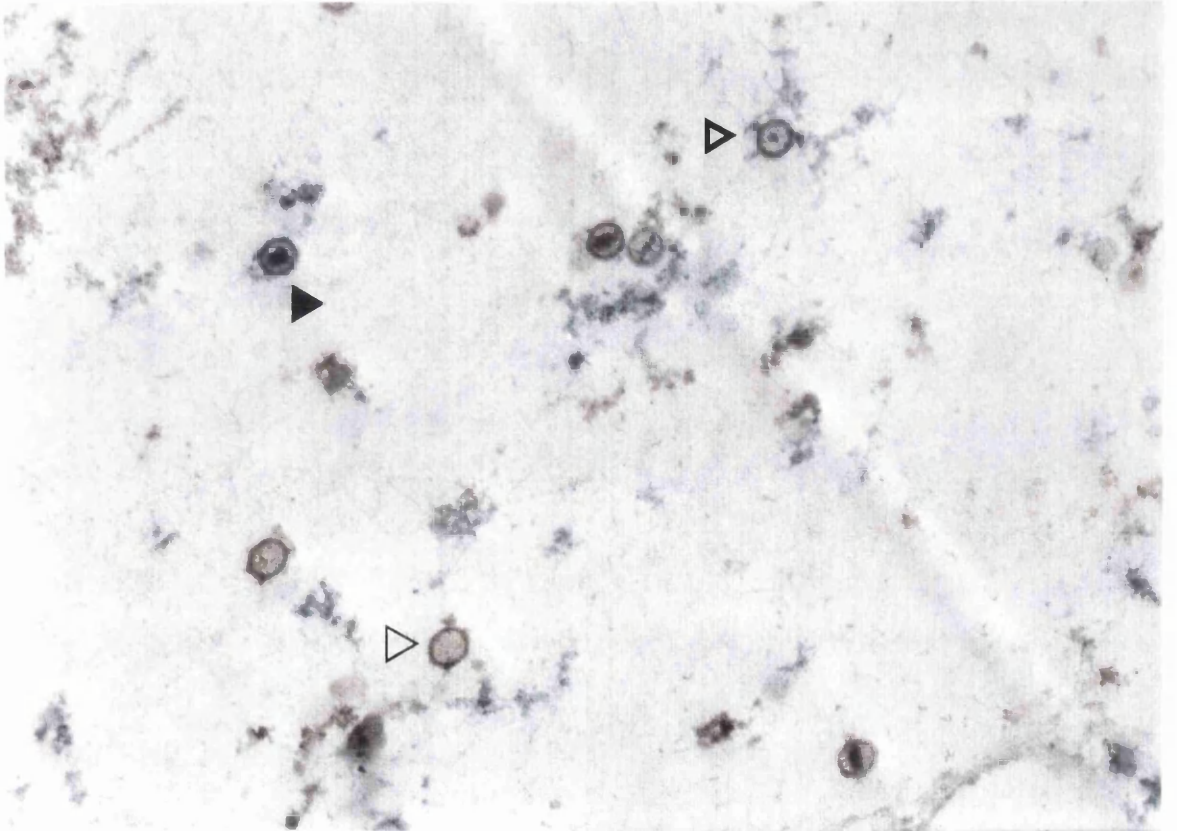
b).



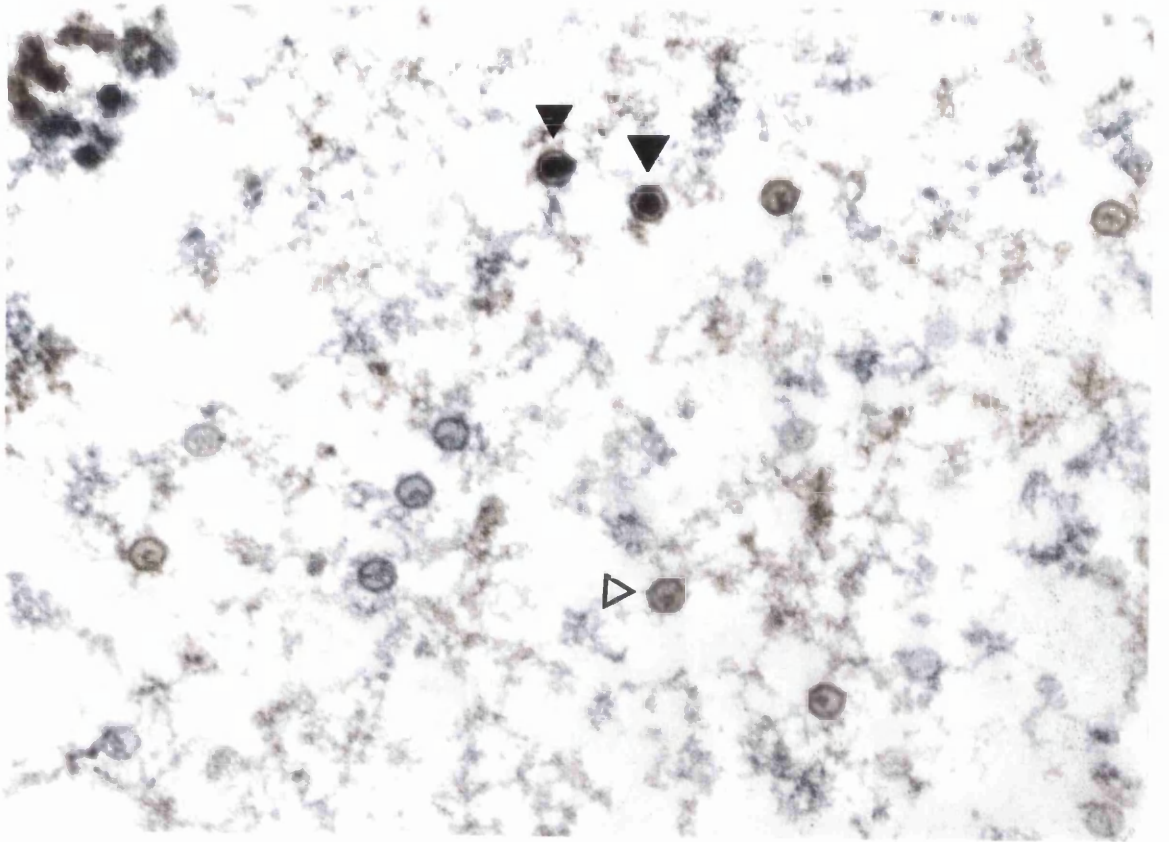
c).



d).



e).



comparison with wt virus. In our experiments we used a higher moi of 20 instead of 5 pfu.cell⁻¹ and examined the cells at a later time of 16 hours pi. Using these conditions larger numbers of *ts1204* and *ts1249* capsids were observed at the NPT after the virus-infected cells were shifted up from the PT. It is therefore likely that the low number of capsids present in the virus-infected cells resulted from an incomplete reversal of the early defect rather than a defect in the assembly of capsids. Interestingly, low numbers of *ts1208* capsids were observed in the nuclei of virus-infected cells at the NPT suggesting that this mutant, like *ts1204* and *ts1249*, may have some impairment at an early stage of infection. It is unlikely that UL25 has a direct role in capsid assembly since large numbers of virus capsids are assembled in the nucleus in the absence of UL25 (McNab *et al.*, 1998).

3.5.7 The Ability of *Ts1249* and *Ts1208* to Package HSV-1 DNA in Cells Infected at the NPT.

A HSV-1 DNA packaging assay was utilised to examine the level of viral DNA packaged by the *ts* mutants in cells infected at the NPT. To overcome the early defect exhibited by *ts1249* in cells infected at the NPT, the cells were adsorbed at the PT of 36°C for 2 hours. This was done in the presence of cycloheximide to prevent viral polypeptide synthesis which may have resulted in the production of low levels of functional UL25 protein and to synchronise mutant, wt virus and marker rescuant infections. At 0 and 24 hours pi samples representing total and packaged HSV-1 DNA were prepared and digested with *Bam*HI prior to electrophoresis through an agarose gel. The electrophoresed DNA was transferred to Hybond-XL membrane and hybridised to ³²P-dGTP labelled HSV-1 Bam g fragment. The membrane was exposed to a phosphorimager screen to obtain the image shown by Figure 3.45. The data were quantified and the approximate level of DNA packaged by each virus in cells infected at the NPT was calculated. Table 3.5 demonstrates that *ts1249* packaged 1.2% of replicated HSV-1 genomic DNA in cells infected at the NPT compared to 25.9% of the marker rescuant virus DNA. This was consistent with the observation that few DNA-containing capsids were observed in the nuclei of cells infected with *ts1249* at the NPT (Figure 3.44b). *Ts*⁺1208MR packaged 11.4% of replicated HSV-1 genomic DNA in cells infected at the NPT. The lower level of DNA packaged by *ts*⁺1208MR compared to *ts*⁺1249MR in cells infected at the NPT provided evidence that at a higher NPT of 39.5°C wt virus capsids package DNA less efficiently than at lower temperatures and explains why fewer DNA-containing capsids were seen in the nucleus of cells infected at 39.5°C than at 39.2°C (Figure 3.44). *Ts1208* only packaged 0.45% of

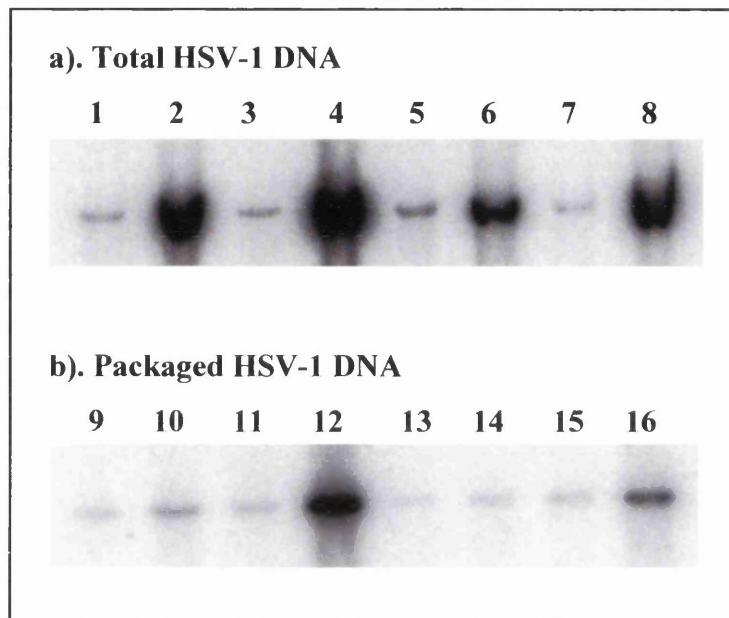


Figure 3.45 Both *Ts1249* and *Ts1208* Package a Low level of HSV-1 DNA in Cells Infected at the NPT.

Vero cells, infected with *ts1249* or *ts⁺1249MR* virus at a moi of 10 pfu.cell⁻¹, were incubated for two hours at 36°C in the presence of 100 µg.ml⁻¹ cycloheximide. After virus adsorption, the cycloheximide was washed out and the virus-infected cells were incubated at the NPT of 39.2°C. Vero cells were infected with *ts1208* or *ts⁺1208MR* virus at a moi of 10 pfu.cell⁻¹ at 39.5°C, virus was adsorbed for 1 hour and incubation continued at this temperature. The cells were harvested at 0 and 24 hours pi and samples representing total DNA and DNase resistant DNA (packaged DNA) were prepared. DNA samples were digested with *Bam*H1 and the fragments were resolved by electrophoresis through a 0.8% TBE-agarose gel. The DNA was transferred to Hybond-XL membrane and probed with ³²P-dGTP labelled HSV-1 Bam g fragment, using Southern hybridisation. **Lanes 1, 9, *ts1249* 0 hours pi. Lanes 2, 10, *ts1249* 24 hours pi. Lanes 3, 11, *ts⁺1249MR* 0 hours pi. Lanes 4, 12, *ts⁺1249MR* 24 hours pi. Lanes 5, 13, *ts1208* 0 hours pi. Lanes 6, 14, *ts1208* 24 hours pi. Lanes 7, 15, *ts⁺1208MR* 0 hours pi. Lanes 8, 16, *ts⁺1208MR* 24 hours pi.**

Virus	<i>Ts</i>1249	<i>Ts</i>⁺1249MR	<i>Ts</i>1208	<i>Ts</i>⁺1208MR
DNA Packaged at NPT.	1.2 %	25.9 %	0.45 %	11.4 %

Table 3.5 The Level of DNA Packaged by *Ts*1249, *Ts*1208 and Marker Rescued Viruses in Cells Infected at the NPT.

The data illustrated in Figure 3.45 were quantified using the Quantity One software package (BIO-RAD). The level of HSV-1 DNA packaged by each virus is expressed as a percentage of the total HSV-1 DNA synthesised by that virus at the NPT.

replicated HSV-1 genomic DNA in cells infected at the NPT and accounted for the low level of DNA-containing capsids observed in the nuclei of cells infected with this virus at the NPT (Figure 3.44d). The DNA packaging process of *ts1208* in cells infected at the NPT was not only compromised by the *ts* mutation in the UL25 protein but also by the constraint imposed by the higher NPT. It is therefore likely that both *ts* mutant viruses have a similar DNA packaging defect in cells infected at the NPT.

3.5.8 The Ability of *Ts1249* and *Ts1208* to Package Amplicon DNA in Cells Infected at the NPT.

An amplicon packaging assay was utilised to examine whether the *ts* mutants could package plasmid DNA. Vero cells were transfected with pSA1, an HSV-1 amplicon containing a packaging signal (the 200 bp HSV-1 u_c -DR1- u_b fragment) and an origin of replication (539 bp of HSV-1 Ori_s) in a pAT153 background. The cells were superinfected with virus at the NPT and at 21 hours pi samples representing total and packaged amplicon DNA were prepared and digested with *Eco*RI and *Dpn*I. The pSA1 amplicon contains *Dpn*I recognition sites which, when methylated, are resistant to cleavage by this enzyme. The transfected pSA1 amplicon is unmethylated as a result of propagation in bacteria deficient in the methylation process and viral replication of the HSV-1 amplicon within the mammalian host cell leads to the methylation of the *Dpn*I sites. Therefore, digestion with *Dpn*I serves to eliminate amplicon DNA that originated from the transfection event leaving only HSV-1 replicated amplicon DNA. The digested DNA samples were resolved by electrophoresis through a agarose gel, transferred to Hybond-XL membrane and probed with ³²P-dGTP labelled pAT153 using Southern blot hybridisation. The membrane was exposed to a phosphorimager screen to obtain the image shown by Figure 3.46. In contrast to the UL28 null mutant virus (gCB) which failed to package any amplicon DNA, both *ts1249* and *ts1208* packaged amplicon DNA although not as efficiently as wt- or marker rescue viruses.

3.5.9 Discussion.

Sequence analysis demonstrated that the defect responsible for the failure of *ts1204* and *ts1249* to synthesise viral polypeptides in cells infected at the NPT resulted from a single base pair change in the UL25 gene leading to the substitution of glutamic acid residue 133 with a lysine. Early indications suggested that *ts1204* was defective in host cell penetration and assembly of functional capsids. However, an immunofluorescence assay demonstrated

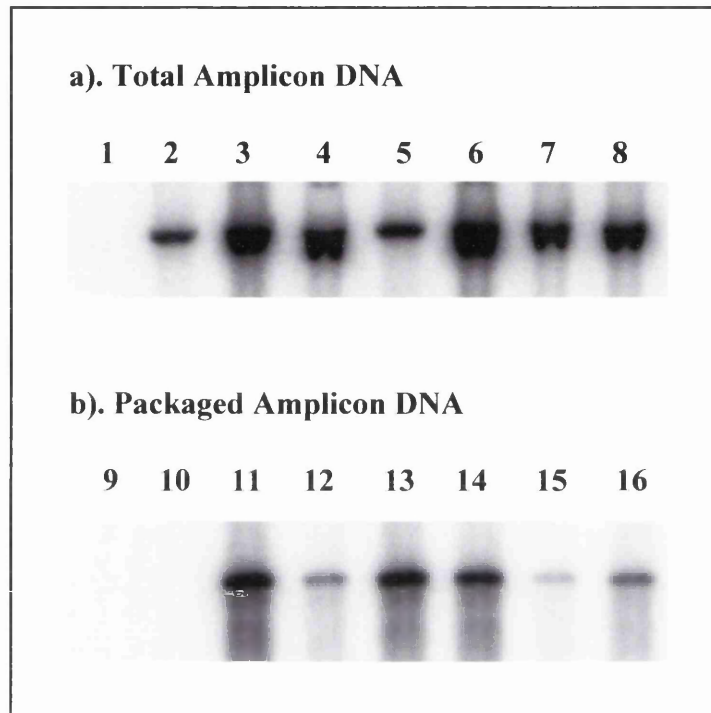


Figure 3.46 Both *Ts1249* and *Ts1208* Package Amplicon DNA in Cells Infected at the NPT.

Vero cells were transfected with pSA1 plasmid. At 12 hours post-transfection the cells were adsorbed with wt virus, *ts1249* or *ts⁺1249MR* at a moi of 10 pfu.cell⁻¹ for two hours at 36°C in the presence of 100 µg.ml⁻¹ cycloheximide. After adsorption, the cycloheximide was washed out and the virus-infected cells were incubated at the NPT of 39.2°C. Cells were infected with *ts1208*, *ts⁺1208MR*, gCB or wt virus at a moi of 10 pfu.cell⁻¹ at 39.5°C, virus adsorbed for 1 hour and incubated at the NPT of 39.5°C. At 21 hours pi the cells were harvested and samples representing total DNA and DNase resistant DNA (packaged DNA) were prepared, digested with *EcoR1* and *DpnI*, and the fragments were resolved by electrophoresis through a 0.8% TBE-agarose gel. The DNA was transferred to Hybond-XL membrane and probed with ³²P-dGTP labelled pAT153 using Southern hybridisation. **Lanes 1, 9**, pSA1 alone. **Lanes 2, 10**, pSA1 and gCB. **Lanes 3, 11**, pSA1 and wt virus. **Lanes 4, 12**, pSA1 and *ts1249*. **Lanes 5, 13**, pSA1 and *ts⁺1249MR*. **Lanes 6, 14**, pSA1 and wt virus. **Lanes 7, 15**, pSA1 and *ts1208*. **Lanes 8, 16**, pSA1 and *ts⁺1208MR*.

that *ts1249* was in fact able to penetrate cells and that *ts1249* capsids were transported to the nuclear periphery in a manner indistinguishable from *ts⁺1249MR* capsids. These results suggested that *ts1249* was defective in a process subsequent to capsid transport to the nuclear periphery, probably in the uncoating of the viral DNA at the nucleus. Electron microscopic analysis demonstrated that a two hour incubation at the PT prior to incubation at the NPT was sufficient reverse the early defect and allow capsid assembly to take place. However, a HSV-1 DNA packaging assay revealed that the level of HSV-1 DNA packaged was reduced in cells infected with *ts1249* at the NPT. This was consistent with the low-level of DNA-containing capsids observed in the nuclei of cells infected with *ts1249* at the NPT. Therefore, in addition to the early defect, the *ts* lesion in the UL25 gene also appeared to affect the DNA packaging process. The precise role of UL25 in the HSV-1 life cycle is not known but UL25 has been proposed to function in retaining the newly packaged viral DNA within the capsid (McNab *et al.*, 1998). The process of uncoating the viral DNA is poorly understood but it possible that proteins involved in the retention of packaged DNA may also be involved in the release of DNA from the capsid. The evidence indicated that the early defect exhibited by *ts1249* may be in the uncoating of the viral DNA at the nucleus. If at the NPT the *ts* lesion within the UL25 gene induces an altered conformation of the protein it is possible that this would result in the inability of UL25 to facilitate the release of the viral DNA from the capsid. This study has therefore provided the first piece of evidence illustrating the involvement of an HSV-1 DNA packaging protein in an early phase of the virus life cycle.

Ts1208 had an in-frame deletion of three base pairs in the coding sequences of UL25 resulting in the loss of valine 161. Earlier studies indicated that *ts1208* was defective in the assembly of functional capsids in cells infected at the NPT. In contrast to *ts1249*, *ts1208* synthesised similar levels of viral polypeptides in cells infected at the NPT compared to cells infected with wt virus or *ts⁺1208MR* at the NPT and electron microscopic analysis demonstrated that *ts1208* assembled capsids in cells infected at the NPT. However, a HSV-1 DNA packaging assay demonstrated that the level of HSV-1 DNA packaged was reduced in cells infected with *ts1208* at the NPT in comparison to *ts⁺1208MR*-infected cells under identical conditions. This was consistent with the low-level of DNA-containing capsids observed in the nuclei of cells infected with *ts1208* at the NPT. These results suggested that the *ts* lesion in the UL25 gene of *ts1208* affected the DNA packaging process.

Both *ts1249* and *ts1208* packaged a reduced amount of amplicon DNA in cells infected at the NPT compared to wt- and marker rescue virus whereas a UL28 null mutant virus did

not package any detectable level of amplicon DNA. Since the UL28 protein is a component of the putative terminase complex it is likely that the UL28 null mutant virus could not process the replicated concatameric amplicon DNA into unit length molecules necessary for packaging into the viral capsid. The ability of both *ts1249* and *ts1208* to package a reduced amount of amplicon DNA in cells infected at the NPT suggested that the UL25 protein functions in a later stage of the DNA packaging process. Additionally, the *ts* mutant viruses appeared to package amplicon DNA more efficiently than HSV-1 DNA in cells infected at the NPT. The reason for this is unknown but it is possible that the smaller amplicon DNA (4.4 Kb) is retained more efficiently than the considerably larger HSV-1 genomic DNA (152 Kb) in capsids containing the mutated form of the UL25 protein and in this respect supported the idea that the UL25 protein is involved in stabilisation/retention of packaged HSV-1 DNA (McNab *et al.*, 1998).

CHAPTER 4

GENERAL DISCUSSION

4.1 The UL25 Protein.

During the initial stages of the project, various recombinant protein expression systems were investigated with a view to obtaining large amounts of soluble UL25 protein in an easily purifiable form. Recombinant UL25 protein was expressed in *E. coli* as MBP- and thioredoxin-fusion proteins and polyhistidine-tagged UL25 was also expressed in *E. coli* as well as in recombinant baculovirus-infected *Sf21* cells. Thioredoxin-UL25 and His-UL25 proteins produced in *E. coli* were almost completely insoluble and modification of the expression conditions, for example, reducing the temperature and altering the IPTG levels, did not increase the solubility of these proteins. The insoluble nature of these proteins was probably a result of the formation of inclusion bodies, consisting of insoluble aggregates of recombinant protein within the bacterial cell. In contrast to His-UL25 protein produced in bacteria, the majority of His-UL25 protein expressed in recombinant baculovirus-infected *Sf21* cells was soluble and this may have been due to more optimal translation conditions within the eukaryotic insect cell. A significant proportion of MBP-UL25 protein synthesised in bacteria was soluble and this may have been due to the MBP-fusion partner which has been reported to increase the solubility of recombinant proteins in *E. coli* (Maina *et al.*, 1998). Despite the extensive optimisation of the His-Tag Purification Procedure (Novagen), purified His-UL25 protein precipitated out of solution at concentrations far below that required for many of the procedures involved in the biochemical analysis of proteins. Therefore, in order to gain an insight into the secondary structure of the UL25 protein, several online bioinformatic software tools were utilised. These analyses demonstrated that a putative coiled-coil region was located within the N-terminal 120 amino acids of the HSV-1 UL25 protein which was conserved in homologues from alpha- beta- and gammaherpesviruses. The N-terminal portion of the UL25 protein is thought to bind HSV-1 DNA and may also be capable of homo-oligomerisation (Ogasawara *et al.*, 2001). Since coiled-coil structures have been shown to mediate these types of interactions, it is possible that the predicted coiled-coil region of the UL25 protein is also involved in these functions (Akhmedov *et al.*, 1999, Krammerer *et al.*, 1999, Procopio *et al.*, 1999). The areas of high sequence conservation identified within the UL25 protein could be analysed using site-directed mutagenesis which may help to determine the functional relevance of these regions. This approach could also be used to examine whether the presence of the putative coiled-coil structure is necessary for the proposed functions of the UL25 protein such as capsid association, DNA binding and genome packaging.

Purification of the UL25 protein to a sufficient concentration and purity would allow the biochemical characterisation of the protein and could provide accurate data concerning the secondary structure of the protein. Providing UL25 could be purified to the concentration and purity required to produce pure crystals of the protein, X-ray crystallographic analysis would generate a detailed three-dimensional structure of the protein. Alternatively, the three-dimensional structure of purified UL25 protein fragments could be obtained using NMR imaging. This technique has the advantage of being able to analyse the structure of a protein whilst in solution and does not rely on the often complicated and lengthy procedure of obtaining protein crystals. However, structural motifs generated by the interaction of two or more distant regions of the protein (such as discontinuous epitopes) will not form if the amino acid residues involved are located within different fragments. Additionally, it is also possible that the protein fragments may not fold correctly to generate a tertiary structure identical to that of the full-length protein.

4.2 Interactions Between UL25 and the HSV-1 Capsid Proteins.

In 2001, Ogasawara *et al.* presented several lines of evidence which indicated that the HSV-1 UL25 protein interacted with both the HSV-1 VP19C and VP5 capsid proteins. An interaction between UL25 and VP19C/VP5 would be consistent with several of the observed biological characteristics of the UL25 protein. Firstly, since VP19C contains a nuclear-localisation signal, the association of UL25 with VP19C in the cytoplasm of HSV-1-infected cells would result in the transport of the UL25 protein to the nucleus, in keeping with the observed nuclear localisation of the UL25 protein during wt virus-infection. Secondly, an interaction between UL25 and VP19C or VP5 would presumably facilitate the binding of the UL25 protein to the capsid. In the first set of experiments performed by Ogasawara *et al.* (2001) the UL25 protein was immobilised on a PVDF sheet and incubated with a sample of HSV-1 virions which had been solubilised with 8 M urea. The virus proteins were renatured by stepwise dialysis and the PVDF sheet was washed to remove unbound proteins. Virion proteins that remained attached to the PVDF sheet, presumably through an interaction with the UL25 protein, were eluted with a buffer containing SDS, resolved by SDS-PAGE and transferred to a nitrocellulose membrane. These proteins were visualised on the membrane using Ponceau S stain which revealed the presence of six proteins of 150, 120, 80, 52, 34 and <34 kDa. The stained protein bands were excised and digested with trypsin and the resulting peptides were purified by reverse-phase high-pressure liquid chromatography and subjected to amino-terminal sequencing.

The 150 and 34 kDa proteins were identified as VP5 and VP23 respectively. At this stage the identity of the 52 kDa protein was not known but the results of subsequent experiments suggested it was probably VP19C (see below). The identities of the remaining proteins were unknown although the 80 kDa protein was thought to be a component of the tegument (see below). It is possible that during the renaturation of the capsid proteins, partial or entire capsid structures were assembled as the proteins refolded to their native conformation. Ogasawara *et al.* (2001) believed that the apparent interaction between UL25 and VP23 was not specific and was mediated through an interaction with the VP19C component of re-assembled triplex complexes.

In the next set of experiments, Ogasawara *et al.* (2001) used far-Western blot analysis to demonstrate that the UL25 protein interacted with both the VP5 and VP19C proteins. Samples of purified B capsids were resolved by SDS-PAGE and capsid proteins were transferred to a PVDF membrane. The membrane was washed with Tris-buffered saline to renature the capsid proteins which were then probed with biotin-labelled UL25. The UL25 protein appeared to interact with capsid proteins of 150 and 52 kDa which, based upon their size, were believed to be VP5 and VP19C respectively. To examine the interaction of UL25 with envelope and tegument components, detergent-treated virions were divided into envelope and capsid-tegument fractions by centrifugation. Samples of these fractions were analysed as before and in addition to VP5 and VP19C, the UL25 protein also appeared to interact with a tegument protein of 80 kDa. The major drawback in the experimental procedures described above were the lack of appropriate controls. Ogasawara *et al.* (2001) were unable to demonstrate that the denatured proteins immobilised on the membranes had folded back to their native conformation following procedures to renature them. It was therefore possible that the observed association between the UL25 and VP5 and VP19C proteins in the far-Western blot analysis did not represent a genuine interaction. If this group had demonstrated that the two triplex proteins interacted with each other in the far-Western blot experiments, this would have indicated that functional interactions were established under the experimental conditions used and would have provided additional evidence to support the observed interaction between UL25 and VP19C and VP5.

To determine that the UL25 and VP19C proteins interacted *in vivo*, Ogasawara *et al.* (2001) examined the intracellular localisation of these proteins in cells transiently expressing UL25 and/or VP19C. This group demonstrated that GFP-tagged UL25 protein localised primarily to the cytoplasm in cells expressing this protein alone. In cells that were cotransfected with plasmids encoding GFP-UL25 and unmodified VP19C proteins, a small

proportion of the GFP-UL25 protein appeared to localise to the nuclei. Ogasawara *et al.* (2001) concluded that GFP-UL25 formed a complex with VP19C in the cytoplasm of cotransfected cells which was transported to the nuclei by virtue of the nuclear localisation signal contained within the VP19C protein. However, the apparent interaction between GFP-UL25 and VP19C appeared far from conclusive since, in the presence of VP19C, the majority of GFP-UL25 still localised to the cytoplasm. The present study found that none of the major HSV-1 capsid proteins, either alone or in combination, had any effect on the intracellular localisation of the UL25 protein in transiently cotransfected cells. This was consistent with observations made by Kaelin *et al.* (2000) who claimed that the PRV VP23, VP5, VP22a and VP24 capsid proteins were unable to translocate the PRV UL25 homologue to the nuclei of transiently cotransfected cells. Additionally, Dr V. Preston has transiently expressed GFP-tagged UL25 protein in Vero cells and has found that, in the presence of the VP19C protein, GFP-UL25 did not appear to localise to the nuclei (unpublished observations).

The present study also examined the ability of the UL25 protein to interact with the triplex proteins using a chromatography assay (data not shown). Purified His-UL25 protein was bound to a nickel-agarose column prior to the addition of the triplex proteins. Since the VP19C protein interacts with the VP23 protein in the cytoplasm of HSV-1-infected cells, the VP23-VP19C protein complex applied to the His-UL25-bound column was a relatively accurate reflection of the status of the VP19C protein found in the cytoplasm of HSV-1-infected cells. The nickel-agarose resin was washed, and the His-UL25 protein was removed from the column using a buffer containing 1 M imidazole. The proteins contained within the column elute were resolved by SDS-PAGE, transferred to nitrocellulose membrane and probed with an antibody specific for the VP23 polypeptide to determine whether triplex complexes were specifically retained on the His-UL25 column. The level of VP23 protein in the elute from the His-UL25 column was not significantly higher than that from a column composed of nickel-agarose alone. This result suggested that under these conditions, the UL25 protein did not interact with the triplex proteins.

The present study found that the His-UL25 protein appeared to associate with herpesvirus capsids generated in the recombinant baculovirus system in the absence of other HSV-1 DNA cleavage and packaging proteins. This finding indicated that the capsid-binding properties of UL25 were mediated by an interaction with one or more of the capsid proteins listed in Table 1.2. The His-UL25 protein also appeared capable of binding to VP5/19C particles suggesting that the association of the UL25 protein with the HSV-1

capsid was facilitated through an interaction with VP5 and/or VP19C and, in this respect, supported the findings of Ogasawara *et al.* (2001). It was possible that the association of UL25 with VP5/19C particles was not specific and represented insoluble aggregates of UL25 that either co-purified with, or were trapped within the VP5/19C particles. To address this possibility, the HSV-1 UL9 ori binding protein was examined for the ability to interact with VP5/19C particles to determine whether a non-capsid associated HSV-1 protein could also bind to these capsid-like structures (data not shown). However, in *Sf21* cells coinfecting with a UL9-expressing recombinant baculovirus and one expressing the VP5 and VP19C proteins, the UL9 protein was not expressed and this was probably a consequence of preferential transcription of the UL19 and UL38 genes under these conditions. Thus, the apparent association of the UL25 protein with VP5/19C particles remains questionable.

Immunoprecipitation analysis of HSV-1-infected cells identified a protein of approximately 55 kDa that appeared to interact with UL25 and this protein was probably of viral origin. The 50 kDa VP19C protein represented an attractive candidate for the unknown UL25-interaction partner especially since data described in the present study suggested UL25 could interact with virus-like particles composed of only the VP5 and VP19C proteins. At the time the immunoprecipitation experiments described in the present study were carried out, there was a very limited supply of polyclonal antibody specific for VP19C. However, there now exists a ready supply of VP19C-specific monoclonal antibody (generated within the Institute of Virology) which could be used in a Western blot assay to determine whether the protein that interacted with UL25 in these experiments was VP19C.

In summary, the means by which the UL25 protein associates with capsids is not yet fully understood and until an interaction between UL25 and a capsid component is identified conclusively, the data indicating that this ability is mediated through an interaction with VP5 and/or VP19C must be interpreted cautiously. Provided the UL25 protein is specifically associated with HSV-1 recombinant capsids, the construction of UL25 gene truncations may help to identify the region(s) of the protein responsible for capsid-association using the recombinant baculovirus capsid assembly system. However, this type of analysis would provide no further information regarding the protein-protein interactions which facilitate this association.

4.3 The Copy Number and Location of the UL25 Protein in HSV-1 Capsids.

The copy number of UL25 per HSV-1 B capsid was estimated to be approximately 40 and this number was consistent with the published figure of 42 ± 17 (Ogasawara *et al.*, 2001). A copy number of 40 immediately indicated that, at least in B capsids, the UL25 protein was unlikely to be located at a unique position. However, it is known that different levels of UL25 protein are found associated with different capsid types; the lowest amount is found in procapsids and the highest is found in C capsids (Sheaffer *et al.*, 2001). Since there is approximately four to sixfold less UL25 protein present in procapsids than in HSV-1 B capsids, it is possible that UL25 is found at one position prior to DNA packaging and that additional copies of UL25 bind to the capsid at different sites following DNA encapsidation to seal/stabilise the packaged genome. Alternatively, the low levels of UL25 protein associated with procapsids examined by Sheaffer *et al.* (2001) may have resulted from a non-specific interaction between UL25 and this capsid type. Therefore, it is possible that the UL25 protein may only associate with the capsid during, or after capsid maturation. It is important to note that the association of UL25 with the capsid is not solely dependent on the DNA packaging process since UL25 is also present within B capsids, albeit in reduced amounts compared to C capsids. The amount of UL25 protein associated with recombinant capsids was similar to the level found in HSV-1 C capsids and it has been suggested that the scaffold structure may regulate the amount of UL25 protein that is able to bind to capsids (Sheaffer *et al.*, 2000). The presence of a scaffold structure within the capsid may serve to prevent the premature association of UL25 protein. The loss of the scaffold structure during DNA packaging could therefore facilitate the binding of UL25 protein to the capsid to ensure that the DNA is packaged efficiently. Accordingly, the elevated levels of UL25 protein found associated with recombinant capsids may have resulted from the reduced level of scaffold present in many of these capsids.

An accurate quantitation of the copy number of the HSV-1 DNA cleavage and packaging proteins within the different capsid types needs to be performed. This could be done by comparing the amount of specific protein within a known number of capsids to standardised amounts of the same protein as determined by amino acid hydrolysis. The analysis could be controlled using the same procedure with one of the capsid proteins for which the copy number is already known. The protein samples used for amino acid hydrolysis must contain protein purified to homogeneity and His-UL25 protein isolated according to the method outlined in section 2.3.0.2 would require additional purification prior to this type of analysis. The UL6 protein is present in approximately equal amounts in

all capsid types, including procapsids and the putative HSV-1 terminase, UL15, is also believed to bind to the UL6 protein (Dr C. White, MRC Institute of Virology, unpublished observations). Thus, this protein represents a potential candidate for a HSV-1 encoded portal protein analogous to that of the ds DNA bacteriophages. Using densitometric analysis to determine the relative amounts of capsid proteins contained within a sample of B capsids resolved by SDS-PAGE and visualised by Coomassie blue staining, Ogasawara *et al.* (2001) indicated that the UL6 protein was present in 44 ± 13 copies per B capsid. This finding strongly suggested that UL6 was not located at a unique position within the HSV-1 capsid and implied that there may be several sites within the capsid available for DNA packaging. Presumably, only one of these potential DNA encapsidation sites is utilised per packaging reaction. According to this model, the DNA packaging machinery must be able to discriminate against capsids that are undergoing DNA encapsidation in order to prevent multiple packaging reactions occurring on the same capsid. Following the initiation of DNA packaging, it is possible that the UL25 protein binds to DNA encapsidation sites that are not in use to ensure that only one DNA packaging reaction occurs per capsid. The very low level of HSV-1 DNA encapsidated in cells infected with *ts1249* at the NPT may have therefore resulted from the inability of this virus to stop DNA packaging commencing at additional sites on the capsid. This model predicts that shorter than unit-length genomes would be found within capsids located in the nuclei of cells infected with a UL25 null mutant virus and this is consistent with observations made by Dr N. Stow following his re-examination of KUL25NS (manuscript submitted for publication).

Indirect immunofluorescent analysis of incoming capsids during the very early stages of HSV-1 infection indicated that at least a part of the UL25 protein was located on the capsid exterior. This result was consistent with data presented by Kaelin *et al.* (2000) who demonstrated that at least a portion of the PRV UL25 homologue was present on infecting PRV capsids. This group went on to show that the PRV UL25 homologue specifically bound the microtubule element of the cellular cytoskeleton. On the basis of these findings, Kaelin *et al.* (2000) concluded that the PRV UL25 homologue was involved in the intracellular transport of infecting capsids. The present study also found that at least some of the HSV-1 UL25 protein localised to the cellular cytoskeleton of transiently transfected cells although the functional significance of this interaction is unknown. It is possible that the UL25 protein functions in the intracellular transport of capsids and the apparent location of at least a portion of the protein on the capsid exterior would place it in an ideal position to influence this process. However, it should be noted that in cells infected at the

NPT, incoming *ts1249* capsids were not impaired in transport to the nucleus. Presumably, it would be easier for additional copies of UL25 protein to bind to the capsid following DNA packaging if the protein was located on the capsid exterior. However, since the scaffolding protein is extruded from the procapsid before, or during the DNA packaging process, there obviously exists a mechanism whereby protein molecules can traverse the procapsid shell prior to capsid maturation. It is therefore possible that the majority of the UL25 protein is located within the capsid shell with only a small proportion of the protein found on the capsid exterior. The only antibody available which bound to UL25 in this context was a rabbit polyclonal antibody raised against denatured GST-UL25 fusion protein. The UL25-specific mouse monoclonal and polyclonal antibodies raised against soluble His-UL25 failed to react with infecting HSV-1 capsids. The ability of the UL25-specific rabbit polyclonal antibody to bind to the region of the UL25 protein on the capsid exterior may have therefore resulted from a rabbit-specific immune response and/or the form by which the antigen was presented to the animal. Alternatively, it was possible that the UL25-specific monoclonal antibodies only recognised a limited portion of the UL25 protein and that this part of the protein was not located on the capsid surface.

Recombinant capsid-associated UL25 protein was found to be resistant to 2 M GuHCl extraction whereas HSV-1 B capsid-associated UL25 was not. Since 2 M GuHCl treatment has been reported to remove the VP26 decorating protein, the pentons, peripentonal triplexes and scaffolding proteins from HSV-1 capsids (Newcomb & Brown, 1991), it is possible that the UL25 protein interacted, at least partly, with one or more of these capsid elements of HSV-1 B capsids but not recombinant capsids. With an estimated copy number of 40, the UL25 protein could potentially interact with every penton of the capsid. Alternatively, if the UL25 protein associates with either the triplex and/or the hexon elements of the HSV-1 capsid, a copy number of 40 indicated that UL25 may only be capable of interacting with a subset of these capsid components. Using immunogold labelling techniques to identify the location of HSV-1 B capsid-bound anti-UL25 antibodies, Ogasawara *et al.* (2001) presented data which indicated that the UL25 protein associated with the penton component of this capsid type. However, these data were far from conclusive and suffered from the lack of appropriate controls such as capsids assembled in the absence of UL25. This study and the present study also found that the majority of UL25 protein was removed from HSV-1 B capsids following 2 M GuHCl treatment and these observations supported the idea that the UL25 protein may, at least in part, associate with the pentons and/or peripentonal triplexes of these capsids.

Cryoelectron microscopy and three-dimensional image reconstruction have been used to examine HSV-1 capsids at a resolution of 8.5 Å (Zhou *et al.*, 1998). Although this process has been used to examine the molecular structure of the HSV-1 capsid in great detail, it suffers from one major drawback: This technique employs icosahedral averaging to obtain the final structure of the HSV-1 capsid and as a result, capsid-associated structures that do not exhibit icosahedral symmetry are not resolved. The HSV-1 DNA cleavage and packaging proteins have not been detected in capsids using this technique and this is probably because they are either asymmetrically ordered and/or present at very low copy numbers within the capsid. The present study found that capsids generated using the recombinant baculovirus system contained elevated levels of UL25 protein. These capsids were analysed using cryoelectron microscopy and three-dimensional image reconstruction to a resolution of approximately 30 Å to determine whether the UL25 protein was icosahedrally ordered (data not shown). However, the results from preliminary experiments indicated that the UL25 protein could not be located in capsids examined under these conditions and this may have been because either the resolution was too low or the UL25 protein was not symmetrically arranged within the capsid.

4.4 The Factors Required to Localise the UL25 Protein to the Nucleus During Wt Virus-Infection.

The nuclear localisation of the UL25 protein during wt HSV-1 infection was not dependent on capsid assembly nor was it dependent on the presence of the VP5 or VP23 proteins. These findings suggested that UL25 might be transported to the nuclei of wt virus-infected cells by virtue of an interaction with one or more viral-encoded proteins other than VP5 and VP23. To determine whether the absence of VP19C protein affected the distribution of UL25 protein in virus-infected cells, the intracellular localisation of UL25 was examined in cells infected with a UL38 null mutant (Person & Desai, 1998). Preliminary experiments revealed that this mutant appeared to have an early replication defect in non-complementing cells since it synthesised reduced levels of UL25 and the capsid proteins in comparison to wt virus (data not shown). It is therefore likely that this virus contained at least one additional mutation. The low level of UL25 protein synthesised in non-complementing cells infected with this virus made it difficult to conclusively identify the intracellular location of this protein under these conditions. In an attempt to overcome this problem, UL38 null mutant virus-infected Vero cells were incubated for up to 24 hours pi to allow higher levels of the UL25 protein to accumulate within the cell.

However, high levels of cpe were observed in mutant-infected cells following extended periods of incubation. The cpe was characterised by the rounding of virus-infected cells and it became virtually impossible to distinguish the cytoplasm from the nuclei in these cells. Therefore, no additional information concerning the factors required for the nuclear localisation of the UL25 protein in wt virus-infected cells was gained from these experiments. Since UL25 is a capsid-associated protein (Ali *et al.*, 1996, McNab *et al.*, 1998), the HSV-1 major capsid proteins were examined for their ability to translocate the UL25 protein to the nuclei of transiently cotransfected cells. As mentioned previously, Ogasawara *et al.* (2001) presented evidence which suggested that the VP19C protein was capable of directing the UL25 protein to the nuclei of cells expressing these two proteins. Using a similar assay, the present study found no evidence to suggest that any of the HSV-1 capsid proteins could relocate the UL25 protein to the nuclei of transiently transfected cells. It is possible that the UL25 protein localised to the nuclei of HSV-1-infected cells through a different network of interactions from that used by the capsid proteins (as illustrated by Figure 1.11). The HSV-1 tegument-associated protein, UL14, is able to translocate the VP26 minor capsid protein to the nuclei of transiently cotransfected cells and represents an additional pathway through which a capsid protein is transported to the nucleus (Yamauchi *et al.*, 2001). Since UL14 has no effect on the intracellular distribution of the UL25 protein (Yamauchi *et al.*, 2001), a different pathway is presumably involved in the transport of UL25 protein to the nuclei of HSV-1 infected cells. It is evident that at least some of the HSV-1 capsid-associated DNA cleavage and packaging proteins are not dependent on the capsid proteins for their localisation to the nuclei of virus-infected cells. The UL28 protein is only directed to the nuclei following a functional interaction with the UL15 protein in the cytoplasm of cells expressing these two proteins (Koslowski *et al.*, 1999, Abbotts *et al.*, 2000). Since the UL25 protein is found associated with B capsids assembled in cells infected with mutants of HSV-1 that lack the UL6, UL15 or UL28 genes, it seems likely that UL25 does not require these proteins to either localise to the nucleus, or to interact with capsids (Yu & Weller, 1998). In summary, the protein-protein interactions responsible for the nuclear localisation of the UL25 protein during HSV-1-infection have yet to be identified and until a genuine UL38 null mutant virus is constructed, it is not possible to exclude the VP19C protein.

The cause of the altered intracellular distribution of UL25 protein in cells infected with HSV-1 A44 at the NPT is unknown but this phenotype may be linked to formation of syncytia. The intracellular localisation of the UL25 protein in cells infected with HSV-1

A44 at the NPT was similar to that observed for tegument proteins such as UL34, which also localise to the perinuclear region of HSV-1-infected cells (Roller *et al.*, 2000, Ye *et al.*, 2000, Reynolds *et al.*, 2001). It is possible that, in wt HSV-1-infected cells, the UL25 protein may act as an anchor for the attachment of tegument proteins to the capsid, and this hypothesis is supported by two lines of evidence. Firstly, as mentioned previously, Ogasawara *et al.* (2001) claimed that the UL25 protein interacted with an unidentified tegument protein of approximately 80 kDa in size. Secondly, data presented by both the present study and by Kaelin *et al.* (2000), suggested that at least a portion of the UL25 protein was located on the capsid exterior. The UL25 protein may have been retained to the perinuclear region of cells infected with HSV-1 A44 at the NPT through an aberrant interaction with a tegument protein which resulted in the transport of decreased amounts of UL25 protein to the cell nuclei. Alternatively, since syn strains of HSV-1 are often more cell-associated and release fewer virions from infected cells than syn⁺ strains, it is possible that the perinuclear distribution of the UL25 protein in cells infected with HSV-1 A44 at the NPT reflected an accumulation of outgoing virus capsids. Indirect immunofluorescent analysis of HSV-1 A44-infected cells was carried out using UL25-specific monoclonal antibody 166 which did not appear to recognise incoming viral capsids during the early stages of HSV-1-infection. However, this finding does not necessarily indicate that this antibody did not bind to outgoing capsids. Since this study presented evidence which indicated that UL25 may be involved in the viral uncoating process, it is possible that the epitope on the UL25 protein, to which monoclonal antibody 166 binds, is masked through either a conformational change in the UL25 protein or an alteration in the nature of the protein-protein interactions involving UL25 during capsid transport to the nuclei of virus-infected cells. This study cannot rule out the possibility that a *ts* lesion was located within the UL25 gene of HSV-1 A44 which affected the ability of this protein to be directed to the nucleus at the elevated temperature and/or any potential interaction between UL25 and a component of the tegument. To investigate this possibility further, the UL25 gene could be cloned from HSV-1 A44 and inserted into a HSV-1 *ts*⁺ 17 syn⁺ background. If the UL25 protein exhibited a similar phenotype in cells infected with this virus at the NPT, this would suggest that there was a *ts* lesion within the UL25 gene of HSV-1 A44.

4.5 Other Interactions Involving the UL25 Protein.

As mentioned previously, Ogasawara *et al.* (2001) presented evidence which suggested that the UL25 protein interacted with an 80 kDa tegument protein. The product of the

UL46 gene, a 78 kDa protein termed VP11/12, is a tegument phosphoprotein reported to modulate the activity of the VP16 α -transinducing factor, and based upon its size, represents a potential candidate for the 80 kDa tegument protein which Ogasawara *et al.* (2001) claimed to interact with the UL25 protein. It is possible that the VP11/12 protein is anchored within the maturing virion through an interaction with the UL25 protein, although there is no additional evidence to support this hypothesis. The present study identified an unknown protein of approximately 55 kDa which appeared to interact specifically with the UL25 protein in an immunoprecipitation assay (Figure 3.39). The HSV-1 UL21 protein is a component of the capsid/tegument and is dispensable for HSV-1 replication in cultured cells (Baines *et al.*, 1994). This protein has a predicted molecular weight of approximately 57 kDa and the PRV UL21 homologue is a capsid protein that has been implicated in the DNA cleavage and packaging process of this virus (de Wind *et al.*, 1992, Wagenaar *et al.*, 2001). This protein therefore represents an attractive candidate for the unidentified protein of approximately 55 kDa that interacted with UL25 in the immunoprecipitation assay shown in Figure 3.39. However, the UL21 protein appears to be extensively modified post-translationally in HSV-1-infected cells and Western-blot analysis of purified HSV-1 virions revealed that UL21 is actually between 62-64 kDa in size (Baines *et al.*, 1994). Nevertheless, it is still necessary to investigate whether or not the unknown protein is UL21.

Ogasawara *et al.* (2001) presented evidence which suggested that the UL25 protein was capable of binding HSV-1 DNA. This observation was particularly relevant to the proposed function of the UL25 protein. It seems logical that a protein which has been implicated in sealing the packaged genome within the capsid could fulfil this function through a direct interaction with the DNA to effectively anchor the genome within the capsid. Ogasawara *et al.* (2001) prepared samples containing purified His-UL25 with and without HSV-1 or baculovirus DNA. The samples were incubated overnight at 4°C to allow any potential protein-DNA interactions to form and electrophoresed through an agarose gel. Separated, full-length genomic DNA, or a corresponding region of the gel if the sample lacked DNA, was extracted and analysed for the presence of UL25 by immunoblotting. Under these conditions, the His-UL25 protein appeared to bind HSV-1 DNA. The His-UL25 protein did not bind to baculovirus DNA in these assays and this finding suggested that UL25 bound to HSV-1 DNA in a sequence-specific manner. However, since this group used full-length HSV-1 genomic DNA, no conclusion could be

formed regarding the specific sequences to which the UL25 protein recognised. The most obvious candidate sequence for recognition by the UL25 protein is the *a* sequence since this sequence provides the *cis*-acting signals necessary for cleavage and packaging of the genome and clearly these experiments need to be repeated using this sequence as a probe. The ability of the UL25 protein to bind to the HSV-1 *a* sequence was investigated by the present study using an electrophoretic mobility shift assay. This experiment was compromised by the necessity to perform the DNA-binding reaction in low-salt conditions. Purified His-UL25 protein was maintained in a buffer containing 1 M NaCl and the protein precipitated out of solution under the low-salt DNA-binding reaction conditions.

4.6 The Further Characterisation of *Ts1249* and *Ts1208*.

Through the use of an indirect immunofluorescence assay which detected incoming capsids very early in the infection process, this study established that the early defect exhibited by *ts1249* was not in the cellular penetration process. Since incoming *ts1249* capsids did not appear impaired in transport from the plasma membrane to the nuclear membrane, it seemed likely that this virus was defective in uncoating the viral genome at the nuclear pore. It is not known precisely how the viral DNA is uncoated but this event does not require *de novo* RNA or protein synthesis indicating cellular and/or virion polypeptides are required for this process (Hochberg & Becker, 1969). The binding of capsids to nuclear pore complexes (NPCs) and subsequent uncoating of the viral genome has been reconstituted in an *in vitro* system described by Ojala *et al.* (2000). They demonstrated that the presence of tegument proteins such as VP1-3, VP13/14, VP16 and VP22 were essential for capsid-NPC binding. Additionally, importin β and Ran, two cellular protein components of the nuclear import machinery, were found to be involved in the binding of capsids to NPCs and this process was independent on the presence of metabolic energy. However, ATP was required for the NPC-bound capsids to release their genomes. No uncoating was observed in the absence of NPC-binding which suggested that this event triggered a conformational change within the capsid that facilitated the release of the viral genome.

The early defect exhibited by *ts1249* appeared identical to the phenotype exhibited by another HSV-1 *ts* mutant, *tsB7*, in cells infected at the NPT (Batterson *et al.*, 1983). This virus contained a *ts* lesion within the UL36 gene which encodes the tegument protein VP1-3 and in cells infected at the NPT, *tsB7* virions were able to bind to the NPC but failed to

release their DNA. VP1-3 is a large protein (270 kDa) which is present in the virion in approximately 12 copies (McNabb & Courtney, 1992). This protein is also believed to constitute part of the tegument material observed around the pentons of isolated capsids (Zhou *et al.*, 1999). Since the viral DNA is thought to exit the capsid through the penton channel (Newcomb & Brown, 1994), it is possible that VP1-3 interacts with components of the NPC to initiate the change that allows DNA to exit from the capsid. Exactly how the UL25 protein is able to influence this process is not known but several possibilities exist. Firstly, since additional copies of UL25 are thought to bind to the capsid following scaffold disassembly and DNA packaging, it is possible that UL25 must be removed from the capsid prior to release of the genome. In cells infected with *ts1249* at the NPT the *ts* lesion within the UL25 gene may render the protein incapable of disassociating from the capsid. Secondly, the *ts* lesion within the UL25 gene may alter the conformation of the protein at the NPT such that the protein blocks the route of DNA exit from capsid by steric hindrance. Thirdly, the UL25 protein may interact with VP1-3 in the HSV-1 virion and this interaction may be either altered or disrupted in cells infected with *ts1249* at the NPT resulting in the inability of VP1-3 to facilitate the uncoating process. Lastly, the UL25 protein may be involved in the docking of the capsid to the NPC either directly or through an interaction with importin β and/or Ran proteins. In *ts1249*-infected cells at the NPT these associations may be suppressed resulting in a defect in the uncoating process. However, it is important to note that although the evidence presented in this study indicated that *ts1249* was unable to release DNA from the capsid in cells infected at the NPT, this was not known for certain. The use of the *in vitro* uncoating assay described by Ojala *et al.* (2000) could determine whether *ts1249* is impaired in genome release at the NPT.

Electron microscopic analysis of *ts1249*-infected cells following a shift-up from the PT to the NPT demonstrated this virus also exhibited a defect in the DNA packaging process. This phenotype was similar to that of *ts1208* which was also impaired in DNA packaging in cells infected at the NPT. The phenotype of these viruses in cells infected at the NPT was different to that of KUL25NS-infected non-complementing cells (McNab *et al.*, 1998). McNab *et al.* (1998) demonstrated that the UL25 null mutant did not package any viral DNA in infected non-complementing cells and the preponderance of A capsids in the nuclei of KUL25NS-infected non-complementing cells led these workers to conclude that the viral DNA was cleaved and packaged, but was not retained within the capsid.

However, Dr N. Stow has re-examined the phenotype of KUL25NS during infection of non-complementing cells and has found that this mutant can package a low-level of HSV-1 and amplicon DNA (manuscript submitted for publication). Both *ts1249* and *ts1208* also encapsidated a low-level of HSV-1 and amplicon DNA in cells infected at the NPT and exhibited a similar phenotype to that of KUL25NS in infected non-complementing cells (Dr N. Stow, MRC Unit of Virology). However, it is possible that in cells infected with the *ts* viruses at the NPT, mutant UL25 was still partially functional and this would explain the observation that the mutant viruses were able to package a low level of genomic DNA. The amount of UL25 protein associated with B capsids isolated from cells infected with *ts1249* at the NPT has subsequently been examined and was approximately four-fold lower than that of wt B capsids (Dr V. Preston, unpublished observations). This finding suggested that the DNA packaging defect exhibited by *ts1249* in cells infected at the NPT was due to the inability of the UL25 protein to interact with the capsid and indicated that *ts1249* acted as a null mutant at the NPT. Therefore, data presented in this study concerning the behaviour of *ts1249* and *ts1208* in cells infected at the NPT, and the findings of Dr N. Stow relating to the phenotype of KUL25NS in infected non-complementing cells, indicated that the UL25 protein did not function solely in the retention of encapsidated DNA and had a more direct role in the DNA packaging process from that suggested by McNab *et al.* (1998). Exactly what this role is remains unknown but since the UL25 protein is not required for cleavage of concatemeric viral DNA it seems likely that this protein functions at a late stage in the packaging process. The UL25 protein can be considered an essential facilitator of the DNA packaging process; maximal levels of viral DNA are packaged in its presence while minimal amounts are encapsidated in its absence. The UL25 protein probably functions to stabilise the highly condensed viral genome during the DNA packaging process possibly through a direct interaction with the DNA.

The HSV-1 UL25 protein appears to perform a similar role to that of the bacteriophage lambda gpD protein (reviewed by Murialdo, 1991). This protein functions at a late stage in the lambda DNA packaging process when approximately 82% of the genome has already been packaged into the prohead. At this point, the prohead expands in a process closely resembling the structural transformation of HSV-1 procapsids, and creates sites in the capsid shell into which gpD is incorporated. The association of gpD with the maturing prohead appears to stabilise the head, possibly through a direct interaction with the outer layers of the DNA within the phage head, and allows packaging of the remaining 18% of the genome. Additionally, lambda null mutants of gpD accumulate large numbers of empty

phage heads, which have undergone prohead expansion, within infected bacterial cells in a manner analogous to the increased levels of A capsids observed in non-complementing cells infected with KUL25NS (McNab *et al.*, 1998). Thus, there are clear parallels in the apparent functions of lambda gpD and HSV-1 UL25 and continued research into the HSV-1 DNA cleavage and packaging process is required in order to assign a specific function to the UL25 DNA packaging protein.

CHAPTER 5

BIBLIOGRAPHY

Bibliography.

- Abbotts, A. P., Preston, V. G., Hughes, M., Patel, A. H. & Stow, N. D. (2000). Interaction of the Herpes Simplex Virus Type 1 Packaging Protein UL15 With Full-Length and Deleted Forms of the UL28 Protein. *Journal of General Virology* **81**, 2999-3009.
- Addison, C., Rixon, F. J., Palfreyman, J. W., O'Hara, M. & Preston, V. G. (1984). Characterization of a Herpes Simplex Virus Type 1 Mutant Which Has a Temperature-Sensitive Defect in Penetration of Cells and Assembly of Capsids. *Virology* **138**, 246-259.
- Addison, C., Rixon, F. J. & Preston, V. G. (1990). Herpes Simplex Virus Type 1 UL28 Gene Product Is Important For the Formation of Mature Capsids. *Journal of General Virology* **71**, 2377-2384.
- Adelman, K., Salmon, B. & Baines, J. D. (2001). Herpes Simplex Virus DNA Packaging Sequences Adopt Novel Structures That are Specifically Recognized by a Component of the Cleavage and Packaging Machinery. *Proceedings of the National Academy of Sciences of the United States of America* **98**, 3086-3091.
- Akhmedov, A. T., Gross, B. & Jessberger, R. (1999). Mammalian SMC3 C-Terminal and Coiled-Coil Protein Domains Specifically Bind Palindromic DNA, Do Not Block DNA Ends, and Prevent DNA Bending. *Journal of Biological Chemistry* **274**, 38216-38224.
- Albrecht, J.-C., Nicholas, J., Biller, D., Cameron, K. R., Biesinger, B., Newman, C., Wittmann, S., Craxton, M. A., Coleman, H., Fleckenstein, B. & Honess, R. W. (1992). Primary Structure of the Herpesvirus Saimiri Genome. *Journal of Virology* **66**, 5047-5058.
- Ali, M. A., Forghani, B. & Cantin, E. M. (1996). Characterization of an Essential HSV-1 Protein Encoded by the UL25 Gene Reported to be Involved in Virus Penetration and Capsid Assembly. *Virology* **216**, 278-283.
- Al-kobaisi, M. F., Rixon, F. J., McDougall, I. & Preston, V. G. (1991). The Herpes Simplex Virus UL33 Gene-Product Is Required For the Assembly of Full Capsids. *Virology* **180**, 380-388.
- Aslani, A., Simonsson, S. & Elias, P. (2000). A Novel Conformation of the Herpes Simplex Virus Origin of DNA Replication Recognised By the Origin Binding Protein. *Journal of Biological Chemistry* **275**, 5880-5887.
- Baer, R., Bankier, A. T., Biggin, M. D., Deininger, P. L., Farrell, P. J., Gibson, T. J., Hatfull, G., Hudson, G. S., S.C., S., Seguin, C., Tuffnell, P. S. & Barrell, B. G. (1984). DNA Sequence and Expression of the B95-8 Epstein Barr Virus Genome. *Nature* **310**, 207-211.

- Baines, J. D., Cunningham, C., Nalwanga, D. & Davison, A. (1997). The UL15 Gene of Herpes Simplex Virus Type 1 Contains Within Its Second Exon a Novel Open Reading Frame that is Translated in Frame With the UL15 Gene Product. *Journal of Virology* **71**, 2666-2673.
- Baines, J. D., Koyama, A. H., Huang, T. M. & Roizman, B. (1994). The UL21 Gene-Products of Herpes Simplex Virus 1 Are Dispensable For Growth in Cultured Cells. *Journal of Virology* **68**, 2929-2936.
- Baines, J. D., Poon, A. P. W., Rovnak, J. & Roizman, B. (1994). The Herpes Simplex Virus 1 UL15 Gene Encodes 2 Proteins and Is Required For Cleavage of Genomic Viral-DNA. *Journal of Virology* **68**, 8118-8124.
- Baines, J. D. & Roizman, B. (1992). The cDNA of UL15, a Highly Conserved Herpes Simplex Virus 1 Gene, Effectively Replaces the 2 Exons of the Wild-Type Virus. *Journal of Virology* **66**, 5621-5626.
- Baines, J. D. & Roizman, B. (1993). The UL10 Gene of Herpes Simplex Virus Type 1 Encodes a Novel Viral Glycoprotein, gM, Which is Present in the Virion and Plasma Membrane of Infected Cells. *Journal of Virology* **67**, 1441-1452.
- Bairoch, A., Bucher, P. & Hofmann, K. (1997). The PROSITE Database, Its Status in 1997. *Nucleic Acids Research* **25**, 217-221.
- Banks, L. M., Halliburton, I. W., Purifoy, D. J. M., Killington, R. A. & Powell, K. L. (1983). Studies on the Herpes Simplex Virus Alkaline Nuclease: Detection of Type-Common and Type-Specific Epitopes on the Enzyme. *Journal of General Virology* **66**, 1-14.
- Batterson, W., Furlong, D. & Roizman, B. (1983). Molecular Genetics of Herpes Simplex Virus. VIII. Further Characterization of a Temperature-Sensitive Mutant Defective in Release of Viral DNA and in other Stages of the Viral Reproductive Cycle. *Journal of Virology* **45**, 397-407.
- Batterson, W. & Roizman, B. (1983). Characterization of the Herpes Simplex Virion-Associated Factor Responsible for the Induction of α Genes. *Journal of Virology* **46**, 371-377.
- Bazinet, C. & King, J. (1982). The DNA Translocating Vertex of dsDNA Bacteriophage. *Annual Review of Microbiology* **39**, 109-129.
- Bearer, E. L., Breakefield, X. O., Schuback, D., Reese, T. S. & LaVail, J. H. (2000). Retrograde Axonal Transport of Herpes Simplex Virus: Evidence for a Single Mechanism and a Role for Tegument. *Proceedings of the National Academy of Sciences of the United States of America* **97**, 8146-8150.
- Boehmer, P. & Lehman, I. (1997). Herpes Simplex Virus DNA Replication. *Annual Review of Biochemistry* **66**, 347-384.

- Bogner, E., Radsak, K. & Stinski, M. F. (1998). The Gene Product of Human Cytomegalovirus Open Reading Frame UL56 Binds the pac Motif and Has Specific Nuclease Activity. *Journal of Virology* **72**, 2259-2264.
- Booy, F., Trus, B., Davison, A. & Steven, A. (1996). The Capsid Architecture of Channel Catfish Virus, An Evolutionary Distinct Herpesvirus, is Largely Conserved in the Absence of Discernible Sequence Homology With Herpes Simplex Virus. *Virology* **215**, 134-141.
- Booy, F. P., Newcomb, W. W., Trus, B. L., Brown, J. C., Baker, T. S. & Steven, A. C. (1991). Liquid-Crystalline, Phage-Like Packing of Encapsidated DNA in Herpes Simplex Virus. *Cell* **64**, 1007-1015.
- Booy, F. P., Trus, B. L., Newcomb, W. W., Brown, J. C., Conway, J. F. & Steven, A. C. (1994). Finding a Needle in a Haystack - Detection of a Small Protein (the 12-Kda VP26) in a Large Complex (the 200-Mda Capsid of Herpes Simplex Virus). *Proceedings of the National Academy of Sciences of the United States of America* **91**, 5652-5656.
- Braun, D. K., Batterson, W. & Roizman, B. (1984). Identification and Genetic Mapping of a Herpes Simplex Virus Capsid Protein That Binds DNA. *Journal of Virology* **50**, 645-648.
- Broll, H., Buhk, H., Zimmermann, W. & Goltz, M. (1999). Structure and Function of the prDNA and the Genomic Termini of the γ_2 -Herpesvirus Bovine Type 4. *Journal of General Virology* **80**, 979-986.
- Bronstein, J. C. & Weber, P. C. (1996). Purification and Characterization of a Herpes Simplex Virus Type 1 Alkaline Nuclease Expressed in *Escherichia coli*. *Journal of Virology* **70**, 2008-2013.
- Bronstein, J. C., Weller, S. K. & Weber, P. C. (1997). The Product of the UL12.5 Gene of Herpes Simplex Virus Type 1 is a Capsid-Associated Nuclease. *Journal of Virology* **71**, 3039-3047.
- Brown, M. & Faulkner, P. (1977). A Plaque Assay for Nuclear Polyhedrosis Virus using a Solid Overlay. *Journal of General Virology* **36**, 361-364.
- Brown, S. M., Ritchie, D. A. & Subak-Sharpe, J. H. (1973). Genetic Studies with Herpes Simplex Virus Type 1. The Isolation of Temperature-Sensitive Mutants, their Arrangement into Complementation Groups and Recombination Analysis Leading to a Linkage Map. *Journal of General Virology* **18**, 329-346.
- Browne, H., Bell, S., Minson, T. & Wilson, D. W. (1996). An Endoplasmic Reticulum Retained Herpes Simplex Virus Glycoprotein H is Absent from Secreted Virions: Evidence for Re-Envelopment During Egress. *Journal of Virology* **70**, 4311-4316.
- Campadelli-Fiume, G., Farabegoli, F., Di Gaeta, S. & Roizman, B. (1991). Origin of Unenveloped Capsids in the Cytoplasm of Cells Infected With Herpes Simplex Virus 1. *Journal of Virology* **65**, 1589-1595.

- Casper, D. L. D. & Klug, A. (1962). Physical Principles in the Construction of Regular Viruses. *Cold Spring Harbour Symposium of Quantitative Biology* **27**, 1-32.
- Catalano, C. E., Cue, D. & Feiss, M. (1995). Virus DNA Packaging: The Strategy Used By Phage λ . *Molecular Microbiology* **16**, 1075-1086.
- Cebrian, J., Berthelot, N. & Laithier, M. (1989). Genome Structure of Cottontail Rabbit Herpesvirus. *Journal of Virology* **63**, 523-531.
- Cerritelli, M. E., Cheng, N., Rosenberg, A. H., McPherson, C. E., Booy, F. P. & Steven, A. C. (1997). Encapsidated Conformation of Bacteriophage T7 DNA. *Cell* **91**, 271-280.
- Challberg, M. (1991). Herpes Simplex Virus DNA Replication. *Seminars in Virology* **2**, 247-256.
- Chang, Y., Cesarman, E., Pessin, M. S., Lee, F., Culpepper, J., Knowles, D. M. & Moore, P. S. (1994). Identification of Herpesvirus-Like DNA Sequences in AIDS-Associated Kaposi's Sarcoma. *Science* **266**, 1865-1869.
- Chang, Y. E. & Roizman, B. (1993). The Product of the UL31 Gene of Herpes Simplex Virus 1 is a Nuclear phosphoprotein Which Partitions With the Nuclear Matrix. *Journal of Virology* **67**, 6348-6356.
- Chang, Y. E., VanSant, C., Krug, P. W., Sears, A. E. & Roizman, B. (1997). The Null Mutant of the UL31 Gene of Herpes Simplex Virus 1: Construction and Phenotype in Infected Cells. *Journal of Virology* **71**, 8307-8315.
- Chang, Y. J. E., Poon, A. P. W. & Roizman, B. (1996). Properties of the Protein Encoded by the UL32 Open Reading Frame of Herpes Simplex Virus 1. *Journal of Virology* **70**, 3938-3946.
- Chartrand, P., Crumpacker, C. S., Schaffer, P. A. & Wilkie, N. M. (1980). Physical and Genetic Analysis of the Herpes Simplex Virus DNA Polymerase Locus. *Virology* **103**, 311-325.
- Chen, D. H., Jiang, H., Lee, M., Liu, F. & Zhou, Z. H. (1999). Three-Dimensional Visualization of Tegument/Capsid Interactions in the Intact Human Cytomegalovirus. *Virology* **260**, 10-16.
- Chi, J. H. I. & Wison, D. W. (2000). ATP-Dependant Localization of the Herpes Simplex Virus Capsid Protein VP26 to sites of Procapsid Maturation. *Journal of Virology* **74**, 1468-1476.
- Chou, J. & Roizman, B. (1989). Characterization of DNA Sequence-Common and Sequence-Specific Proteins Binding to *cis*-Acting Sites for Cleavage of the Terminal *a* Sequence of the Herpes Simplex Virus 1 Genome. *Journal of Virology* **63**, 1059-1068.

- Chowdhury, K. (1991). One Step 'Miniprep' Method for the Isolation of Plasmid DNA. *Nucleic Acids Research* **19**, 2792.
- Cohen, G. H., Ponce De Leon, M., Diggelman, H., Lawrence, W. C., Vernon, S. K. & Eisenberg, R. G. (1980). Structural Analysis of the Capsid Polypeptides of Herpes Simplex Virus Types 1 and 2. *Journal of Virology* **34**, 521-531.
- Comps, M. & Cochenec, N. (1993). A Herpes-Like Virus from the European Oyster *Ostrea edulis* L. *Journal of Invertebrate Pathology* **62**, 201-203.
- Conley, A. F., Knipe, D. M., Jones, P. C. & Roizman, B. (1981). Molecular genetics of Herpes Simplex Virus. VII. Characterisation of a Temperature-Sensitive Mutant Produced by *in vitro* Mutagenesis and Defective in DNA Synthesis and Accumulation of Polypeptides. *Journal of Virology* **37**, 191-206.
- Costa, R. H., Draper, K. G., Banks, L., Powell, K. L., Cohen, G., Eisenberg, R. & Wagner, E. K. (1983). High-Resolution Characterization of Herpes Simplex Virus Type 1 Transcripts Encoding Alkaline Exonuclease and a 50,000-Dalton Protein Tentatively Identified as a Capsid Protein. *Journal of Virology* **48**, 591-603.
- Cotte, L., Drouet, E., Bissuel, F., Denoyel, G. A. & Trepo, C. (1993). Diagnostic Value of Amplification of Human Cytomegalovirus DNA from Gastrointestinal Biopsies from Human Immunodeficiency Virus Infected Patients. *Journal of Clinical Microbiology* **31**, 2066-2069.
- Cuff, J. A., Clamp, M. E., Siddiqui, A. S., Finlay, M. & Barton, G. J. (1998). Jpred: A Consensus Secondary Structure Prediction Server. *Bioinformatics* **14**, 892-893.
- Daikoku, T., Yamashita, Y., Tsurumi, T. & Nishiyama, Y. (1995). The US3 Protein Kinase of Herpes Simplex Virus Type 2 is Associated With Phosphorylation of the UL12 Alkaline Nuclease *in vitro*. *Archives of Virology* **140**, 1637-1644.
- Dasgupta, A. & Wilson, D. W. (1999). ATP Depletion Blocks Herpes Simplex Virus DNA Packaging and Capsid Maturation. *Journal of Virology* **73**, 2006-2015.
- Davison, A. & Wilkie, N. (1981). Nucleotide Sequence of the Joint Between the L and S Segments of Herpes Simplex Virus Types 1 and 2. *Journal of General Virology* **55**, 315-331.
- Davison, A. J. (1992). Channel Catfish Virus: A New Type of Herpesvirus. *Virology* **186**, 9-14.
- Davison, A. J. & McGeoch, D. J. (1995). Herpesviridae. In *Molecular Basis of Viral Evolution*, pp. 290-309. Edited by A. Gibbs, C. H. Calisher & F. Garcia-Arenal. Cambridge: Cambridge University Press.
- Davison, A. J. & Scott, J. E. (1986). The Complete DNA Sequence of Varicella-Zoster Virus. *Journal of General Virology* **67**, 1759-1816.

- Davison, M. D., Rixon, F. J. & Davison, A. J. (1992). Identification of Genes Encoding 2 Capsid Proteins (VP24 and VP26) of Herpes Simplex Virus Type 1. *Journal of General Virology* **73**, 2709-2713.
- de Wind, N., Wagenaar, F., Pol, J., Kimman, T. & Berns, A. (1992). The Pseudorabies Virus Homologue of Herpes Simplex Virus UL21 Gene Product is a Capsid Protein Which is Involved in Capsid Maturation. *Journal of Virology* **66**, 7096-7103.
- Deiss, L. P., Chou, J. & Frenkel, N. (1986). Functional Domains Within the *a* Sequence Involved in the Cleavage-Packaging of Herpes Simplex Virus DNA. *Journal of Virology* **59**, 605-618.
- Deiss, L. P. & Frenkel, N. (1986). Herpes Simplex Virus Amplicon: Cleavage of Concatemeric DNA Is Linked to Packaging and Involves Amplification of the Terminally Reiterated *a* Sequence. *Journal of Virology* **57**, 933-941.
- Deng, H. & Dewhurst, S. (1998). Functional Identification and Analysis of *cis*-Acting Sequences Which Mediate Genome Cleavage and Packaging in Human Herpesvirus 6. *Journal of Virology* **72**, 320-329.
- Desai, P., Deluca, N. A., Glorioso, J. C. & Person, S. (1993). Mutations in Herpes Simplex Virus Type 1 Genes Encoding VP5 and VP23 Abrogate Capsid Formation and Cleavage of Replicated DNA. *Journal of Virology* **67**, 1357-1364.
- Desai, P., DeLuca, N. A. & Person, S. (1998). Herpes Simplex Virus Type 1 VP26 is Not Essential for Replication in Cell Culture but Influences Production of Infectious Virus in the Nervous System of Infected Mice. *Virology* **247**, 115-124.
- Desai, P. & Person, S. (1996). Molecular Interactions Between the HSV-1 Capsid Proteins as Measured by the Yeast Two-Hybrid System. *Virology* **220**, 516-521.
- Desai, P. J. (2000). A Null Mutation in the UL36 Gene of Herpes Simplex Virus Type 1 Results in Accumulation of Unenveloped DNA-Filled Capsids in the Cytoplasm of Infected Cells. *Journal of Virology* **74**, 11608-11618.
- Dilanni, C. L., Mapelli, C. & Drier, D. A. (1993). *In Vitro* Activity of the Herpes Simplex Virus Type 1 Protease With Peptide Substrates. *Journal of Biological Chemistry* **268**, 25449-25454.
- Dolan, A., Jamieson, F.E., Cunningham, C., Barnett, B.C. & McGeoch, D.J. (1998). The Genome Sequence of Herpes Simplex Virus Type 2. *Journal of Virology* **72**, 2010-2021.
- Dolter, K. E., Ramaswamy, R. & Holland, T. C. (1994). Syncytial Mutations in the Herpes Simplex Virus Type1 gK (UL53) Gene Occur in Two Distinct Domains. *Journal of Virology* **68**, 8277-8281.

- Draper, K. G., Devi-Rao, G., Costa, R. H., Blair, E. D., Thompson, R. L. & Wagner, E. K. (1986). Characterization of the Genes Encoding Herpes Simplex Virus Type 1 and 2 Alkaline Exonucleases and Overlapping Proteins. *Journal of Virology* **57**, 1023-1036.
- Dube, P., Tavares, P., Lurz, R. & Van Heel, M. (1993). The Portal Protein of Bacteriophage SPP1: A DNA Pump With 13-Fold Symmetry. *EMBO Journal* **12**, 1303-1309.
- Earnshaw, W. & Harrison, S. C. (1977). DNA Arrangement in Isometric Phage Heads. *Nature* **268**, 598-602.
- Elgadi, M. M., Hayes, C. E. & Smiley, J. R. (1999). The Herpes Simplex Virus vhs Protein Induces Endoribonucleolytic Cleavage of Target RNAs in Cell Extracts. *Journal of Virology* **73**, 7153-7164.
- Elliott, G., Mouzakis, G. & O'Hare, P. (1995). VP16 Interacts Via Its Activation Domain With VP22, a Tegument Protein of Herpes Simplex Virus, and Is Relocated to a Novel Macromolecular Assembly in Coexpressing Cells. *Journal of Virology* **69**, 7932-7941.
- Elliott, G. & O'Hare, P. (1999). Live-Cell Analysis of a Green Fluorescent Protein-Tagged Herpes Simplex Virus Infection. *Journal of Virology* **73**, 4110-4119.
- Farrell, M. J., Dobson, A. T. & Feldman, L. T. (1991). Herpes Simplex Virus Latency-Associated Transcript is a Stable Intron. *Proceedings of the National Academy of Sciences of the United States of America* **88**, 790-794.
- Forrester, A., Farrell, H., Wilkinson, G., Kaye, J., Davis-Poynter, N. & Minson, T. (1992). Construction and Properties of a Mutant of Herpes Simplex Virus Type 1 With Glycoprotein H Coding Sequences Deleted. *Journal of Virology* **66**, 341-348.
- Gaffney, D., McLauchlan, J., Whitton, J. & Clements, J. (1985). A Modular System for the Assay of Transcription Regulatory Signals: The Sequence TAATGARAT is Required for Herpes Simplex Virus Immediate Early Gene Activation. *Nucleic Acids Research* **13**, 7847-7863.
- Gao, M., Matusick-kumar, L., Hurlburt, W., Ditusa, S. F., Newcomb, W. W., Brown, J. C., McCann, P. J., Deckman, I. & Colonno, R. J. (1994). The Protease of Herpes Simplex Virus Type 1 Is Essential For Functional Capsid Formation and Viral Growth. *Journal of Virology* **68**, 3702-3712.
- Geraghty, R. J., Krummenacher, C., Cohen, G. H., Eisenberg, R. J. & Spear, P. G. (1998). Entry of Alphaherpesviruses Mediated by Poliovirus Receptor-Related Protein 1 and Poliovirus Receptor. *Science* **280**, 1618-1620.
- Gibson, W. & Roizman, B. (1972). Proteins Specified by Herpes Simplex Virus. VIII. Characterisation and Composition of Multiple Capsid Forms of Subtypes 1 and 2. *Journal of Virology* **10**, 1044-1052.

- Gibson, W. & Roizman, B. (1974). Proteins Specified by Herpes Simplex Virus. X. Staining and Radiolabelling Properties of B Capsid and Virion Proteins in Polyacrylamide Gels. *Journal of Virology* **13**, 155-165.
- Goldstein, J. N. & Weller, S. K. (1998a). The Exonuclease Activity of HSV-1 UL12 is Required for *in vivo* Function. *Virology* **244**, 442-457.
- Goldstein, J. N. & Weller, S. K. (1998b). *In vitro* Processing of Herpes Simplex Virus Type 1 DNA Replication Intermediates by the Viral Alkaline Nuclease, UL12. *Journal of Virology* **72**, 8772-8781.
- Gominak, S., Cros, D. & Paydarfar, D. (1990). Herpes Simplex Labialis and Trigeminal Neuropathy. *Neurology* **40**, 151-152.
- Goodman, J. L. & Engel, J. P. (1991). Altered Pathogenesis in Herpes Simplex Virus Type 1 Infection Due to a Syncytial Mutation Mapping to the Carboxy Terminus of Glycoprotein B. *Journal of Virology* **65**, 1770-1778.
- Goshima, F., Watanabe, D., Takakuwa, H., Wada, K., Daikoku, T., Yamada, M. & Nishiyama, Y. (2000). Herpes Simplex Virus UL17 Protein is Associated With B Capsids and Colocalises With ICP35 and VP5 in Infected Cells. *Archives of Virology* **145**, 417-426.
- Guo, P., Peterson, C. & Anderson, D. (1987). Prohead and DNA-gp3-Dependent ATPase Activity of the DNA Packaging Protein gp16 of Bacteriophage ϕ 29. *Journal of Molecular Biology* **197**, 229-236.
- Guo, P., Zhang, C., Chen, C., Garver, K. & Trottier, M. (1998). Inter-RNA Interaction of Phage ϕ 29 pRNA to Form a Hexameric Complex for Viral DNA Transportation. *Molecular Cell* **2**, 149-155.
- Harris-Hamilton, E. & Bachenheimer, S. L. (1985). Accumulation of Herpes Simplex Virus Type 1 RNAs of Different Kinetic Class in the Cytoplasm of Infected Cells. *Journal of Virology* **53**, 144-151.
- Harrison, S. C. (1983). Packaging of DNA into Bacteriophage Heads: A Model. *Journal of Molecular Biology* **171**, 577-580.
- Hayward, G. S., Jacob, R. J., Wadsworth, S. C. & Roizman, B. (1975). Anatomy of Herpes Simplex Virus DNA: Evidence for Four Populations of Molecules That Differ in the Relative Orientations of Their Long and Short Segments. *Proceedings of the National Academy of Sciences of the United States of America* **72**, 4243-4247.
- He, X. & Lehman, I. R. (2001). An Initial ATP-Independent Step in the Unwinding of a Herpes Simplex Virus Type 1 Origin of Replication by a Complex of the Viral Origin-Binding Protein and Single-Strand DNA-Binding Protein. *Proceedings of the National Academy of Sciences of the United States of America* **98**, 3024-3028.

- He, X., Treacy, M. N., Simmons, D. M., Ingraham, H. A., Swanson, L. S. & Rosenberg, M. G. (1989). Expression of a Large Family of POU-Domain Regulatory Proteins in Mammalian Brain Development. *Nature* **340**, 35-42.
- Hochberg, E. & Becker, Y. (1969). Adsorption, Penetration and Uncoating of Herpes Simplex Virus. *Journal of General Virology* **2**, 231-241.
- Hoffmann, P. J. & Cheng, Y.-C. (1979). DNase Induced After Infection of KB Cells by Herpes Simplex Virus Type 1 or 2. *Journal of Virology* **32**, 449-457.
- Holland, T. C., Marlin, S. D., Levine, M. & Glorioso, J. (1983). Antigenic Variants of Herpes Simplex Virus Selected With Glycoprotein-Specific Monoclonal Antibodies. *Journal of Virology* **45**, 672-682.
- Honess, R. & Roizman, B. (1974). Regulation of Herpesvirus Macromolecular Synthesis I. Cascade Regulation of the Synthesis of Three Groups of Viral Proteins. *Journal of Virology* **14**, 8-19.
- Honess, R. & Roizman, B. (1975). Regulation of Herpesvirus Macromolecular Synthesis I. Cascade Regulation of the Synthesis of Three groups of Viral Polypeptides. *Proceedings of the National Academy of Sciences of the United States of America* **72**, 1276-1280.
- Hong, Z., Beaudet-Miller, M., Durkin, J., Zhang, R. & Kwong, A. D. (1996). Identification of a Minimal Hydrophobic Domain in the Herpes Simplex Virus Type 1 Scaffolding Protein which is Required for Interaction with the Major Capsid Protein. *Journal of Virology* **70**, 533-540.
- Hutchinson, L., Goldsmith, K., Snoddy, D., Ghosh, H., Graham, F. L. & Johnson, D. C. (1992). Identification and Characterization of a Novel Herpes Simplex Virus Glycoprotein, gK, Involved in Cell Fusion. *Journal of Virology* **66**, 5603-5609.
- Jones, D. T. (1999). Protein Secondary Structure Prediction Based on Position-Specific Scoring Matrices. *Journal of Molecular Biology* **292**, 195-202.
- Johnson, P. A., Best, M. G., Friedmann, T. & Parris, D. A. (1991). Isolation of a Herpes Simplex Virus Type 1 Deleted for the Essential UL42 Gene and Characterisation of its Null Phenotype. *Journal of Virology* **65**, 700-710.
- Johnson, D. C., Frame, M. C., Ligas, M. W., Cross, A. M. & Stow, N. D. (1988). Herpes Simplex Virus Immunoglobulin G Fc Receptor Activity Depends on a Complex of Two Viral Glycoproteins, gE and gI. *Journal of Virology* **62**, 1347-1354.
- Kaelin, K., Dezelee, S., Masse, M. J., Bras, F. & Flamand, A. (2000). The UL25 Protein of Pseudorabies Virus Associates With Capsids and Localizes to the Nucleus and to Microtubules. *Journal of Virology* **74**, 474-482.

- Kennard, J., Rixon, F. J., McDougall, I. M., Tatman, J. D. & Preston, V. G. (1995). The 25 Amino-Acid-Residues At the Carboxy-Terminus of the Herpes Simplex Virus Type 1 UL26.5 Protein Are Required For the Formation of the Capsid Shell Around the Scaffold. *Journal of General Virology* **76**, 1611-1621.
- Kirkitadze, M. D., Barlow, P. N., Price, N. C., Kelly, S. M., Boutell, C. J., Rixon, F. J. & McClelland, D. A. (1998). The Herpes Simplex Virus Triplex Protein, VP23, Exists as a Molten Globule. *Journal of Virology* **72**, 10066-10072.
- Kitts, P. A., Ayres, M. D. & Possee, R. D. (1990). Linearization of Baculovirus DNA Enhances the Recovery of Recombinant Virus Expression Vectors. *Nucleic Acids Research* **18**, 55667-55672.
- Kitts, P. A. & Possee, R. D. (1993). A Method for Producing Recombinant Baculovirus Expression Vectors at High Frequency. *BioTechniques* **14**, 810-817.
- Knipe, D. M., Batterson, W., Nosal, C., Roizman, B. & Buchan, A. (1981). Molecular Genetics of Herpes Simplex Virus VI. Characterization of a Temperature-Sensitive Mutant Defective in the Expression of All Early Viral Gene Products. *Journal of Virology* **38**, 539-547.
- Knopf, C. W. & Weisshart, K. (1990). Comparison of Exonucleolytic Activities of Herpes Simplex Virus Type-1 DNA Polymerase and DNase. *European Journal of Biochemistry* **191**, 263-273.
- Koch, H.-G., Delius, H., Matz, B., Flugel, R. M., Clarke, J. & Darai, G. (1985). Molecular Cloning and Physical Mapping of the Tupaia Herpesvirus Genome. *Journal of Virology* **55**, 86-95.
- Koslowski, K. M., Shaver, P. R., Casey, J. T., Wilson, T., Yamanaka, G., Sheaffer, A. K., Tenney, D. J. & Pederson, N. E. (1999). Physical and Functional Interactions between the Herpes Simplex Virus UL15 and UL28 DNA Cleavage and Packaging Proteins. *Journal of Virology* **73**, 1704-1707.
- Krammerer, R. A., Frank, S., Schulthess, T., Landwehr, R., Lustig, A. & Engel, J. (1999). Heterodimerization of a Functional GABA_B Receptor is Mediated by Parallel Coiled-Coil Alpha-Helices. *Biochemistry* **38**, 13263-13269.
- Kristie, T. M., Pomerantz, J. L., Twomey, T. C., Parent, S. A. & Sharp, P. A. (1995). The Cellular C1 Factor of the Herpes Simplex Virus Enhancer Complex is a Family of Polypeptides. *Journal of Biological Chemistry* **270**, 4387-4394.
- Kristie, T. M., Vogel, J. L. & Sears, A. E. (1999). Nuclear Localization of the C1 Factor (Host Cell Factor) in Sensory Neurones Correlates with Reactivation of Herpes Simplex Virus from Latency. *Proceedings of the National Academy of Sciences of the United States of America* **96**, 1229-1233.

- Krummenacher, C., Nicola, A. V., Whitbeck, J. C., Lou, H., Hou, W., Lambris, J. D., Geraghty, R. J., Spear, P. G., Cohen, G. H. & Eisenberg, R. J. (1998). Herpes Simplex Virus Glycoprotein D Can Bind to Poliovirus Receptor-Related Protein 1 or Herpesvirus Entry Mediator, Two Structurally Unrelated Mediators of Virus Entry. *Journal of Virology* **72**, 7064-7074.
- Kwong, A. D. & Frenkel, N. (1987). Herpes Simplex Virus-Infected Cells Contain a Function(s) That Destabilises Both Host and Viral mRNAs. *Proceedings of the National Academy of Sciences of the United States of America* **84**, 1926-1930.
- Kwong, A. D., Kruper, J. A. & Frenkel, N. (1988). Herpes Simplex Virus Virion Host Shutoff Function. *Journal of Virology* **62**, 912-921.
- La Boissière, S., Hughes, T. & O'Hare, P. (1999). HCF-Dependent Nuclear Import of VP16. *EMBO Journal* **18**, 480-489.
- Lamberti, C. & Weller, S. K. (1996). The Herpes Simplex Virus Type 1 UL6 Protein is Essential for Cleavage and Packaging but Not for Genomic Inversion. *Virology* **226**, 403-407.
- Lamberti, C. & Weller, S. K. (1998). The Herpes Simplex Virus Type 1 Cleavage/Packaging Protein, UL32, is Involved in Efficient Localization of Capsids to Replication Compartments. *Journal of Virology* **72**, 2463-2473.
- Larson, S. B., Koszelak, S., Day, J., Greenwood, A., Dodds, A. & McPherson, A. (1993). Three-Dimensional Structure of Satellite Tobacco Mosaic Virus at 2.9 Å Resolution. *Journal of Molecular Biology* **231**, 375-391.
- Laurent, A.-M., Madjar, J.-J. & Greco, A. (1998). Translational Control of Viral and Host Protein Synthesis During the Course of Herpes Simplex Virus Type 1 Infection: Evidence That Initiation of Translation is the Limiting Step. *Journal of General Virology* **79**, 2765-2775.
- Lee, W.-C. & Fuller, A. O. (1993). Herpes Simplex Virus Type 1 and Pseudorabies Virus Bind to a Common Saturable Receptor on Vero Cells That Is Not Heparan Sulphate. *Journal of Virology* **67**, 5088-5097.
- Lehman, I. R. & Boehmer, P. E. (1999). Replication of Herpes Simplex Virus DNA. *Journal of Biological Chemistry* **274**, 28059-28062.
- Ligas, M. W. & Johnson, D. C. (1988). A Herpes Simplex Virus Mutant in Which Glycoprotein D Sequences are Replaced by β -Galactosidase Sequences Binds to But is Unable to Penetrate Into Cells. *Journal of Virology* **62**, 1486-1494.
- Lillycrop, K. A., Dent, C. L., Wheatley, S. C., Beech, N. M., Ninkina, N. N., Wood, J. N. & Latchman, D. S. (1991). The Octamer-Binding Protein Oct-2 Represses HSV Immediate-Early Genes in Cell-Lines Derived from Latently Infectable Sensory Neurons. *Neuron* **7**, 381-390.

- Lillicrop, K. A., Howard, M. K., Estridge, J. K. & Latchman, D. S. (1994). Inhibition of Herpes Simplex Virus Infection by Ectopic Expression of Neuronal Splice Variants of the Oct-2 Transcription Factor. *Nucleic Acids Research* **22**, 815-820.
- Liu, F. & Roizman, B. (1991a). The Herpes Simplex Virus 1 Gene Encoding a Protease Also Contains Within Its Coding Domain the Gene Encoding the More Abundant Substrate. *Journal of Virology* **65**, 5149-5156.
- Liu, F. Y. & Roizman, B. (1991b). The Promoter, Transcriptional Unit, and Coding Sequence of Herpes Simplex Virus 1 Family 35 Proteins Are Contained Within and in Frame With the UL26 Open Reading Frame. *Journal of Virology* **65**, 206-212.
- Liu, F. Y. & Roizman, B. (1993). Characterization of the Protease and Other Products of Amino-Terminus-Proximal Cleavage of the Herpes Simplex Virus UL26 Protein. *Journal of Virology* **67**, 1300-1309.
- Livingstone, C. & Jones, I. (1989). Baculovirus Expression Vectors With Single-Strand Capability. *Nucleic Acids Research* **17**, 2366.
- Locker, H. & Frenkel, N. (1979). *Bam*I, *Kpn*I, and *Sal*I Restriction Enzyme Maps of the DNAs of Herpes Simplex Virus Strains Justin and F: Occurrence of Heterogeneities in Defined Regions of the Viral DNA. *Journal of Virology* **32**, 429-441.
- Lupas, A., Van Dyke, M. & Stock, J. (1991). Predicting Coiled Coils from Protein Sequences. *Science* **252**, 1162-1164.
- Lycke, E., Hamarck, B., Johansson, M., Krotchwil, A., Lycke, J. & Svennerholm, B. (1988). Herpes Simplex Virus Infection of the Human Sensory Neuron An Electron Microscopy Study. *Archives of Virology* **101**, 87-104.
- McMahan, L. & Schaffer, P. A. (1990). The Repressing and Enhancing Functions of the Herpes Simplex Virus Regulatory Protein ICP27 Map to the C-Terminal Regions and are Required to Modulate Viral Gene Expression Very Early in Infection. *Journal of Virology* **64**, 3471-3485.
- MacPherson, I. & Stoker, M. (1962). Polyoma Transformation of Hamster Cell Clones - An Investigation of Genetic Factors Affecting Cell Competence. *Virology* **16**, 147-151.
- Maina, C. V., Riggs, P. D., Grandea, A. G. I., Slatko, B. E., Moran, L. S., Tagliamonte, J. A., McReynolds, L. A. & Guan, C. (1988). A Vector to Express and Purify Foreign Proteins in *Escherichia coli* by Fusion to, and Separation From, Maltose Binding Protein. *Gene* **74**, 365-373.
- Martin, D. & Weber, P. (1996). The *a* Sequence is Dispensable for Isomerisation of the Herpes Simplex Type 1 Genome. *Journal of Virology* **70**, 8801-8812.

- Martinez, R., Sarisky, R. T., Weber, P. C. & Weller, S. K. (1996a). Herpes Simplex Virus Type 1 Alkaline Nuclease is Required for Efficient Processing of Viral DNA Replication Intermediates. *Journal of Virology* **70**, 2075-2085.
- Martinez, R., Shao, L., Bronstein, J. C., Weber, P. C. & Weller, S. K. (1996b). The Product of a 1.9-kb mRNA Which Overlaps the HSV-1 Alkaline Nuclease Gene (UL12) Cannot Relieve the Growth Defects of a Null Mutant. *Virology* **215**, 152-164.
- Matusick-Kumar, L., Hulburt, W., Weinheimer, S. P., Newcomb, W. W., Brown, J. C. & Gao, M. (1994). Phenotype of the Herpes Simplex Virus Type 1 Protease Substrate ICP35 Mutant Virus. *Journal of Virology* **68**, 5384-5394.
- McGeoch, D., Dolan, A., Donald, S. & Rixon, F. (1985). Sequence Determination and Genetic Content of the Short Unique Region in the Genome of Herpes Simplex Virus Type 1. *Journal of Molecular Biology* **181**, 1-13.
- McGeoch, D. J., Dalrymple, M. A., Davison, A. J., Dolan, A., Frame, M. C., McNab, D., Perry, L. J., Scott, J. E. & Taylor, P. (1988). The Complete DNA-Sequence of the Long Unique Region in the Genome of Herpes Simplex Virus Type 1. *Journal of General Virology* **69**, 1531-1574.
- McLauchlan, J. & Rixon, F. J. (1992). Characterization of Enveloped Tegument Structures (L-Particles) Produced By Alpha herpesviruses - Integrity of the Tegument Does Not Depend on the Presence of Capsid or Envelope. *Journal of General Virology* **73**, 269-276.
- McNabb, D. S. & Courtney, R. J. (1992). Characterization of the Large Tegument Protein (ICP1/2) of Herpes Simplex Virus Type 1. *Virology* **190**, 221-232.
- McNab, A. R., Desai, P., Person, S., Roof, L. L., Thomsen, D. R., Newcomb, W. W., Brown, J. C. & Homa, F. L. (1998). The Product of the Herpes Simplex Virus Type 1 UL25 Gene is Required for Encapsidation but Not for Cleavage of Replicated Viral DNA. *Journal of Virology* **72**, 1060-1070.
- McVoy, M., Nixon, D. & Adler, S. (1997). Circularization and Cleavage of Guinea Pig Cytomegalovirus Genomes. *1997* **71**, 4209-4217.
- McVoy, M. A., Nixon, D. E., Adler, S. P. & Mocarski, E. S. (1998). Sequences Within the Herpesvirus-Conserved *pac1* and *pac2* Motifs Are Required For Cleavage and Packaging of the Murine cytomegalovirus Genome. *Journal of Virology* **72**, 48-56.
- Mellerick, D. M. & Fraser, N. W. (1987). Physical State of the Latent Herpes Simplex Virus Genome in a Mouse Model: Evidence Suggesting an Episomal State. *Virology* **158**, 265-275.
- Mocarski, E. S. & Roizman, B. (1981). Site-Specific Inversion Sequences of the Herpes Simplex Virus Genome: Domain and Structural Features. *Proceedings of the National Academy of Sciences of the United States of America* **78**, 7047-7051.

- Mocarski, E. S. & Roizman, B. (1982). Structure and Role of the Herpes Simplex Virus DNA in Inversion, Circularization and Generation of Virion DNA. *Cell* **31**, 89-97.
- Montgomery, R. I., Warner, M. S., Lum, B. J. & Spear, P. G. (1996). Herpes Simplex Virus-1 Entry into Cells Mediated by a Novel Member of the TNF/NGF Receptor Family. *Cell* **87**, 427-436.
- Morgan, C., Rose, H., Holden, M. & Jones, E. (1959). Electron Microscopic Observations on the Development of Herpes Simplex Virus. *Journal of Experimental Medicine* **110**, 643-656.
- Morrison, E. E., Stevenson, A. J., Wang, Y.-F. & Meredith, D. M. (1998). Differences in the Intracellular Localization and Fate of Herpes Simplex Virus Tegument Proteins Early in the Infection of Vero Cells. *Journal of General Virology* **79**, 2517-2528.
- Murialdo, H. (1991) Bacteriophage Lambda DNA Maturation and Packaging. *Annual Reviews in Biochemistry* **60**, 125-153.
- Nasseri, M. & Mocarski, E. (1988). The Cleavage Recognition Signal is Contained Within Sequences Surrounding an *a-a* Junction in Herpes Simplex Virus DNA. *Virology* **167**, 25-30.
- Newcomb, W. W. & Brown, J. C. (1991). Structure of the Herpes Simplex Virus Capsid - Effects of Extraction With Guanidine-Hydrochloride and Partial Reconstitution of Extracted Capsids. *Journal of Virology* **65**, 613-620.
- Newcomb, W. W. & Brown, J. C. (1994). Induced Extrusion of DNA From the Capsid of Herpes Simplex Virus Type 1. *Journal of Virology* **68**, 433-440.
- Newcomb, W. W., Homa, F. L., Thomsen, D. R., Booy, F. P., Trus, B. L., Steven, A. C., Spencer, J. V. & Brown, J. C. (1996). Assembly of the Herpes Simplex Virus Capsid: Characterization of Intermediates Observed During Cell-Free Capsid Formation. *Journal of Molecular Biology* **263**, 432-446.
- Newcomb, W. W., Homa, F. L., Thomsen, D. R., Trus, B. L., Cheng, N. Q., Steven, A., Booy, F. & Brown, J. C. (1999). Assembly of the Herpes Simplex Virus Procapsid From Purified Components and Identification of Small Complexes Containing the Major Capsid and Scaffolding Proteins. *Journal of Virology* **73**, 4239-4250.
- Newcomb, W. W., Homa, F. L., Thomsen, D. R., Ye, Z. P. & Brown, J. C. (1994). Cell-Free Assembly of the Herpes Simplex Virus Capsid. *Journal of Virology* **68**, 6059-6063.
- Newcomb, W. W., Trus, B. L., Booy, F. P., Steven, A. C., Wall, J. S. & Brown, J. C. (1993). Structure of the Herpes Simplex Virus Capsid - Molecular Composition of the Pentons and the Triplexes. *Journal of Molecular Biology* **232**, 499-511.

- Newcomb, W. W., Trus, B. L., Cheng, N., Steven, A. C., Sheaffer, A. K., Tenney, D. J., Weller, S. K. & Brown, J. C. (2000). Isolation of Herpes Simplex Virus Procapsids from Cells Infected with a Protease-Deficient Mutant Virus. *Journal of Virology* **74**, 1663-1673.
- Nicholson, P., Addison, C., Cross, A. M., Kennard, J., Preston, V. G. & Rixon, F. J. (1994). Localization of the Herpes Simplex Virus Type 1 Major Capsid Protein VP5 to the Cell-Nucleus Requires the Abundant Scaffolding Protein VP22a. *Journal of General Virology* **75**, 1091-1099.
- Ogasawara, M., Suzutani, T., Yoshida, Y. & Azuma, M. (2001). Role of the UL25 Gene Product in Packaging DNA into the Herpes Simplex Virus Capsid: Location of UL25 Product in the Capsid and Demonstration that it Binds DNA. *Journal of Virology* **75**, 1427-1436.
- Oien, N. L., Thomsen, D. R., Wathen, M. W., Newcomb, W. W., Brown, J. C. & Homa, F. L. (1997). Assembly of Herpes Simplex Virus Capsids Using the Human Cytomegalovirus Scaffold Protein: Critical Role of the C Terminus. *Journal of Virology* **71**, 1281-1291.
- Ojala, P. M., Sodeik, B., Ebersold, M. W., Kutay, U. & Helenius, A. (2000). Herpes Simplex Virus Type 1 Entry into Host Cells: Reconstitution of Capsid Binding and Uncoating at the Nuclear Pore complex *In Vitro*. *Molecular and Cellular Biology* **20**, 4922-4931.
- Overton, H., McMillan, D., Hope, L. & Wong-Kai-In, P. (1994). Production of Host Shutoff-Defective Mutants of Herpes Simplex Virus Type 1 by Inactivation of the UL13 Gene. *Virology* **202**, 97-106.
- Overton, H. A., McMillan, D. J., Klavinskis, L. S., Hope, L., Ritchie, A. J. & Wong-Kai-In, P. (1992). Herpes Simplex Virus Type 1 UL13 Encodes a Phosphoprotein That is a Component of the Virion. *Virology* **190**, 184-192.
- Patel, A. H. & Maclean, J. B. (1995). The Product of the UL6 Gene of Herpes Simplex Virus Type 1 is Associated With Virus Capsids. *Virology* **206**, 465-478.
- Patel, A. H., Rixon, F. J., Cunningham, C. & Davison, A. J. (1996). Isolation and Characterization of Herpes Simplex Virus Type 1 Mutants Defective in the UL6 Gene. *Virology* **217**, 111-123.
- Penfold, M. E. T., Armati, P. & Cunningham, A. L. (1994). Axonal Transport of Herpes Simplex Virions to Epidermal Cells: Evidence for a Specialised Mode of Virus Transport and Assembly. *Proceedings of the National Academy of Sciences of the United States of America* **91**, 6529-6533.
- Perdue, M. L., Cohen, J. C., Kemp, M. C., Randall, C. C. & O'Callaghan, D. (1975). Characterization of Three Species of Nucleocapsids of Equine Hepes Virus Type 1 (EHV-1). *Virology* **64**, 187-204.

- Person, S. & Desai, P. (1998). Capsids are Formed in a Mutant Virus Blocked at the Maturation Site of the UL26 and UL26.5 Open Reading Frames of Herpes Simplex Virus Type 1 but are Not Formed in a Null Mutant of UL38 (VP19C). *Virology* **242**, 193-203.
- Person, S., Laquerre, S., Desai, P. & Hempel, J. (1993). Herpes Simplex Virus Type 1 Capsid Protein, VP21, Originates Within the UL26 Open Reading Frame. *Journal of General Virology* **74**, 2269-2273.
- Pertuiset, B., Boccara, M., Cebrian, J., Berthelot, N., Chousterman, S., Puvion-Dutilleul, F., Sisman, J. & Sheldrick, P. (1989). Physical Mapping and Nucleotide Sequence of a Herpes Simplex Virus Type 1 Gene Required for Capsid Assembly. *Journal of Virology* **63**, 2169-2179.
- Poon, A. P. W. & Roizman, B. (1993). Characterization of a Temperature-Sensitive Mutant of the U_L15 Open Reading Frame of Herpes Simplex Virus 1. *Journal of Virology* **67**, 4497-4503.
- Poteete, A. R. & King, J. (1977). Functions of Two New Genes in Salmonella Phage P22 Assembly. *Virology* **76**, 725-739.
- Preston, C. M. (2000). Repression of Viral Transcription During Herpes Simplex Virus Latency. *Journal of General Virology* **81**, 1-19.
- Preston, V. G., Coates, J. A. V. & Rixon, F. J. (1983). Identification and Characterization of a Herpes Simplex Virus Gene Product Required For Encapsulation of Virus DNA. *Journal of Virology* **45**, 1056-1064.
- Preston, V. G., Rixon, F. J., McDougall, I. M., McGregor, M. & Alkobaisi, M. F. (1992). Processing of the Herpes Simplex Virus Assembly Protein- ICP35 Near Its Carboxy Terminal End Requires the Product of the Whole of the UL26 Reading Frame. *Virology* **186**, 87-98.
- Procopio, W. N., Pelavin, P. I., Lee, W. M. & Yeilding, N. M. (1999). Angiopoietin-1 and -2 Coiled-Coil Domains Mediate Distinct Homo-Oligomerization Patterns, But Fibrinogen-Like Domains Mediate Ligand Activity. *Journal of Biological Chemistry* **274**, 30196-30201.
- Purves, F. C., Spector, D. & Roizman, B. (1991). The Herpes Simplex Virus 1 Protein-Kinase Encoded By the U_S3 Gene Mediates Posttranslational Modification of the Phosphoprotein Encoded By the U_L34 Gene. *Journal of Virology* **65**, 5757-5764.
- Rao, V. B. & Black, L. W. (1988). Cloning, Overexpression, and Purification of the Terminase Proteins gp16 and gp17 of Bacteriophage T4. Construction of a Defined in vitro DNA Packaging System Using Purified Terminase Proteins. *Journal of Molecular Biology* **200**, 475-488.
- Raucina, J., Matis, J. & Lesso, J. (1984). Defective Glycoprotein C of the Syncytial Strain of Herpes Simplex Virus Type 1. *Acta Virology* **28**, 457-63.

- Reynolds, A. E., Fan, Y. & Baines, J. D. (2000). Characterization of the UL33 Gene Product of Herpes Simplex Virus 1. *Virology* **266**, 310-318.
- Reynolds, A. E., Ryckman, B. J., Baines, J. D., Zhou, Y., Liang, L. & Roller, R. J. (2001). U_L31 and U_L34 Proteins of Herpes Simplex Virus Type 1 Form a Complex That Accumulates at the Nuclear Rim and Is Required for Envelopment of Nucleocapsids. *Journal of Virology* **75**, 8803-8817.
- Rhim, J. & Schell, K. (1967). Cytopathic and Plaque Assay of Rubella Virus in a Line of African Green Monkey Kidney Cells (Vero). *Proceedings of the Society of Experimental Biology and Medicine* **125**, 475-488.
- Rixon, F. J. (1993). Structure and Assembly of Herpesviruses. *Seminars in Virology* **4**, 135-144.
- Rixon, F. J., Addison, C., McGregor, A., Macnab, S. J., Nicholson, P., Preston, V. G. & Tatman, J. D. (1996). Multiple Interactions Control the Intracellular Localization of the Herpes Simplex Virus Type 1 Capsid Proteins. *Journal of General Virology* **77**, 2251-2260.
- Rixon, F. J., Cross, A. M., Addison, C. & Preston, V. G. (1988). The Products of Herpes Simplex Virus Type 1 Gene UL26 Which Are Involved in DNA Packaging Are Strongly Associated With Empty But Not With Full Capsids. *Journal of General Virology* **69**, 2879-2891.
- Rixon, F. J., Davison, M. J. & Davison, A. J. (1990). Identification of the Genes Encoding Two Capsid Proteins of Herpes Simplex Virus Type 1 by Direct Amino Acid Sequencing. *Journal of General Virology* **71**, 1211-1214.
- Rixon, F. J. & McNab, D. (1999). Packaging-Competent Capsids of a Herpes Simplex Virus Temperature- Sensitive Mutant Have Properties Similar to Those of *in vitro*-Assembled Procapsids. *Journal of Virology* **73**, 5714-5721.
- Robertson, B. J., McCann, P. J., Matusick-Kumar, L., Preston, V. G. & Gao, M. (1997). Na, an Autoproteolytic Product of the Herpes Simplex Virus Type 1 Protease, Can Functionally Substitute for the Assembly Protein ICP35. *Journal of Virology* **71**, 1683-1687.
- Roizman, B. (1979). The Structure and Isomerisation of Herpes Simplex Virus Genomes. *Cell* **16**, 481-494.
- Roizman, B., Desrosiers, R., Fleckstein, B., Lopez, C., Minson, A. & Studdert, M. (1992). The Family *Herpesviridae*: An Update. *Archives of Virology* **123**, 425-449.
- Roller, R. J., Zhou, Y. P., Schnetzer, R., Ferguson, J. & DeSalvo, D. (2000). Herpes Simplex Virus Type 1 U_L34 Gene Product is Required for Viral Envelopment. *Journal of Virology* **74**, 117-129.
- Rost, B. & Sandler, C. (1993). Prediction of Protein Sequences at Better than 70% Accuracy. *Journal of Molecular Biology* **232**, 584-599.

- Saad, A., Zhou, Z. H., Jakana, J., Chiu, W. & Rixon, F. J. (1999). Roles of Triplex and Scaffolding Proteins in Herpes Simplex Virus Type 1 Capsid Formation Suggested by Structures of Recombinant Particles. *Journal of Virology* **73**, 6821-6830.
- Salmon, B. & Baines, J. D. (1998). Herpes Simplex Virus DNA Cleavage and Packaging: Association of Multiple Forms of U_L15-Encoded Proteins With B Capsids Requires at Least the U_L6, U_L17, and U_L28 Genes. *Journal of Virology* **72**, 3045-3050.
- Salmon, B., Cunningham, C., Davison, A. J., Harris, W. J. & Baines, J. D. (1998). The Herpes Simplex Virus Type 1 U_L17 Gene Encodes Virion Tegument Proteins that are Required for Cleavage and Packaging of Viral DNA. *Journal of Virology* **72**, 3779-3788.
- Salmon, B., Nalwanga, D., Fan, Y. & Baines, J. D. (1999). Proteolytic Cleavage of the Amino Terminus of the U_L15 Gene Product of Herpes Simplex Virus Type 1 is Coupled With Maturation of Viral DNA Into Unit-Length Genomes. *Journal of Virology* **73**, 8338-8348.
- Saltzman, R. L., Quirk, M. R. & Jordan, M. C. (1988). Disseminated Cytomegalovirus Infection - Molecular Analysis of Virus and Leucocyte Interactions in Viremia. *Journal of Clinical Investigation* **81**, 75-81.
- Sandri-Goldin, R. M. (1998). Interactions Between a Herpes Simplex Virus Regulatory Protein and Cellular mRNA Processing Pathways. *Methods* **16**, 95-104.
- Sarisky, R. & Weber, P. (1994). Requirement for double Stranded Breaks but Not for Specific Sequences in Herpes Simplex Virus Type 1 Genome Isomerisation Events. *Journal of Virology* **68**, 34-47.
- Sarmiento, M., Haffey, M. & Spear, P. G. (1979). Membrane Proteins Specified by Herpes Simplex Viruses. III. Role of Glycoprotein VP7 (B₂) in Virion Infectivity. *Journal of Virology* **29**, 1149-1158.
- Schaffer, P. A., Aron, G. M., Biswal, N. & Benyesh-Melnick, M. (1973). Temperature-Sensitive Mutants of Herpes Simplex Virus Type 1: Isolation, Complementation and Partial Characterization. *Virology* **52**, 57-71.
- Schek, N. & Bachenheimer, S. L. (1985). Degradation of Cellular mRNAs Induced by a Virion-Associated Factor During Herpes Simplex Virus Infection of Vero Cells. *Journal of Virology* **55**, 601-610.
- Schrag, J. D., Venkataram, P., Rixon, F. J. & Chiu, W. (1989). Three-Dimensional Structure of the HSV-1 Nucleocapsid. *Cell* **56**, 651-660.
- Shao, L., Rapp, L. M. & Weller, S. K. (1993). Herpes Simplex Virus 1 Alkaline Nuclease Is Required For Efficient Egress of Capsids From the Nucleus. *Virology* **196**, 146-162.

- Sheaffer, A. K., Newcomb, W. W., Brown, J. C., Gao, M., Weller, S. K. & Tenney, D. J. (2000). Evidence for Controlled Incorporation of Herpes Simplex Virus Type 1 UL26 Protease Into Capsids. *Journal of Virology* **74**, 6838-6848.
- Sheaffer, A. K., Newcomb, W. W., Gao, M., Yu, D., Weller, S. K., Brown, J. C. & Tenney, D. J. (2001). Herpes Simplex Virus DNA Cleavage and Packaging Proteins Associate With the Procapsid Prior to Its Maturation. *Journal of Virology* **75**, 687-698.
- Shieh, M.-T. & Spear, P. G. (1994). Herpesvirus Induced Cell Fusion That Is Dependent on Cell Surface Heparan Sulphate or Soluble Heparin. *Journal of Virology* **68**, 1224-1228.
- Shulman, M., Wilde, C. D. & Köhler, G. (1978). A Better Cell Line for Making Hybridomas Secreting Specific Antibodies. *Nature* **276**, 269-270.
- Schulz, T. F. (1998). Kaposi's Sarcoma-Associated Herpesvirus (Human Herpesvirus-8). *Journal of General Virology*. **79**, 1573-1591.
- Simpson, A. A., Tao, Y., Leiman, P. G., Badasso, M. O., He, Y., Jardine, P. J., Olson, N. H., Morais, M. C., Grimes, S., Anderson, D. L., Baker, T. S. & Rossmann, M. G. (2000). Structure of the Bacteriophage ϕ 29 DNA Packaging Motor. *Nature* **408**, 745-750.
- Skepper, J. N., Whiteley, A., Browne, H. & Minson, A. (2001). Herpes Simplex Virus Nucleocapsids Mature to Progeny Virions by an Envelopment-Deenvelopment-Reenvelopment Pathway. *Journal of Virology* **75**, 5697-5702.
- Smibert, C. A., Johnson, D. C. & Smiley, J. R. (1992). Identification and Characterization of the Virion Induced Host Shutoff Product of Herpes Simplex Virus Gene UL41. *Journal of General Virology* **73**, 467-470.
- Smith, G. A., Gross, S. P. & Enquist, L. W. (2000). Herpesviruses Use Bidirectional Fast-Axonal Transport to Spread in Sensory Neurons. *Proceedings of the National Academy of Sciences of the United States of America* **98**, 3466-3470.
- SmithKline Beecham Corporation (1998). Use of HSV-1 UL-15 and VP5 in Identifying Anti-Viral Agents. European Patent Application Number 98301123.0
- Sodeik, B., Ebersold, M. W. & Helenius, A. (1997). Microtubule-Mediated Transport of Incoming Herpes Simplex Virus 1 Capsids to the Nucleus. *Journal of Cell Biology* **136**, 1007-1021.
- Southern, S. (1975). Detection of Specific Sequences Among DNA Fragments Separated by Electrophoresis. *Journal of Molecular Biology* **98**, 503-517.
- Spaete, R. & Mocarski, E. S. (1985). The *a* Sequence of the Cytomegalovirus Genome Functions as a Cleavage/Packaging Signal for Herpes Simplex Virus Defective Genomes. *Journal of Virology* **54**, 817-824.

- Spear, P. G. (1993). Entry of Alphaherpesviruses Into Cells. *Seminars in Virology* **4**, 167-180.
- Spencer, J. V., Newcomb, W. W., Thomsen, D. R., Homa, F. L. & Brown, J. C. (1998). Assembly of the Herpes Simplex Virus Capsid: Preformed Triplexes Bind to the Nascent Capsid. *Journal of Virology* **72**, 3944-3951.
- Steven, A. C., Booy, F. P., Greenstone, H. L., Trus, B. L., Newcomb, W. W. & Brown, J. C. (1992). DNA-Phage Assembly As a Model For Herpesvirus Capsid Assembly. *Faseb Journal* **6**, A136.
- Steven, A. C. & Spear, P. G. (1997). Herpesvirus Capsid Assembly and Envelopment. In *Structural Biology of Viruses*, pp. 312-351. Edited by W. Chiu, R. Burnett & R. Garcea. New York: Oxford University Press.
- Steven, A. C., Roberts, C. R., Hay, J., Bisher, M. E., Pun, T. & Trus, B. L. (1986). Hexavalent Capsomers of Herpes Simplex Virus Type 2: Symmetry, Shape, Dimensions and Oligomeric Status. *Journal of Virology* **57**, 578-584.
- Stevens, J. G. & Cook, M. L. (1971). Latent Herpes Simplex Virus in Spinal Ganglia of Mice. *Science* **173**, 843-845.
- Stevens, J. G., Wagner, E. K., Devi-Rao, G. B., Cook, M. L. & Feldman, L. (1987). RNA Complementary to a Herpesvirus Alpha Gene mRNA is Predominant in Latently Infected Neurons. *Science* **235**, 1056-1059.
- Stow, N. D., Hammarsten, O., Arbuckle, M. I. & Elias, P. (1993). Inhibition of Herpes Simplex Virus Type 1 DNA Replication by Mutant Forms of the Origin-Binding Protein. *Virology* **196**, 413-418.
- Stow, N. D., McMonagle, A. & Davison, A. (1983). Fragments From Both Termini of the Herpes Simplex Virus Type 1 Genome Contain Signals Required for Encapsidation of Viral DNA. *Nucleic Acids Research* **11**, 8205-8219.
- Stow, N. & Wilkie (1976). An Improved Technique for Obtaining Enhanced Infectivity With Herpes Simplex Virus Type 1 DNA. *Journal of General Virology* **33**, 447-458.
- Strauss, H. & King, J. (1984). Steps in the Stabilization of Newly Packaged DNA During Phage P22 Morphogenesis. *Journal of Molecular Biology* **172**, 523-543.
- Strobel-Fidler, M. & Francke, B. (1980). Alkaline Deoxyribonuclease Induced by Herpes Simplex Virus Type 1: Composition and Properties of the Purified Enzyme. *Virology* **103**, 493-501.
- Szilágyi, J. F. & Cunningham, C. (1991). Identification and Characterization of a Novel Non-Infectious Herpes Simplex Virus-Related Particle. *Journal of General Virology* **72**, 661-668.

- Tatman, J. D., Preston, V. G., Nicholson, P., Elliott, R. M. & Rixon, F. J. (1994). Assembly of Herpes Simplex Virus Type-1 Capsids Using a Panel of Recombinant Baculoviruses. *Journal of General Virology* **75**, 1101-1113.
- Taus, N. S. & Baines, J. D. (1998). Herpes Simplex Virus 1 DNA Cleavage/Packaging: The UL28 Gene Encodes a Minor Component of B Capsids. *Virology* **252**, 443-449.
- Taus, N. S., Salmon, B. & Baines, J. D. (1998). The Herpes Simplex Virus 1 UL17 Gene is Required for Localization of Capsids and Major and Minor Capsid Proteins to Intranuclear Sites Where Viral DNA is Cleaved and Packaged. *Virology* **252**, 115-125.
- Taylor-Wiedeman, J., Sissons, J., Borysiewicz, L. & Sinclair, J. (1991). Monocytes are a Major site of Persistence of Human Cytomegalovirus in Peripheral Blood Mononuclear Cells. *Journal of General Virology* **72**, 2059-2064.
- Tengelsen, L. A., Pederson, N. E., Shaver, P. R., Wathen, M. W. & Homa, F. L. (1993). Herpes Simplex Virus Type 1 DNA Cleavage and Encapsidation Require the Product of the UL28 Gene - Isolation and Characterization of 2 UL28 Deletion Mutants. *Journal of Virology* **67**, 3470-3480.
- Thomsen, D. R., Newcomb, W. W., Brown, J. C. & Homa, F. L. (1995). Assembly of the Herpes Simplex Virus Capsid - Requirement For the Carboxyl-Terminal 25 Amino-Acids of the Proteins Encoded By the UL26 and UL26.5 Genes. *Journal of Virology* **69**, 3690-3703.
- Thomsen, D. R., Roof, L. L. & Homa, F. L. (1994). Assembly of Herpes Simplex Virus (HSV) Intermediate Capsids in Insect Cells Infected With Recombinant Baculoviruses Expressing HSV Capsid Proteins. *Journal of Virology* **68**, 2442-2457.
- Trus, B. L., Booy, F. P., Newcomb, W. W., Brown, J. C., Homa, F. L., Thomsen, D. R. & Steven, A. C. (1996). The Herpes Simplex Virus Procapsid: Structure, Conformational Changes Upon Maturation, and Roles of the Triplex Proteins VP19c and VP23 in Assembly. *Journal of Molecular Biology* **263**, 447-462.
- Trus, B. L., Gibson, W., Cheng, N. Q. & Steven, A. C. (1999). Capsid Structure of Simian Cytomegalovirus from Cryoelectron Microscopy: Evidence for Tegument Attachment Sites. *Journal of Virology* **73**, 2181-2192.
- Trus, B. L., Homa, F. L., Booy, F. P., Newcomb, W. W., Thomsen, D. R., Cheng, N. Q., Brown, J. C. & Steven, A. C. (1995). Herpes Simplex Virus Capsids Assembled in Insect Cells Infected With Recombinant Baculoviruses - Structural Authenticity and Localization of VP26. *Journal of Virology* **69**, 7362-7366.
- Trus, B. L., Newcomb, W. W., Booy, F. P., Brown, J. C. & Steven, A. C. (1992). Distinct Monoclonal-Antibodies Separately Label the Hexons or the Pentons of Herpes Simplex Virus Capsid. *Proceedings of the National Academy of Sciences of the United States of America* **89**, 11508-11512.

- Trybala, E., Svennerholm, B., Bergstrom, T., Oloffson, S., Jeansson, S. & Goodman, J. L. (1993). Herpes Simplex Virus Type 1-Induced Hemagglutination: Glycoprotein C Mediates Virus Binding to Erythrocyte Surface Heparan Sulphate. *Journal of Virology* **67**, 1278-1285.
- Turtinen, L., Saltzman, R., Jordan, M. & Haase, A. (1987). Interactions of Human Cytomegalovirus With Leucocytes, *in vivo* Analysis by *in situ* Hybridisation. *Microbial Pathogenesis* **3**, 287-297.
- Twigg, A. & Sherratt, D. (1980). Trans Complementable Copy Number Mutants of Plasmid ColE1. *Nature* **283**, 216-218.
- Umene, K. & Nishimoto, T. (1996). Replication of Herpes Simplex Virus Type 1 DNA is Inhibited in a Temperature-Sensitive Mutant of BHK-21 Cells Lacking RCC1 (Regulator of Chromosome Condensation) and Virus DNA Remains Linear. *Journal of General Virology* **77**, 2261-2270.
- Valpuesta, J. M. & Carracosa, J. L. (1994). Structure of Viral Connectors and Their Function in Bacteriophage Assembly and DNA Packaging. *Quarterly Reviews of Biophysics* **27**, 107-155.
- Valpuesta, J. M., Fujisawa, H., Marco, S., Carazo, J. M. & Carrascosa, J. (1992). Three-Dimensional Structure of T3 Connector Purified from Overexpressing Bacteria. *Journal of Molecular Biology* **224**, 103-112.
- Varmuza, S. L. & Smiley, J. R. (1985). Signals for Site-Specific Cleavage of HSV DNA: Maturation Involves Two Separate Cleavage Events at Sites Distal to the Recognition Sequences. *Cell* **41**, 793-802.
- Vaughn, J. C., Goodwin, R. H., Tompkins, G. J. & McCawley, P. (1977). The Establishment of Two Cell Lines From the Insect *Spodoptera frugiperda* (Lepidoptera: Noctuidae). *In Vitro* **13**, 213-217.
- Wadsworth, S., Jacob, R. J. & Roizman, B. (1975). Anatomy of Herpes Simplex Virus DNA. II. Size, Composition, and Arrangement of Inverted Terminal Repeats. *Journal of Virology* **15**, 1487-1497.
- Wagenaar, F., Pol, J. M., de Wind, N. & Kimman, T. G. (2001). Deletion of the UL21 Gene in Pseudorabies Virus Results in the Formation of DNA-Deprived Capsids: An Electron Microscopy Study. *Veterinary Research* **32**, 47-54.
- Wagner, E. K. & Bloom, D. C. (1997). Experimental Investigation of Herpes Simplex Virus Latency. *Clinical Microbiology Reviews* **10**, 419-443.
- Ward, P. L., Ogle, W. O. & Roizman, B. (1996). Assemblons: Nuclear Structures Defined by Aggregation of Immature Capsids and Some Tegument Proteins of Herpes Simplex Virus 1. *Journal of Virology* **70**, 4623-4631.

- Weinheimer, S. P., McCann III, P. J., O'Boyle II, D. R., Stevens, J. T., Boyd, B. A., Drier, D. A., Yamanaka, G. A., Dilanni, C. L., Deckman, I. C. & Cordingly, M. G. (1993). Autoproteolysis of Herpes Simplex Virus Type 1 Protease Releases an Active Catalytic Domain Found in Intermediate Capsid Particles. *Journal of Virology* **67**, 5813-5822.
- Weller, S. K., Seghatoleslami, M. R., Shao, L., Rowse, D. & Carmichael, E. P. (1990). The Herpes Simplex Virus Type 1 Alkaline Nuclease Is Not Essential For Viral-DNA Synthesis - Isolation and Characterization of a LacZ Insertion Mutant. *Journal of General Virology* **71**, 2941-2952.
- White, E. & Cipriani, R. (1989). Specific Disruption of Intermediate Filaments and the Nuclear Lamina by the 19-kDa product of the Adenovirus E1B Oncogene. *Proceedings of the National Academy of Sciences of the United States of America* **86**, 9886-9890.
- Wildy, P. & Watson, D. (1963). Electron Microscopic Studies on the Architecture of Animal Viruses. *Cold Spring Harbour Symposia of Quantitative Biology* **27**, 25-47.
- Wilson, D. W., Davis-Poynter, N. & Minson, A. C. (1994). Mutations in the Cytoplasmic Tail of Herpes Simplex Virus Glycoprotein H Suppress Cell Fusion by a Syncytial Strain. *Journal of Virology* **68**, 6985-6993.
- Wingfield, P. T., Stahl, S. J., Thomsen, D. R., Homa, F. L., Booy, F. P., Trus, B. L. & Steven, A. C. (1997). Hexon-Only Binding of VP26 Reflects Differences Between the Hexon and Penton Conformations of VP5, the Major Capsid Protein of Herpes Simplex Virus. *Journal of Virology* **71**, 8955-8961.
- Wittels, M. & Spear, P. G. (1991). Penetration of Cells by Herpes Simplex Virus Does Not Require a Low pH-Dependent Endocytic Pathway. *Virus Research* **18**, 271-290.
- Wohlrab, F., Chatterjee, S. & Wells, R. (1991). The Herpes Simplex Virus 1 Segment Inversion Site is Specifically Cleaved by a Virus-Induced Nuclear Endonuclease. *Proceedings of the National Academy of Sciences of the United States of America* **88**, 6432-6436.
- Yamauchi, Y., Wada, K., Goshima, F., Takakuwa, H., Daikoku, T., Yamada, M. & Nishiyama, Y. (2001). The UL14 Protein of Herpes Simplex Virus Type 2 Translocates the Minor Capsid Protein VP26 and the DNA Cleavage and Packaging UL33 Protein into the Nucleus of Coexpressing Cells. *Journal of General Virology* **82**, 321-330.
- Yao, X., Matecic, M. & Elias, P. (1997). Direct Repeats of the Herpes Simplex Virus a sequence Promote Nonconservative Homologous Recombination that is Not Dependent on XPF/ERCC4. *Journal of Virology* **71**, 6842-6849.
- Ye, G. J., Vaughan, K. T., Vallee, R. B. & Roizman, B. (2000). The Herpes Simplex Virus 1 UL34 Protein Interacts with a Cytoplasmic Dynein Intermediate Chain and Targets the Nuclear Membrane. *Journal of Virology* **74**, 1355-1363.

- Yu, D., Sheaffer, A. K., Tenney, D. J. & Weller, S. K. (1997). Characterization of ICP6:lacZ Insertion Mutants of the UL15 Gene of Herpes Simplex Virus Type 1 Reveals the Translation of Two Proteins. *Journal of Virology* **71**, 2656-2665.
- Yu, D. & Weller, S. K. (1998a). Genetic Analysis of the UL15 Gene Locus for the Putative Terminase of Herpes Simplex Virus Type 1. *Virology* **243**, 32-44.
- Yu, D. & Weller, S. K. (1998b). Herpes Simplex Virus Type 1 Cleavage and Packaging Proteins UL15 and UL28 are Associated With B but Not C Capsids During Packaging. *Journal of Virology* **72**, 7428-7439.
- Zhang, F., Lemieux, S., Wu, X., St-Arnaud, D., McMurray, C. T., Major, F. & Anderson, D. (1998). Function of Hexameric RNA in Packaging of Bacteriophage ϕ 29 DNA In Vitro. *Molecular Cell* **2**, 141-147.
- Zhou, Z. H., Chen, D. H., Jakana, J., Rixon, F. J. & Chiu, W. (1999). Visualization of Tegument-Capsid Interactions and DNA in Intact Herpes Simplex Virus Type 1 Virions. *Journal of Virology* **73**, 3210-3218.
- Zhou, Z. H., Chiu, W., Haskell, K., Spears, H., Jakana, J., Rixon, F. J. & Scott, L. R. (1998). Refinement of Herpesvirus B-Capsid Structure on Parallel Supercomputers. *Biophysical Journal* **74**, 576-588.
- Zhou, Z. H., Macnab, S. J., Jakana, J., Scott, L. R., Chiu, W. & Rixon, F. J. (1998). Identification of the Sites of Interaction Between the Scaffold and Outer Shell in Herpes Simplex Virus-1 Capsids by Difference Electron Imaging. *Proceedings of the National Academy of Sciences of the United States of America* **95**, 2778-2783.
- Zhou, Z. H., Prasad, B. V. V., Jakana, J., Rixon, F. J. & Chiu, W. (1994). Protein Subunit Structures in the Herpes Simplex Virus A-Capsid Determined From 400-Kv Spot-Scan Electron Cryomicroscopy. *Journal of Molecular Biology* **242**, 456-469.
- Zimmermann, J. & Hammerschmidt, W. (1995). Structure and Role of the Terminal Repeats of Epstein-Barr Virus in Processing and Packaging of Virion DNA. *Journal of Virology* **69**, 3147-3155.